U.PORTO

DOUTORAMENTO

BIOLOGIA MOLECULAR E CELULAR

Cross-regulation of mitochondrial function and cell cycle progression in budding yeast

Ana Cláudia Leite

D

2023

Ana Cláudia Leite. Cross-regulation of mitochondrial function and cell cycle progression in budding yeast

Cross-regulation of mitochondrial function and cell cycle progression in budding yeast

Ana Cláudia Ribeiro Leite

D.ICBAS 2023

SEDE ADMIISTRATIVA

INSTITUTO DE CIÊNCIAS BIOMÉDICAS ABEL SALAZAR

FACULDADE DE CIÊNCIAS

Ana Cláudia Ribeiro Leite

Cross-regulation of mitochondrial function and cell cycle progression in budding yeast

Tese de Candidatura ao grau de Doutor em Biologia Molecular e Celular;
Programa doutoral da Universidade do Porto (Instituto de Ciências Biomédicas Abel Salazar e Faculdade de Ciências)

Orientador – Doutora Clara Isabel Ferreira Pereira
Categoria – Investigador Auxiliar
Afiliação – Instituto de Investigação e Inovação em Saúde (i3S), Universidade do Porto

Coorientador – Doutor Vitor Manuel Vieira da Costa
Categoria – Professor Associado
Afiliação – Instituto de Ciências Biomédicas Abel Salazar (ICBAS) e Instituto de Investigação e Inovação em Saúde (i3S), Universidade do Porto

Financial Support

This work was funded by National Funds through Fundação para a Ciência e a Tecnologia (FCT) (UIDB/04293/2020 and IF/00889/2015 to Clara Pereira) as well as by NORTE 2020 under PORTUGAL 2020 Partnership Agreement through the European Regional Development Fund (Norte-01-0145-FEDER-000008). The author was supported by a PhD fellowship from FCT (SFRH/BD/135921/2018).

A autora esclarece que na elaboração desta tese foram incluídos os artigos publicados ou manuscritos submetidos para publicação abaixo indicados, e declara ter participado ativamente na conceção e execução das experiências que estiveram na origem da mesma, assim como na sua interpretação, discussão e redação.

The author declares that in the elaboration of this thesis published articles or manuscripts submitted for publication were included as listed below and declares that she participated actively in the conception and execution of the experiments that produced such data, as well as in their interpretation, discussion and in the manuscript writing.

Ao abrigo do disposto do no 2, alínea a) do artigo 31° do Decreto-Lei n.º 115/2013 de 7 de agosto, fazem parte integrante desta tese de doutoramento os seguintes trabalhos já publicados ou submetidos para publicação:

List of publications:

Ana Cláudia Leite, Telma S. Martins, Ana Campos, Vitor Costa and Clara Pereira, Phosphoregulation of the ATP synthase beta subunit stimulates mitochondrial activity for G2/M progression, Advances in Biological Regulation, 2022, 85:100905 (DOI: 10.1016/j.jbior.2022.100905).

Ana Cláudia Leite*, Telma S. Martins*, Rute R. Cesário, Vitor Teixeira, Vitor Costa and Clara Pereira, Mitochondrial respiration promotes Cdc37-dependent stability of the Cdk1 homolog Cdc28, Journal of Cell Science, 2023, 136:jcs260279 (DOI: 10.1242/jcs.260279).
*Co-first authors with equal contribution

Ana Cláudia Leite, Maria Barbedo, Vitor Costa and Clara Pereira, The APC/C activator Cdh1p plays a role in mitochondrial metabolic remodeling in yeast, International Journal of Molecular Sciences, 2023, 24:4111 (DOI: 10.3390/ijms24044111).

Ana Cláudia Leite, Vitor Costa and Clara Pereira, Mitochondria and the cell cycle in budding yeast, under revision.

Agradecimentos

Este trabalho de doutoramento contou com o apoio de inúmeras pessoas que direta ou indiretamente contribuíram para a sua elaboração e concretização. A todas quero expressar o meu agradecimento:

À minha orientadora Clara Pereira, por ter sido uma peça fundamental no meu crescimento enquanto cientista, mas também enquanto pessoa. Agradeço a orientação, o apoio e a constante partilha de conhecimentos ao longo deste percurso. Foi um enorme privilégio ter partilhado contigo esta experiência!

Ao meu co-orientador Vitor Costa, por me ter dado a oportunidade de integrar o seu grupo de investigação e por toda a disponibilidade que sempre demonstrou durante esta jornada. Agradeço também todas as críticas e sugestões que em muito contribuíram para a qualidade deste trabalho.

A todos os membros do grupo Yeast Signalling Networks, pela boa disposição e energia no laboratório. Agradeço também pela ajuda constante e partilha de conhecimentos. Vou recordar com carinho todos os momentos passados no laboratório! Em particular quero realçar o meu agradecimento a antigos membros do grupo que contribuíram diretamente para a realização deste trabalho, nomeadamente Ana Moura, Inês Claro, Ana Campos e Maria Tavares. Agradeço também ao grupo Phenotypic Evolution pela boa disposição e entreajuda com que sempre me presentaram.

À minha família e amigos que sempre tiveram uma palavra de incentivo e coragem nos momentos certos. Em especial, à minha mãe, a quem todas as palavras são poucas para exprimir o meu agradecimento. Agradeço por todo o amor e paciência, por teres acreditado em mim e permitido que chegasse até aqui. Todas as minhas conquistas são reflexo do teu apoio incondicional!

Ao Marco, por partilhares comigo todos os momentos de alegria e sobretudo os de desânimo ao longo deste percurso. Agradeço pelas longas discussões científicas, mas essencialmente pelo constante encorajamento e apoio que nunca me deixaram desistir. Esta conquista também se deve a ti!

Abstract

Accumulating evidence suggests an integrated regulation of mitochondria and the cell cycle in distinct organisms. In budding yeast, a well-established example is the coordinated movement and positional control of mitochondria during the different phases of the cell cycle. In addition, mitochondrial bioenergetics, including mitochondrial respiration and ATP production, also change with cell cycle phases both in yeast and mammalian cells. In turn, mitochondrial defects often led to a cell cycle delay or arrest, indicating mitochondrial function can also regulate cell cycle progression. However, the molecular mechanisms underlying this co-regulation remain largely unknown.

Recently, it was shown that the phosphorylation of ATP synthase catalytic beta subunit (Atp2p in yeast) at T124/T317 upregulates Atp2p levels, impacting on ATP synthase activity and mitochondrial function. Remarkably the two Atp2p phosphosites are regulated by the PP2A-like Sit4p phosphatase, which plays a role in cell cycle regulation, and lie on putative anaphase-promoting complex/cyclosome (APC/C) recognition motifs. In this thesis, we set out to investigate if Atp2p phosphorylation was cell cycle-dependent and whether APC/C targeted Atp2p for degradation, in a phosphorylation regulated manner. Our results showed that Atp2p levels and phosphorylation are associated with cell cycle, with an increase at G2/M phase. Phosphorylation of Atp2p, possibly by the polo-like kinase Cdc5p, stimulates mitochondrial membrane potential, respiration and ATP production at G2/M and promotes cell cycle progression at this phase. Importantly, we also found that APC/C is not directly involved in the regulation of Atp2p stability. However, Atp2p levels increased in the absence of the APC/C coactivator Cdh1p. This unexpected result led us to investigate the general role of Cdh1p in the mitochondrial proteome composition. We identified 14% of the total mitochondrial proteins as having altered abundance in the *cdh1*Δ cells. About one third were upregulated proteins which included subunits of the mitochondrial respiratory chain, enzymes from tricarboxylic acid cycle and regulators of the mitochondrial organization, suggesting a metabolic remodelling towards an increase in mitochondrial respiration. This result was confirmed by an increase in mitochondrial oxygen consumption and cytochrome *c* oxidase activity in Cdh1p deficient cells. Interestingly, the increased mitochondrial respiration in *cdh1*Δ cells is mediated by the upregulation of the transcription factor Yap1p, indicating an indirect effect of Cdh1p in mitochondrial remodelling.

Cdc28p is the major kinase involved in the regulation of the cell cycle progression in yeast. We found that the absence of Atp2p, or of other proteins involved in mitochondrial respiration, inhibits proliferation of cells expressing Cdc28p conditional mutants. Cell growth defects in these double mutants is associated with aggravated cell cycle arrest, mitochondrial dysfunction and a strong decrease in mutant Cdc28p steady-state protein

levels. We also found that Cdc28p instability in mitochondrial mutants is due to an impairment in the Hsp90-Cdc37 chaperone system, a complex vital for the folding and activity of several yeast kinases, including Cdc28p. These results suggest that mitochondrial dysfunction can also trigger a cell cycle checkpoint arrest by directly affecting Cdc28p levels.

Overall, this thesis provided novel insights into the mechanisms underlying the coordination of mitochondrial function and cell cycle progression.

Resumo

Várias evidências apontam para uma regulação integrada da mitocôndria e do ciclo celular em diversos organismos. Um bom exemplo desta co-regulação na levedura é o movimento coordenado e posicional da mitocôndria durante as diferentes fases do ciclo celular. Além disso, a bioenergética mitocondrial, que inclui a respiração mitocondrial e a produção de ATP, também varia consoante as fases do ciclo celular tanto em células de levedura como de mamífero. Por sua vez, defeitos mitocondriais induzem atrasos ou paragens no ciclo celular, o que indica que a função mitocondrial também regula a progressão do ciclo celular. No entanto, os mecanismos moleculares subjacentes a esta co-regulação permanecem largamente desconhecidos.

Recentemente, foi reportado que a fosforilação da subunidade beta (Atp2p em levedura) da ATP sintase nas T124/T317 aumenta os níveis de Atp2p e influencia a atividade da ATP sintase e a função mitocondrial. Curiosamente, os dois locais de fosforilação são regulados pela fosfatase Sit4p, que desempenha um papel no ciclo celular e, encontram-se em motivos de reconhecimento do complexo promotor de anáfase/ciclossoma (APC/C). Assim, nesta tese propusemo-nos a investigar se a fosforilação de Atp2p é dependente do ciclo celular e se a proteína Atp2p é um alvo direto do APC/C, sendo esta regulação dependente da fosforilação. Os resultados revelam que tanto os níveis como o estado de fosforilação de Atp2p variam com o ciclo celular, com um aumento na fase G2/M. A fosforilação de Atp2p, possivelmente pela cinase Cdc5p, estimula o potencial de membrana mitocondrial, a respiração e a produção de ATP em G2/M e promove também a progressão do ciclo celular. Adicionalmente, os resultados mostram que o APC/C não está diretamente envolvido na regulação da estabilidade de Atp2p. No entanto, os níveis de Atp2p aumentam na ausência de um dos co-ativadores do APC/C, Cdh1p. Este resultado inesperado conduziu à análise do papel do Cdh1p na composição do proteoma mitocondrial. A abundância de 14% das proteínas mitocondriais está alterada nas células *cdh1*Δ. Aproximadamente um terço destas proteínas tem os níveis aumentados e nestas incluem-se subunidades da cadeia respiratória, enzimas do ciclo do ácido tricarboxílico e reguladores da organização mitocondrial, o que sugere uma reorganização metabólica no sentido de aumentar a respiração mitocondrial. Este resultado foi confirmado pelo aumento do consumo de oxigénio e atividade do citocromo *c* oxidase em células deficientes em Cdh1p. O aumento da respiração mitocondrial nas células *cdh1*Δ é mediado pelo aumento da atividade do fator de transcrição Yap1p, o que aponta para um efeito indireto do Cdh1p na remodelação mitocondrial.

Na levedura, a proteína Cdc28p constitui a principal cinase envolvida da regulação do ciclo celular. A ausência de Atp2p, ou outras proteínas envolvidas na respiração mitocondrial,

inibe a proliferação de células que expressam mutantes condicionais de Cdc28p. Os defeitos no crescimento desses duplos mutantes estão associados com atrasos severos no ciclo celular, disfunção mitocondrial e uma forte redução dos níveis basais de Cdc28p. Os resultados demonstram ainda que a instabilidade de Cdc28p na ausência de proteínas mitocondriais deve-se à disfunção do complexo chaperona constituído pelas proteínas Hsp90-Cdc37, que é crucial para o enrolamento e atividade de diversas cinases na levedura, como Cdc28p. Estes resultados sugerem que a disfunção mitocondrial pode induzir atrasos no ciclo celular através da redução dos níveis de Cdc28p.

Em conclusão, os resultados apresentados nesta tese oferecem novas perspetivas sobre os mecanismos subjacentes à coordenação da função mitocondrial com a progressão do ciclo celular.

Table of contents

Abbreviations

2D – two dimension

Acetyl-CoA – acetyl coenzyme A

ADP – adenosine diphosphate

AIM – altered inheritance rate of mitochondria

AMP - adenosine monophosphate

AMPK – AMP-activated protein kinase

ANOVA – analysis of variance

APC/C – anaphase-promoting complex/cyclosome

ATP – adenosine triphosphate

AU – arbitrary units

AUC – area under the curve

cAMP – cyclic AMP

Cdc – cell division cycle

Cdk – cyclin-dependent kinase

COX – cytochrome *c* oxidase

DAPI – 4′,6-diamidino-2-phenylindole

D-box – destruction box

DHE – dihydroethidium

DIC – differential interference contrast

$DiOC_6(3)$ – 3,3′-dihexyloacarbocyanide iodine

FAD – flavin adenine dinucleotide

$FADH_2$ – reduced flavin adenine dinucleotide

FC – fold change

FCCP – carbonyl-cyanide 4-(trifluoromethoxy)-phenylhydrazone

GA – geldanamycin

GFP – green fluorescent protein

GLS1 – glutaminase 1

GO – gene ontology

GPS – group-based prediction system

GTP – guanosine triphosphate

HA – hemagglutinin

HPLC-MS/MS – high performance liquid chromatography tandem mass spectrometry

IMM – inner mitochondrial membrane

IMS – intermembrane space

MEN – mitotic exit network

Mff – mitochondrial fission factor

MMS – methyl methanesulfonate

mtDNA – mitochondrial DNA

mtGFP – mitochondria-targeted green fluorescent protein

MTOC – microtubules-organizing center

NADH – reduced nicotinamide adenine dinucleotide

NAO – 10-N-Nonyl acridine orange

ns – not significant

OCR – oxygen consumption rate

OD – optical density

ONPG – *o*-nitrophenyl-β-d-galactopyranoside

OMM – outer mitochondrial membrane

OXPHOS – oxidative phosphorylation

PACE – proteasome associated control elements

PAGE – polyacrylamide gel electrophoresis

PCR – polymerase chain reaction

PDS – post diauxic shift

PFKFB3 – 6-phosphofructo-2-kinase/fructose-2,6-bisphosphatase 3

Pi – phosphate group

pI – isoeletric point

PKA – protein kinase A

PTM – post-translational modification

ROS – reactive oxygen species

rpm – rotations per minute

RTG – retrograde response

SCF – SKP1-CUL1-F-box protein

SD – standard deviation

SDS – sodium dodecyl sulfate

SEM – standard error of the mean

SPB – spindle pole body

TCA – tricarboxylic acid

TIM – translocase of the inner membrane

TOM – translocase of the outer membrane

TOR – target of rapamycin

TORC1 – TOR complex 1

Ts – temperature sensitive

TTC – tetrazolium chloride

List of figures

List of tables

CHAPTER 1.

General introduction

This chapter comprises parts from the following publication:

Ana Cláudia Leite, Vitor Costa and Clara Pereira, Mitochondria and the cell cycle in budding yeast, submitted.

1. Mitochondria – an overview

Mitochondria arose around two billion years ago from the engulfment of an α-proteobacterium by a precursor of the eukaryotic cell (Lane and Martin, 2010). In the late 19th century, Benda named these organelles mitochondria, derived from the Greek words' "mitos" (meaning thread) and "chondrion" (meaning granule). Along evolution, by allowing the integration of different cell signaling pathways, mitochondria become a central modulator of cell fate whose dysfunction is implicated in many human pathologies such as neuromuscular and neurodegenerative diseases as well as some forms of cancer and diabetes (Friedman and Nunnari, 2014).

Mitochondria are essential intracellular organelles with a major role in generating cellular energy in the form of adenosine triphosphate (ATP). Decades of research revealed that mitochondria are also involved in other important cellular processes namely amino acid and lipid metabolism, heme and iron-sulfur (Fe/S) cluster biosynthesis, and maintenance of cellular redox state (Lasserre *et al.*, 2015; Malina *et al.*, 2018). Mitochondria are organized as a network of interconnected double-membrane tubules. The outer and inner mitochondrial membranes (OMM and IMM, respectively) delineate the two aqueous compartments: the intermembrane space (IMS) and the mitochondrial matrix (Malina *et al.*, 2018). The assigned *Saccharomyces cerevisiae* mitochondrial proteome comprises ~1000 different soluble, peripheral and integral mitochondrial membrane proteins (Vögtle *et al.*, 2017).

As a part of the evolution process, the overall form and composition of mitochondria have dramatically changed and most of the mitochondrial genomic material was lost or transferred to the nuclear genome (Friedman and Nunnari, 2014). The existence of mitochondrial genome (mtDNA) makes mitochondria unique organelles. While the exact number of genes located in mtDNA can differ among species, the mtDNA always encode proteins required for protein synthesis and core subunits (seven in yeast) of the oxidative phosphorylation (OXPHOS) complexes (Foury *et al.*, 1998). Since the mitochondrial genome encodes only a fraction of the mitochondrial proteins, the mitochondrial biogenesis requires coordination between mitochondria and the nucleus. In this sense, mitochondrial biogenesis involves the import of nucleus-encoded proteins translated in cytosolic ribosomes (Friedman and Nunnari, 2014; Neupert and Herrmann, 2007) that are found in the proximity to the OMM (Margeot *et al.*, 2002). The import of precursor proteins requires the presence of specific targeting signals, being the most frequent a cleavable N-terminal extension termed presequence. Normally it consists of about 10 to 80 amino acid residues that have the potential to form amphipathic α-helical segments with a net positive charge.

However, many mitochondrial precursors lack N-terminal presequences and instead contain internal targeting sequences (Neupert and Herrmann, 2007).

Yeast can survive without mtDNA, as long as fermentable carbon sources, such as glucose, are present in the growth medium. Even in the presence of oxygen, yeast cells generate ATP primarily by glycolysis with ethanol as the major fermentation product. However, when yeast grow on non-fermentable carbon sources, such as ethanol or glycerol, respiration and therefore the integrity of the mitochondrial genome become obligatory (Gancedo, 1998). Though yeast can survive loss of mtDNA in fermenting media, in any condition it cannot survive loss of mitochondria due to its role in the biosynthesis of essential cellular metabolites.

Considering the fundamental importance of mitochondria to the cell, mitochondrial biogenesis, morphology and activity are continuously adjusted in response to cellular requirements, including cell cycle progression and division.

1.1. Mitochondrial bioenergetics

The most well-known role ascribed to mitochondria as the cell's powerhouse is the generation of usable energy in the form of ATP, being the host of the tricarboxylic acid (TCA) cycle and OXPHOS (Malina *et al.*, 2018).

The TCA cycle, also known as the citric acid cycle or Krebs cycle, takes place in mitochondrial matrix and its main function is to produce reduced nicotinamide adenine dinucleotide (NADH) as electron donor for the respiratory chain. Several studies have also uncovered the role of TCA cycle as a source of metabolic intermediates that acts as signaling molecules and as building blocks of synthesis for cellular components (Osellame *et al.*, 2012).

Before entering the TCA cycle, energy-rich nutrients, such as sugars, fats and proteins are metabolized to acetyl-coenzyme A (acetyl-CoA). Regarding to sugars, they enter the mitochondria as pyruvate, after undergoing glycolysis in the cytosol, where they are converted to acetyl-CoA by pyruvate dehydrogenase. Fatty acids are converted to acetyl-CoA inside mitochondria by β-oxidation and amino acids are converted in pyruvate, acetyl-CoA or other intermediates by several different enzymes (Bartlett and Eaton, 2004; Maechler *et al.*, 2006; Osellame *et al.*, 2012). The first step of TCA cycle is the transfer of the acetyl group of acetyl-CoA to the four-carbon oxaloacetate, forming citrate. This six-carbon citrate molecule is oxidized back to oxaloacetate, in a series of seven enzymatic steps, with the formation of carbon dioxide, NADH and reduced flavin adenine dinucleotide ($FADH_2$). The oxaloacetate re-enter in a new TCA cycle, while the energy generated is

passed to the mitochondrial electron transport chain by the NADH and $FADH_2$ (Osellame *et al.*, 2012).

The respiratory chain, located in the IMM consist of a series of multisubunit protein complexes and generates an electrochemical gradient across the membrane that is ultimately used to promote ATP production by complex V (ATP synthase) in the final step of OXPHOS (Aretz *et al.*, 2020; Foury *et al.*, 1998).

Electrons from NADH enter the electron transport chain by binding to the largest of the respiratory complexes, NADH dehydrogenase, or complex I. While in mammals the whole complex consists of 45 subunits, in budding yeast NADH is oxidized by an internal NADH:ubiquinone oxidoreductase, also called internal NADH dehydrogenase (Bakker *et al.*, 2001). The two electrons donated by NADH are initially transferred to a flavin mononucleotide prosthetic group and then through a series of iron-sulfur clusters to coenzyme Q. The passage of electrons from NADH to complex I is accompanied by the translocation of four protons across the IMM.

Coenzyme Q, also called ubiquinone, is a small lipid soluble redox molecule carrier that can freely diffuse through the mitochondrial membrane to donate its electrons to the complex III, cytochrome *c* reductase. This enzyme, the smallest of the electron transport complexes, oxidizes coenzyme Q and transfer the electrons to two molecules of cytochrome *c*, a water-soluble redox protein bound to the outer face of the IMM that also plays a well-known role in apoptosis (Ow *et al.*, 2008). Linked to the oxidation of coenzyme Q, two protons are deposited in the IMS and an additional two protons are translocated from the mitochondrial matrix. In complex IV, or cytochrome *c* oxidase (COX), the electrons are finally used in the production of two H_2O molecules from one O_2 molecule. Alongside this reaction, four protons are translocated from the mitochondrial matrix (Liu *et al.*, 2011; Osellame *et al.*, 2012).

A distinct protein complex, entirely encoded by nuclear DNA, known as succinate dehydrogenase or complex II, is responsible for the reduction of FAD to $FADH_2$ in the TCA cycle and is itself part of the electron transport chain. The electrons from succinate are transferred to FAD and then to coenzyme Q and to complexes III and IV, as described above (Zhou *et al.*, 2011).

The free energy derived from the passage of the electrons is the power source for the pumping of protons against their concentration gradient through complexes I, III and IV. The redox reactions coupled to proton transfer from the matrix to the IMS generates a proton motive forced composed of a pH and electrical differential across the membrane. The potential energy stored in this electrochemical gradient is then harvested and used for ATP synthesis (Rich, 2003). This coupling mechanism was first proposed by Peter Mitchell in 1961 (Mitchell, 1961), resulting in their award of the 1978 Nobel Prize in Chemistry. The

fifth protein complex, responsible for coupling the energetically favorable flow of proton to the synthesis of ATP in the final step of OXPHOS, is ATP synthase or complex V (Osellame *et al.*, 2012).

Mitochondrial ATP synthase is a complex formed by 15-18 subunits and is encoded by both nuclear and mitochondrial genomes. It consists of two domains – the F_o domain embedded in the IMM and a soluble hydrophilic F_1 domain that projects into the mitochondrial matrix – giving the enzyme its alternate name of F_oF_1 ATPase (Nakamoto *et al.*, 2008). The water-soluble F_1-domain is composed of three α and three β subunits. These subunits are arranged alternately and the catalytic sites that bind adenosine diphosphate (ADP) and inorganic phosphate (Pi) are in the β subunits. The F_1-domain is connected to the membrane-embedded ring-like subunit c oligomer of the F_0-domain by a central (formed by γ, δ and ε subunits) and a peripheral (formed by OSCO, b, d and F6 subunits) stalk. The yeast enzyme has two additional subunits, i and k, which belong to the membrane part. As protons cross the membrane via the proton channel in the membrane part, the rotor turns inside the $\alpha\beta$ trimer of the F_1-domain. As the rotating stalk passes each binding site, conformational changes are induced that catalyzes ATP synthesis, resulting in 3 ATP molecules by each turn (Nakamoto *et al.*, 2008; Osellame *et al.*, 2012). This mechanism was first described by Paul Boyer and John Walker, for which they were awarded the Nobel Prize in Chemistry in 1997.

In addition to proton leakage uncoupling the membrane from ATP production, electron leakage also occurs across the electron transport chain complexes. Rather than being passed to oxygen to form water at complex IV, premature leakage of electrons allows their reaction with oxygen to form the superoxide anion radical ($O_2^{\bullet -}$). Superoxide is a highly reactive molecule and can damage proteins, lipids, and DNA. Superoxide produced by mitochondria is a major cause of cellular oxidative distress that may underlie many pathologies and aging (Brand *et al.*, 2004; Osellame *et al.*, 2012). However, superoxide radicals can be converted by superoxide dismutases into hydrogen peroxide, which at low levels acts as a redox signaling molecule in physiological oxidative stress responses to promote health, a condition known as oxidative eustress (Sies, 2017).

1.2. Mitochondrial morphology

Mitochondria are highly dynamic organelles and depending on the cell type and metabolic requirements can have different morphologies, from small spheres to long tubules. The two interconverting forms are balanced by the opposing processes of fusion and fission. The importance of fission and fusion homeostasis has been highlighted by the

association of proteins that regulate mitochondrial dynamics with neurodegenerative and neurological disorders (Palmer *et al.*, 2011).

During mitochondrial fusion, two individual mitochondria can encounter each other and merge both their OMM and IMM resulting in a single and larger mitochondrion. Conversely, a mitochondrion can divide by fission into two or more smaller mitochondria (Detmer and Chan, 2007; Roy *et al.*, 2015). This equilibrium is crucial to the maintenance of normal mitochondrial functions. Fusion is important for mixing mitochondrial contents and maintaining electric conductivity throughout the mitochondria (Hoppins, 2014). In contrast, mitochondrial fission maintains the number of mitochondria in proliferating cells and ensures the elimination of damaged mitochondria through a process called mitophagy (Elgass *et al.*, 2013; Hoppins, 2014).

The main regulators of mitochondrial dynamics, the dynamin-related GTPases, were first identified in model organisms. The first fusion component, *fuzzy onions* (Fzo), was identified in *Drosophila melanogaster* (Hales and Fuller, 1997) and led to the discovery of mitofusion homologs in yeast (Fzo1p) (Rapaport *et al.*, 1998) and mammals (Mfn1 and Mfn2) (Santel and Fuller, 2001), components of the OMM. Generally, the fusion of two mitochondria involves three steps: the tethering of mitochondria; the increasing of the contact surface area and the decreasing of the distance between the two membranes; and the fusion of the two outer membranes due to GTP-dependent conformational change (Tilokani *et al.*, 2018). The fusion of the IMM occurs downstream and is mediated by Mgm1p (Opa1 in mammals) (Tilokani *et al.*, 2018; Wong *et al.*, 2003). The opposite process is mediated by dynamin-related protein Dnm1p (Bleazard *et al.*, 1999; Sesaki and Jensen, 1999) (Drp1 in mammals), which was identified together with its receptor Fis1p using yeast genetics (Mozdy *et al.*, 2000). Dnm1p is a cytosolic protein that once activated is translocated to the OMM, multimerizes and creates a ring-like structure that constricts and divides the organelle, in a GTP-dependent manner (Tilokani *et al.*, 2018).

2. Cell cycle

The eucaryotic cell cycle is a highly conserved process and comprises two main phases: interphase and M phase. Interphase is the longest period and consists of three distinct stages: G1, S and G2 phases. The shorter period known as M phase involves the mitosis (nuclear division) and cytokinesis (cell division) (reviewed in (Murray, 2004)). In budding yeast, cell division is asymmetric, yielding a large mother cell and a small daughter cell. The budding is initiated when the mother cell reaches a critical size, starting at same time as DNA replication. To allow bud formation and nucleus migration to the bud neck, the duplication of the spindle pole bodies, and the reorganization of the microtubules occur

early in the yeast cell cycle, which lacks a clear definition between G2 and M phases (Forsburg and Nurse, 1991). In addition to DNA replication, other biosynthetic processes take place to achieve two-fold increases of all the other cell components, including organelles (Johnston *et al.*, 1977).

The progression through the different phases is regulated by the interaction of cyclin-dependent kinases with their activating subunits, the cyclins. Cyclins are unstable proteins whose protein and transcriptional levels vary periodically through the cell cycle (Sherr and Roberts, 2004). In mammalian cells, D-type cyclins regulate G1 phase, E-type cyclins regulate G1/S transition, A-type cyclins regulate S phase and G2 and B-type cyclins regulate M phase. In budding yeast, the cyclin-dependent kinase Cdc28p is the main regulator of the cell cycle as, in addition controlling mitotic commitment, it controls bud initiation, DNA replication, spindle formation and chromosome separation (Mendenhall and Hodge, 1998). The association of Cdc28p with two families of cyclins, the G1 cyclins (Cln1-3) and the B-type cyclins (Clb1-6) provide substrate specificity through the different phases (Sherr and Roberts, 2004).

To maintain the order, integrity and fidelity of the cell cycle, the cells developed control mechanisms known as cell cycle checkpoints. In the presence of defects or unfavorable conditions, inhibitory signals are produced resulting in a reversible cell cycle arrest mainly by the inhibition of cyclin-Cdk complexes (Salazar-Roa and Malumbres, 2017). For instance, if the nucleus fails to translocate into the bud during anaphase, the Mitotic Exit Network (MEN), a Ras-like GTPase signal transduction cascade, prevents activation of the essential Cdc14p and cells arrest in anaphase without exiting mitosis (Bardin *et al.*, 2000). In addition, a START checkpoint, found in late G1 phase, allows yeast to commit to the cell cycle and start DNA replication, or if conditions are not favorable, e.g. due to nutrients limitation, arrest the cell cycle and enter a stationary or G0 phase (Werner-Washburne *et al.*, 1993).

2.1. Anaphase-promoting complex/Cyclosome

The anaphase-promoting complex or cyclosome (APC/C) is a large multi-subunit cullin-RING E3 ubiquitin ligase that drive the cell cycle by tagging key regulators with polyubiquitin chains, promoting their destruction by the 26S proteosome (reviewed in (Peters, 2006; Pines, 2006; Thornton and Toczyski, 2006)). APC/C also plays a role to regulate meiosis and has been implicated in post-mitotic functions, including metabolic functions (Almeida *et al.*, 2010; Colombo *et al.*, 2010).

The first structural analysis of APC/C was obtained by cryo-EM from human cells (Gieffers *et al.*, 2001), *Xenopus laevis* egg extracts (Dube *et al.*, 2005) and budding yeast

(Passmore *et al.*, 2005). In all three cases, APC/C is an asymmetric triangular complex composed of an outer wall that encloses an internal cavity. In most eukaryotes, APC/C comprises 13 different subunits, most of which are highly conserved and essential for activity. These subunits are arranged in two large domains, known as 'platform' and 'arc lamp'. The 'platform' contains the catalytic core (APC2 and APC11) and the 'arc lamp' provides a scaffolding element and a binding site for the coactivator/substrate (Bodrug *et al.*, 2021).

In addition to E2 enzymes, APC/C activity is dependent on one of several coactivators that associate transiently with APC/C at specific periods of cell cycle. The best-known coactivators are Cdc20p and Cdh1p, which are encoded by all eucaryotic genomes (Peters, 2006). These coactivators are characterized by the presence of sequence elements that mediate APC/C binding, namely N-terminal C-box (Schwab *et al.*, 2001) and C-terminal Ile-Arg motifs (IR-tail) (Passmore *et al.*, 2003; Vodermaier *et al.*, 2003). Additionally, APC/C co-activators contain a C-terminal WD40 domain that is believed to recognize APC/C substrates by interacting with specific recognition motifs in these substrates (Kraft *et al.*, 2005).

Substrate recognition by the APC/C is based on two distinct recognition signals that are present in most APC/C substrates in one or more copies. The best-defined is the destruction box (D-box), a nine-residue motif (RxxLxxxxN), first characterized in B-type cyclins (Glotzer *et al.*, 1991). Another APC/C degron, the KEN box (KENxxxN) (Pfleger and Kirschner, 2000) is often present in APC/C substrates usually in addition to the D-box. The recognition of two distinct degrons contributes to substrate specify, with Cdc20 being more dependent on the D-box and Cdh1p more dependent on the KEN box (Burton and Solomon, 2001; Pfleger *et al.*, 2001). However, D- and KEN boxes are often found in substrates of both Cdc20 and Cdh1.

The interaction between APC/C and coactivators is tightly regulated to ensure that APC/C substrates are targeted for degradation at the correct time during cell cycle. Cdc20 can only associate efficiently with APC/C in mitosis after the phosphorylation of several APC/C subunits by the mitotic kinases Cdk1 and Plk1 (Kramer *et al.*, 2000; Rudner and Murray, 2000). At metaphase, APC/C-Cdc20 facilitates sister-chromatid separation by destruction of securin (Cohen-Fix *et al.*, 1996; Waizenegger *et al.*, 2000) and initiates degradation of cyclins, decreasing the activity of Cdks (Clute and Pines, 1999; Shirayama *et al.*, 1999).

By contrast, Cdk1-dependent phosphorylation of Cdh1 prevents its binding to APC/C (Kramer *et al.*, 2000; Zachariae *et al.*, 1998), limiting APC/C-Cdh1 activity to late mitosis and G1 when Cdk activity is low and protein phosphatases like Cdc14p in yeast remove the phosphates (Visintin *et al.*, 1998). APC/C-Cdh1 is responsible for the degradation of a

broader substrates than APC/C-Cdc20, including spindle-associated proteins, mitotic cyclins and kinases and the coactivator Cdc20 (Peters, 2006). In budding yeast, it was also reported that, in addition to regulate the binding to APC/C, Cdk-dependent phosphorylation cause nuclear export of Cdh1p (Jaquenoud *et al.*, 2002). Since APC/C subunits and Cdc20 were detected within the nucleus (Jaquenoud *et al.*, 2002; Shirayama *et al.*, 1998; Zachariae *et al.*, 1996), it is assumed that ubiquitination by APC/C occurs in the nuclear compartment and that Cdh1p export inactivates the APC/C at G1/S transition. However, in yeast several APC/C-Cdh1p substrates are found both inside and outside the nucleus, such as the polo kinase Cdc5p (Charles *et al.*, 1998; Lee *et al.*, 2005) and the cyclin Clb2p (Hood *et al.*, 2001; Schwab *et al.*, 1997) or even reside exclusively outside the nucleus, such as Iqg1p (Epp and Chant, 1997; Ko *et al.*, 2007) and Hsl1p (Barral *et al.*, 1999; Burton and Solomon, 2000). Further work is necessary to clarify whether APC/C-Cdh1 may be active in the cytoplasm.

3. Coordination between mitochondria and cell cycle in budding yeast

3.1. Mitochondrial inheritance during cell division

Mitochondrial inheritance, the transfer of mitochondria from the mother to the daughter cell during cell division, is essential for daughter cell viability, as mitochondria are self-replicating and cannot be formed *de novo*. The mitochondrial movement and distribution during cell cycle progression reveals an intimate and coordinated interplay between these processes (Figure 1.1). Early in the cell cycle (at the beginning of the S phase), mitochondria align along polarized actin cables that extend from the mother cell into the bud, and a portion of the mitochondrial network is transported into the growing bud (Boldogh *et al.*, 2001). Mitochondria, like most organelles, are transported into the bud by Myo2p, a processive type V myosin motor, which binds to mitochondria via the Rab-type GTPase, Ypt11p, and the mitochondrial membrane protein, Mmr1p, and walks them along actin cables (Chernyakov *et al.*, 2013). Post-transport, Mmr1p also anchors mitochondria at the bud tip (Swayne *et al.*, 2011). Simultaneously, a portion of the mitochondrial network is anchored to the cell cortex of the mother cell by the Num1p and Mdm36p tethers (Klecker *et al.*, 2013; Lackner *et al.*, 2013) or the mitochondrial F-box protein Mfb1p (Pernice *et al.*, 2016), ensuring about half the mitochondria is retained in the mother cell. During S and G2 phases, mitochondria continue a poleward movement toward the bud at a constant rate as it enlarges (Simon *et al.*, 1997). Mitochondria also grow with the growing cell until a set-point of mitochondria volume relative to size is reached (Rafelski *et al.*, 2012). After cytokinesis, mitochondria are released from the poles of the dividing cells and distributed throughout the cytoplasm (Boldogh *et al.*, 2001). This precise coordination of mitochondrial

inheritance with cell cycle events suggests a common regulatory mechanism. Transcriptional regulation may be involved as distinct transcriptome studies showed that *MMR1*, *YPT11* and *NUM1*, which encode Myo2p adaptors, are differentially expressed as a function of the cell cycle (Campbell *et al.*, 2020; Granovskaia *et al.*, 2010; Orlando *et al.*, 2008; Spellman *et al.*, 1998). Remarkably, several other genes affecting mitochondrial inheritance, many of unclear function named Altered Inheritance rate of Mitochondria (AIM) were also found to oscillate with the cell cycle. The most consistently altered AIMs among the different studies include *AIM20*, *AIM32*, *AIM44* and *AIM17* (Campbell *et al.*, 2020; Granovskaia *et al.*, 2010; Orlando *et al.*, 2008; Spellman *et al.*, 1998). Analysis of the role of these genes during cell cycle will certainly aid in the elucidation of the coordination between mitochondria inheritance and cell division. This coordination is also likely achieved by post-translational modifications (PTMs), since mitochondrial transport into the bud, but not bud emergence, is delayed in the absence of the type 2C protein phosphatase Ptc1p (Roeder *et al.*, 1998).

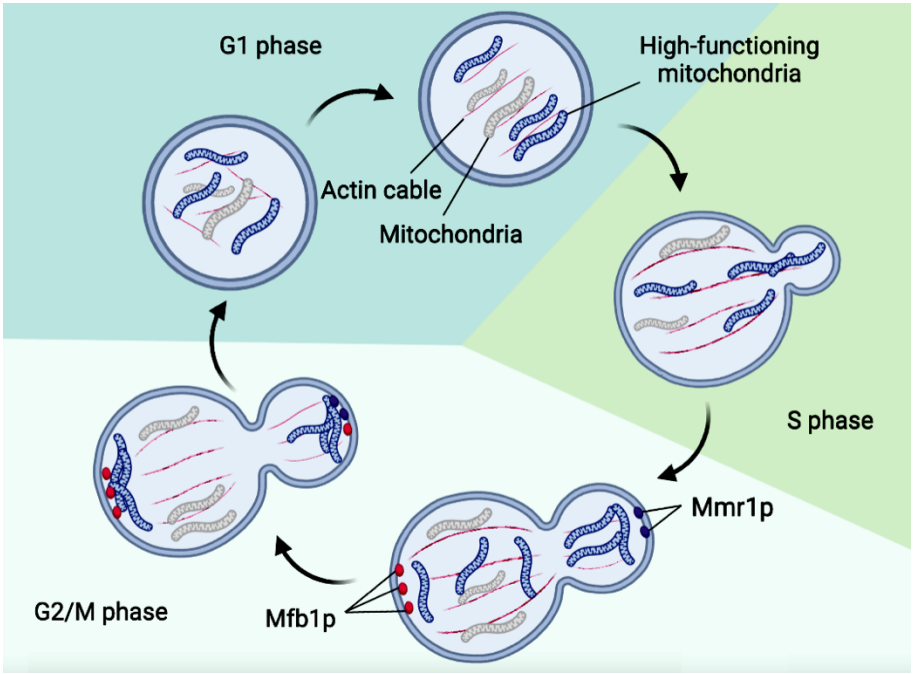

Figure 1.1. Mitochondrial inheritance during cell division. During G1 phase, mitochondria align along polarized actin cables (in red). During bud growth in the S and G2 phases, mitochondria move from mother to daughter cell. Healthier mitochondria (blue tubules) are preferentially retained at the tip of the mother cell and at the bud tip. After cytokinesis, mitochondrial are released from the poles and redistributed in the dividing cells (see text for more details).

Although bud emergence and organelle inheritance are cell cycle-linked, arresting cell cycle progression does not block these processes (Li *et al.*, 2021; Yang *et al.*, 1999). This indicates that bud emergence and mitochondrial inheritance are triggered at certain cell cycle phase but are not dependent on cell cycle progression to completion once triggered.

Mitochondrial inheritance relies on mitochondrial transport and membrane anchoring processes, but also on the mitochondrial fusion and fission machinery. In yeast, the main regulators of mitochondrial fusion are Fzo1p, Mgm1p and Ugo1p, which facilitate OMM and IMM fusion cooperatively. Mitochondrial fission, the opposite process, is mediated by cytosolic Dnm1p, which is recruited to sites of mitochondrial fission by Fis1p, Caf4p and Mdv1p to form a distinctive constriction ring (Westermann, 2010). In mammalian cells, the regulation of mitochondrial fission by cell cycle machinery is well established. Cdk1-regulated Drp1 stimulates mitochondrial fission in mitosis, facilitating mitochondrial portioning during cell division (Horn *et al.*, 2011; Taguchi *et al.*, 2007) (see section 4). In budding yeast, mitochondrial networks are more interconnected than in mammalian cells (Viana *et al.*, 2020) and there is no evidence of mitochondrial fragmentation at any phase of the cell cycle. On the contrary, mitochondria are primarily a single continuous reticulum during undisturbed cell cycle progression. Nevertheless, mitochondrial fusion machinery plays a role in mitochondrial inheritance in budding yeast, since the maintenance of a fused mitochondria is important for mitochondrial transport across the bud neck and for retention in the mother cell (Böckler *et al.*, 2017; Higuchi-Sanabria *et al.*, 2016). The absence of the core fusion components, Fzo1p or Mgm1p, promotes not only mitochondrial fragmentation but also significant mitochondrial inheritance defects. For instance, deletion of *FZO1* results in a 60% decrease in mitochondria in the bud (Böckler *et al.*, 2017; Higuchi-Sanabria *et al.*, 2016). Mitochondrial fusion may be indirectly controlled by cell cycle signaling since Cdc28p phosphorylates the mitochondrial protein import machinery at the M phase, favoring Mgm1p import and increasing its abundance (Harbauer *et al.*, 2014).

Although mitochondrial morphology seems unaltered during regular cell division, in some setting it is affected by cell cycle progression. For instance, in aged cells, an oscillatory behavior of mitochondrial dynamics occurs in coordination with cell cycle progression. Aged cells exhibit a transient formation of mitochondrial clusters upon budding, whose purpose is unclear but hypothesized to play a role in the asymmetric inheritance of less fit mitochondria (Fehrmann *et al.*, 2013) (see section 3.2). In addition, during yeast meiosis for gamete formation (sporulation), mitochondria are arranged around the meiotic nucleus in a very specific pattern (Miyakawa *et al.*, 1984). It was recently found that this mitochondrial remodeling at meiosis is due to the regulation of the mitochondrial plasma membrane anchoring through the destruction of the tethers Num1p and Mdm36p. Interestingly, Num1p and Mdm36p are phosphorylated and consequently degraded by the meiosis-specific kinase Ime2p (Sawyer *et al.*, 2018). This implies that mitochondrial remodeling in meiosis is directly regulated by the cell cycle signaling.

3.2. Mitochondrial quality control during cell division

In budding yeast, a mother cell can produce only a limited number of daughter cells before it stops dividing. Independently of the replicative age of the mother, each bud is born young, as a consequence of asymmetric yeast cell division. Segregation of aging determinants, such as lower functioning mitochondria, to the mother cell is vital for overall fitness and survival of the growing colony (McFaline-Figueroa *et al.*, 2011). Mitochondria that are anchored in the bud tip and destined for inheritance by the daughter cell were shown to have lower levels of reactive oxygen species (ROS) and oxidative damage, a more-reducing redox potential and a higher mitochondrial membrane potential ($\Delta\psi$) than mitochondria in mother cells (Higuchi *et al.*, 2013; Lai *et al.*, 2002; McFaline-Figueroa *et al.*, 2011). A mechanism controlling the quantity, in addition to the quality, of mitochondria inherited by the bud seems also to be in place. Though the mitochondria-to-cell size ratio decreases in aging mother cells, buds always attain the same ratio (Rafelski *et al.*, 2012).

The mechanism that favors the partitioning of the fittest mitochondria to daughter cells is not completely understood, but it appears to involve actin dynamics and the mitochondria anchorage machinery. Actin cables, which are F-actin bundles that serve as tracks for anterograde and retrograde cargo movement, undergo retrograde flow that is driven, in part, by actin polymerization and assembly (Yang and Pon, 2002). To be transported into the bud, the mitochondria must overcome the retrograde flow of the actin cables. Well-functioning mitochondria are apparently more mobile and thus will preferentially move into the bud, contributing to the bud asymmetric inheritance of the fittest mitochondria (Higuchi *et al.*, 2013). Anchorage of mitochondria is vital for inheritance of the organelle by buds and its retention in mother cells. Since actin cables undergo retrograde flow, anchorage of mitochondria in the bud tip ensures that the organelle is retained in the daughter cell. Mmr1p, the adaptor that facilitates actin-based transport of mitochondria to the bud (Itoh *et al.*, 2004), was later found to contribute to anchorage of the fittest mitochondria to the bud tip. Upon deletion or overexpression of *MMR1*, the asymmetric inheritance of qualitatively different mitochondria is lost (McFaline-Figueroa *et al.*, 2011). The F-box protein, Mfb1p, also contributes to the anchorage of high-functioning mitochondria in the bud in a cell cycle-regulated manner (Pernice *et al.*, 2016). Mfb1p tethers mitochondria at the mother tip throughout the cell cycle but in late M phase its levels at the bud tip increase. As cells progress towards cytokinesis, Mfb1p contributes to the anchorage of high-functioning mitochondria at the bud (Pernice *et al.*, 2016). Mbf1p association to mitochondria in the bud may be regulated by proteolysis by Skp1p (Kondo-Okamoto *et al.*, 2006), an essential component of the SKP1-CUL1-F-box (SCF) protein ubiquitin ligase complex, which mediates the ubiquitination and degradation of several key cell cycle regulatory proteins for

cell cycle progression (Petroski and Deshaies, 2005). Unexpectedly, Mfb1p also contributes to the retention of a population of higher functioning mitochondria in the mother cell tip, suggesting Mfb1p prevents depletion of all high-functioning mitochondria from mother cell (Pernice *et al.*, 2016).

Mitochondrial dynamics also plays a role in mitochondrial quality control. While, as referred before, fusion is important for mitochondrial accumulation at the bud tip, fission seems to play a role in the segregation of the fittest mitochondria to the bud. Deletion of *DNM1*, encoding for a mitochondrial fission protein, results in a single continuous reticulum of mitochondria and leads to loss of the asymmetry in mitochondrial $\Delta\psi$ between mother and daughter cells. On the other hand, deletion of genes encoding for mitochondrial OMM or IMM fusion proteins (Fzo1p and Mgm1p), which cause mitochondrial fragmentation, improve the segregation of high $\Delta\psi$ mitochondria to the bud (Higuchi-Sanabria *et al.*, 2016). Notably, Dnm1p levels exhibit cell cycle oscillations, with a peak at G2/M (Campbell *et al.*, 2020). Since Mfb1p levels at the bud also increases at mitosis, it suggests the segregation of the fittest mitochondria to the bud may predominantly occur late in the cell cycle.

It is not clear how qualitatively different mitochondria are identified and selected for anchorage. Regarding Mfb1p, this protein does not seem to actively sense mitochondrial function since its localization or function in mitochondrial anchorage is not affected by treatments that induce mitochondrial oxidation or a drop in $\Delta\psi$ (Pernice *et al.*, 2016).

Interestingly, the localization of Mfb1p during division depends on the correct asymmetric inheritance of spindle microtubules-organizing centers (MTOCs). In yeast, the pre-existent (old) spindle pole body (SPB) segregates towards the daughter cell, whereas the newly synthetized SPB is retained by the mother. Inverting MTOC fate affects the localization of Mfb1p and abolishes the asymmetric segregation of functionally distinct mitochondria between the mother and daughter cells. This reinforces that the control of mitochondrial quality is intrinsically linked with cell cycle processes (Manzano-López *et al.*, 2019).

3.3. mtDNA replication and inheritance

Mitochondrial function in respiratory metabolism requires expression of the mitochondrial genome. The mtDNA must, therefore, be faithfully inherited to prevent propagation of respiratory-incompetent mitochondria. Unlike nuclear DNA, the replication of mtDNA in yeast is not strictly coupled with the cell division cycle but occurs continuously and arresting the cell cycle does not prevent mtDNA replication (Conrad and Newlon, 1982; Newton and Fangman, 1975). In fact, although the mtDNA copy number can change in response to physiological conditions, mtDNA synthesis is mostly coupled to cell growth

(Conrad and Newlon, 1982). In yeast, mtDNA copy number was found to correlate linearly with the size of the mitochondrial network (Osman *et al.*, 2015), which in turns correlates with cell volume (Rafelski *et al.*, 2012), suggesting that mtDNA is linked to cell volume and not determined by cell cycle events. Notwithstanding, the amount of mtDNA seems to influence nuclear replication. The mtDNA is organized as DNA-protein complexes termed nucleoids that distribute throughout the mitochondrial network (Miyakawa, 2017). Although the segregation of mt-nucleoids into daughter cells is dependent on the movement of mitochondrial structures, these two events are not necessarily coupled. In fact, mtDNA is actively transported into the bud by a yet poorly characterized nucleoid segregation apparatus. Abf2p is one of the most important proteins involved in the nucleoid organization and maintenance. Cells lacking Abf2p exhibit impaired mtDNA inheritance and altered nucleoid morphology (Zelenaya-Troitskaya *et al.*, 1998). Moderate overexpressing of Abf2p, which elevates the amount of mtDNA by 50-150%, also accelerates nuclear DNA replication and overall cell proliferation (Blank *et al.*, 2008). The cells exhibit a shortened G1 phase due to acceleration of START. The accelerated cell cycle commitment is dependent on active respiration since it is lost when Abf2p is overexpressed in respiratory incompetent (*rho*$^{-}$) cells (Blank *et al.*, 2008). Also hinting to a common regulation of mtDNA and nuclear DNA are the observation made on the proteasomal lid subunit Rpn11p. It was found that a conditional mutation in Rpn11p leads to over-replication of both mitochondrial and nuclear DNA, associated to mitochondrial dysfunction and cell cycle arrest (Rinaldi *et al.*, 1998). In addition to its role in the proteasome, Rpn11p was later found to be involved in mitochondrial dynamics (Rinaldi *et al.*, 2008). This suggests that, similarly to Abf2p, Rpn11p may primarily affect mtDNA replication, which then positively influences nuclear replication. While increased mtDNA accelerates entry into S phase, the opposite also holds true, with the absence of mtDNA leading to a delay in G1 to S phase transition (Crider *et al.*, 2012).

In addition, several observations suggest that mtDNA stability/inheritance can by jointly regulated with nuclear stability. The first evidence emerged with the characterization of cell division cycle (cdc) mutants. Two temperature sensitive cdc mutants, *cdc5* and *cdc27*, were shown to have a defect in the acquisition of both nuclear and mitochondrial DNA when incubated at restrictive temperature (Dutcher, 1982). Cdc5p is a polo-like kinase and Cdc27p is a subunit of the ubiquitin-protein ligase APC/C, both playing essential function in mitosis (Botchkarev and Haber, 2018; Zachariae and Nasmyth, 1999). Cdc28p, the essential component of the cell cycle oscillator, also affects mitotic transmission of both nuclear and mitochondrial DNA. Cells bearing the *cdc28-srm* mutation, a non-temperature sensitive mutation, have reduced rates of spontaneous *petite* formation and simultaneously affects the maintenance of the yeast chromosomes and plasmids. In addition, the *cdc28-*

srm allele also leads to a decreased sensitivity of yeast cells to the mutagenic action of ethidium bromide (Devin *et al.*, 1990). This effect on the mutability of the mtDNA was also found for a conditional *cdc28-1* mutant at permissive or semi-permissive temperatures (Koltovaya *et al.*, 1998). Two other proteins, Net1p and Hfi1p, are also involved in chromosome maintenance and the formation of mitochondrial lesions. Net1p is a component of the RENT complex and plays a role in the regulation of the mitotic exit (Visintin *et al.*, 1999). The reason why nuclear and mitochondrial DNA stability are coupled in these cell cycle mutants remains unexplained, but it suggests a common regulatory mechanism. Loss of proteins with a role in mitochondrial function or morphology, such as Mdm1p, Mdm10p, Mdm12p and Erv1p, which were shown to impair mtDNA inheritance, also hinder nuclear inheritance with a cdc phenotype (García-Rodríguez *et al.*, 2009; Lisowsky, 1994; McConnell *et al.*, 1990). In the cases of Mdm10p and Mdm12p, loss of mtDNA was reported to be the primary defect that hinder nucleus inheritance due to the activation of a cell cycle checkpoint (Crider *et al.*, 2012; García-Rodríguez *et al.*, 2009) (see section 3.4). It will be interesting to assess if a similar activation of a mitochondrial checkpoint occurs in the remaining mutants.

Recently, novel findings shed new light on the integration of mitochondrial and nuclear inheritance. In addition to anchoring mitochondria to the cell cortex, as referred above, Num1p clusters also function as a cortical anchor for dynein, where it contributes to orient the mitotic spindle and nuclear segregation (Heil-Chapdelaine *et al.*, 2000). In cells with impaired mitochondrial inheritance due to a double mutation in the mitochondrial Myo2p adapters, Mmr1p and Ypt11p, Num1p clusters fail to assemble in the bud. Since Num1p clusters also serve to anchor dynein to the plasma membrane, defects in the mitochondrial-driven assembly of Num1p lead to defects in dynein-mediated spindle positioning (Kraft and Lackner, 2017).

These results provide a mechanism leading to an integrated positioning and inheritance of mitochondria and nucleus during the cell cycle (Anderson *et al.*, 2022; Kraft and Lackner, 2017) and may explain joint defects in mitochondrial and nuclear inheritance. Interestingly, the mitochondrial fission protein Fis1p, which plays a role in mitochondrial morphology and mtDNA stability (Rapaport *et al.*, 1998), also affects spindle formation (Estela *et al.*, 2011). Deletion of *FIS1* leads to the formation of aberrant shorter mitotic spindles during cell division and results in an increased number of cells with undivided nucleus in the bud neck. In agreement with these defects, the *fis1* mutant exhibits a G2/M phase delay (Estela *et al.*, 2011). These data point for a previous unsuspected role of mitochondria in spindle positioning/formation in yeast that certainly warrants further investigation.

3.4. Mitochondrial checkpoint?

The primary function of a checkpoint is to ensure that critical events during nuclear inheritance occur with fidelity and at the correct time as cells divide. Upon detection of an error, such as DNA damage or a failure of spindle assembly, these checkpoints block progression of the cell cycle, promote repair of the error, and allow for cell cycle progression after the problem has been corrected.

As mitochondria are essential for yeast survival, they must be faithfully inherited. The proteins Mdm10p, Mdm12p and Mmm1p form a complex required for mitochondria movement, inheritance and morphology (Boldogh *et al.*, 2003). The deletion of these genes results in an impaired mitochondrial inheritance and defective cytokinesis, leading to a multi-budded phenotype (García-Rodríguez *et al.*, 2009). Inhibition of cytokinesis was found to occur due to a MEN-linked checkpoint (García-Rodríguez *et al.*, 2009). MEN is an essential signaling pathway that contributes to the release and activation of the phosphatase Cdc14p, which in turn promotes mitotic exit and initiates cytokinesis (Stegmeier and Amon, 2004; Surana *et al.*, 2002). In *mdm10*Δ cells, alteration in MEN signaling leads to a delay in the release of Cdc14p from the nucleolus and inhibition of cytokinesis and contractile ring closure. It was thus proposed that severe defects in mitochondrial inheritance trigger a regulatory system involving MEN that inhibits cytokinesis and halts cell cycle progression. In accordance with its surveillance role, disturbing the MEN-linked checkpoint was found to result in defects in mitochondrial portioning (García-Rodríguez *et al.*, 2009).

Curiously, the *rpn11-m1* mitochondrial morphology defect (see section 3.3) is suppressed by overexpression of Cdc14p (Esposito *et al.*, 2011). Cdc14p overexpression also alleviates the mitochondrial morphology defect caused by deficiency in Mmm2p/Mdm34p (Esposito *et al.*, 2011), which are involved in anchoring of mitochondria to the actin cytoskeleton and maintenance of mtDNA nucleoids (Youngman *et al.*, 2004). These results suggest that Cdc14p relays on mitochondrial defects but also has an active role in mitochondrial regulation.

However, not all mutants resulting in severe inheritance defects trigger a cell cycle arrest. In a Myo2p conditional mutant, the inheritance of mitochondria into buds is inhibited but cytokinesis is able to progress normally, producing unviable daughters without mitochondria (Chernyakov *et al.*, 2013). This suggests that the activation of the mitochondrial checkpoint may be more complex than assumed and it is not simply the absence of mitochondria that is sensed. As an alternative, Myo2p may play a role in the sensing of mitochondrial inheritance defects or in the activation of the checkpoint, and the checkpoint is not activated in mutated Myo2p cells. Further studies are necessary to elucidate this matter.

Adding complexity to this topic, distinct checkpoints may be triggered by different mitochondrial defects. Indeed, defects in mtDNA do not affect the above discussed cytokinesis checkpoint, but it seems to trigger a distinct checkpoint at the G1 to S phase transition (Crider *et al.*, 2012). Absence of mtDNA in buds inhibits G1 to S phase transition in about half of the cells, and this is not a consequence of loss of mitochondrial respiration, since cells containing mtDNA with no coding information exhibit wild-type cell cycle progression. It seems this checkpoint monitor the amount of inherited mtDNA itself and not the loss of genes encoded by mtDNA. Notably, the mtDNA inheritance checkpoint is dependent on Rad53p (Crider *et al.*, 2012), a protein kinase involved in the arrest at G1 to S phase transition in response to nuclear DNA damage (Allen *et al.*, 1994). This suggests a temporal and mechanistic coordination in monitoring fidelity of nuclear and mitochondrial DNA during cell cycle progression. Curiously, Rad53p itself plays a role in mtDNA stability (O'Rourke *et al.*, 2005) and regulation of mtDNA copy number (Taylor *et al.*, 2005). It is possible that reduced mtDNA levels activate Rad53p, which delays START while stimulating mtDNA replication.

Several more mutants with dysfunctional mitochondria exhibit cell cycle arrest, by mechanisms that remain to be delineated. However, they are suggestive of a mitochondrial checkpoint. For instance, a strain carrying mutations in both *GCS1* and *SED1* loses mtDNA at high rates and is defective for re-entry into the mitotic cell cycle from stationary phase (Drebot *et al.*, 1987).

Pam16p, a subunit of the import motor (PAM complex), is required for preprotein translocation into the mitochondrial matrix. In cells expressing a temperature-sensitive allele (*pam16-I61N*), incubation at non-permissive temperatures causes abnormal mitochondria morphology and respiratory defects that are also accompanied by a G1 cell cycle arrest (Short *et al.*, 2012).

Upon deletion of the cardiolipin synthase gene *CRD1*, cells lose mtDNA leading to a G2/M arrest. The cell cycle defect is due to the upregulation of the protein kinase Swe1p (Chen *et al.*, 2010), a morphogenesis checkpoint protein that regulates the G2/M transition by inhibiting Cdc28p (Booher *et al.*, 1993; Lew, 2003). Interestingly, the expression of *SWE1* is dependent on the mitochondrial retrograde response (Chen *et al.*, 2010). In yeast, activation of the mitochondrial retrograde response, a pathway of communication from mitochondria to the nucleus, allows adaptation to mitochondrial dysfunction (Butow and Avadhani, 2004). The key event is the Rtg2p-mediated translocation of the Rtg1p-Rtg3p transcription factor from the cytoplasm to the nucleus (Sekito *et al.*, 2000). Deletion of *RTG2* or *RTG3* in the *rho*^{0}*cdr1*Δ mutant suppresses the elevated *SWE1* expression, suggesting the retrograde regulation can, at least in some settings, mediate the activation of cell cycle checkpoints.

3.5. Regulation of mitochondrial bioenergetics during the cell cycle

Studies using self-synchronized cycling yeast provided the first evidence that, in addition to mitochondrial inheritance, mitochondrial function could also be synchronous with the cell cycle. Under nutrient-steady growth conditions, cells display metabolic cycles between conditions of high-oxygen consumption and low-oxygen consumption (Klevecz *et al.*, 2004; Tu *et al.*, 2005). This metabolic cycle seems to be partially synchronized with the cell cycle, giving raise to the hypothesis that the restriction of DNA replication to the low-oxygen consumption of the metabolic cycle protects genome integrity (Chen *et al.*, 2007). However, since periodic oxygen consumption was latter observed, even in the absence of cell division (Slavov *et al.*, 2011), it is likely that the observed drastic oscillations in mitochondrial respiration in yeast in continuous culture are not driven by cell cycle progression but intrinsic to the metabolic oscillator.

Nevertheless, several studies point to alterations in mitochondrial function during the cell cycle progression. Transcriptome studies demonstrated that several nuclear-encoded mitochondrial proteins are expressed as a function of the cell cycle. The mitochondrial transcripts correspond to 5 to 16% of all the cell cycle-regulated mRNAs (Blank *et al.*, 2020; Campbell *et al.*, 2020; Cho *et al.*, 1998; Granovskaia *et al.*, 2010; Orlando *et al.*, 2008; Spellman *et al.*, 1998). The mitochondrial periodic transcriptomes show enrichments in processes mainly related to mitochondrial respiration and biogenesis. Regarding protein expression, which is often not predicted by mRNA, mitochondrial proteins correspond to approximately 20% of the total cell cycle-regulated proteins. Similarly to the transcriptome, the mitochondrial proteome suggests cell cycle oscillations in mitochondrial respiration, organization and mitochondrial translation (Blank *et al.*, 2020; Campbell *et al.*, 2020).

In addition, it was shown by quantitative fluorescence microscopy that the mitochondrial volume increases, particularly at G2/M, suggesting that mitochondrial biogenesis increases at this phase, possibly in response to increased energy demands (Campbell *et al.*, 2020). Mitochondrial biogenesis involves the import of nuclear-encoded proteins into mitochondria via a series of complex molecular machines (Schmidt *et al.*, 2011). Presequence-carrying preproteins and most of the noncleavable precursors are imported by the translocase of the outer membrane (TOM) and the translocase of the inner membrane (TIM23), two highly conserved mechanism that constitute the main mitochondrial protein import machineries. The observation that *TOM6* mRNA and Tom6p levels exhibit a moderate increase at G2/M (Spellman *et al.*, 1998) led to the finding that the TOM complex assembly is cell cycle regulated (Harbauer *et al.*, 2014). Importantly, Tom6p is also phophoregulated at G2/M by Cdc28p, which enhances Tom6p efficient import into mitochondria. Phosphorylation of Tom6p promotes the assembly of the TOM core component Tom40p and import of fusion

GTPases, especially Mgm1p, at G2/M phase (Figure 1.2). Recently, Tom5p and Tom22p were also described as periodic proteins (Campbell *et al.*, 2020). Since they are both phosphoregulated, it suggests that several TOM components may potentially be cell cycle regulated. By stimulating mitochondrial biogenesis, the cell cycle-regulation of Tom6p leads to an increase in mitochondrial respiration in mitosis (Harbauer *et al.*, 2014). Interestingly, in mammals, the Cdc28p homologue Cdk1, phosphorylates several subunits of the respiratory complex I at G2/M transition. Regulation of complex I by Cdk1 enhances mitochondrial respiration and ATP production (Wang *et al.*, 2014). This suggests the role of Cdc28p in mitochondrial regulation during cell cycle progression may be conserved.

The observed increase in respiratory activity at G2/M, partially controlled by Cdc28p-dependent phosphorylation of Tom6p supports a cell cycle-dependent regulation of mitochondrial activity (Figure 1.2). Preventing the phosphorylation of Tom6p delays cell cycle progression indicating that enhanced mitochondrial function is important to support cell cycle progression, presumably by helping meet energetics demands. Cell division is one of the cellular processes that requires high energy levels, as it involves the replication of DNA and the entire contents of the cell. However, recent data points for the maintenance of the cell cycle-oscillator controlling mitotic entry and exit as the most energetically costlier process in cell division (Rodenfels *et al.*, 2019). This second hypothesis is more in accordance with the observed increase in yeast mitochondrial activity at G2/M and not during the growth phases.

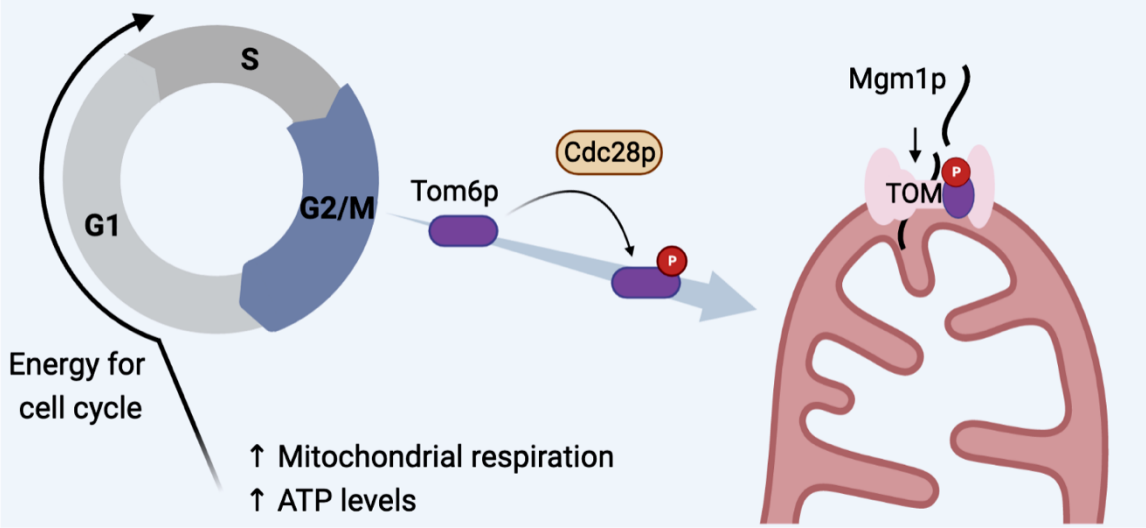

Figure 1.2. Mitochondrial bioenergetics during cell cycle. The phosphorylation of Tom6p (in purple) in G2/M phase enhances the activity of the TOM complex in the mitochondrial outer membrane, promoting protein import, especially Mgmg1p. The regulation of this mitochondrial protein ultimately enhances the respiration-driven energy production by mitochondria, contributing for cell cycle progression (see text for more details).

Although alterations in mitochondrial respiration suggest that ATP production may vary during the cell cycle, studies using an ATP-biosensor in undisturbed live cells showed that the concentration of ATP is maintained fairly at a constant level. Non-significant alterations were found either during cell cycle progression in fermenting or respiring conditions (Takaine *et al.*, 2019).

3.6. Signaling pathways in mitochondria-cell cycle coordination

How is the regulation of mitochondrial function coordinated with the cell cycle? Yeast grows and divide at maximal rates when glucose is available. This requires a coordination between the metabolic regulation and the multiplicity of structural events required for cellular duplication, which is mediated by several bifunctional proteins, with roles both in mitochondrial function and cell cycle regulation, allowing an adaptative cellular response to the energetic requirements of cell division.

One of these proteins is Tor1p, a serine/threonine protein kinase highly conserved among eukaryotes. Tor1p is a subunit of the Target of Rapamycin (TOR) complex 1 (TORC1), which is involved mainly in the growth control by stimulating ribosome biogenesis and translation when nutrients are available (Moreno-Torres *et al.*, 2015). Growth control is intrinsically linked with cell cycle regulation (Turner *et al.*, 2012). Recently it was shown that TORC1 activity towards ribosome biogenesis oscillates in synchrony with the budding yeast cell cycle in undisturbed cells. In addition, TORC1 coordinates growth with G1/S cell cycle progression, by promoting the expression of the G1 cyclins that activate Cdc28p and by destabilizing the Cdc28p inhibitors (for instance, Sic1p) (Barbet *et al.*, 1996; Moreno-Torres *et al.*, 2015; Zinzalla *et al.*, 2007). TORC1 also impacts on G2/M transition (Nakashima *et al.*, 2008).

In addition to its role in cell cycle, TORC1 negatively regulates mitochondrial function in the presence of glucose (Bonawitz *et al.*, 2007). Reduced TORC1 signaling increases mitochondrial respiration and $\Delta\psi$ (Bonawitz *et al.*, 2007; Pan *et al.*, 2011; Pan and Shadel). Interestingly, the enhanced mitochondrial bioenergetics are not mediated by an increase mitochondrial biogenesis but rather associated with an increase in the translation of mtDNA-encoded OXPHOS subunits that enhances the density of OXPHOS complexes (Bonawitz *et al.*, 2007; Pan *et al.*, 2011; Pan and Shadel). Whether TORC1 activity, similarly to ribosome biogenesis, oscillates with the cell cycle to modulate mitochondrial bioenergetics is unknown.

One of TORC1 downstream effectors is Sit4p, a type 2A-related serine-threonine protein phosphatase. Sit4p can serve broad pleiotropic functions, which include the regulation of mitochondria and of cell cycle. Sit4p is required for the normal accumulation

of G1 cyclin mRNAs and for the execution of START, bud emergence and SPB duplication (Clotet *et al.*, 1999; Di Como *et al.*, 1995; Sutton and Freiman, 1997; Sutton *et al.*, 1991). Sit4p is also required for the transcriptional repression of mitochondria by glucose (Jablonka *et al.*, 2006), by regulating transcriptional repressors of mitochondrial function such as Hxk2p (Barbosa *et al.*, 2016). In yeast, glucose is the preferred carbon source, and the expression of genes such as those involved in respiration are repressed when glucose levels are high (Conrad *et al.*, 2014). Interestingly, the role of Sit4p in mitochondrial transcriptional repression seems to be connected with its role in cell cycle progression, as preventing mitochondria derepression in *sit4*Δ cells by expressing a phosphoresistant $Hxk2^{S15A}$ mutant also suppresses the G1 arrest of Sit4p-deficient cells (Barbosa *et al.*, 2016).

Sit4p is also involved in the regulation of Snf1p (for “Sucrose non-fermenting”), a serine/threonine protein kinase. Snf1p/AMPK are central components of signal transduction pathways that are activated in response to nutrient limitation (Hardie and Carling, 1997). In yeast, Snf1p is activated by phosphorylation, mediated by Sak1p, Tos3p or Elm1p, and inhibited by the dephosphorylation catalyzed by Sit4p or Glc7p. Similarly to Sit4p, Snf1p is involved in glucose repression (Young *et al.*, 2012). In the absence of glucose, Snf1p is required for the expression of glucose-repressed genes, including genes involved in respiration. Consistently, cells lacking Snf1p are unable to grow on respiratory carbon sources. Paradoxically, studies in high glucose conditions indicate that loss of Snf1p causes an increased cellular dependence of mitochondrial function as cells lacking Snf1p showed an increased oxygen consumption and their growth and energy production is sustained mainly by OXPHOS (Nicastro *et al.*, 2015; Tripodi *et al.*, 2018).

Snf1p is also involved in cell cycle control. Loss of Snf1p affects proper expression of the *CLB5* gene and decreases the expression of G1-specific genes, inducing a G1/S transition delay (Busnelli *et al.*, 2013; Nicastro *et al.*, 2015; Pessina *et al.*, 2010). In addition, Snf1p has a role in the regulation of mitosis, contributing to the correct alignment of mitotic spindle along the mother-bud axis (Tripodi *et al.*, 2018). Since loss of Snf1p impairs both mitochondrial respiration and delays cell cycle progression, Snf1p is also a potential player in the coordination of both processes.

The cAMP-activated protein kinase A (cAMP-PKA) pathway, the main pathway activated by glucose, is also a good candidate to integrate mitochondrial regulation with cell cycle progression. In yeast, cAMP levels and PKA activity oscillate in synchrony with the cell cycle (Guerra *et al.*, 2022; Smith *et al.*, 1990). In addition, cAMP-PKA plays a prominent role in the regulation of START (Cocklin and Goebl, 2011; Mizunuma *et al.*, 2013), and is involved in the control of mitotic exit by negatively regulating the APC/C (Irniger *et al.*, 2000). The cAMP-PKA pathway also plays a role in mitochondrial function under respiratory

conditions (lactate). By inducing the transcription of nuclear-encode mitochondrial proteins, cAMP-PKA pathway modulates the mitochondrial enzyme content but not the total mass, increasing the oxidative phosphorylation capacity of the cells (Chevtzoff *et al.*, 2005; Dejean *et al.*, 2002). On the other hand, in glucose media, PKA plays a role in the inhibition of mitochondrial biogenesis. By phosphorylating a subunit of the preprotein translocase of the outer membrane (TOM complex) in non-respiring conditions, PKA inhibits protein import of nuclear-encoded mitochondrial proteins (Schmidt *et al.*, 2011). In addition, it may regulate the *in vivo* functions of Abf2p, controlling the mtDNA content in response to glucose availability (Cho *et al.*, 2001).

Another interesting example of a bifunctional protein with a major role in the regulation of both cell cycle and mitochondrial function is Grr1p (for “Glucose repression resistant”). As the name suggests, Grr1p was originally characterized by its role in sensing glucose levels and subsequent activation of glucose repression pathways (Flick and Johnston, 1991). Mutants lacking Grr1p are thus derepressed even in the presence of high glucose conditions and exhibit a strong defect in respiratory conditions (Dimmer *et al.*, 2002; Romero Antonia *et al.*, 2018). Grr1p is also a nonessential F-box subunit of the SCF E3 ubiquitin ligase complex. The SCF complex, together with APC/C, are responsible for the polyubiquitination and consequent degradation by the 26S proteasome of cell cycle regulators (Teixeira and Reed, 2013). Grr1p mediates the recognition of specific substrates such as the cyclins Cln1p and Cln2p (Barral *et al.*, 1995), promoting its ubiquitination and proteasomal degradation (Cardozo and Pagano, 2004). Targets involved in both glucose repression and cell cycle progression are degraded by the SCF-Grr1p complex. The Grr1p-Skp1p interaction is enhanced by high glucose levels (Li and Johnston, 1997), allowing to couple mitochondrial glucose repression with cell cycle regulation via ubiquitin-mediated protein degradation.

It is highly probable that more regulators with dual functions in mitochondria and cell cycle regulation exist. Elucidation of all the complex regulatory networks that allow for the intimate coordination of mitochondrial inheritance/function with cell cycle progression will be a challenging task.

4. Coordination between mitochondria and cell cycle in higher eukaryotes

Several studies support a bidirectional relationship between mitochondria and the cell cycle also in mammalian cells, suggesting that alterations in intracellular circumstances during cell cycle progression are coordinated with metabolic and morphological alterations of mitochondria.

In fact, several efforts were made to understand how the cells sense its underlying metabolic status and the AMPK was identified as an intracellular sensor for AMP levels (Corton *et al.*, 1994). AMPK is activated following ATP depletion, which cause a rise in the AMP:ATP ratio within the cell. Once activated, AMPK plays an important role in maintaining the energy balance and ATP homeostasis, stimulating ATP-generating processes and inactivating ATP-consuming pathways, like cell cycle progression (Carling, 2004). AMPK promotes the phosphorylation of p53 at serine-15, which prevents p53 degradation, induces the expression of its target gene p21, promoting cyclin E degradation and suppression of G1 progression (Igata *et al.*, 2005; Imamura *et al.*, 2001; Jones *et al.*, 2005). These results showed that G1/S transition is an energy-sensitive process in which enhanced ATP is required. In this sense, it was found an upregulation of the glycolytic activator 6-phosphofructo-2-kinase/fructose-2,6-bisphosphatase 3 (PFKFB3) in mitotically committed cells. Overexpression of PFKFB3 promotes cell proliferation by increasing the expression of central cell cycle molecules, namely cyclin D3 (Yalcin *et al.*, 2009). In addition, it was shown that upregulation of nuclear PFKFB3 increases the expression of Cdc25C, a M-phase-promoting phosphatase, and decreases the expression of the Cdk1 inhibitor p27 (Yalcin *et al.*, 2009). It was also described that glutaminase 1 (GLS1), a mitochondrial enzyme involved in the hydrolysis of glutamine into glutamate and ammonia, is very active during G1/S progression but also during G2/M transitions. These results suggest that glutamine metabolization is also crucial for proper cell cycle progression (Colombo *et al.*, 2011).

The levels of these metabolic enzymes are regulated by the APC/C-Cdh1 complex (Almeida *et al.*, 2010; Colombo *et al.*, 2011). As described above, APC/C is a central regulator of the cell cycle that targets key substrates to promote both mitotic exit and progression through G1. It was reported that a decrease in APC/C-Cdh1 activity at late G1 enhances glycolysis and glutaminolysis, due to a decreased APC/C-Cdh1-mediated degradation of PFKFB3 and GLS1. Overall, these changes enable cells to overcome the nutrient-sensitive checkpoint that controls G1/S transition (Almeida *et al.*, 2010; Colombo *et al.*, 2011; Kalucka *et al.*, 2015). Accordingly, in the presence of an energetic stress like a decline in bioenergetics or a mitochondrial defect, the cells can become reversibly arrested at the G1/S boundary of the cell cycle (Lee and Finkel, 2013). The coordination of metabolic activities with the G2/M transition is poorly characterized. The finding that Cdk1, involved in mitosis initiation, is indirectly regulated by AMPK (Shen *et al.*, 2018) suggests that a metabolic checkpoint may also regulate G2/M transition.

It was also proposed mitochondrial biogenesis is enhanced during the cell cycle as a means to build mitochondria for cell division. The biosynthesis of mitochondrial membrane components like cardiolipin and mitochondrial proteins is proposed to occur in S phase

(Jahnke *et al.*, 2009; Martínez-Diez *et al.*, 2006). In addition, the expression of mitochondrial biogenesis factors (PGC-1α, PPAR-α, PPAR-δ and NOS1) increase at S phase (Jahnke *et al.*, 2009). In agreement, it was proposed that mitochondria in G1/S boundary have a significantly higher $\Delta\psi$ and a burst of respiratory activity (Herzig *et al.*, 2000; Schieke *et al.*, 2008; Van den Bogert *et al.*, 1988). Enhanced respiratory activity was also associated with increased ROS levels (Jahnke *et al.*, 2009) that promote G1 to S transition (Burdon, 1995; Deng *et al.*, 2003; Sattler *et al.*, 1999). Other authors however reported a peak of mitochondrial activity in G2/M transition (Martínez-Diez *et al.*, 2006; Wang *et al.*, 2014; Xie *et al.*, 2019). Whether the peak in mitochondrial activity in mammalian cells may vary between cell types or the discrepancy arise from distinct methodologies is unclear.

Progression through cell cycle requires increased ATP production and consequently enhanced mitochondrial bioenergetics (Bao *et al.*, 2013; Xie *et al.*, 2019). ATP is generated via OXPHOS which in mammalian cells is composed of five complexes in which the complex I is the largest with 46 subunits. It is known that complex I is essential for mitochondrial respiration, but it was also proposed that it is required for proper cell cycle progression as disruption of complex I retards the G1/S transition (Owusu-Ansah *et al.*, 2008). It was recently shown that Cdk1-cyclin B relocates to the mitochondrial matrix and phosphorylates at least five subunits of the complex I during G2. Respiratory chain complex I phosphorylation and activation by Cdk1 enhance mitochondrial respiration, with increased ATP generation (Wang *et al.*, 2014). Accordingly, the deficient phosphorylation of the complex I delays G2/M transition with loss of the enhanced mitochondrial activity (Wang *et al.*, 2014).

In contrast with budding yeast, in mammalian cells it was reported that the mitochondrial morphology changes as cells progress through the cell cycle (Arakaki *et al.*, 2006; Kanfer and Kornmann, 2016; Mitra *et al.*, 2009). In interphase, mitochondria exist as highly interconnected tubular structures or long spiral forms of tubules. During G1 progression, mitochondria fuse into a giant, hyperfused and hyperactive tubular network with higher ATP producing capacity (Mitra *et al.*, 2009) (Figure 1.3). The presence of a hyperfused mitochondria is important for G1 to S transition and proper cell cycle progression. Inducing mitochondria hyperfusion by Drp1 inhibition leads to increased levels of cyclin E and initiation of DNA replication in quiescent cells, independent of growth factors (Mitra *et al.*, 2009). Further evidence will be needed to uncover the regulation of cyclin E levels by hyperfused mitochondria. Upon G1/S progression, this hyperfused mitochondrial network is fragmented, with the greatest fragmentation occurring during mitosis, favoring the stochastic segregation of mitochondria into the cells, where the filamentous shape is reformed (Lee *et al.*, 2007; Martínez-Diez *et al.*, 2006; Mitra *et al.*, 2009). The mitochondrial

fission during mitosis is also favored by the degradation of Mfn1 promoted by Cdk1-cyclin B activity (Park and Cho, 2012).

It has been proposed that the regulation of Drp1 by the cell cycle machinery plays an essential role in controlling cell cycle-dependent changes in morphology. Once the cells exit mitosis, Drp1 is targeted for degradation by APC/C-Cdh1 (Horn *et al.*, 2011) favoring the increase in mitochondrial fusion and the formation of a hyperfused network at G1/S transition (Mitra *et al.*, 2009). As the cell cycle progresses, the activation of interphase Cdk-cyclin complexes during G1/S transition results in phosphorylation and inactivation of APC/C-Cdh1 complex, producing a rise in Drp1 levels and Drp1 stabilization, shifting the balance to favor mitochondrial fission at the onset of S phase (Taguchi *et al.*, 2007).

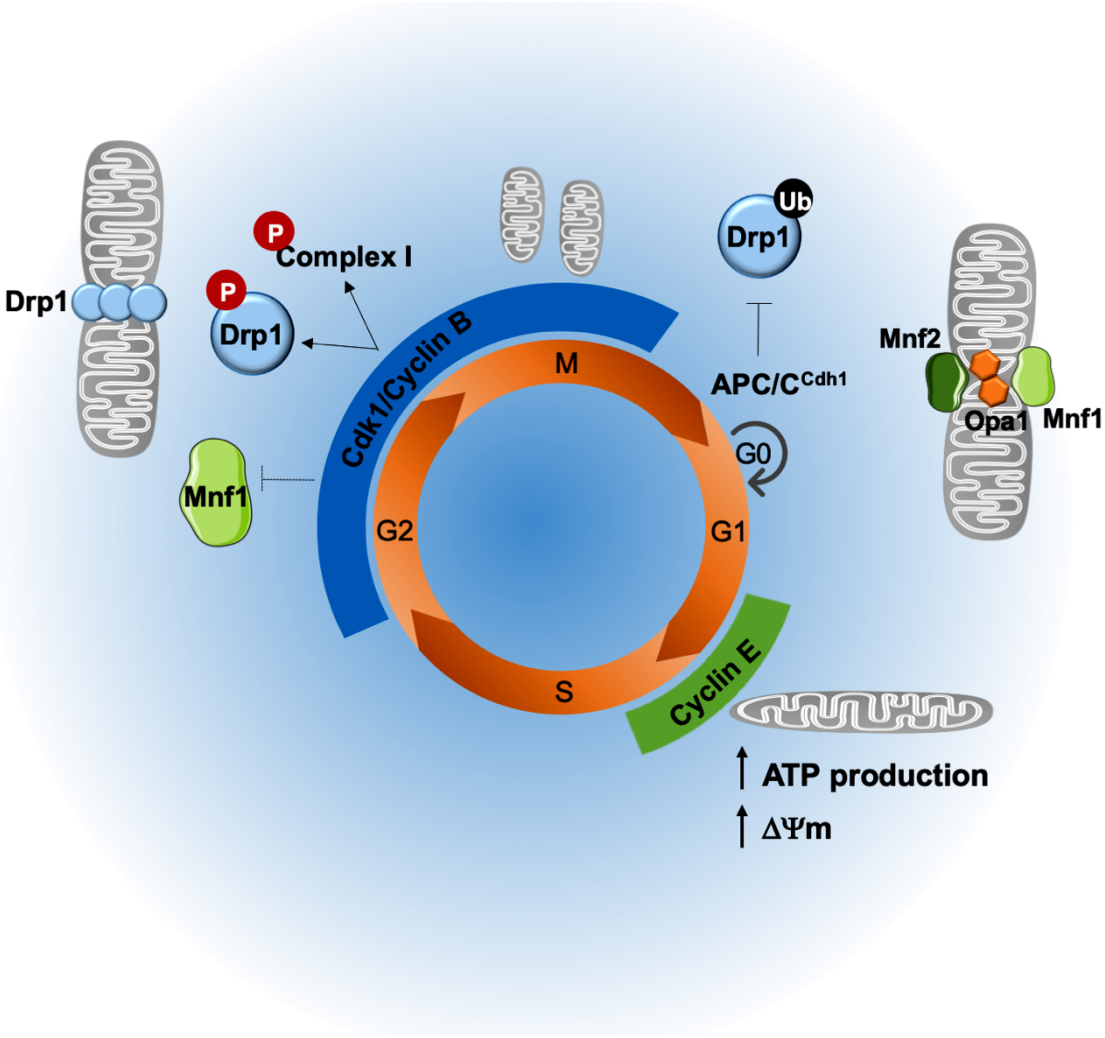

Figure 1.3. Mitochondrial dynamics and bioenergetics are coordinated with cell cycle progression in mammalian cells. During G1, mitochondria fuse into a hyperfused and hyperactive network that regulates cyclin E levels and enhances energy production to presumably allow G1 to S transition. At G2/M, Cdk1-cyclin B simultaneously promotes mitosis, enhances mitochondrial respiration and activates Drp1, favouring mitochondrial segregation into daughter cells. After mitotic exit, Drp1 is targeted for degradation by the APC/C-Cdh1, allowing the reassembly of the mitochondrial network (see text for more details).

Drp1 activity is also regulated by phosphorylation. In response to the mitotic regulators Ras-related protein Ral-A/Aurora A, Cdk1-cyclin B activates Drp1 by phosphorylation on serine-616 leading to mitochondrial fragmentation during G2/M transition (Kashatus *et al.*, 2011; Salazar-Roa and Malumbres, 2017; Xie *et al.*, 2019). In addition, Drp1 recruitment is enhanced indirectly by AMPK, through the phosphorylation of the mitochondrial fission factor (Mff), linking energy sensing to mitochondrial dynamics (Otera *et al.*, 2010; Toyama *et al.*, 2016).

The importance of Drp1 and proper mitochondrial fission during cell cycle is highlighted by the studies showing that inhibition of Drp1 delayed S phase entry (Mitra *et al.*, 2009) and induces a partial G2/M arrest (Qian *et al.*, 2012; Rehman *et al.*, 2012). Although it is unclear how Drp1 mediate normal cell cycle progression, it has been shown that Drp1 inhibition leads to increased levels of cyclin E, especially during G2/M transition (Mitra *et al.*, 2009; Parker *et al.*, 2015; Qian *et al.*, 2012). In Drp1-depleted cells, a persistent mitochondrial hyperfusion leads to cell cycle defects characteristic of aberrant expression of cyclin E, such as replication stress, centrosome overduplication and chromosomal instability, eventually leading to aneuploidy (Qian *et al.*, 2012).

CHAPTER 2.

Main aims and thesis outline

Accumulating evidence suggest that cellular bioenergetics adjusts to the increased energy consumption during cell cycle progression. Although this coordination is not fully understood, mitochondria has emerged as an important player in integrating these two cellular processes. The main aim of this thesis was to further understand the cross-regulation between cell cycle progression and mitochondrial function and explore the mechanisms and molecular players involved in this coordination. For this purpose, we took advantage of the budding yeast *Saccharomyces cerevisiae*, that was used to uncover the findings described across the chapters of this thesis:

Chapter 3 focuses on how mitochondrial bioenergetics adjusts to support the energetic demands of cell cycle progression. We demonstrated that the levels and phosphorylation of the ATP synthase catalytic beta subunit (Atp2p in yeast) vary during cell cycle progression, with an increase at the G2/M phase. The implications for mitochondrial function and cell cycle are further discussed in chapter 3.

Chapter 4 provides a proteomic characterization of yeast mitochondria in the absence of the APC/C coactivator Cdh1p. The observations presented in this chapter suggest absence of Cdh1p leads to a metabolic remodelling towards to an increase mitochondrial respiration. The mechanism underlying this mitochondrial remodelling is explored in chapter 4.

Chapter 5 unveils a new link between the yeast cyclin-dependent kinase, Cdc28p, and mitochondrial respiration. The observations presented in this chapter suggest that, through the modulation of the Hsp90p-Cdc37p chaperone system, mitochondrial function can also trigger cell cycle checkpoint arrest by directly affecting Cdc28p levels.

Finally, chapter 6 summarizes the main findings and final conclusions of this thesis, showing the implications of the new findings while opening questions for future works.

CHAPTER 3.

Phosphoregulation of the ATP synthase beta subunit stimulates mitochondrial activity for G2/M progression

This chapter was based on the following published paper:

Ana Cláudia Leite, Telma S. Martins, Ana Campos, Vitor Costa and Clara Pereira, Phosphoregulation of the ATP synthase beta subunit stimulates mitochondrial activity for G2/M progression, Advances in Biological Regulation, 2022, 85:100905 (DOI: 10.1016/j.jbior.2022.100905).

Phosphoregulation of the ATP synthase beta subunit stimulates mitochondrial activity for G2/M progression

Abstract

Mitochondrial ATP synthase is a multifunctional enzyme complex involved in ATP production. We previously reported that the ATP synthase catalytic beta subunit (Atp2p in yeast) is regulated by the 2A-like protein phosphatase Sit4p, which targets Atp2p at T124/T317 impacting on ATP synthase levels and mitochondrial respiration. Here we report that Atp2-T124/T317 is also potentially regulated by Cdc5p, a polo-like mitotic kinase. Since both Cdc5p and Sit4p have established roles in cell cycle regulation, we investigated whether Atp2-T124/T317 phosphorylation was cell cycle-related. We present evidence that Atp2p levels and phosphorylation vary during cell cycle progression, with an increase at G2/M phase. Atp2-T124/T317 phosphorylation stimulates mitochondrial membrane potential, respiration and ATP levels at G2/M phase, indicating that dynamic Atp2p phosphorylation contributes to mitochondrial activity at this specific cell cycle phase. Preventing Atp2p phosphorylation delays G2/M to G1 transition, suggesting that enhanced bioenergetics at G2/M may help meet the energetic demands of cell cycle progression. However, mimicking constitutive T124/T317 phosphorylation or overexpressing Atp2p leads to mitochondrial DNA instability, indicating that reversible Atp2p phosphorylation is critical for homeostasis. These results indicate that transient phosphorylation of Atp2p, a protein at the core of the ATP production machinery, impacts on mitochondrial bioenergetics and supports cell cycle progression at G2/M.

Keywords: Atp2p phosphorylation, Bioenergetics, Cell cycle, Mitochondria, Yeast.

3.1. Introduction

Sit4p is a serine/threonine protein phosphatase of the PP2A-like phosphatase family that regulates several distinct cellular processes. Of note, Sit4p plays a major role in the transcriptional regulation of mitochondrial biogenesis. By targeting the Snf1p kinase, member of the AMP-activated protein kinase family (Ruiz *et al.*, 2011), Sit4p promotes the repression of respiratory genes under high glucose (fermentative) conditions. We have found that Sit4p also directly dephosphorylates mitochondrial proteins, including the catalytic beta subunit (Atp2p) of the mitochondrial ATP synthase complex (Pereira *et al.*, 2018). Phosphorylation of Atp2p at either T124 or T317 increases the stability of Atp2p and the mitochondrial content of the entire ATP synthase complex, resulting in higher mitochondrial respiration and cellular ATP levels (Pereira *et al.*, 2018). Phosphoregulation of Atp2p is thus a novel mechanism contributing to the control of ATP synthase, particularly relevant as this is the key flux-controlling enzyme for the respiratory metabolism (Nilsson and Nielsen, 2016).

Sit4p also plays a role in cell cycle regulation. It is required for the normal accumulation of G1 cyclin RNAs and for the execution of the control point called START which is required for DNA synthesis, bud emergence and spindle pole body duplication, contributing for correct cell cycle (Clotet *et al.*, 1999; Di Como and Arndt, 1996; Di Como *et al.*, 1995; Fernandez-Sarabia *et al.*, 1992; Jiang, 2006). Interestingly, the role of Sit4p in mitochondrial transcriptional repression seems to be connected with its role in cell cycle progression, as preventing mitochondrial derepression in the *sit4*Δ mutant also abolished the G1 arrest (Barbosa *et al.*, 2016). Such a coordination between the cell cycle progression and mitochondrial activity is supported by numerous studies in synchronous populations of distinct organisms. Mitochondrial mass increases during G1/S phase, whereas mitochondrial activity seems to increase at S and most notoriously at G2/M phase (Harbauer *et al.*, 2014; Martínez-Diez *et al.*, 2006; Montemurro *et al.*, 2017; Wang *et al.*, 2014). The coordination of mitochondrial function with cell cycle involves the activity of the cyclin-dependent kinase 1 (Cdk1), a master regulator of cell cycle. In yeast, phosphorylation of the outer membrane translocase Tom6p by Cdk1 (Cdc28p) during mitosis indirectly increases mitochondrial protein influx. This favors mitochondrial biogenesis and consequently cellular respiratory activity, which contributes for mitotic progression (Harbauer *et al.*, 2014). In mammalian cells, it was shown that Cdk1-cyclin B is able to relocate to the mitochondrial matrix and phosphorylates at least five subunits of respiratory chain complex I, enhancing mitochondrial respiration and ATP production (Wang *et al.*, 2014). This increase in mitochondrial activity seems important for cell cycle progression since loss of complex I phosphorylation by Cdk1-cyclin B in mammalian cells slowed G2/M

transition (Wang *et al.*, 2014). Likewise, cell cycle progression is blocked by mutations affecting the respiratory chain complexes I or IV in *Drosophila* (Mandal *et al.*, 2005) or treating HeLa cells with the ATP synthesis inhibitor oligomycin (Xiong *et al.*, 2012). In addition to mitochondrial bioenergetics, cell cycle-dependent changes in mitochondrial morphology, essential for the completion of cytokinesis and for the proper distribution of mitochondria into daughter cells, have been described (Taguchi *et al.*, 2007). While a bidirectional connection between mitochondrial activity and cell division is now established, the molecular effectors connecting both processes warrant further investigation.

In this study, we report that Atp2-T124/T317 phosphorylation dynamics is cell cycle-regulated, leads to increased mitochondrial activity at G2/M and helps support cell cycle progression.

3.2. Results

3.2.1. The yeast polo-like kinase Cdc5p is involved in Atp2p regulation

The ATP synthase catalytic beta subunit (Atp2p in yeast) is dephosphorylated at residues T124/T317 by the phosphatase Sit4p (Pereira *et al.*, 2018) and phosphorylated by unknown kinase(s). To identify potential kinase regulators of Atp2-T124/T317 we performed an *in silico* analysis. Using the software Group-based Prediction System (GPS), four kinases were identified as potential regulators of Atp2-T124/T317 sites, namely yeast Ipl1p and Pkc1p and two mammalian kinases whose closest homologs in yeast are Cdc5p and Hrr25p (Figure 3.1A). Notably, both Pkc1p and Hrr25p kinases were reported to share substrates with Sit4p (Mehlgarten *et al.*, 2009; Torres *et al.*, 2002). Plus, using STRING analysis (Szklarczyk *et al.*, 2018) we found Sit4p and the putative Atp2p kinase regulators Cdc5p, Ipl1p, Pkc1p and Hrr25p have significant interactions (PPI enrichment p-value:0.000868) indicating some biological connection (Figure 3.1B).

A

Residues	Predicted kinase	Score	Yeast homologue kinase
T124/T317	PLK	9.9/8.6	Cdc5p
T124/T317	Ipl1/AUR	8.7/3.5	Ipl1p
T124/T317	yPkc1/PKC	8.2/11.9	Pkc1p
T124/T317	CK1	2.4/-0.7	Hrr25p

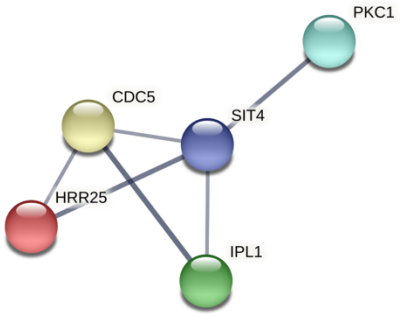

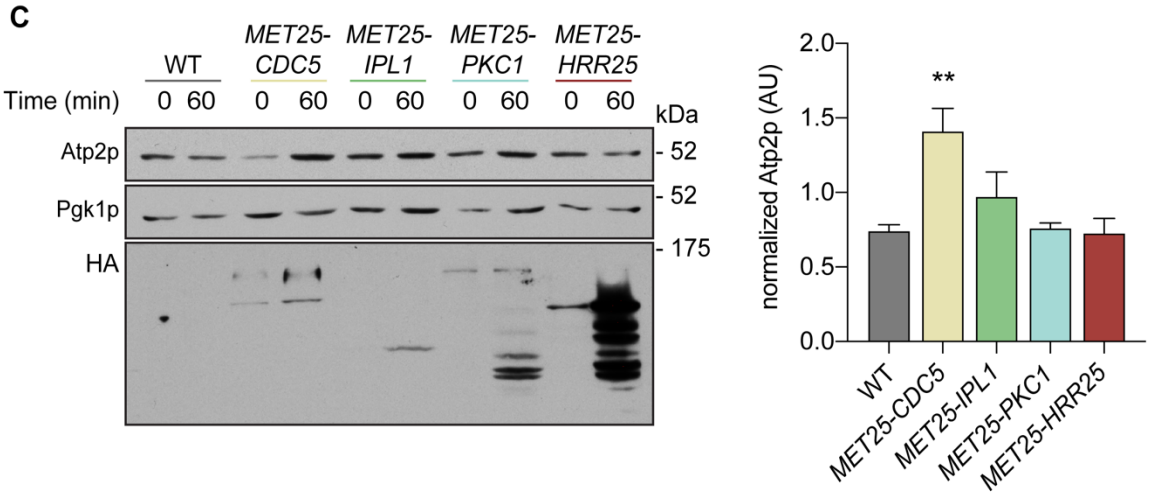

Figure 3.1. Cdc5p kinase is involved in Atp2p regulation. (A) Table showing the GPS 3.0 predicted kinases and respective yeast homologs. Kinase score values for each Atp2p phosphosite were update using GPS 5.0 *S. cerevisiae* specific module. (B) Interaction network of Sit4p and the predicted Atp2p regulatory kinases. Interactions were mapped by searching STRING database version 11.5 with a confidence cut-off of 0.4. In the association network, proteins are presented as nodes connected with line thickness representing the strength of data support. (C) Immunodetection of Atp2p and indicated kinases under regulation of *MET25* promotor (HA-tagged) in cells grown in non-inducing conditions (0 min) or shifted to inducing (60 min) conditions. Pgk1p is shown as loading control. Fold change of Atp2p levels between the 0 and 60 min is shown (mean ± SEM, $n = 3$, **, $p < 0.01$, one-way ANOVA).

Since Atp2p phosphorylation at the T124 and T317 was associated with increased Atp2p levels (Pereira *et al.*, 2018), we used this as a readout to identify the kinase(s) responsible for phosphorylating Atp2p. For that, we manipulated the candidate kinases expression by replacing the endogenous promoters with a methionine inducible promoter *MET25* while simultaneously adding an HA tag. Regulated kinase overexpression was attained by incubating cells with excess methionine (non-inducing conditions; t0), or with low methionine (inducing conditions). Kinase overexpression was induced for 60 min, a time point in which kinase expression was highest (Figure 3.1C). We found that Ipl1p, Pkc1p and Hrr25p overexpression had no effect on Atp2p accumulation, while Cdc5p overexpression increased Atp2p levels (Figure 3.1C). These results suggest that from these kinases only Cdc5p may be involved in Atp2p phosphoregulation and mitochondrial function. Supporting

this hypothesis, Cdc5p overexpression resulted in a significant increase in the respiratory rate (Figure 3.7).

3.2.2. Atp2p levels and phosphorylation are regulated during cell cycle progression

Even though Atp2-T124/T317 phosphorylation plays a clear function in regulating mitochondrial respiration, its physiological context is unknown. Cdc5p, a conserved polo-like kinase, is an important cell cycle regulator, participating in multiple events from S phase to cytokinesis (Botchkarev and Haber, 2018). Since both Sit4p and Cdc5p play a role in cell cycle regulation, we postulated that Atp2p phosphoregulation may be cell cycle-related. To test this hypothesis, we monitored Atp2p levels during cell cycle progression. Cells were arrested in G1 with α-factor and synchronously released into the cell cycle and time-course Atp2p levels analysed by Western blotting. Cell cycle progression was monitored by flow cytometry analysis of DNA content and by monitoring the abundance of Cdc20p, a cell cycle marker of mitosis (Figure 3.2A). To evaluate the contribution of Atp2-T124/T317 phosphorylation, we constructed a phosphoresistant Atp2p mutant with both residues mutated into alanine (T124A/T317A). *ATP2* WT and T124A/T317A mutant were expressed from a vector under the control of its own native promotor in the absence of endogenous *ATP2* and the *BAR1* gene. We observed that Atp2-WT levels vary during cell cycle progression with two small peaks at G1 and G2/M phases. However, only the peak at G2/M phase was suppressed when the phosphoresistant Atp2-T124A/T317A version was expressed (Figure 3.2A) indicating Atp2-T124/T317 phosphorylation contributes to Atp2p protein stability specifically at G2/M phase of the cycle. Since Atp2-T124/T317 phosphorylation can be detected by a shift in the protein isoelectric point (pI) (Pereira *et al.*, 2018), we assessed the dynamics of Atp2p phosphorylation during the cell cycle by two-dimension (2D) gel electrophoresis followed by Western blot analysis of Atp2p. In synchronous WT cells, Atp2p shifts towards the acidic end at both S (50 min) and G2/M (110 min) phases, in comparison to G1 phase cells (0 min) (Figure 3.2B). However, only the shift at the G2/M phase was abolished upon expression of the phosphoresistant Atp2p version, indicating that the phosphorylation of T124 and T317 occurs only at G2/M, and the pI shift at the S phase is likely due to an unrelated modification. Interestingly, for both Atp2-WT and Atp2-T124A/T317A, we observed a second Atp2p band with a lower molecular weight at G2/M phase. Thus, in addition to Atp2-T124/T317 phosphorylation, Atp2p may exhibit other modifications contributing to a dynamic regulation of this protein during cell cycle progression.

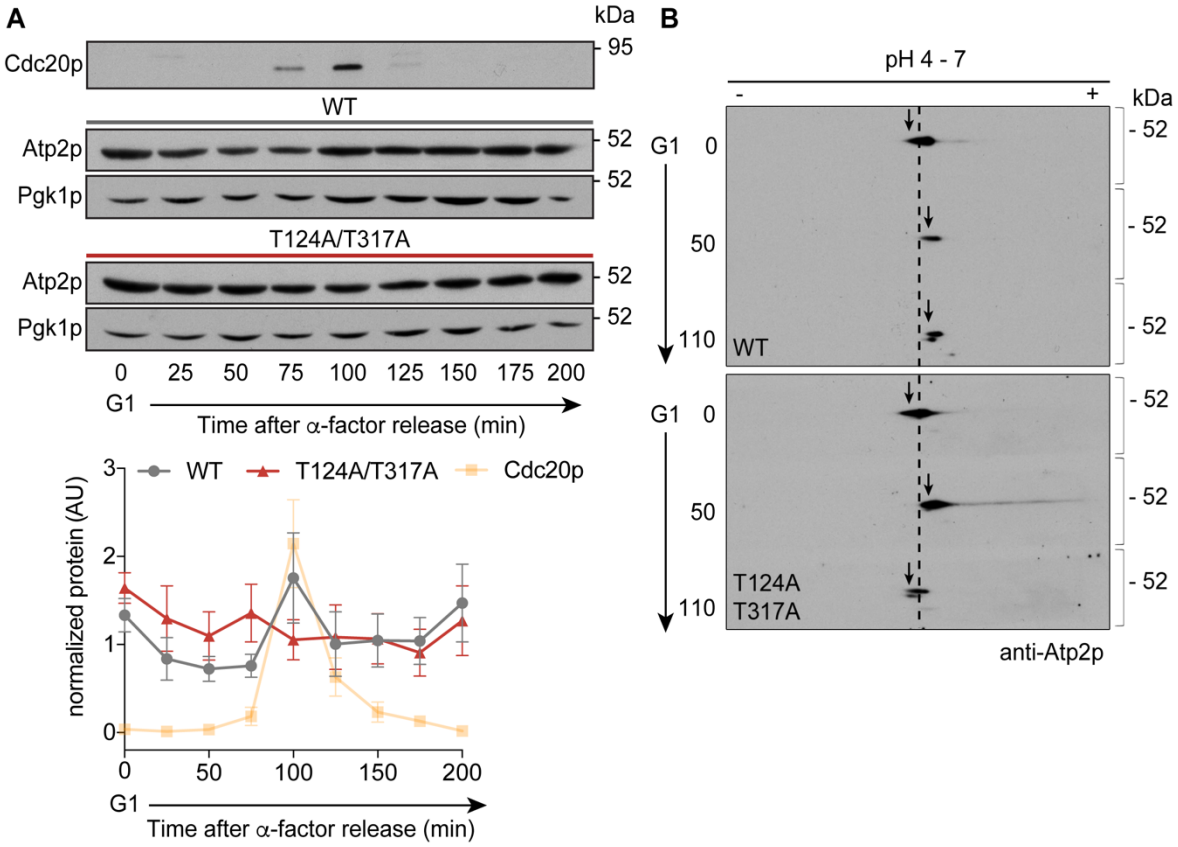

Figure 3.2. Atp2p protein levels and phosphorylation oscillate during the cell cycle. (A) Immunodetection of Atp2p on total protein extracts of *bar1*Δ*atp2*Δ expressing Atp2-WT and Atp2-T124A/T317A cells after synchronization with α-factor and release. Cdc20p profile, used as a marker of mitosis, is only shown for WT (Cdc20p appeared at approximately the same time in both strains). Pgk1p is shown as loading control. Graph represents the relative amount of Atp2p or Cdc20p along time (mean ± SEM, *n* = 5). (B) Total proteins extracts obtained at 0, 50 and 110 min after release from α-factor were separated by 2D-gel electrophoresis and immunoblotted to detect Atp2p. Each time point was transferred to individual nitrocellulose membranes, and membranes aligned for joint immunodetection. A representative image is shown (*n* = 3).

3.2.3. APC/C is not directly involved in the regulation of Atp2p levels

Throughout the cell cycle, the abundance of several proteins is regulated through ubiquitin-mediated proteolysis in a timely and specific manner (Teixeira and Reed, 2013). One key component of the degradation system is the ubiquitin protein anaphase promoting complex/cyclosome (APC/C). Substrate recognition by the APC/C complex is based on specific recognition motifs that are present in most APC/C substrates. The best-defined motif is the destruction box (D-box), with a consensus of RxxLxxxN (x is any amino acid). Phosphorylation of the recognition motif in the substrate frequently prevents APC/C recognition, providing an additional mechanism to regulate substrate stability (Holt, 2012). Remarkably, Atp2p phosphorylation residues lie in sequences resembling destruction boxes (Figure 3.3A) which lead us to hypothesize that APC/C may control the degradation of unphosphorylated Atp2p. To address if Atp2p is a substrate of APC/C, Atp2p expression

was analysed by Western blot in total proteins lysates upon downregulation of the following APC/C subunits: Cdh1p and Cdc20p, the temporally activated subunits involved in substrate recognition; and Cdc16p, an essential member of the complex. We found Atp2p accumulated at higher levels in proliferating *cdh1*Δ cells (Figure 3.3B). Since *CDC20* and *CDC16* are essential genes, the endogenous promotor was replaced by *GAL1* and Atp2p levels were analysed after glucose repression of *CDC20* and *CDC16*. To overcome the fact that addition of glucose inhibits mitochondrial biogenesis and hence Atp2p levels, we analysed the Atp2p decrease relative to WT cells in the same conditions. We found that Atp2p stability was not affected by Cdc20p downregulation, but Atp2p levels increased in cells lacking the core APC/C subunit Cdc16p (Figure 3.3B). These results were consistent with the hypothesis that APC/C in complex with Cdh1p may target Atp2p. To investigate if Atp2p is an APC/C target, its putative D-box recognition motifs were mutated by site-directed mutagenesis. If Atp2p is an APC/C substrate, eliminating recognition by the APC/C cofactors should result in protein stabilization. We constructed two mutants, in which only the canonical leucines were replaced by alanines (L125A/L318A) or the additional residues composing the putative D-boxes (RxxLxxI and QxxLxxD) were also replaced by alanines (D-box). *ATP2* carrying these mutations was expressed (from a vector controlled by the native promotor) in WT cells lacking the endogenous *ATP2* and its protein levels assessed by Western blot. These mutants were compared with the phosphomimetic version (T124D/T317D), whose effect they should mimic, in accordance with the hypothesis that phosphorylation masks the D-box. However, no differences in Atp2p stability were observed (Figure 3.3C) arguing against Atp2p being targeted by APC/C. Furthermore, overexpression of APC/C subunits Cdc20p and Cdh1p or a constitutively active Cdh1-m11 form (lacking the 11 Cdk inhibitory-phosphorylation sites) (Zachariae *et al.*, 1998) did not promote Atp2p degradation (Figure 3.3D). Since APC/C promotes ubiquitination of its substrates targeting them for proteasome-dependent degradation (Jin *et al.*, 2008), we also used a strain carrying a temperature-sensitive mutation in Cim3p (*cim3-1*), an essential component of the 26S proteasome, that at restrictive temperature stabilizes polyubiquitinated proteins (Ghislain *et al.*, 1993). We found that Atp2p was not stabilized in *cim3-1* cells at the restrictive temperature, indicating that Atp2p is unlikely degraded by the ubiquitin-proteosome pathway (Figure 3.3E). In conclusion, although low APC/C-Cdh1p activity affects Atp2p levels, overall results indicate that Atp2p is not a direct APC/C substrate.

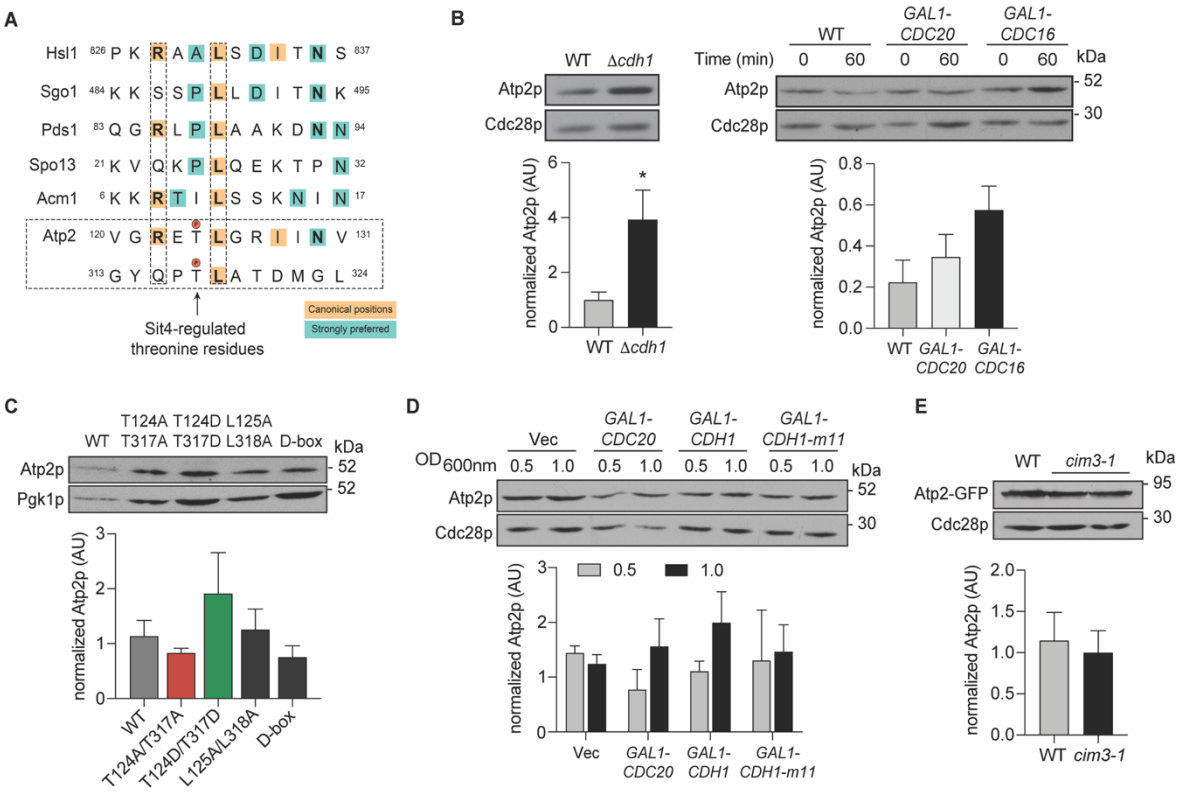

Figure 3.3. Non-phosphorylated Atp2p is not targeted by APC/C. (A) Preference of the D-box-binding pocket and representative experimentally validated yeast D-box instances. The putative D-boxes present in Atp2p and the Sit4p-phosphorylated residues are also shown. (B) Immunodetection of Atp2p upon APC/C downregulation. *cdh1*Δ cells were collected after overnight growth (mean ± SEM, $n = 4$, *, $p < 0.05$, Student's *t*-test). Cells expressing APC/C subunits under regulation of *GAL1* promotor were collected after 60 min in repressing conditions (2% glucose)). Cdc28p is shown as loading control. Fold change of Atp2p levels between the 0 and 60 min is shown (mean ± SEM, $n = 4$). (C) Immunodetection of Atp2p in *atp2*Δ cells expressing WT, phosphomutant Atp2p (T124A/T317A or T124D/T317D) or Atp2p containing mutations on putative APC/C recognition motifs (L125A/L318A or D-box). Pgk1p is shown as loading control. Graph represents the relative amount of Atp2p normalized to Pgk1p (mean ± SEM, $n = 4$). (D) Immunodetection of Atp2p in cells carrying vectors for *GAL1* promotor-induced overexpression of Cdc20p, Cdh1p and Cdh1-m11. At early log phase, cells were transferred to induction media (2% of galactose) and collected at the indicated densities. Cdc28p is shown as loading control. Graph represents the relative amount of Atp2p normalized to Cdc28p (mean ± SEM, $n = 3$). (E) Immunodetection of Atp2p in temperature-sensitive proteasome-deficient (*cim3-1*) or WT cells expressing an integrating Atp2p-GFP, grown at the restrictive temperature (37 °C). Graph represents the relative amount of Atp2p normalized to Cdc28p (mean ± SEM, $n = 3$).

3.2.4. Atp2p phosphorylation and levels impact on mitochondrial genome stability

Cells expressing single phosphomimetic mutants Atp2-T124D or -T317D were shown to exhibit increased Atp2p levels (Pereira *et al.*, 2018). However, in cells expressing the double phosphomimetic version (T124D/T317D) we did not observe the anticipated cumulative effect neither a consistent Atp2p accumulation similar to the single mutants. In addition, we found that Atp2-T124D or -T317D single mutants exhibited a higher specific

growth rate (0.143 ± 0.006 and 0.127 ± 0.004, respectively) on non-fermentative (respiratory) media containing glycerol as carbon source (Figure 3.4A), but cells expressing the Atp2-T124D/T317D double mutant grew poorly than single mutants (0.053 ± 0.050) (Figure 3.4A). ATP synthase function has been reported to influence the stability of mitochondrial (mt) DNA (Contamine and Picard, 2000), indispensable for the biogenesis of respiratory-competent mitochondria. Considering the above data, we evaluated the impact of Atp2-T124D/T317D phosphomimetic mutant on mtDNA stability by determining the percentage of respiration-deficient petite colony formation, using the tetrazolium chloride (TTC) staining. Colonies with functional mitochondria are stained red while smaller white colonies represent respiratory-deficient cells (Figure 3.4B). We found no differences in cells expressing the T124A/T317A version in relation to WT cells; however, the percentage of *petite* colonies increased in cells expressing the Atp2p version mimicking constitutive T124/T317 phosphorylation (Figure 3.4C). To evaluate if the presumed sustained high Atp2p levels in the T124D/T317D mutant could be the source of the mtDNA instability, WT Atp2p was overexpressed from its own promotor (vector pRS316) or under the control of the strong *MET25* promoter (vector pUG23). We found an *ATP2* expression-dependent increase in respiratory-incompetent cells (Figure 3.4D) indicating increased Atp2p levels are sufficient to cause mtDNA instability. These results suggest that Atp2-T124/T317 phosphorylation, but also its reversibility, is important for mitochondrial physiology.

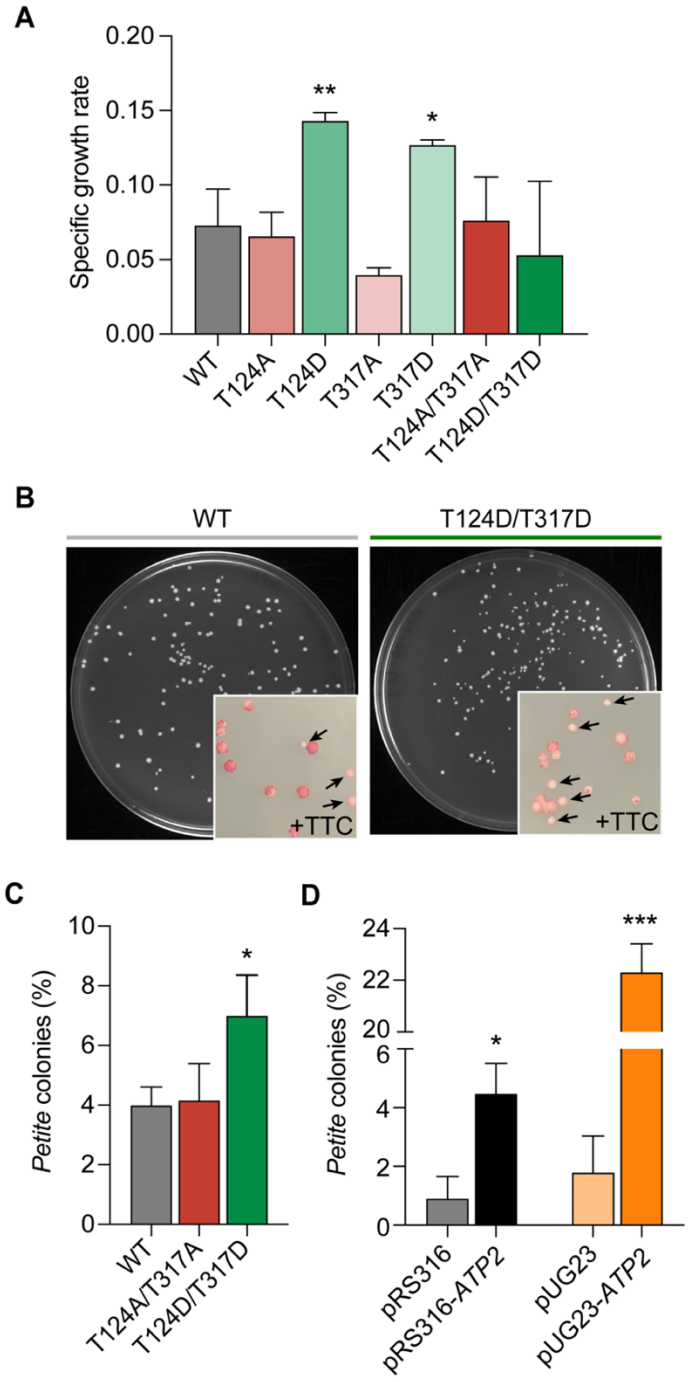

Figure 3.4. Atp2p phosphorylation and levels impact on mitochondrial DNA stability. (A) The specific growth rate of *atp2*Δ cells expressing WT or Atp2p phosphomutants cultured on glycerol-containing media. Specific growth rate was calculated using the change in OD_{600nm} measurements as a function of time. The values represent the mean ± SD (n = 3, *, $p < 0.05$, **, $p < 0.01$, one-way ANOVA). (B) Examples of plates containing *atp2*Δ cells expressing WT Atp2p or phosphomimetic version (T124D/T317D) overlaid with TTC soft agar where red colonies represent cells with functional mitochondria while smaller white colonies represent respiratory deficient cells (indicated by arrows). (C) Frequency of petite colonies in *atp2*Δ cells expressing WT Atp2p or phosphomutant versions (T124A/T317A, T124D/T317D) (mean ± SEM, n = 7, *, $p < 0.05$, one-way ANOVA). (D) Frequency of petite colonies in WT cells with an extra copy of *ATP2* expressed under its own promoter (pRS316) or under the strong *MET25* promoter (pUG23) (mean ± SEM, $n \geq 3$, *, $p < 0.05$, ***, $p < 0.001$, Student's *t*-test).

3.2.5. Atp2p phosphorylation is required for mitochondrial function at G2/M and for efficient cell cycle progression

To further understand the role of Atp2-T124/T317 phosphorylation during cell cycle progression, we assessed several parameters of mitochondrial function in cells expressing Atp2-WT or Atp2-T124A/T317A, synchronously progressing through the cell cycle at time 0, 50 and 110 min corresponding to G1, S and G2/M phases, respectively. We started by evaluating mitochondrial biogenesis in live cells using flow cytometry-detection of nonyl acridine orange (NAO) fluorescence, which binds cardiolipin in mitochondria, correlating with mitochondrial mass (Goswami *et al.*, 2012). The mean fluorescence intensity of NAO-stained cells increased significantly in S phase when compared to cells in G1 (Figure 3.5A) but no further significant changes were observed at G2/M (Figure 3.5A). The mitochondrial mass was similar in Atp2-WT and Atp2-T124A/T317A cells, indicating Atp2-T124/T317 phosphorylation does not impact on mitochondrial biogenesis irrespective of the cell cycle stage. Next, we measured mitochondrial membrane potential (Δψm) in synchronously cells using the lipophilic, cationic fluorescent probe $DiOC_6(3)$. $DiOC_6(3)$ unspecific binding was subtracted through the analysis of the FCCP responsive potential (histograms shown in Figure 3.8) and the values were normalized to the mitochondrial mass. We did not find significant alterations in Δψm for cells expressing Atp2-WT during cell cycle progression. The phosphoresistant Atp2p strain exhibited a decrease in Δψm, already noticeable at cells in S phase, but only significant at G2/M cells. We also analysed total cellular ATP levels measured with the use of a luciferin/luciferase assay. We found ATP levels did not differ significantly along cell cycle phases (Figure 3.5C). However, preventing Atp2-T124/T317 phosphorylation led to reduced cellular ATP levels at G2/M phase (Figure 3.5C).

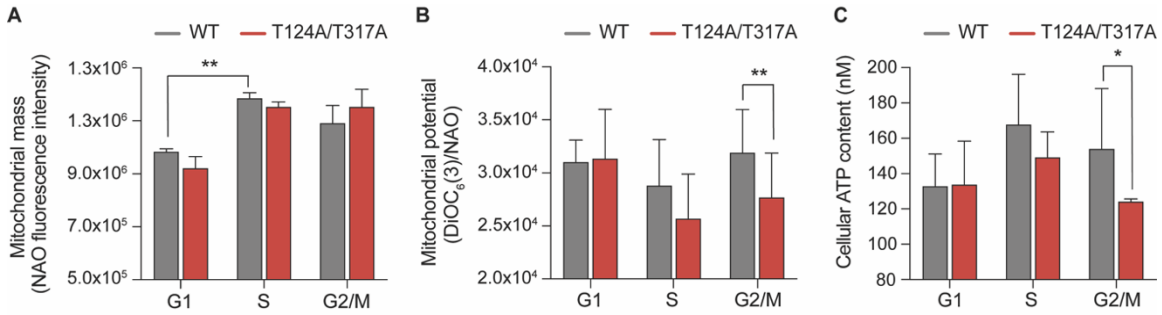

Figure 3.5. Preventing Atp2p phosphorylation decreases mitochondrial membrane potential and ATP content at G2/M. (A–C) Samples from synchronized WT and T124A/T317A cell cultures were collected at time 0 min (G1), time 50 min (S) and time 110 min (G2/M) after release from G1 arrest. (A) The mitochondrial mass was determined by staining the cells with the dye NAO and analysed by flow cytometry (mean ± SEM, $n = 4$, **, $p < 0.01$, Student's *t*-test). (B) The Δψm was determined by staining the cells with the dye $DiOC_6(3)$ and analysed by flow cytometry. Bar graphs represent FCCP-responsive $DiOC_6(3)$ staining normalized to mitochondrial mass (mean ± SEM, $n = 5$, **, $p < 0.01$, Student's *t*-test). (C) ATP content in whole cells (mean ± SEM, $n = 4$, *, $p < 0.05$, Student's *t*-test).

Phosphoregulation of the ATP synthase beta subunit stimulates mitochondrial activity for G2/M progression

We also monitored mitochondrial respiration during cell cycle progression. Oxygen consumption rate slightly increased close to the S phase in both the WT and T124A/T314A mutant, which may be owed to the increase in mitochondrial mass that we observed at this phase. Close to mitosis (125 min), we observed a second peak in respiration in WT cells but not in the phosphoresistant mutant (Figure 3.6A). Together with the reduced Δψm and ATP content, it indicates that Atp2p phosphorylation contributes to the mitochondrial function specifically at G2/M phase.

The impact of Atp2p phosphorylation on cell growth was evaluated by measuring the OD_{600nm} in cells expressing WT and phosphoresistant Atp2p synchronously progressing through the cell cycle. The initial growth curves of both strains were similar up to 125 min (G2/M) where the growth of the phosphoresistant strain was delayed (Figure 3.6B). As expected, the effect is more noticeable in cells completely lacking Atp2p (Figure 3.6B). Since this result suggests a delay in cell cycle, cell cycle progression was analysed in these cells by flow cytometry. We found cell cycle progresses similarly in the phosphoresistant mutant until G2/M phase when the transition to G1 was delayed (Figure 3.6C). The comparison of the percentage of cells in G1 at 125 and 150 min after G1 release shows that only half of the Atp2-T124A/T317A cells re-entered into G1 phase compared to WT cells. A more aggravated delay in G1 entry was observed in the absence of Atp2p, but a significant number of these cells also arrested in G1 throughout the cell cycle (Figure 3.6C).

Overall, these results suggest that Atp2p phosphorylation may be required to meet the energetic demands of G2/M to G1 progression.

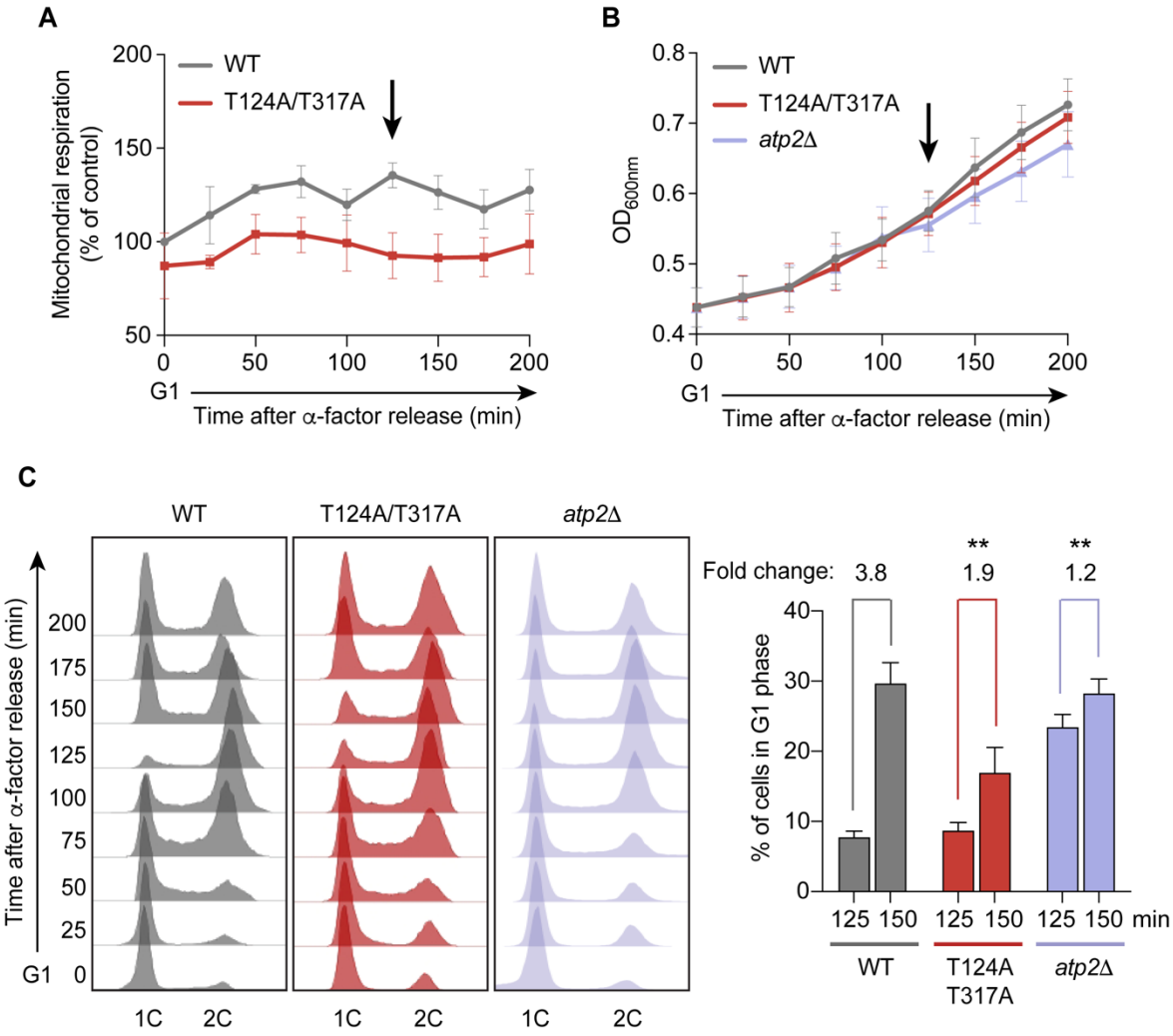

Figure 3.6. Preventing Atp2p phosphorylation delays G2/M to G1 transition. (A–C) Samples from synchronized WT, T124A/T317A and *atp2*Δ cell cultures were taken at the indicated time points after release from G1 arrest. (A) The mitochondrial respiration was determined by measuring oxygen consumption rate in whole cells (mean ± SEM, $n = 4$). (B) Growth was measured by monitoring the OD_{600nm} over time (mean ± SEM, $n = 4$). (C) Cell-cycle progression was monitored by the analysis of DNA content by flow cytometry. Representative histograms are shown. Quantification of G1 cells at 125 and 150 min after release and the fold change is shown (mean ± SEM, $n = 4$, *, $p < 0.05$, **, $p < 0.01$, one-way ANOVA).

3.3. Discussion

Though ATP synthase is extensively studied, there are critical gaps in our knowledge of the physiological relevance of ATP synthase phosphoregulation. And yet, ATP synthase seems heavily regulated by phosphorylation, as more than 136 phosphorylation sites were already identified, with beta subunit as the most frequent phosphorylated subunit in the complex (Castellanos and Lanning, 2019). Plus, many of these phosphorylation sites are physiologically relevant and were already implicated in a wide-range of conditions such as insulin-resistance, heart protection from ischemic episodes, mitochondrial iron overload or cancer (reviewed in (Johnson and Ogbi, 2011)).

Phosphoregulation of the ATP synthase beta subunit stimulates mitochondrial activity for G2/M progression

In here, we provide evidence that ATP synthase beta subunit or Atp2p (ATP5B in mammals) is also phosphoregulated during cell cycle progression. The phosphorylated residues are potentially regulated by the Cdc5p kinase. Cdc5p is an essential and highly conserved mitotic regulator that starts to be expressed in S phase and remains high until the end of cell division (Charles *et al.*, 1998; Cheng *et al.*, 1998). The phosphatase Sit4p, on the other hand, appears to be more active at the G1/S transition (Sutton *et al.*, 1991). This timeframe of activities fits well with a phosphoregulation of Atp2p by Sit4p/Cdc5p. Interestingly, mutations in *CDC5* were shown to affect both nuclear and mitochondrial transmission in yeast (Dutcher, 1982) already pointing for a role for Cdc5p in mitochondrial regulation. Atp2p is likely phosphoregulated before mitochondrial protein import since matrix proteins are not easily accessible to kinases/phosphatases. Interestingly, mitochondrial protein import is enhanced at G2/M phase (Harbauer *et al.*, 2014), which may facilitate the increase of phosphorylated Atp2p in mitochondria at this phase. The mechanism by which Atp2p phosphorylation leads to increased protein levels is still unclear. Atp2-T124/T317 phosphorylation did not decrease Atp2p degradation by the cytosolic proteasomal system, but it may reduce Atp2p turnover by the mitochondrial autonomous proteolytic systems. In fact, Atp2p stability is regulated by the intramitochondrial Lon-like Protease Pim1 (Bayot *et al.*, 2010), but whether Atp2p phosphorylation impacts on this process needs further investigation.

From our results, it has also become clear that a tight control over Atp2p-T124/T317 phosphorylation must occur in physiological conditions, as expressing an Atp2p mutant mimicking constitutive phosphorylation (T124D/T317D) increased mtDNA instability. Interestingly, while we found Atp2p overexpression is sufficient to cause loss of mtDNA, on the other hand, Atp2p is indispensable for yeast cells to survive loss of mtDNA (Contamine and Picard, 2000), highlighting the importance of regulated Atp2p levels for the maintenance of the mitochondrial genome. This effect may be relevant in many tumour types in which beta subunit/ATP5B levels are high and play an essential role in tumour progression and metastasis (Li *et al.*, 2017; Liu *et al.*, 2021; Lu *et al.*, 2009).

We showed that Atp2-T124/T317 phosphorylation increases at G2/M phase, where it stimulates the mitochondrial respiratory activity, Δψm and ATP production. In accordance, a regulated enhancement of mitochondrial function at mitotic exit has been reported in both yeast (Campbell *et al.*, 2020; Harbauer *et al.*, 2014) and human cells (Montemurro *et al.*, 2017; Sweet and Singh, 1999; Wang *et al.*, 2014), suggesting mitochondrial activity is particularly relevant at this phase. An increase in respiration during S and G2/M may fulfil increased energy requirements for DNA and lipid synthesis and chromosome segregation (Salazar-Roa and Malumbres, 2017). Preventing Atp2-T124/T317 phosphorylation not only prevents G2/M-enhanced mitochondrial bioenergetics, but it also delays G2/M to G1

transition. This indicates that cell cycle regulates mitochondrial function, but also that mitochondrial function regulates cell cycle progression, reiterating observations from previous works (Harbauer *et al.*, 2014; Mandal *et al.*, 2005; Wang *et al.*, 2014; Xiong *et al.*, 2012).

The corresponding Atp2-T124/T317 residues in the human beta subunit ATP5B (hT140 and hT334) are also phosphorylated (Rigbolt *et al.*, 2011; Tsai *et al.*, 2015). Since mammalian ATP5B also increases at G2/M phase (Martínez-Diez *et al.*, 2006), ATP synthase beta subunit cell cycle phosphoregulation may be a conserved process.

In conclusion, we present evidence that Atp2-T124/T317 phosphorylation stimulates mitochondrial function at G2/M phase contributing to fuel cell cycle progression. By providing evidence for a direct link between the ATP synthase complex - the core hub of oxidative phosphorylation - and the cell cycle, our results uncover a novel mechanism underlying the complex interplay between mitochondrial function and cell cycle regulation.

3.4. Material and methods

3.4.1. Yeast strains and growth conditions

The *Saccharomyces cerevisiae* strains used are all BY4741 derivative and are listed in Table 3.1. To generate *bar1*Δ*atp2*Δ cells, *bar1*Δ strain was transformed with a DNA fragment containing HIS3MX and the flanking regions of *ATP2*. Gene deletion was confirmed by PCR.

Table 3.1. *S. cerevisiae* strains used in this study.

Strain	Genotype	Source
BY4741 (WT)	Mat *a his3Δ1 leu2Δ0 met15Δ0 ura3Δ0*	Euroscarf
*bar1*Δ	BY4741; *bar1*Δ*::KanMX4*	This study
*cdh1*Δ	BY4741; *cdh1*Δ*::KanMX4*	Euroscarf
*atp2*Δ	BY4741; *atp2*Δ*::MXHIS6*	Lab collection
*bar1*Δ *atp2*Δ	BY4741; *bar1*Δ*::KanMX4 atp2*Δ*::MXHIS3*	This study
*bar1*Δ*ATP2-GFP* (WT)	BY4741; *bar1*Δ*::MXHIS3 ATP2-GPF::KanMX4*	This study
cim3-1	BY4741; *bar1::MXHIS3 atp2-GPF::KanMX4 cim3-1::URA3*	This study
Atp2-WT	BY4741; *bar1*Δ*::KanMX4 atp2*Δ*::ATP2-WT*	This study
Atp2-T124A/T317A	BY4741; *bar1*Δ*::KanMX4 atp2*Δ*::ATP2-T124A/T317A*	This study
Cdc20-FLAG	BY4741; *bar1*Δ*::KanMX4 Cdc20-6Gly-3FLAG-hphMX4*	This study
Met25-Pkc1	BY4741; *Nat-Met25-3HA-PKC1*	This study
Met25-Ipl1	BY4741; *Nat-Met25-3HA-IPL1*	This study
Met25-Cdc5	BY4741; *Nat-Met25-3HA-CDC5*	This study
Met25-Hrr15	BY4741; *Nat-Met25-3HA-HRR25*	This study
Gal1-Cdc5	BY4741; *KanMX6-Gal1-3HA-CDC5*	This study
Gal1-Cdc20	BY4741; *KanMX4-Gal1-3HA-CDC20*	This study
Gal1-Cdc16	BY4741; *KanMX4-Gal1-3HA-CDC16*	This study

Mutations T124A/T317A, T124D/T317D, L125A/L318A and R122A/L125A/N130A/Q315A/L318A/D321A were introduced into the wild type ATP2 gene

cloned in the pRS316 vector using the Q5 Site-Directed Mutagenesis Kit (New England Biolabs). Fidelity of all substitutions was confirmed by sequencing. To construct the *cim3-1* expressing strains, *CIM3-1* sequence was amplified and fused to the *URA3* integrating cassette using overlap extension PCR. This product was then integrated into *bar1::MXHIS3 atp2-GPF::KanMX4* strain.

For Cdh1p and Cdc20p overexpression, cells were transformed with plasmids (pEG-[KT]-CDC20 and pEG-[KT]-CDH1 (Burton and Solomon, 2000) and for Cdh1-m11 overexpression cells were transformed with pRS416-GALL-3HA-Cdh1-m11 plasmid (Zachariae and Nasmyth, 1999). *URA3* marker in pEG-[KT]-CDH1 was replaced by *HIS3* using *in vivo* cloning by yeast homologous recombination in accordance to (Oldenburg *et al.*, 1997).

The overexpression plasmid pUG23-*ATP2* was generated by insertion of the PCR-derived *ATP2* coding region in the SalI and SpeI restriction sites of the centromeric vector pUG23-*MET25* (Niedenthal *et al.*, 1996). Cells were selected in minimal medium lacking histidine. Fidelity of the construct was confirmed by sequencing.

To generate an integrative Atp2p phosphoresistant mutant, *bar1*Δ*atp2*Δ strain was transformed with a DNA fragment containing *ATP2-T124A/T317A* or *ATP2-WT* (control) and selected by recovery of growth in respiratory (3% glycerol) media. Integration was confirmed by PCR and DNA sequencing of the gene.

Epitope-tagged strains were constructed by standard PCR-based homologous recombination (Janke *et al.*, 2004; Longtine *et al.*, 1998), using plasmids pYM-N36-MET25pr-3HA-NAT-NT2, pFa6a-6xGly-3xFLAG-hphMX4 and pFa6a-KanMX6-pGAL1-3HA as template. Strains were transformed by the standard lithium acetate procedure (Gietz and Schiestl, 2007).

Cells were grown in rich medium [YPGal: 1% (w/v) yeast extract, 2% (w/v) bactopeptone, 2% (w/v) galactose] or synthetic complete medium [SC: 0.67% (w/v) Bacto-yeast nitrogen base w/o amino acids, 2% (w/v) glucose and 0.2% (w/v) Dropout mix] lacking uracil/histidine.

Cells with candidate kinases under the regulation of the inducible *MET25* promoter and wild type cells were grown overnight until log-phase in SCGal supplemented with 3 mM L-methionine and harvested (t = 0). The remaining cells were washed twice with ddH2O, transferred to SCGal supplemented with 0.01 mM L-methionine (inducing conditions) and grown for 60 min before harvesting (t = 60).

For *cim3-1* and wild type cells carrying Atp2-GFP, log-phase cultures were grown in YPGal overnight at the permissive temperature (24 ºC), followed by incubation at the restrictive temperature (37 ºC) for 3h.

Cultures were routinely grown in an orbital shaker at 140 r.p.m, 26 ºC.

3.4.2. Cell cycle arrest and synchronization

Synchronized cultures were generated by block and release with 100 ng/mL α-factor peptide (GenScript) for 3h at 26 ºC. Cell cycle arrest was monitored by phase contrast microscopy until >95% of the cells exhibited the "shmoo" morphology. To release, cells were washed and resuspended in medium without α-factor peptide and cells collected at specified time points for the different assays. To validate the arrest and release protocol, parallel samples was usually collected for DNA content analyses by flow cytometry.

3.4.3. SDS-PAGE and Western blot

For immunoblotting, yeast cell extracts were resuspended at identical cell densities in sodium dodecyl sulfate (SDS) loading dye, and lysed by boiling for 10 min and 1 min vortexing with glass beads. Protein samples were separated using SDS-polyacrylamide gels and transferred to nitrocellulose membranes (Hybond-C, GE Healthcare).

The primary antibodies used were raised against mammalian ATP synthase beta subunit (1:7000; ab128743, Abcam), yeast Cdc28p (G-7) (1:100, sc-515762, Santa Cruz Biotechnology), yeast Pgk1p (1:20000, 22C5D8, Invitrogen), FLAG (1:500, M2, Sigma-Aldrich), HA (1:1000, Y-p11, Santa Cruz Biotechnology) and GFP (1:5000, Roche).

Secondary antibodies used were anti-mouse IgG-HRP (1:5000, Molecular probes) and anti-rabbit IgG-HRP (1:10000, Sigma).

Membranes were incubated with WesternBright ECL (Advansta), exposed to LucentBlue X-ray film (Advansta), scanned on a Molecular Imager GS900, and quantified using Image Lab Software version 6.1 (Bio-Rad).

3.4.4. Cell cycle analysis

For cell cycle analysis, cells were fixed overnight and DNA content was analysed by flow cytometry using 10 mM SYTOX Green (Molecular Probes) basically as in (Haase and Reed, 2002). Cells were acquired using the FL1 detector in a BD Accuri C6. Cell cycle distribution was estimated using FlowJo v10 software version.

3.4.5. Petite frequency assay

The generation of cells lacking respiratory competency was performed using the tetrazolium overlay technique as previously described in (Hess *et al.*, 2009), with minor modifications. All the strains were initially grown at 26 ºC for 24h and a dilution was plated on a YPD plate with 1% of glucose or on a SC plate supplemented with 0.05 mM of L-methionine. After 48h at 26 ºC, the *petite* frequency was evaluated by overlaying with soft agar (1.5%) diluted in 0.067 M sodium phosphate buffer pH 7.0 containing 0.1% 2,3, 5–

triphenyltetrazolium chloride (TTC) (Carl Roth). Colonies with functional mitochondria were stained red while colonies without functional mitochondria remained white. The ratio of white colonies to total colonies gives the *petite* frequency.

3.4.6. Mitochondrial mass and mitochondrial membrane potential

The total mitochondrial mass was determined using 10-N-Nonyl acridine orange (NAO, Invitrogen), a dye that binds to cardiolipin present specifically on the mitochondrial membrane basically as described in (Goswami *et al.*, 2012). Briefly, the cells were incubated in culture medium containing 10 μM NAO for 30 min and fluorescence intensity measured using the BD Accuri C6 flow cytometer.

The Δψm was analysed using 3,3′-dihexyloacarbocyanide iodine ($DiOC_6(3)$, Molecular Probes), a dye that accumulates in the mitochondrial matrix according to the Δψm (Perry *et al.*, 2011). The cells were harvested and incubated in culture medium containing 40 nM DiOC6(3) for 30 min at room temperature in the dark with constant shaking. As a negative control, the cells were preincubated with 10 μM carbonyl-cyanide 4-(trifluoromethoxy)-phenylhydrazone (FCCP, Sigma) 15 min before fluorescent dye staining, which leads to a collapse of Δψm. At least 20.000 cells were analysed per sample and the DiOC6(3) membrane potential-related fluorescence was recorded using FL1 detector in a BD Accuri C6 flow cytometer. The collected data was analysed using FlowJo software version 10 to determine the median green fluorescence intensity for each curve.

3.4.7. ATP levels

ATP levels were quantified in whole cells as described in (Ashe *et al.*, 2000) with the following minor modifications: 100 μL of the culture were collected by centrifugation and resuspended in 20 μL of 10% (w/v) trichloroacetic acid. ATP was measured using Enliten luciferin/luciferase reagent kit (Promega) in a Sinergy luminometer against ATP standard solutions.

3.4.8. Oxygen consumption

The oxygen consumption rate was measured in whole cells (1×10^7 in PBS buffer) from cultures grown in YPGal media, using a Clark-type oxygen electrode coupled to an Oxygraph plus system (Hansatech). Data were analysed using the OxyTrace + software.

3.4.9. 2D-gel electrophoresis

Proteins extracted from whole cells were focused in nonlinear IPG strips (Immobiline DryStrip gels pH 4–7, 7 cm, GE Healthcare) as described in (Pereira *et al.*, 2018).

Immunodetection was performed with primary antibody against mammalian ATP synthase beta subunit (1:5000; ab128743, Abcam).

3.4.10. Statistical analysis

Data were analysed in GraphPad Prism Software v8.4.3 (GraphPad Software). Values were compared by one-way ANOVA or by Student's *t*-test, *, $p < 0.05$; **, $p < 0.01$; ***, $p < 0.001$.

3.5. Acknowledgments

The authors would like to thank Mark Solomon (University of Yale, USA) and Wolfgang Seufert (University of Regensburg, Germany) for generously providing the plasmids expressing Cdh1p and Cdc20p, and expressing Cdh1-m11, respectively. The authors acknowledge the support of the i3S Scientific Platform Translational Cytometry.

3.6. Supplementary material

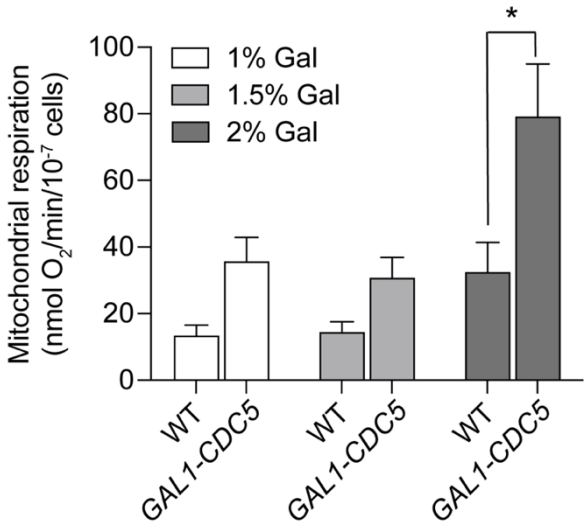

Figure 3.7. Cdc5p overexpression increases respiratory rate. *GAL1-CDC5* strain was constructed by standard PCR-based homologous recombination (Janke *et al.*, 2004; Longtine *et al.*, 1998), using pFa6a-KanMX6-pGAL1-3HA plasmid as template. Cells were grown in semi-repressive media containing 1% galactose and 1% glucose, in 1.5% galactose and 0.5% glucose, or in inducing media containing 2% galactose. The mitochondrial respiration was determined by measuring oxygen consumption rate using a Clark oxygen electrode (mean ± SEM, $n = 4$, *, $p<0.05$, two-way ANOVA, Tukey's test).

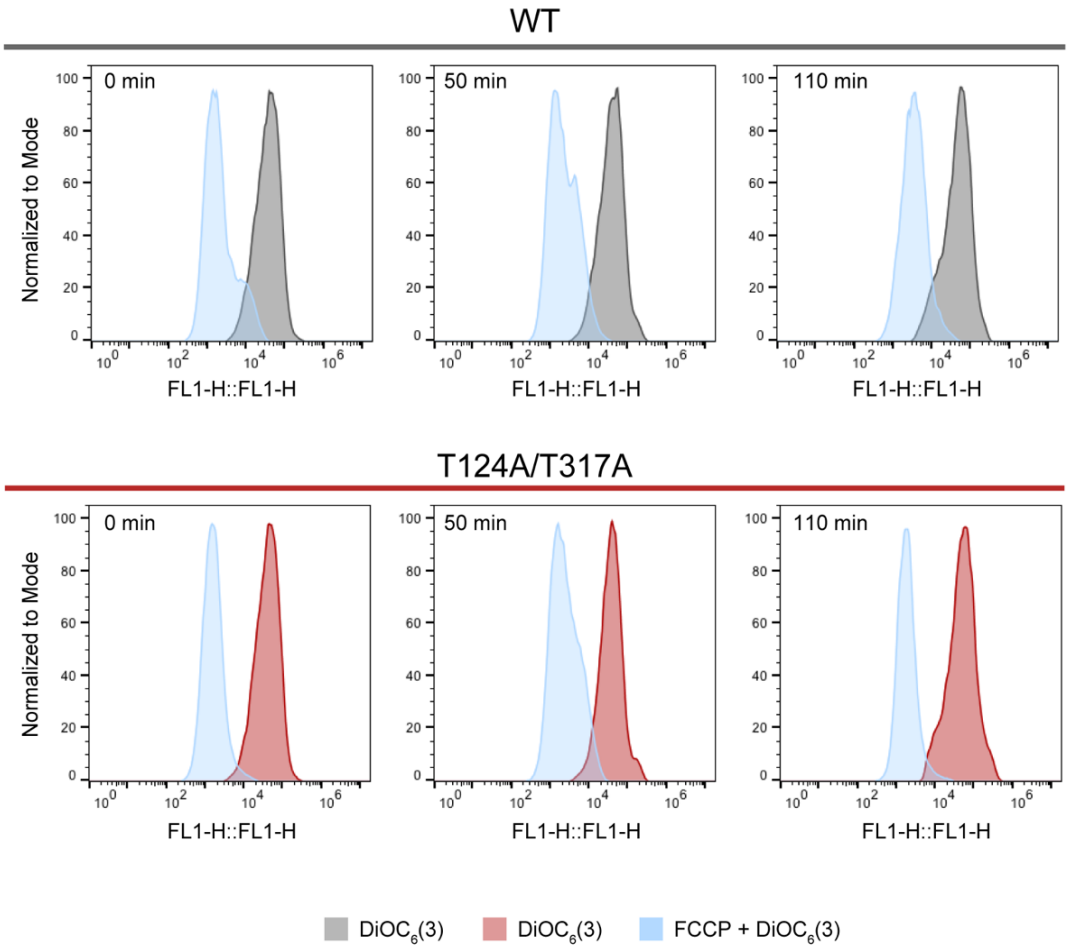

Figure 3.8. Preventing Atp2p phosphorylation decreases mitochondrial inner membrane potential. Samples from synchronized WT and T124A/T317A cell cultures were taken at the indicated time points after release from G1 arrest. Addition of the FCCP protonophore, which dissipates the Δψm, lead to a substantial reduction of the $DiOC_6(3)$ uptake for all analysed samples.

CHAPTER 4.

The APC/C activator Cdh1p plays a role in mitochondrial metabolic remodelling in yeast

This chapter was based on the following paper:

Ana Cláudia Leite, Maria Barbedo, Vitor Costa and Clara Pereira, The APC/C activator Cdh1p plays a role in mitochondrial metabolic remodelling in yeast, under revision.

The APC/C activator Cdh1p plays a role in mitochondrial metabolic remodelling in yeast

Abstract

Cdh1p is one of the two substrate adaptor proteins of the anaphase promoting complex/cyclosome (APC/C), an ubiquitin ligase that regulates proteolysis during cell cycle. In this work, using a proteomic approach, we found 135 mitochondrial proteins whose abundance was significantly altered in the *cdh1*Δ mutant, with 43 upregulated proteins and 92 downregulated proteins. The group of significantly upregulated proteins included subunits of the mitochondrial respiratory chain, enzymes from the tricarboxylic acid cycle and regulators of mitochondrial organization, suggesting a metabolic remodelling towards an increase in mitochondrial respiration. In accordance, mitochondrial oxygen consumption and cytochrome *c* oxidase activity increased in Cdh1p-deficient cells. These effects seem to be mediated by the transcriptional activator Yap1p, a major regulator of the yeast oxidative stress response. *YAP1* deletion suppressed the increased Cyc1p levels and mitochondrial respiration in *cdh1*Δ cells. In agreement, Yap1p is transcriptionally more active in *cdh1*Δ cells and responsible for the higher oxidative stress tolerance of *cdh1*Δ mutant cells. Overall, our results unveil a new role for APC/C-Cdh1p in the regulation of the mitochondrial metabolic remodelling through Yap1p activity.

Keywords: Cdh1p, Mitochondria, Proteomics, Yap1p, Yeast

4.1. Introduction

Mitochondria are essential organelles that play a critical role in several cellular functions including ATP synthesis by the oxidative phosphorylation system (OXPHOS). The biogenesis of the OXPHOS system requires the concerted expression of the nuclear and the mitochondrial genomes (Ulery *et al.*, 1994). In yeast, the mitochondrial proteome is largely dependent on substrate availability. The presence of glucose induces the catabolite repression of mitochondrial function (Brauer *et al.*, 2005; Ulery *et al.*, 1994). The transition from fermentative to respiratory metabolism (known as diauxic shift) and shift to nonfermentable carbon sources trigger a major metabolic reorganization with the transcriptional upregulation of many genes required to promote not only an increase in mitochondrial biogenesis and mitochondrial mass, but also a remodelling of mitochondria function towards a more respiratory mode, with an increase in OXPHOS complexes and tricarboxylic acid (TCA) enzymes (Di Bartolomeo *et al.*, 2020; Ohlmeier *et al.*, 2004; Renvoisé *et al.*, 2014). The mitochondrial regulation is achieved mainly at the transcriptional level by the concerted regulation of multiple transcription factors by glucose-sensing signalling pathways (reviewed in (Kayikci and Nielsen, 2015)). Signalling pathways also seem to impact on mitochondrial metabolic reprogramming independently of the carbon source. By modulating the transcription of nuclear-encoded mitochondrial proteins, the cAMP-dependent protein kinase A (PKA) pathway regulates the mitochondrial enzyme content, and not the total mass, increasing the oxidative phosphorylation capacity of the cells (Chevtzoff *et al.*, 2005; Dejean *et al.*, 2002). Likewise, reduced TOR signalling increases mitochondrial oxygen consumption, in part, by up-regulating the translation of mitochondrial genome-encoded OXPHOS subunits, enhancing the density of OXPHOS complexes (Bonawitz *et al.*, 2007; Pan and Shadel, 2009). The type 2A-related serine-threonine phosphatase Sit4p is one of the TOR complex 1 (TORC1) downstream effectors that plays a role in mitochondrial glucose repression (Jablonka *et al.*, 2006) and impacts on OXPHOS activity. Sit4p modulates the phosphorylation status of several mitochondrial proteins, including the ATP synthase catalytic beta subunit (Atp2p in yeast) (Pereira *et al.*, 2018). In the absence of Sit4p, the phosphorylation of Atp2p leads to an increase in the ATP synthase levels, impacting the activity of the respiratory chain complexes and enhancing overall mitochondrial respiration (Pereira *et al.*, 2018).

We recently reported that the Atp2p levels increase in the absence of the anaphase-promoting complex/cyclosome (APC/C) activator Cdh1p (Leite *et al.*, 2022). APC/C is an E3 ubiquitin ligase responsible for the ubiquitin-dependent degradation of many cell cycle regulators (King *et al.*, 1995; Sudakin *et al.*, 1995) and its activity is primarily regulated through the temporal activation of two cofactors, Cdc20p and Cdh1p (also known as Hct1p) (Schwab *et al.*, 2001; Visintin *et al.*, 1997). Cdc20p and Cdh1p carry conserved receptor

domains to recognize specific sequence signals such as the destruction box and the KEN box that provide substrate selectivity (Burton and Solomon, 2001). Unlike Cdc20p, Cdh1p is not essential in yeast, though *cdh1*Δ cells exhibit a prolonged cell cycle and are sensitive to different types of stress, such as caffeine, alkalinity and hyperosmotic stress (Simpson-Lavy *et al.*, 2009). In addition to targeting mitotic regulators, emerging evidence suggest that Cdh1p have cell cycle-independent functions both in yeast (Thornton and Toczyski, 2003) and mammals (Li and Zhang, 2009). Although Atp2p is not an APC/C-Cdh1p direct target (Leite *et al.*, 2022), the fact that its protein abundance is affected in cells lacking Cdh1p raises the question of whether Cdh1p may play a role in the regulation of mitochondrial function.

In the current study, we performed a mitochondrial proteomic analysis and found that deletion of *CDH1* impacts on the abundance of many mitochondrial proteins in yeast. Overall, absence of Cdh1p promotes a shift towards a higher mitochondrial respiratory metabolism, which is dependent on the basic leucine zipper (bZIP) transcription factor Yap1p.

4.2. Results

4.2.1. *CDH1* deletion leads to a remodelling of the mitochondrial proteome and promotes mitochondrial respiration

To evaluate the impact of APC/C-Cdh1p activity on yeast mitochondria, the mitochondrial proteome of wild type (wt) and *CDH1*-deleted cells was analysed by high-resolution mass spectrometry (HPLC-MS/MS). Quantification of mitochondrial proteins was performed with normalization based on total peptide amount. Cells were grown to mid-log phase under semi-respiratory conditions, using galactose as a carbon source to obtain a higher mitochondrial mass, and mitochondria were then isolated by differential centrifugation. The proteomic data obtained gave a high level of replicate reproducibility with a total of 922 proteins previously reported as mitochondrial, representing a coverage of 90-100%, depending on the reference proteome used (Morgenstern *et al.*, 2017; Vögtle *et al.*, 2017). Only these proteins were used for further data treatment.

To evaluate overall changes in the mitochondrial proteome upon *CDH1* deletion, we used biological triplicate proteomic data for significance testing of the protein abundance changes in a pairwise manner. Student's *t* test was used to identify differential protein expression between wt and *cdh1*Δ cells and represented in a volcano plot (Figure 4.1A). To analyse changes in protein abundance, a cut-off of p-value < 0.05 and an absolute log2 fold change (log2 FC) > 0.3 was applied. A total of 135 proteins exhibited altered protein abundance in the absence of Cdh1p activity, with 43 upregulated and 92 downregulated

proteins (Figure 4.1B). The top up- and downregulated mitochondrial proteins are listed in Table 4.2 and Table 4.3, respectively.

The proteins that increased the most in *cdh1*Δ cells are four succinate dehydrogenase subunits (Complex II), Sdh1p, Sdh3p, Sdh4p and Sdh6p. Among the most abundant proteins are also two Cytochrome *c* oxidase (Complex IV; Cox2p, Cox5p) subunits, two subunits of Cytochrome bc_1 complex (Complex III; Qcr2p and Rip1p) as well as the NADH:ubiquinone oxidoreductase (equivalent to mammalian Complex I; Ndi1p). This shows that deletion of *CDH1* increases the abundance of proteins from all respiratory chain complexes. Among the most overrepresented proteins are also the respiratory chain soluble carrier Cytochrome *c* isoform 1 (Cyc1p), Aconitase (Aco1p) and the ADP/ATP translocator isoform (Aac1p), also involved in the respiratory metabolism. As we previously found, Atp2p was statistically significantly upregulated in *cdh1*Δ cells, but stayed below our defined threshold.

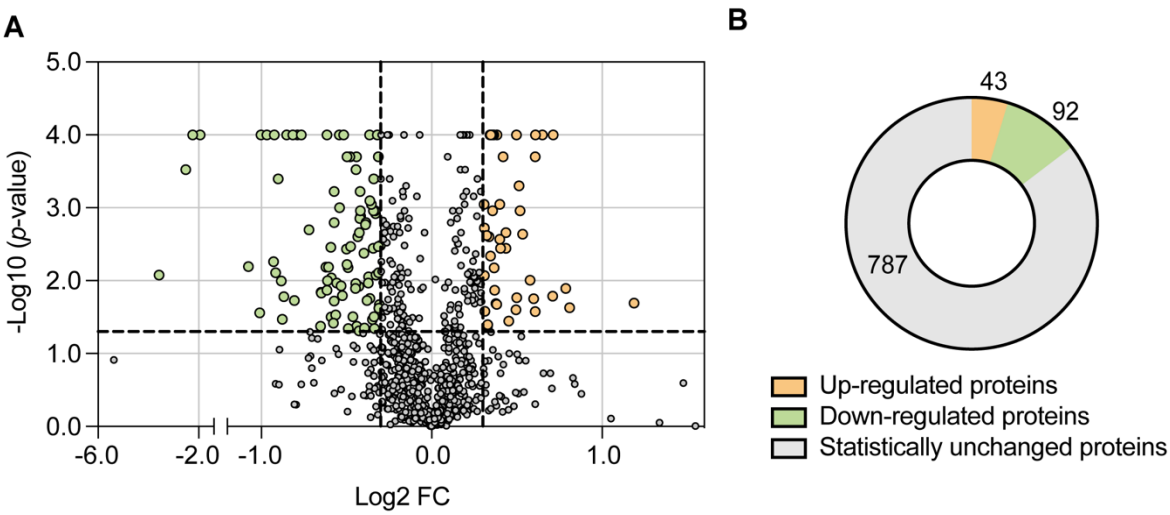

Figure 4.1. A total of 135 mitochondrial proteins exhibited significantly altered abundance in Cdh1p-deficient cells. (A) Volcano plot showing differentially expressed proteins in *cdh1*Δ mutant. Log-transformed *p*-values (*t*-test) are plotted against log-transformed fold change (FC). The horizontal dashed line marks a *p*-value of 0.05. Vertical dashed lines indicate a Log2 FC of ± 0.3. The upregulated and downregulated mitochondrial proteins are highlighted in orange and green, respectively. The plot was cropped between -1.4 and -1.2 Log2 FC to improve data visualization. (B) Diagram depicting the number of mitochondrial proteins up- and downregulated in *cdh1*Δ mutant cells.

To identify the biological processes most impacted in *cdh1*Δ cells, a gene ontology (GO)-term enrichment analysis on biological processes was run using STRING v11.0 database (Szklarczyk *et al.*, 2018). This analysis showed that among the 43 upregulated mitochondrial proteins, the TCA cycle and mitochondrial respiration were the most represented processes (Figure 4.2A). Our results are consistent with the mitochondrial proteome analysis of yeast grown in respiratory conditions (versus fermentative) in which

an overrepresentation of proteins associated to these processes have been reported (Casanovas *et al.*, 2015; Di Bartolomeo *et al.*, 2020; Renvoisé *et al.*, 2014). We also found that proteins associated with mitochondrial protein synthesis and mitochondrial organization are enriched in the *cdh1*Δ mutant, namely several proteins involved in respiratory complexes assembly and two proteins involved in mitochondrial morphology, Fis1p and Dnm1p. Since both proteins are involved in fission, we analysed the mitochondrial network morphology in the *cdh1*Δ mutant but found no alterations in mitochondrial morphology (Figure 4.8). However, this was not entirely unexpected, as increased Fis1p and Dnm1p abundance are also associated to the proteome remodelling that occurs upon the transition to a respiration metabolism, and this is not associated to mitochondrial fragmentation (Casanovas *et al.*, 2015; Di Bartolomeo *et al.*, 2020).

On the other hand, the 92 downregulated proteins include proteins from diverse functional categories, with fatty acid metabolism (Cat2p and Oar1p among the most abundant in this category) and amino acid metabolism (glycine catabolism and aspartate synthesis) as the most relevant downregulated biological process in the *cdh1*Δ mutant.

These results suggest that deletion of *CDH1* promotes a metabolic remodelling towards an increased respiratory metabolism, demonstrated by the upregulation of proteins involved in energy generation. An increase in the abundance of proteins associated to the respiratory chain and TCA cycle are hallmarks in the transition from fermentative to respiratory growth conditions (Di Bartolomeo *et al.*, 2020). To confirm these results, oxygen consumption in the *cdh1*Δ mutant was evaluated in whole cells in the conditions used for the proteomic analysis. In accordance, the results showed a 1.8-fold increase in mitochondrial respiration in *cdh1*Δ cells compared to wt cells (Figure 4.2B). We also assessed the oxygen consumption rate of *cdh1*Δ cells from post-diauxic shift (PDS) cells, when yeast switch their growth from fermentation to mitochondrial respiration. At PDS, the oxygen consumption rate in *cdh1*Δ cells was similar to that in wt cells (Figure 4.2B), indicating that Cdh1p does not regulate the normal derepression of respiratory genes at the diauxic shift. This suggests that either Cdh1p plays a role in mitochondrial function only in proliferating cells, or that it exhibits an early catabolite derepression.

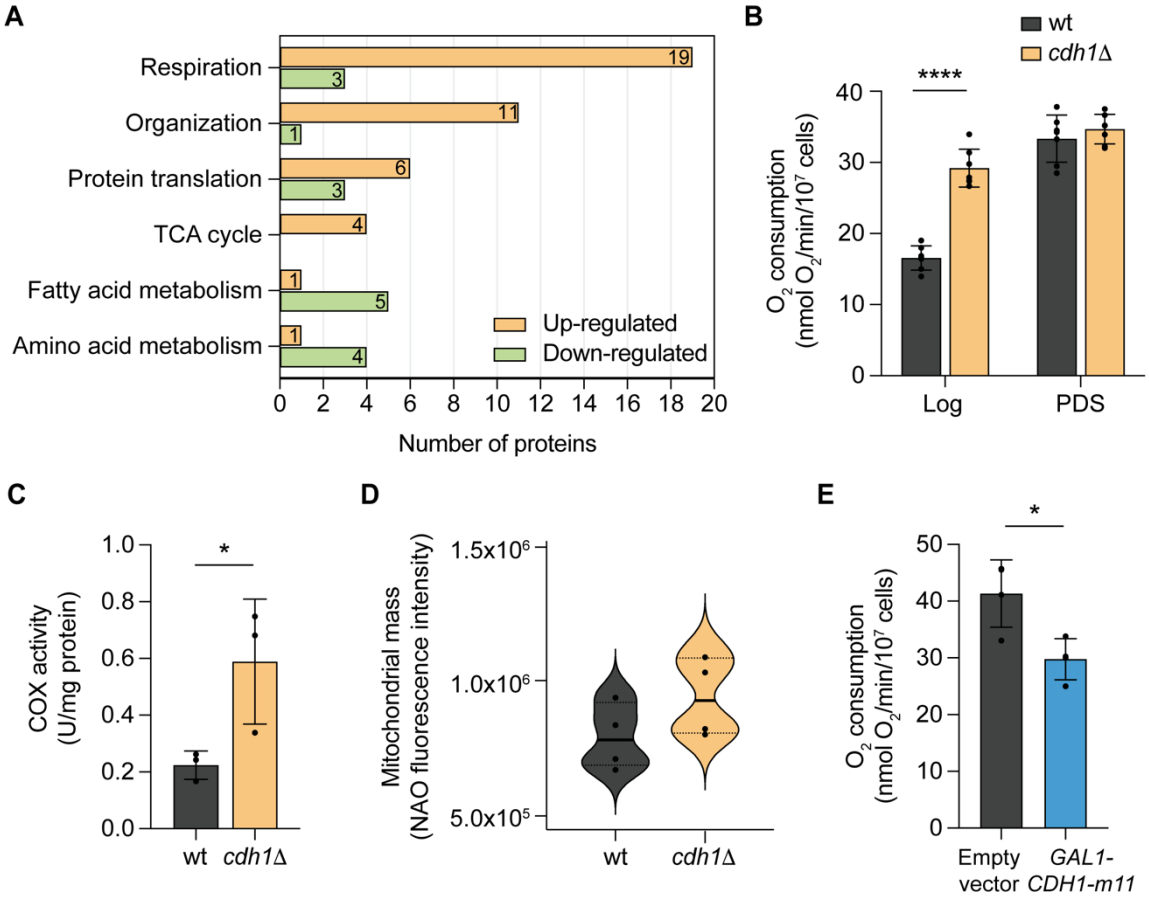

Figure 4.2. *CDH1* deletion promotes a metabolic remodeling towards an increased respiratory metabolism. (A) Gene ontology (GO)-term enrichment analysis on biological processes for statistically altered proteins using STRING v11.0. (B) Cells were grown until mid-log or post-diauxic shift (PDS) phase and the respiratory rate was obtained measuring oxygen consumption rate in whole cells. Values are the mean ± SD (n = 7); ****, $p < 0.0001$; t-test. (C) Cells were grown until mid-log phase and cytochrome c oxidase activity was determined by following the rate of cytochrome c oxidation. Values are the mean ± SD (n = 3); *, $p < 0.05$; t-test. (D) Cells were grown until early-log phase and the mitochondrial mass was determined by staining the cells with the dye nonyl acridine orange (NAO) and analyzed by flow cytometry (n = 4). (E) For the Cdh1p overexpression assay, cells were grown in raffinose media until mid-log phase and oxygen consumption rate measured after 3h of addition of 4% galactose. Values are the mean ± SD (n = 4); *, $p < 0.05$; t-test.

The increase in mitochondrial respiration in mid-log *cdh1*Δ cells was further supported by the increased activity of the respiratory complex cytochrome *c* oxidase (COX) (from 0.22 U/mg protein in wt to 0.59 U/mg protein in *cdh1*Δ mutant; Figure 4.2C). Since the remodelling towards a more respiratory metabolism is often accompanied by an increase in mitochondrial biogenesis, we performed *in vivo* measurements of mitochondrial mass, using nonyl acridine orange (NAO) fluorescence. We found that the mitochondrial mass is mildly increased in *cdh1*Δ cells when compared to wt cells, but the difference was not statistically significant ($7.9x10^5 \pm 1.2x10^5$ to $9.4x10^5 \pm 1.5x10^5$, mean ± SD, Figure 4.2D). This indicates that the increased mitochondrial respiration in *cdh1*Δ cells is mostly due to an increase in the respiratory capacity of mitochondria than to an increase in mitochondrial

mass. Furthermore, overexpression of a constitutively active Cdh1-m11 form (lacking the 11 Cdk inhibitory-phosphorylation sites) (Zachariae *et al.*, 1998) results in a decrease in mitochondrial respiration compared to wt cells expressing the empty vector (Figure 4.2E).

4.2.2. The transcription factors Yap1p and Rpn4p mediate the induction of mitochondrial respiration in *cdh1*Δ cells

Since Cdh1p is part of an E3 ubiquitin ligase complex, it is possible that part of the mitochondrial proteins could be regulated by Cdh1p-mediated proteolysis. However, given the high number of altered proteins, with a high proportion of downregulated proteins, it is most likely that Cdh1p is impacting on mitochondrial proteins indirectly, possibly through the modulation of transcription factor(s). The repository YEASTRACT+ (Yeast Search for Transcriptionally Regulators And Consensus Tracking) (Teixeira *et al.*, 2022) was used to predict the transcription factors that might be responsible for the protein expression patterns in *cdh1*Δ cells. This led to the identification of four transcription factors as possibly regulating the adaptive responses to *CDH1* deletion (Figure 4.3A). This list includes Pdr3p (regulator of the pleiotropic drug resistance), Gcn4p (regulator of amino acid biosynthetic genes in response to amino acid starvation), Yap1p (regulator of the oxidative stress response) and Rpn4p (regulator of the proteasome). To investigate whether these transcription factors mediate the effects of *CDH1* deletion on mitochondrial function, double mutant strains deleted both in *CDH1* and in the individual transcription factors were constructed. The absence of the selected transcription factors on the *cdh1*Δ mitochondrial phenotype was first evaluated by measuring oxygen consumption rate. Our results show that deletion of *PDR3* and *GCN4* did not significantly affect *cdh1*Δ high oxygen consumption. On the other hand, both *YAP1* and *RPN4* deletion restored *cdh1*Δ respiration to wt levels (Figure 4.3B). We also assessed the impact of the transcription factors deletion on cell growth by measuring optical density (OD_{600nm}) over time (Figure 4.3C). For quantitative evaluation of growth and statistical analysis purposes, the area under each growth curve was also calculated (AUC; values in Figure 4.9). Cells lacking Cdh1p exhibited a significant growth delay when compared to wt cells, which can be attributed to the accumulation of cell cycle progression substrates, like Clb2p and Ase1p (Visintin *et al.*, 1997). Deletion of *PDR3*, *RPN4* and *YAP1* improved the growth of *cdh1*Δ cells. This effect was more significant for YAP1 deletion that, despite not reverting *cdh1*Δ growth to wt levels (AUC of 19.4), almost doubled the AUC from 6.7 in *cdh1*Δ cells to 12.5 in *yap1*Δ*cdh1*Δ cells. This suggests that *YAP1* genetically interacts with *CDH1* and contributes to the *cdh1*Δ mutant slow growth phenotype.

A

Transcription factor	% in up-regulated proteins	*p* value	% in down-regulated proteins	*p* value
Pdr3p	97.7	1.0×10^{-4}	95.6	5.4×10^{-6}
Gcn4p	93.0	1.1×10^{-2}	100.0	0.1×10^{-10}
Yap1p	97.7	1.1×10^{-4}	97.8	7.8×10^{-8}
Rpn4p	97.7	2.6×10^{-5}	97.8	3.8×10^{-9}

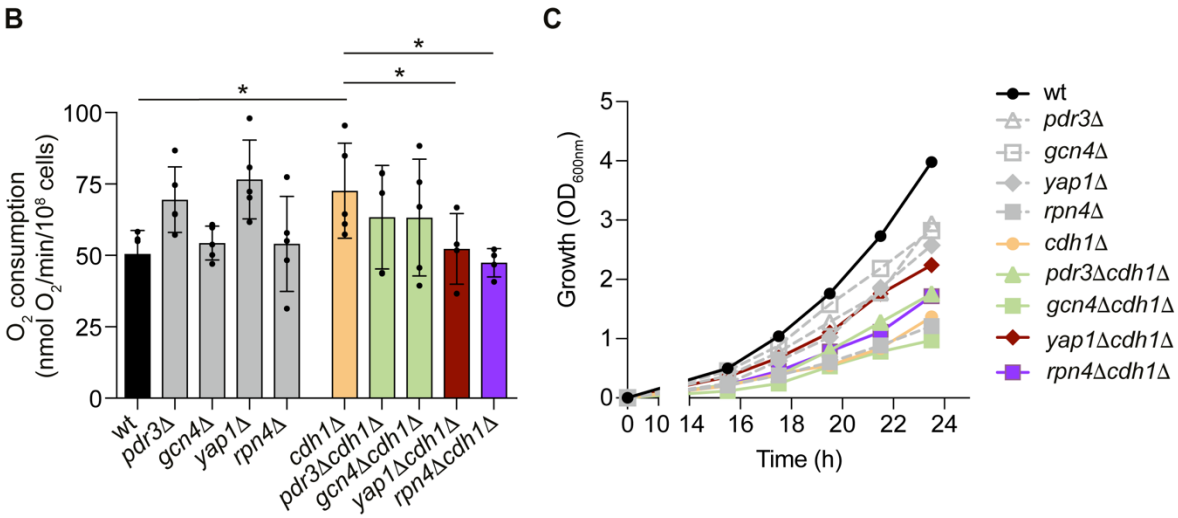

Figure 4.3. The transcription factors Yap1p and Rpn4p are required for the increase of mitochondrial respiration in the *cdh1*Δ mutant. (A) Table showing the YEASTRACT+ predicted transcription factors that might regulate the mitochondrial proteins altered in *cdh1*Δ cells. (B) Cells were grown until late-log phase and the respiratory rate was obtained measuring oxygen consumption rate in whole cells. Values are the mean ± SD (n = 4); *, $p < 0.05$; one-way ANOVA followed by Tukey's multiple-comparison test. (C) The growth of the indicated strains was monitored over time by optical density (OD_{600nm}) measurements. Values are the mean (n = 3).

To further evaluate this functional relationship, we assessed how the deletion of *RPN4* and *YAP1* affected the expression of mitochondrial proteins previously identified as upregulated (Cyc1p and Cox2p) in *cdh1*Δ cells. Cyc1p and Cox2p were among the proteins identified by YEASTRACT+ as potentially transcriptionally regulated by Yap1p and Rpn4p. Tim22p, which was found unaltered *cdh1*Δ cells, was also analysed as a control of mitochondrial mass. Accordingly, we found Cyc1p and Cox2p, but not Tim22p, accumulated at higher levels in proliferating *cdh1*Δ cells (Figure 4.4). Our results also show that Cyc1p levels were significantly decreased after deletion of both *YAP1* and *RPN4* in *cdh1*Δ cells. Cox2p levels also decreased in the double mutants when compared with *cdh1*Δ cells, but the difference was not statistically significant (Figure 4.4).

Overall, these results suggest that transcription factors Yap1p and Rpn4p function as Cdh1p downstream effectors in the regulation of mitochondrial protein levels. Interestingly, Yap1p and Rpn4p are functionally related, as *YAP1* itself contains a Proteasome Associated Control Elements (PACE) sequence in its promotor targeted by Rpn4p (Fleming

et al. , 2002) while *RPN4*, in turn, can be transcriptionally regulated by Yap1p (Owsianik *et al.* , 2002).

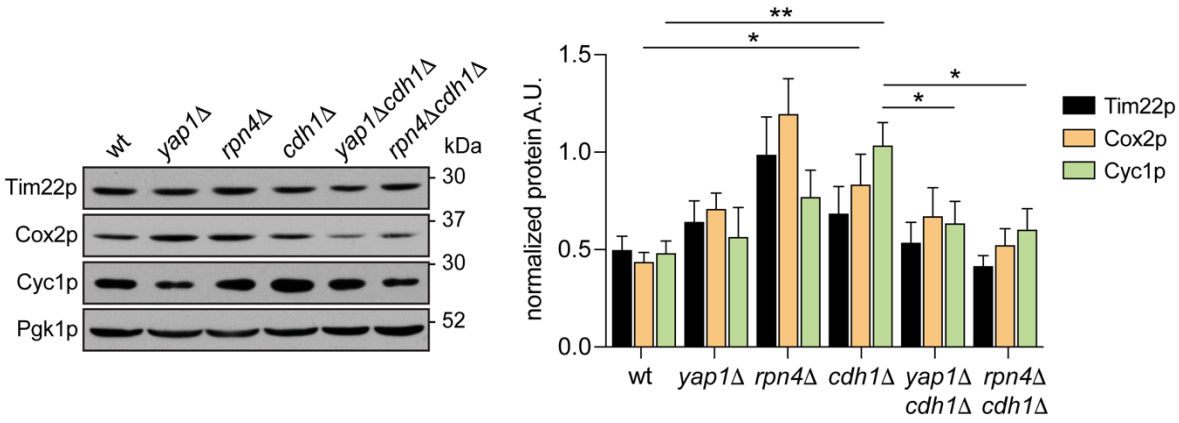

Figure 4.4. The upregulation of Cyc1p in the *cdh1*Δ mutant is mediated by the transcription factors Yap1p and Rpn4p. Cells with the indicated genotypes were grown until mid-log phase and Cox2p and Cyc1p levels on total proteins extracts were assessed by immunodetection. Tim22p (inner mitochondrial protein unchanged in *cdh1*Δ cells) is shown as control of mitochondrial mass. A representative blot is shown. Graph represents the relative amount of Tim22p, Cox2p and Cyc1p normalized to Pgk1p. Values are the mean ± SEM (n = 5); *, $p < 0.05$; **, $p < 0.01$; t-test.

4.2.3. *CDH1* deletion does not impact on Rpn4p activity

Yeast Rpn4p is a C_2H_2 zinc finger transcription factor that is responsible for the expression of genes associated with proteasome biogenesis and activity and with ubiquitin-dependent proteolysis (Mannhaupt *et al.*, 1999; Xie and Varshavsky, 2001). Inhibition of proteasome activity results in a Rpn4p stabilization, which binds to PACE sequences, found in Rpn4p-recognized promotors, upregulating its target genes (Mannhaupt *et al.*, 1999).

We next investigated the hypothesis that the direct targeting of Rpn4p by APC/C-Cdh1p may account for the mitochondrial alterations induced by *CDH1* deletion. For that, the levels of Rpn4p were evaluated by Western blot, in cells expressing HA-tagged endogenous Rpn4p. We found that Rpn4p stability was not increased by *CDH1* deletion (Figure 4.5A), suggesting that Rpn4p is not a direct substrate of APC/C-Cdh1p. In addition, it suggests that Rpn4p is not more active in *cdh1*Δ cells, as Rpn4p stabilization is associated to its activity (Dohmen *et al.*, 2007). To confirm this, we assessed Rpn4p transcriptionally activity using a Rpn4p-driven GFP reporter (Work and Brandman, 2020). As a positive control, wt cells were incubated with 60 μM of the proteasome inhibitor MG132 for 2h. As shown in Figure 4.5B, GFP fluorescence was significantly elevated in MG132-treated cells while *RPN4*-deleted cells showed a strong decrease, validating the reporter specificity. However, loss of Cdh1p did not affect Rpn4p transcriptional activity, supporting the hypothesis that Rpn4p is not more active in *CDH1*-deleted cells. These results suggest that Rpn4p activation is not the primary cause leading to Cdh1p-mediated upregulation of mitochondrial respiration.

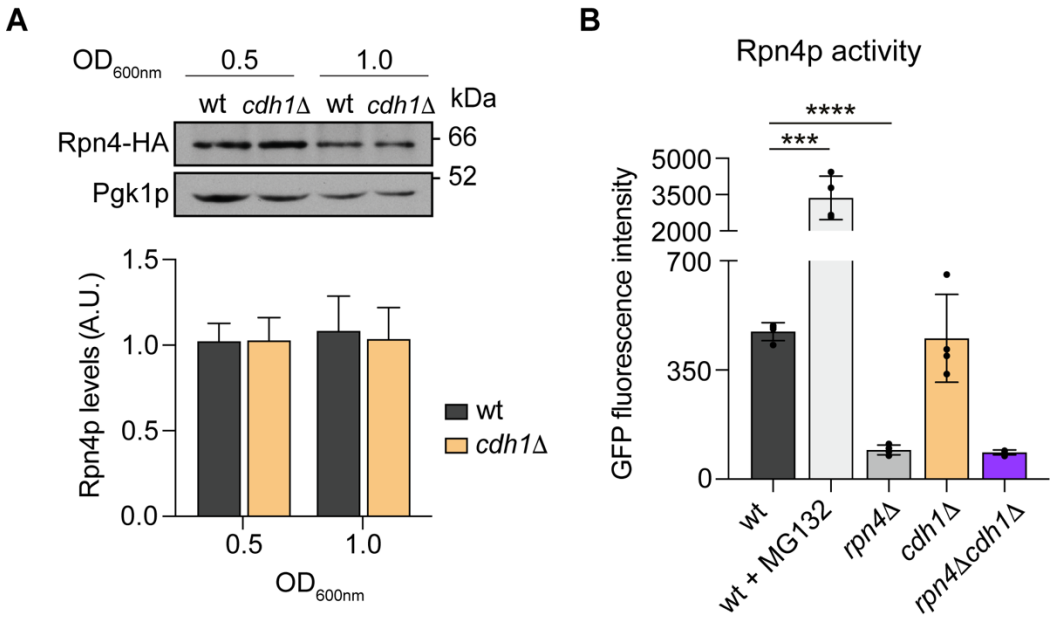

Figure 4.5. Rpn4p levels or activity are not altered in *cdh1*Δ mutant cells. (A) Wt or *cdh1*Δ cells endogenously expressing hemagglutinin (HA)-tagged Rpn4p were grown to early and mid-log phase and analyzed by immunoblotting using anti-HA and anti-Pgk1p (loading control) antibodies. A representative blot is shown. Graph represents the relative amount of Rpn4-HA normalized to Pgk1p. Values are the mean ± SEM (*n* = 4). (B) Cells with the indicated genotypes harboring a GFP reporter for Rpn4p activity were grown to early-log phase. As a positive control, wt cells were treated with the proteasome inhibitor MG132. The GFP fluorescence intensity was determined by flow cytometry. The values are the mean ± SD (*n* = 4), ***, $p < 0.001$; ****, $p < 0.0001$; *t*-test.

4.2.4. Yap1p is more active in *cdh1*Δ cells

Yeast Yap1p is a leucine zipper (bZIP) transcription factor that activates the expression of genes encoding several antioxidant proteins (Delaunay *et al.*, 2002). Yap1p is activated in response to different reactive oxygen species (ROS), such as hydrogen peroxide (H_2O_2), by a mechanism that inhibits its nuclear export, thus promoting Yap1p nuclear accumulation and activation (Coleman Sean *et al.*, 1999; Kuge *et al.*, 1997; Wemmie *et al.*, 1997). Besides its well-known role in the oxidative stress response, Yap1p is also involved in the yeast response to metals and unrelated drugs (Wemmie *et al.*, 1997) and seems to play a role in mitochondrial regulation (Jun *et al.*, 2012; Li *et al.*, 2020; Zyrina Anna *et al.*, 2017).

We next investigated the hypothesis that the direct targeting of Yap1p by APC/C-Cdh1p may account for the mitochondrial alterations induced by *CDH1* deletion. For that, we compared the steady-state level of the Yap1p protein in wt and *cdh1*Δ cells. The Yap1-9Myc protein was expressed from a vector under the regulation of its native promoter in the *yap1*Δ and *yap1*Δ*cdh1*Δ mutants. As shown in Figure 4.6A, no difference was detected in the protein levels of Yap1p at OD_{600nm} 0.5 suggesting Yap1p is not a Cdh1p direct substrate. In addition, the levels of Yap1p were also not affected by expression of a constitutively active Cdh1-m11 form (lacking the 11 Cdk inhibitory-phosphorylation sites) (Zachariae *et*

al., 1998) or after mutation in a potential APC/C recognition motif predicted using GPS-ARM 1.0 (Figure 4.10). Intriguingly, at OD_{600nm} 1.0, Yap1p levels were even decreased in cells lacking Cdh1p (Figure 4.5A). It was previously reported that Yap1p activity is mostly controlled by the disruption of Yap1p nuclear export without affecting protein levels (Maeta *et al.*, 2004; Wemmie *et al.*, 1997). However, a decrease in Yap1p protein levels is often observed following its activation (Gulshan *et al.*, 2012; Maeta *et al.*, 2004; Wemmie *et al.*, 1997). Therefore, our results suggest that Yap1p is not a direct Cdh1p target, but its transcriptional activity might be indirectly regulated by Cdh1p. To investigate this hypothesis, we monitored Yap1p transcriptional activity in *cdh1*Δ cells, using a Yap1p-dependent lacZ reporter (pRS415-AP-1-CYC-LacZ) (Maeta *et al.*, 2004). As a positive control, wt cells were treated with 5 mM H_2O_2 for 1.5h, which triggered a significantly increase in β-galactosidase activity (Figure 4.5B). On the other hand, the Yap1p-dependent β-galactosidase activity in *yap1*Δ cells was dramatically decreased, confirming the reporter specificity. Notably, the results showed a 1.7-fold increase of β-galactosidase activity in *cdh1*Δ cells compared to wt cells, indicating that Yap1p transcriptional activity is increased in cells lacking Cdh1p.

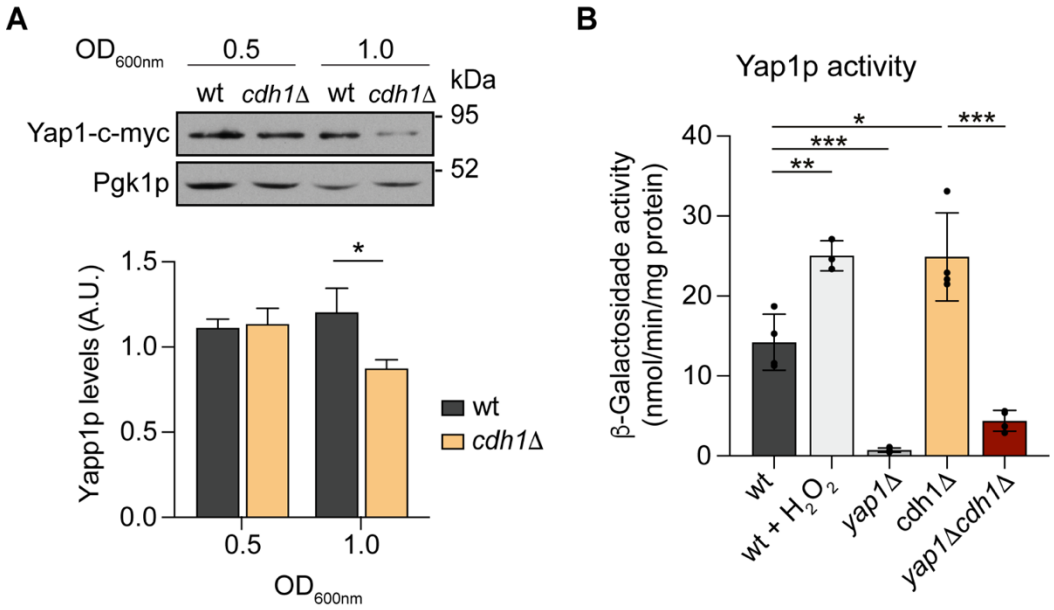

Figure 4.6. *CDH1* deletion leads to Yap1p activation. (A) *yap1*Δ and *yap1*Δ*cdh1*Δ cells harboring pRS315-Yap1-c-Myc plasmid were grown to early and mid-log phase and total protein extracts were separated by SDS-PAGE and analyzed by immunoblotting using anti-c-myc and anti-Pgk1p. A representative blot is shown. Graph represents the relative amount of Yap1-c-myc normalized to Pgk1p. Values are the mean ± SEM ($n = 4$); *, $p < 0.05$; *t*-test. (B) Cells with the indicated genotypes harboring pRS415-AP-1-CYC1-LacZ reporter were grown to mid-log phase. As a positive control, wt cells were exposed to hydrogen peroxide (H_2O_2). The specific β-galactosidase activity was determined using *o*-nitrophenyl-β-d-galactopyranoside (ONPG) as a substrate. The values are the mean ± SD ($n = 4$), *, $p < 0.05$; **, $p < 0.01$; ***, $p < 0.001$; *t*-test.

4.2.5. Yap1p mediate the oxidative stress resistance of *cdh1*Δ cells

Since Yap1p is a major oxidative stress response regulator in yeast, we asked whether its increased transcriptional activity in *cdh1*Δ cells led to an increase in oxidative stress resistance. To test this hypothesis, cells were grown in solid media in the presence of H_2O_2. As expected, deletion of *YAP1* dramatically increases the H_2O_2 sensitivity (Figure 4.7A). In contrast, cells lacking Cdh1p presented a higher oxidative stress resistance compared to wt cells, particularly evident at the higher H_2O_2 concentration used. The increase in H_2O_2 resistance was dependent on Yap1p since its deletion in *cdh1*Δ cells restored oxidative stress sensitivity (Figure 4.7A). In contrast, *cdh1*Δ cells, but not *yap1*Δ cells, were more sensitive to methyl methanesulfonate (MMS) comparing to wt (Figure 4.7A), as reported for several other stressors (Simpson-Lavy *et al.*, 2009). These findings indicate that *cdh1*Δ cells are unexpectedly resistant to oxidative stress, and that this occurs due to Yap1p activation.

Under physiological conditions, mitochondria serve a major source of ROS that are mainly generated from the mitochondrial respiratory chain as a normal consequence of aerobic respiration (Aon *et al.*, 2012; Balaban *et al.*, 2005). Since *CDH1* deletion led to an upregulation of mitochondrial respiration, we investigated its effect on ROS levels using dihydroethidium (DHE) as a probe that becomes fluorescent upon oxidation by superoxide radicals and hydrogen peroxide. At early-log phase, approximately 1% of wt cells exhibited ROS accumulation, whereas 10% of *cdh1*Δ cells displayed DHE staining (Figure 4.10B). ROS levels in the *yap1*Δ*cdh1*Δ double mutant were similar to that in *cdh1*Δ cells (Figure 4.7B). Since *YAP1* deletion lowered the increase in mitochondrial respiration in *cdh1*Δ cells, but not the ROS levels, we questioned whether the higher ROS levels in *cdh1*Δ cells may underlie Yap1p activation in these cells and precede the mitochondrial remodelling. To test this hypothesis, we analysed Yap1p transcriptional activity in *cdh1*Δ cells after overexpression of the mitochondrial superoxide dismutase (Sod2p) using Yep352-*SOD2* plasmid (Vilaça *et al.*, 2014). Overexpression of *SOD2* decreased the Yap1p-dependent β-galactosidase activity in *cdh1*Δ cells comparing to cells expressing the empty-vector (Figure 4.7C). However, *SOD2* overexpression did not fully lower the Yap1p activity in the *cdh1*Δ mutant to the levels observed in wt cells overexpressing *SOD2*. This result led us to hypothesized that in *cdh1*Δ cells Yap1p is transcriptionally more active, leading to an increase in mitochondrial respiration, which result in higher mitochondrial ROS production. These in turn, in a positive feedback loop, further favours Yap1p activation in these cells.

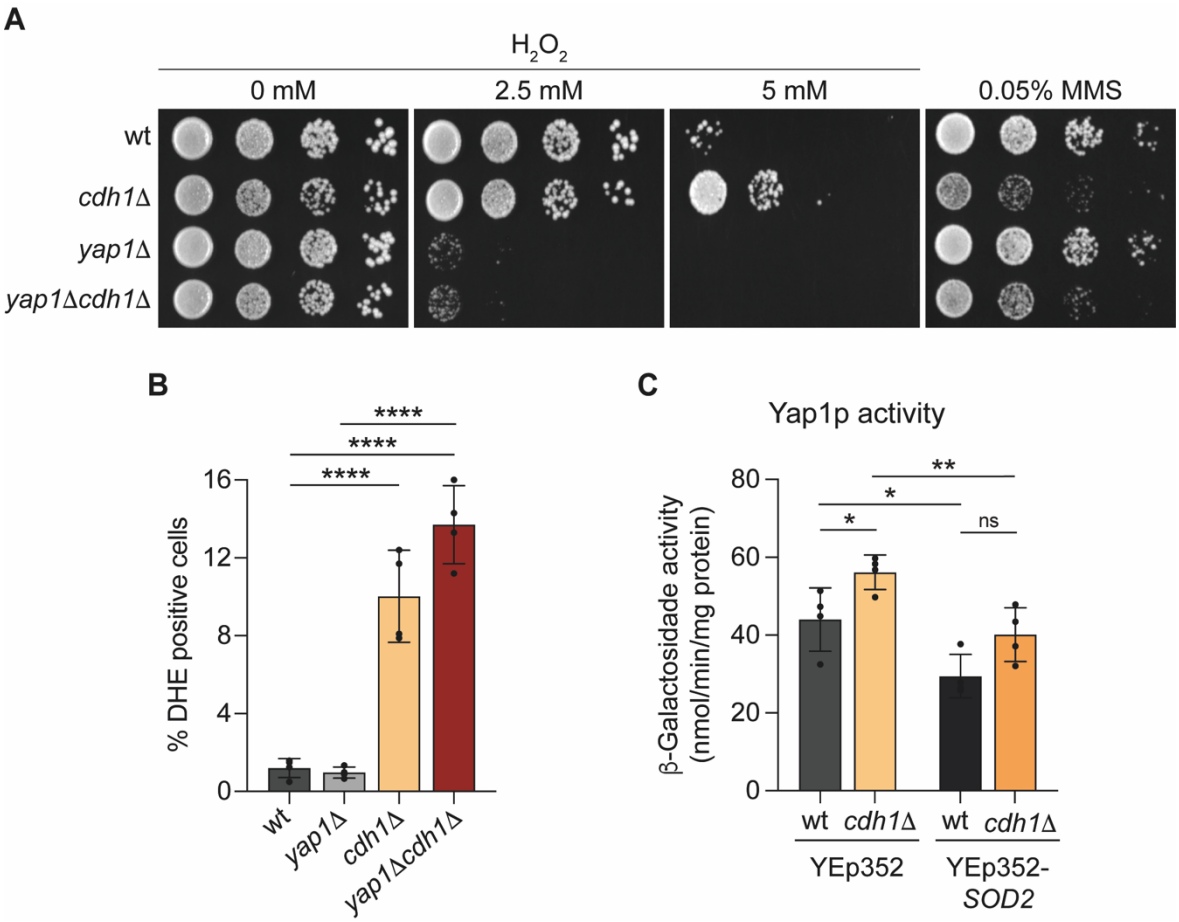

Figure 4.7. Yap1p mediates the oxidative stress resistance of the *cdh1Δ* strain. (A) H_2O_2 and methyl methanesulfonate (MMS) sensitivity of wt, *cdh1*Δ, *yap1*Δ and *yap1*Δ*cdh1*Δ cells. Cells were grown until mid-log phase and ten-fold dilutions were spotted onto YPGal plates without a stressor or with 2.5 - 5 mM H_2O_2 or 0.05% MMS. Plates were incubated at 26 °C for 2 days. A representative image is shown (n = 3). (B) Cells with the indicated genotypes were grown until early-log phase and cellular ROS levels were assessed by flow cytometry using the fluorescent probe dihydroethidium (DHE). The values are the mean ± SD (n = 4), ****, $p < 0.0001$; one-way ANOVA followed by Tukey's multiple-comparison test. (C) Cells with the indicated genotypes harboring pRS415-AP-1-CYC1-LacZ reporter were grown to mid-log phase. The specific β-galactosidase activity was determined using *o*-nitrophenol-β-d-galactopyranoside (ONPG) as a substrate. The values are the mean ± SD (n = 4), ns, not significant, *, $p < 0.05$; **, $p < 0.01$; t-test.

4.3. Discussion

In this work, we investigated the role of Cdh1p in the control of mitochondrial function using a proteomic approach. Cdh1p has a well-known role in ubiquitination of cell cycle substrates, regulating cell cycle processes such as G1/S transition and mitotic exit (Schwab *et al.*, 2001). This study provides for the first-time evidence that Cdh1p also plays a role in the regulation of mitochondrial functional remodelling and provides a global overview of the specific mitochondrial changes elicited by *CDH1* deletion. We found that deletion of *CDH1* causes a shift in mitochondrial proteome composition to promote a more respiratory mode, which was confirmed by measuring oxygen consumption and COX activity. Besides the canonical functions of APC/C, some studies in mammalian cells point to a role for Cdh1p in

the regulation of metabolism and mitochondrial morphology (Horn *et al.*, 2011; Lambhate *et al.*, 2021). APC/C-Cdh1 impacts on mitochondrial morphology by ubiquitinating Drp1 (the Dnm1p homologue) contributing to the maintenance of a dynamic balance between mitochondrial fission and fusion during mitotic exit (Horn *et al.*, 2011). Though we also found an increase in Dnm1p levels in cells lacking Cdh1p, due to the high number of mitochondrial proteins altered in the *cdh1*Δ mutant (135), with about two-thirds being downregulated, it is more likely these are indirect effects. However, we cannot discard the hypothesis that, among the upregulated proteins, some might be direct targets and subject to Cdh1p-regulated proteolysis. In fact, many mitochondrial proteins have potential Cdh1p canonical recognition motifs. However, the APC/C motifs are very common in the proteome (Pfleger and Kirschner, 2000) and, thus, are not strong substrate predictors and need to be experimentally validated.

The upregulation of mitochondrial respiration in *cdh1*Δ mutant was suppressed upon deletion of genes encoding the transcription factors Yap1p or Rpn4p, supporting an indirect regulation of mitochondrial function. Though both Yap1p and Rpn4p, a downstream target of Yap1p (Yokoyama *et al.*, 2006), were required for mitochondrial functional remodelling in the *cdh1*Δ mutant, only Yap1p was found to be more active in these cells. Due to the functional relation between Yap1p and Rpn4p, Rpn4p may contribute to Yap1p effects, but the upregulation of Yap1p function is likely the main trigger for the mitochondrial alterations in *cdh1*Δ cells. Yap1p is the main oxidative stress response regulator in yeast, but several works point for a potential role for Yap1p in mitochondrial function. Indeed, it was demonstrated that the transcription factor Yap1p is directly involved in the regulation of iron export from the mitochondria (Li *et al.*, 2020) and plays a role in the mitochondrion-to-nucleus signalling during growth on ethanol (Zyrina Anna *et al.*, 2017). Importantly, Yap1p overexpression leads to an increase in the abundance of mitochondrial proteins associated to respiration (Jun *et al.*, 2012), supporting our observations that increased Yap1p activity can lead to an enhancement in mitochondrial respiration in *cdh1*Δ cells. Interestingly, in the same study, authors also report Yap1p overexpression triggers alterations in proteins associated to cell cycle and growth regulation. Though Cdh1p can have cell cycle-independent functions, its main role is the regulation of cell cycle progression. Since we and others have found a synchronization between cell cycle progression and mitochondrial respiration in yeast (Harbauer *et al.*, 2014; Leite *et al.*, 2022), it will be interesting to assess if the role of Cdh1p in the regulation of mitochondrial function is cell cycle-independent or occurs during cell cycle progression. In fact, the oxygen consumption during cell cycle progression is lowest in G1, the phase in which Cdh1p is more active (Harbauer *et al.*, 2014; Leite *et al.*, 2022). Likewise, the lower effect in the mitochondrial proteome remodelling in the *cdh1*Δ mutant compared to the transition to growth in respiratory substrates, fits well

with the maximum oscillations found in mitochondrial respiration during cell cycle progression (about 1.3-fold) (Leite *et al.*, 2022). In addition, Cdh1p does not seem to play a role in the traditional diauxic shift transition to respiration, as it did not affect the yeast respiration in PDS phase. In addition, Yap1p and Rpn4p are not important players in mitochondrial transcriptional regulation at this phase, with Msn2p and Msn4p (Boy-Marcotte *et al.*, 1998), Cat8p (Haurie *et al.*, 2001) and Sip4p (Vincent and Carlson, 1998) as the main transcriptional factors involved in mitochondrial derepression. This suggests that Cdh1p impacts on mitochondrial respiration in proliferating cells independently of the canonical carbon source-responsive pathways.

A remaining question is also how APC/C-Cdh1p regulates the activity of Yap1p to promote the induction of mitochondrial respiration. We provide evidence that *CDH1* deletion affects Yap1p activity but not its protein levels. It is therefore possible that Cdh1p may regulated the proteins involved in the regulation of Yap1p activity/nuclear export. Since we found that *cdh1*Δ cells exhibit higher ROS levels than wt cells, it is also possible that Yap1p is being activated by the oxidative environment of *cdh1*Δ cells. Curiously, though Yap1p seem involved in the upregulation of respiration in *cdh1*Δ cells, Yap1p transcriptionally activity has been described to be also induced by mitochondrial respiration (Jamieson, 1992; Stephen *et al.*, 1995). The mitochondria respiratory chain is the major source of endogenous ROS (Aon *et al.*, 2012) and therefore transition to mitochondrial respiratory growth is accompanied by the induction of cellular antioxidant defences, which allows the cells to become intrinsically more tolerant to oxidants than fermentatively grown yeast (Jamieson, 1992; Stephen *et al.*, 1995). Activation of Yap1p in *cdh1*Δ cells may allow to coordinate mitochondrial respiration with oxidant resistance, particularly vital if the regulation of mitochondrial function by Cdh1p occurs during cell division, as ROS are particularly harmful to replicating DNA (Chen *et al.*, 2007) and can lead to cell cycle arrest (Flattery-O'Brien and Dawes, 1998). Interestingly, two additional transcription factors, Tos4p and Pdr3p, implicated in the DNA damage response were reported to be positively regulated by Cdh1p (Ostapenko *et al.*, 2012). Together with our results, this suggests Cdh1p may play a broader role than believed in the cellular transcriptional responses to different environmental stresses.

In conclusion, our study reveals a novel role for Cdh1p in the regulation of mitochondrial metabolic remodelling contributing to our understanding of the signalling pathways controlling cellular energy homeostasis. Regulation of mitochondrial metabolism occurs after glucose exhaustion, in the presence of alternative respiratory carbon sources and even during cell cycle progression (Harbauer *et al.*, 2014; Leite *et al.*, 2022). Mitochondrial metabolic remodelling also occurs in response to diverse signalling pathways (Bonawitz *et al.*, 2007; Chevtzoff *et al.*, 2005; Dejean *et al.*, 2002; Jablonka *et al.*, 2006; Pan and Shadel,

2009) reinforcing the importance of fine-tuning mitochondrial function with energetic demands. We also report that Cdh1p impacts on Yap1p transcriptional activity, which underlies both the *cdh1*Δ mutant resistance to oxidative stress and the upregulated mitochondrial respiration. The integration of mitochondrial function with the induction of antioxidant defences through Yap1p may be important to maintain the cellular redox balance in *cdh1*Δ cells.

4.4. Materials and Methods

4.4.1. Yeast strains and growth conditions

The *Saccharomyces cerevisiae* strains used are all BY4741 derivative and are listed in Table 4.1. To generate *cdh1*Δ::*HIS3* strain, *cdh1*Δ*::KanMX4* was transformed with a DNA fragment containing *HIS3MX*. To construct double mutant strains, the DNA fragment containing *cdh1*Δ::*HIS3* was amplified and transformed in the deletion strains. To generate Rpn4-HA*cdh1*Δ::*kan* strain, Rpn4-HA:*HIS3* was transformed with a DNA fragment containing *cdh1*Δ*::KanMX4*. Strains were transformed by the standard lithium acetate procedure (Gietz and Schiestl, 2007). Gene deletion was confirmed by PCR. For overexpression of Cdh1-m11 and Sod2p, cells were transformed with the plasmids pRS416-GALL-3HA-Cdh1-m11 (Zachariae *et al.*, 1998) and Yep352-SOD2 (Vilaça *et al.*, 2014), respectively.

Cells were grown in rich medium [YPGal: 2% (w/v) galactose, 1% (w/v) yeast extract, 2% (w/v) bactopeptone] or synthetic complete medium [SC: 0.67% (w/v) Bacto-yeast nitrogen base w/o amino acids, 2% (w/v) glucose and 0.2% (w/v) Dropout mix] lacking uracil/leucine, as appropriate. For Cdh1-m11 overexpression, cells were grown in YPRaff medium [YPRaff: 2% (w/v) raffinose, 1% (w/v) yeast extract, 2% (w/v) bactopeptone] overnight until mid-log phase and cultured with 4% galactose for 3h before oxygen consumption analysis.

Cultures were routinely grown at 26 °C in an orbital shaker at 140 r.p.m.

Table 4.1. *S. cerevisiae* strains used in this study.

Strain	Genotype	Source
BY4741 (wt)	Mat *a his3Δ1 leu2Δ0 met15Δ0 ura3Δ0*	Euroscarf
*cdh1*Δ::kan	BY4741; *cdh1*Δ*::KanMX4*	Euroscarf
*cdh1*Δ	BY4741; *cdh1*Δ*::HIS3MX6*	This study
*yap1*Δ	BY4741; yap*1*Δ*::KanMX4*	Euroscarf
*rpn4*Δ	BY4741; *rpn4*Δ*::KanMX4*	Euroscarf
*gcn4*Δ	BY4741; *gcn4*Δ*::KanMX4*	Euroscarf
*pdr3*Δ	BY4741; *pdr3*Δ*::KanMX4*	Euroscarf
*yap1*Δ*cdh1*Δ	BY4741; yap*1*Δ*::KanMX4 cdh1*Δ*::HIS3MX6*	This study
*rpn4*Δ*cdh1*Δ	BY4741; *rpn4*Δ*::KanMX4 cdh1*Δ*::HIS3MX6*	This study
*gcn4*Δ*cdh1*Δ	BY4741; *gcn4*Δ*::KanMX4 cdh1*Δ*::HIS3MX6*	This study
*pdr3*Δ*cdh1*Δ	BY4741; *pdr3*Δ*::KanMX4 cdh1*Δ*::HIS3MX6*	This study

*rpn4*Δ::hph	BY4741; *rpn4*Δ*::hphMX4*	This study
Rpn4-HA	BY4741; Rpn4-HA:HIS3	(Work and Brandman, 2020)
Rpn4-HA*cdh1*Δ::kan	BY4741; Rpn4-HA:HIS3 *cdh1*Δ*::KanMX4*	This study

4.4.2. Mitochondrial isolation

For isolation of an enriched mitochondrial fraction, wt and *cdh1*Δ cells were grown to mid-log phase (OD_{600nm} = 1.4) in YPGal medium and digested enzymatically with zymolyase (5mg/g of cells) at 37 °C for 30 min. The homogenized spheroplasts were subjected to differential centrifugation basically as described in (Lange *et al.*, 1999).

4.4.3. Protein identification by HPLC-MS/MS

Biological triplicates from wt and *cdh1*Δ cells were solubilized with 100 mM Tris pH 8.5, 1% (w/v) sodium deoxycholate, 10 mM tris(2-carboxyethyl) phosphine and 40 mM chloroacetamide for 10 min at 95 °C at 1000 r.p.m. Each sample was processed for proteomics analysis following the solid-phase-enhanced sample-preparation (SP3) protocol as described in (Hughes *et al.*, 2019). Enzymatic digestion was performed with Trypsin/LysC (2 μg) overnight. Protein identification and quantitation was performed by nanoLC-MS/MS composed by an Ultimate 3000 liquid chromatography system coupled to a Q-Exactive Hybrid Quadrupole-Orbitrap mass spectrometer (Thermo Scientific), as previously described (Osório *et al.*, 2021). This equipment is composed by an Ultimate 3000 liquid chromatography system coupled to a Q-Exactive Hybrid Quadrupole-Orbitrap mass spectrometer (Thermo Scientific).

The raw data was processed using Proteome Discoverer 2.5.0.400 software (Thermo Scientific) and searched against the UniProt database for the *Saccharomyces cerevisiae* Proteome 2020_03 together with a common contaminant database from MaxQuant (version 1.6.2.6, Max Planck Institute of Biochemistry). The Sequest HT search engine was used to identify tryptic peptides. Peptide confidence was set to high. The processing node Percolator was enabled with the following settings: maximum delta Cn 0.05; decoy database search target FDR 1%, validation based on q-value. Protein label free quantitation was performed with the Minora feature detector node at the processing step. Precursor ions quantification was performing at the processing step with the following parameters: Peptides to use unique plus razor, precursor abundance based on intensity and normalization based on total peptide amount.

The mass spectrometry proteomics data have been deposited to the ProteomeXchange Consortium via the PRIDE (Perez-Riverol *et al.*, 2022) partner repository with the dataset identifier PXD039879.

4.4.4. Mitochondrial mass analysis

The total mitochondrial mass was determined using 10-N-Nonyl acridine orange (NAO, Invitrogen), a dye that binds to cardiolipin present specifically on the mitochondrial membrane (Goswami *et al.*, 2012). Briefly, wt and *cdh1*Δ cells were grown to mid-log phase in YPGal medium and incubated in culture medium containing 10 μM NAO for 30 min. Fluorescence intensity measured using the BD Accuri C6 flow cytometer. Data were analysed with FlowJo v10 software version.

4.4.5. Oxygen consumption rate and COX activity

The oxygen consumption was measured polarographically in whole cells resuspended in PBS buffer, from cultures grown in YPGal medium to mid-log or PDS phase, using a Clark-type oxygen electrode coupled to an Oxygraph plus system (Hansatech). Data were analysed using the OxyTrace^{+} software. The respiratory rate was obtained by dividing the oxygen consumed per min by the number of cells used in the experiment.

Cytochrome *c* oxidase activity was determined by measuring cytochrome *c* oxidation as previously described (Poyton *et al.*, 1995).

4.4.6. SDS-PAGE and western blot

For immunoblotting, yeast cell extracts were resuspended at identical cell densities in sodium dodecyl sulphate (SDS) loading dye and lysed by boiling for 6 min and vortexing for 5 min with glass beads. Protein samples were separated into 7.5%-10% SDS-PAGE gels and transferred to nitrocellulose membranes (Hybond-C, GE Healthcare).

The primary antibodies used were raised against yeast Tim22p (1:500, sc-14042, Santa Cruz Biotechnology), yeast Cox2p (1:6000, 4B12A5, ThermoFisher Scientific), yeast Cytochrome c (1:10000, Davids Biotechnologie), yeast Pgk1p (1:30000, 22C5D8, ThermoFisher Scientific), HA (1:1000, Y-p11, Santa Cruz Biotechnology) and *c*-Myc (1:1000, ThermoFisher Scientific).

Secondary antibodies used were anti-goat IgG-HRP (1:5000), anti-mouse IgG-HRP (1:10000, Molecular probes) and anti-rabbit IgG-HRP (1:10000, Sigma).

Membranes were incubated with WesternBright ECL (Advansta), exposed to LucentBlue X-ray film (Advansta), scanned on a Molecular Imager GS900, and quantified using Image Lab Software version 6.1 (Bio-Rad).

4.4.7. Fluorescent reporter assay measurements

Cells harbouring a GFP reporter for Rpn4p activity (Work and Brandman, 2020) were grown in YPGal until early-log phase. To assess Rpn4 activity under proteasomal stress

conditions, wt cells were treated with 60 μM of MG132 (Merck) for 2 h. Cells were then centrifuged, washed and resuspended in PBS buffer. Cells were acquired using the FL1 detector in a BD Accuri C6 Flow cytometer and data were analysed with FlowJo v10 software version.

4.4.8. β-galactosidase assay

Cells harbouring pRS415-AP-1-*CYC1-LacZ* plasmid (Maeta *et al.*, 2004) were grown in YPGal until mid-log phase. To assess Yap1p activity under oxidative stress conditions, wt cells were treated with 3 mM H_2O_2 (Merck) for 1.5 h. The β-galactosidase activity was measured in a liquid assay using *o*-nitrophenyl-β-D-galactoside (ONPG; Merck) as previously described (Almeida *et al.*, 2008) using 60 μg of total protein.

4.4.9. Oxidative stress and DNA damage resistance

Wt, *cdh1*Δ, *yap1*Δ and *yap1*Δ*cdh1*Δ strains were grown overnight at 26 °C in YPGal medium until mid-log phase. Each culture was then diluted to OD_{600nm} = 0.1 and ten-fold dilutions were performed using PBS buffer. Cells were spotted in YPGal plates, used within 48h of preparation, supplemented with 0, 2.5 and 5 mM of H_2O_2 (Merck) and 0.05% (v/v) of methyl methanesulfonate (MMS, ThermoFisher Scientific). Cells were incubated for 2 days at 26 °C.

4.4.10. ROS levels

Cells were grown overnight at 26 °C in YPGal medium until mid-log phase and incubated with 5 μg/ml dihydroethidium (DHE) for 30 min at room temperature in the dark. Cells were then centrifuged, washed and resuspended in PBS buffer. Cells were acquired using the FL3 detector in a BD Accuri C6 Flow cytometer and data were analysed with FlowJo v10 software version.

4.5. Acknowledgments

The HA-tagged Rpn4p strain and the Rpn4p activity reporter were kindly provided by Onn Brandman (Stanford University, USA). The authors acknowledge the support of the i3S Scientific Platforms, Translational Cytometry and Proteomics (supported by the Portuguese Mass Spectrometry Network, integrated in the National Roadmap of Research Infrastructures of Strategic Relevance (ROTEIRO/0028/2013; LISBOA-01-0145-FEDER-022125, with assistance of Hugo Osório).

4.6. Supplementary material

Table 4.2. Mitochondrial proteins significantly upregulated in Cdh1p-deficient cells.

UniProtID	Gene name	Description
Q00711	SDH1	Succinate dehydrogenase [ubiquinone] flavoprotein subunit
P33421	SDH3	Succinate dehydrogenase [ubiquinone] cytochrome b subunit
P37298	SDH4	Succinate dehydrogenase [ubiquinone] cytochrome b small subunit
Q3E785	SDH6	Succinate dehydrogenase assembly factor 1
P00431	CCP1	Cytochrome *c* peroxidase
Q3E846	COA6	Cytochrome *c* oxidase assembly factor 6
P00410	COX2	Cytochrome *c* oxidase subunit 2
P00044	CYC1	Cytochrome *c* isoform 1
P54861	DNM1	Dynamin-related protein
P40515	FIS1	Mitochondrial fission 1 protein
P04710	AAC1	ADP,ATP carrier protein 1
P19414	ACO1	Aconitate hydratase
P32316	ACH1	Acetyl-CoA hydrolase
P33416	HSP78	Heat shock protein 78
P40513	MAM33	Mitochondrial acidic protein MAM33
P07259	URA2	Protein URA2
P41903	TES1	Peroxisomal acyl-coenzyme A thioester hydrolase 1
P32451	BIO2	Biotin synthase
P43567	AGX1	Alanine-glyoxylate aminotransferase 1
P50896	PSP1	Protein PSP1
P53123	MRM2	rRNA methyltransferase 2
P32785	FMT1	Methionyl-tRNA formyltransferase
P11325	NAM2	Leucine-tRNA ligase
P04039	COX8	Cytochrome *c* oxidase subunit 8
P33303	SFC1	Succinate/fumarate mitochondrial transporter
Q06409	DCK1	DOCK-like protein 1
P37293	NAT2	Putative N-terminal acetyltransferase 2
P87275	AIM11	Altered inheritance of mitochondria protein 11
P32502	GCD7	Translation initiation factor eIF-2B subunit beta
P33759	MRPS5	37S ribosomal protein S5
P32340	NDI1	Rotenone-insensitive NADH-ubiquinone oxidoreductase
P40033	RSM18	37S ribosomal protein RSM18
P40858	MRPL49	54S ribosomal protein L49
P07257	QCR2	Cytochrome bc_1 complex subunit 2

P00424	COX5A	Cytochrome *c* oxidase subunit 5A
P28778	MRP17	37S ribosomal protein MRP17
P07253	CBP6	Cytochrome B pre-mRNA-processing protein 6
Q02950	MRP51	37S ribosomal protein MRP51
P00175	CYB2	Cytochrome b2
P10127	ADH4	Alcohol dehydrogenase 4
Q99297	ODC2	Mitochondrial 2-oxodicarboxylate carrier 2
P08067	RIP1	Cytochrome bc_1 complex subunit Rieske
P32839	BCS1	Mitochondrial chaperone BCS1

Table 4.3. Mitochondrial proteins significantly downregulated in Cdh1p-deficient cells.

UniProtID	Gene name	Description
Q04409	EMI2	Putative glucokinase-2
Q05473	MRX8	MIOREX complex component 8
Q06681	YSP2	Membrane-anchored lipid-binding protein YSP2
P25578	PGS1	CDP-diacylglycerol-glycerol-3-phosphate 3-phosphatidyltransferase
Q12031	ICL2	Mitochondrial 2-methylisocitrate lyase
P13188	GLN4	Glutamine-tRNA ligase
Q06563	SYM1	Protein SYM1
P53918	ESBP6	Uncharacterized transporter ESBP6
P53311	MPC3	Mitochondrial pyruvate carrier 3
P12887	UNG1	Uracil-DNA glycosylase
P53252	PIL1	Sphingolipid long chain base-responsive protein PIL1
Q12230	LSP1	Sphingolipid long chain base-responsive protein LSP1
P38631	FKS1	1,3-beta-glucan synthase component FKS1
P48015	GCV1	Aminomethyltransferase
P47031	IML2	Inclusion body clearance protein IML2
Q03653	EFR3	Protein EFR3
P32660	DNF1	Phospholipid-transporting ATPase DNF1
Q03558	OYE2	NADPH dehydrogenase 2
Q12207	NCE102	Non-classical export protein 2
P23337	GSY1	Glycogen [starch] synthase isoform 1
P40165	NNR1	NAD(P)H-hydrate epimerase
P54003	SUR7	Protein SUR7

P43581	HXT10	Hexose transporter HXT10
P12945	NAT1	N-terminal acetyltransferase A complex subunit NAT1
Q12359	ATO3	Ammonia transport outward protein 3
P53322	TNA1	High-affinity nicotinic acid transporter
P32333	MOT1	TATA-binding protein-associated factor MOT1
P53198	ERP6	Protein ERP6
P32843	YME2	Mitochondrial escape protein 2
Q07878	VPS1	Vacuolar protein sorting-associated protein 13
P04806	HXK1	Hexokinase-1
P15179	MSD1	Aspartate-tRNA ligase
Q01802	AAT1	Aspartate aminotransferase
Q02863	UBP16	Ubiquitin carboxyl-terminal hydrolase 16
P32796	CAT2	Carnitine O-acetyltransferase
Q08970	MMT2	Mitochondrial metal transporter 2
P00045	CYC7	Cytochrome *c* isoform 2
P16862	PFK2	ATP-dependent 6-phosphofructokinase subunit beta
P17709	GLK1	Glucokinase-1
P38087	YMC2	Carrier protein YMC2
Q06683	IRC3	Putative ATP-dependent helicase IRC3
Q06143	DIC1	Mitochondrial dicarboxylate transporter
P23500	MRS4	Mitochondrial RNA-splicing protein MRS4
P39003	HXT6	High-affinity hexose transporter HXT6
P36064	CMC1	COX assembly mitochondrial protein
P53230	TAM41	Phosphatidate cytidylyltransferase
P35731	OAR1	3-oxoacyl-[acyl-carrier-protein] reductase
P07271	PIF1	ATP-dependent DNA helicase PIF1
Q03640	TCB3	Tricalbin-3
P16603	NCP1	NADPH-cytochrome P450 reductase
P33302	PDR5	Pleiotropic ABC efflux transporter of multiple drugs
P32568	SNQ2	Protein SNQ2
P38885	AIM46	Altered inheritance of mitochondria protein 46
P0CX55	RPS18A	40S ribosomal protein S18-A
P53121	FLC3	Putative flavin carrier protein 3
P32891	DLD1	D-lactate dehydrogenase [cytochrome] 1
P34227	PRX1	Peroxiredoxin PRX1
P38323	MCX1	ATP-dependent clpX-like chaperone

P27697	COQ8	Atypical kinase COQ8
P04807	HXK2	Hexokinase-2
P53081	NIF3	NGG1-interacting factor 3
P33893	PET112	Glutamyl-tRNA(Gln) amidotransferase subunit B
P22936	APN1	Apurinic-apyrimidinic endonuclease 1
P40202	CCS1	Superoxide dismutase 1 copper chaperone
Q12375	ORT1	Mitochondrial ornithine transporter 1
P48564	MRX6	MIOREX complex component 6
Q02889	MGR2	Protein MGR2
P30624	FAA1	Long-chain-fatty-acid-CoA ligase 1
P49095	GCV2	Glycine dehydrogenase (decarboxylating)
P38756	TCD1	tRNA threonylcarbamoyladenosine dehydratase 1
Q12428	PDH1	Probable 2-methylcitrate dehydratase
P36008	TEF4	Elongation factor 1-gamma 2
P36015	YKT6	Synaptobrevin homolog YKT6
Q06705	CSR1	Phosphatidylinositol transfer protein CSR1
Q08001	LAM6	Membrane-anchored lipid-binding protein LAM6
P23301	HYP2	Eukaryotic translation initiation factor 5A-1
P10834	PET54	Protein PET54
P46367	ALD4	Potassium-activated aldehyde dehydrogenase
P07246	ADH3	Alcohol dehydrogenase 3
P40012	HEM14	Protoporphyrinogen oxidase
P00360	TDH1	Glyceraldehyde-3-phosphate dehydrogenase 1
P39726	GCV3	Glycine cleavage system H protein
P12709	PGI1	Glucose-6-phosphate isomerase
Q04472	MGR3	Mitochondrial inner membrane i-AAA protease supercomplex subunit MGR3
Q12283	MCT1	Malonyl CoA-acyl carrier protein transacylase
P38072	SCO2	Protein SCO2
P38152	CTP1	Tricarboxylate transport protein
Q03218	MMT1	Mitochondrial metal transporter 1
Q02771	PET117	Protein PET117
P48813	GNP1	High-affinity glutamine permease
Q12171	MDM32	Mitochondrial distribution and morphology protein 32
P53320	MTM1	Mitochondrial carrier protein MTM1

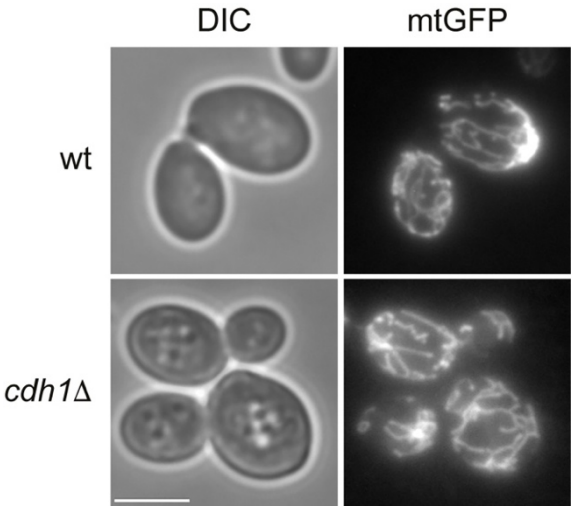

Figure 4.8. Deletion of *CDH1* did not affect mitochondrial morphology. Yeast wt and *cdh1*Δ cells transformed with a pYX142mtGFP plasmid [Westermann and Neupert, 2000] were grown overnight at 26 °C in YPGal until mid-log phase. Cells were then imaged by fluorescence microscopy and images acquired by epifluorescence in a Zeiss Axio Imager Z1 microscope with Nomarski optics with an Axiocam MR3.0 camera and analysed using the Axivision 4.7 software. Images were collected at 0.4 μm z-intervals. Representative DIC images from 4 independent experiments are merged with maximum intensity projections from the mitochondrial GFP signal. Scale bar: 5 μm.

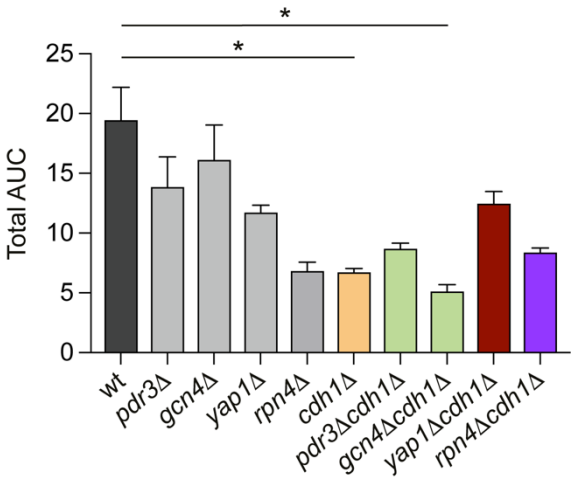

Figure 4.9. Area under the growth curves calculated from data presented in Figure 4.3, in arbitrary units (A.U.). Values presented are the mean ± SEM (*n* = 3), *, p < 0.05, Welch's *t* test of the area under the curve.

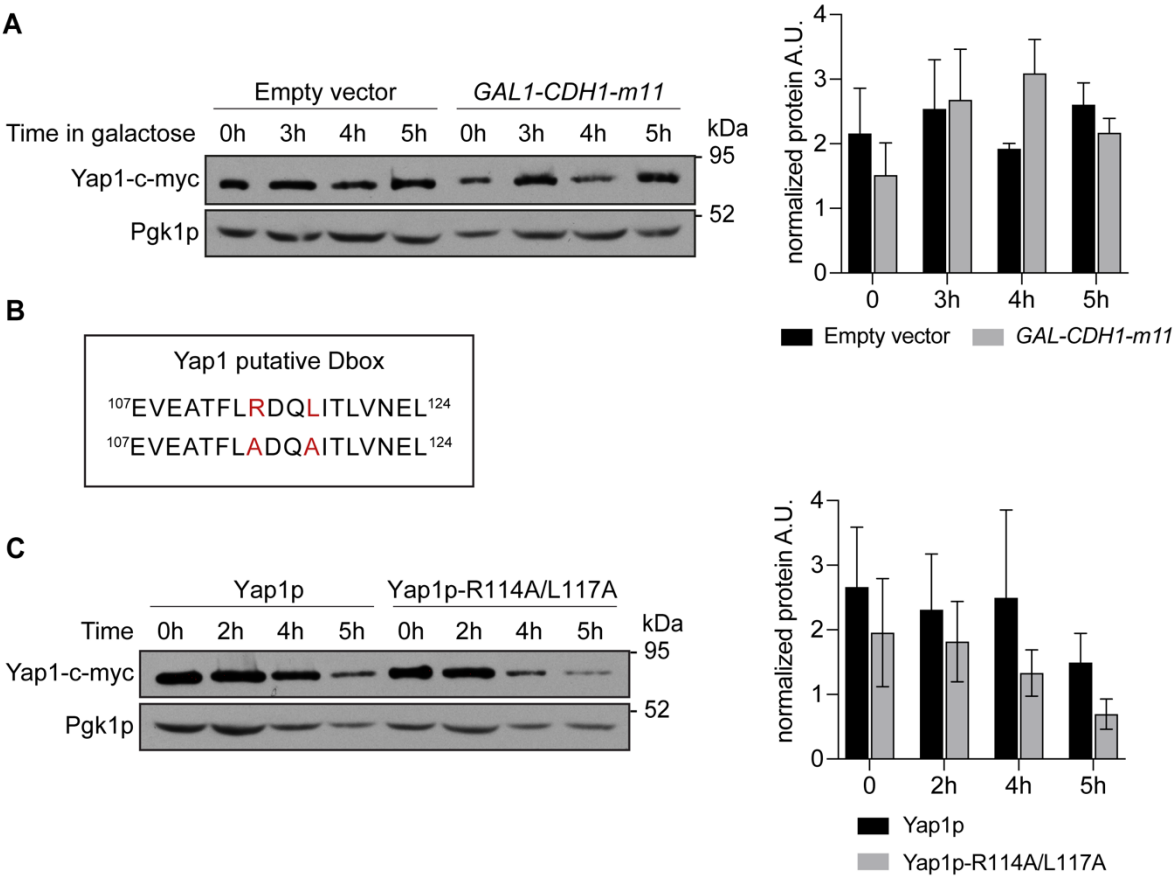

Figure 4.10. Overexpressing Cdh1-m11 or mutating a putative Cdh1p recognition motif (destruction box) in Yap1p did not affect Yap1p stability. (A) *yap1*Δ cells harboring pRS315-Yap1-c-Myc plasmid and carrying vector for *GAL1* promotor-induced overexpression of Cdh1-m11 were grown in YPRaffinose. At early-log phase, 4% of galactose was added and cells were collected at indicated time points. Total protein extracts were separated by SDS-PAGE and analyzed by immunoblottig using anti-c-myc and anti-Pgk1p (loading control) antibodies. A representative blot is shown. Graph represents the relative amount of Yap1-c-myc normalized to Pgk1p. Values are the mean ± SEM (*n* = 2). (B) Schematic representation of one putative destruction box (D-box) in Yap1p predicted using GPS-ARM 1.0. (C) *yap1*Δ cells harboring pRS315-Yap1-c-Myc or pRS315-Yap1-R114A/L117A-c-Myc plasmid were grown in YPGal to early-log phase. The R114A/L117A mutation was introduced using the Q5 Site-Directed Mutagenesis Kit (New England Biolabs). Cells were collected at indicated time points and total protein extracts were separated by SDS-PAGE and analyzed by immunoblotting using anti-c-myc and anti-Pgk1p (loading control) antibodies. A representative blot is shown. Graph represents the relative amount of Yap1-c-myc normalized to Pgk1p. Values are the mean ± SEM (*n* = 2).

CHAPTER 5.

Mitochondrial respiration promotes Cdc37p-dependent stability of the Cdk1 homolog Cdc28p

This chapter was based on the following paper:

Ana Cláudia Leite*, Telma S. Martins*, Rute R. Cesário, Vitor Teixeira, Vitor Costa and Clara Pereira, Mitochondrial respiration promotes Cdc37-dependent stability of the Cdk1 homolog Cdc28, Journal of Cell Science, 2023, 136:jcs260279 (DOI: 10.1242/jcs.260279).

*Co-first authors with equal contribution

Mitochondrial respiration promotes Cdc37p-dependent stability of the Cdk1 homolog Cdc28p

Abstract

Cdc28p, the homolog of mammalian Cdk1, is a conserved key regulatory kinase for all major cell cycle transitions in yeast. We have found that defects in mitochondrial respiration (including deletion of *ATP2*, an ATP synthase subunit) inhibit growth of cells carrying a degron allele of Cdc28p (*cdc28-td*) or temperature-sensitive mutations (*cdc28-1* and *cdc28-1N)* at semi-permissive temperatures. Loss of cell proliferation in the *atp2*Δ*cdc28-td* double mutant is associated with aggravated cell cycle arrest and mitochondrial dysfunction, including mitochondrial hyperpolarization and fragmentation. Unexpectedly, in mutants defective in mitochondrial respiration, steady-state protein levels of mutant *cdc28* are strongly reduced, accounting for the aggravated growth defects. Stability of Cdc28p is promoted by the Hsp90p-Cdc37p chaperone complex. Our results showed that *atp2*Δ*cdc28-td* double mutant cells, but not single mutants, are sensitive to chemical inhibition of the Hsp90-Cdc37 complex, and exhibit reduced levels of additional Hsp90p-Cdc37p client kinases, suggesting an inhibition of this complex. In agreement, overexpression of *CDC37* improved *atp2*Δ*cdc28-td* cell growth and Cdc28p levels. Overall, our study shows that simultaneous disturbance of mitochondrial respiration and Cdc28p activity reduces the capacity of Cdc37p to chaperone client kinases, leading to growth arrest.

Keywords: Cell cycle, Chaperone, Mitochondria, Signalling, Yeast.

5.1. Introduction

The eukaryotic cell cycle is controlled by cyclin-dependent kinases (CDKs). In *Saccharomyces cerevisiae*, a single CDK, Cdc28p, is necessary and sufficient for cell cycle regulation. Cdc28p (Cdk1 in mammals; Cdc2 in *S. pombe*) targets more than 200 substrates, and its activity and specificity are provided by the binding to one of nine cyclin subunits, divided in two groups, the G1 cyclins and B-type cyclins. The regulation of the different phase-specific cyclins is tightly controlled by oscillatory mechanisms that provide alternate periods of low and high levels of the different cyclin-Cdc28p activities, ensuring orderly progression through the cell cycle (Orlando *et al.*, 2008; Spellman *et al.*, 1998). In addition to cyclins, Cdc28p activity is regulated by the presence of Cdc28p inhibitors and by post-translational modifications (PTMs) such as phosphorylation (Mendenhall and Hodge, 1998). Transcriptional and translational regulation of Cdc28p seems to be of minor importance, given that the amount of Cdc28p is normally present at constant levels (and in excess) throughout the cell cycle (Mendenhall and Hodge, 1998). Cdc28p steady-state levels are promoted by Cdc37p (Farrell and Morgan, 2000), an Hsp90p co-chaperone that specifically targets protein kinases (Kimura *et al.*, 1997). Cdc37p promotes Cdc28p folding and/or stabilization and mediates Cdc28p activation by promoting formation of the Cdc28p-Cln and Cdc28p-Clb2p complexes (Mendenhall and Hodge, 1998), and is thus critical for proper cell cycle progression.

Cdc28p controls the timing of mitotic commitment, DNA replication and repair, spindle formation, chromosome separation and cytokinesis (Mendenhall and Hodge, 1998). It also affects processes not directly associated with the cell cycle, but coordinated with it, such as cell growth and bud morphogenesis (McCusker *et al.*, 2007), lipid synthesis (Kurat *et al.*, 2009), carbohydrate metabolism (Ewald *et al.*, 2016) and vacuole inheritance (Peng and Weisman, 2008). Cdc28p has also been reported to impact on mitochondrial DNA (mtDNA) stability (Devin *et al.*, 1990; Koltovaya *et al.*, 1998) and to favour mitochondrial protein import and bioenergetic activity at G2/M phase (Harbauer *et al.*, 2014).

Mitochondria play a number of key roles in eukaryotic cells, including ATP synthesis by oxidative phosphorylation (OXPHOS). The OXPHOS system is composed of four respiratory chain complexes, which are responsible for electron transport and generation of a proton gradient across the inner mitochondrial membrane, and the ATP synthase uses this proton gradient to drive the aerobic synthesis of ATP. *S. cerevisiae* is tolerant to mutations that inactivate the electron transport chain or OXPHOS due to its good fermenting capacity. In fact, this species can tolerate a partial deletion or complete loss of mtDNA when grown on a fermentable carbon source. Even so, the mitochondrial compartment is essential for yeast cell growth as it is required for essential biosynthetic pathways, such as amino acid synthesis and iron-sulfur cluster biogenesis (Lill *et al.*, 2012). It is therefore not

surprising that severe defects in mitochondrial inheritance trigger a checkpoint that inhibits cytokinesis (García-Rodríguez *et al.*, 2009). Plus, cells that have lost their mtDNA (*rho*^{0} cells) exhibit defects in G1 to S progression (Crider *et al.*, 2012). Taken together, these pieces of evidence point to a two-way communication between mitochondrial function and cell cycle progression.

Here, we report that mitochondrial OXPHOS mutations inhibit growth in Cdc28p conditional mutants by impairing the activity of the Hsp90p co-chaperone Cdc37p and further compromising Cdc28p levels. This work presents mitochondrial dysfunction as a new factor affecting Cdc37p activity, expanding our knowledge on the complex networks involved in cell division decisions.

5.2. Results

5.2.1. Mitochondrial OXPHOS defects inhibit growth of Cdc28p conditional mutants

In this study, to improve our understanding of the interplay between cell cycle regulation and mitochondrial function, we investigated the genetic interaction between *CDC28* and *ATP2*, which encode a key cell cycle regulatory kinase and the catalytic subunit of the F_oF_1-ATP synthase, respectively. In the presence of glucose, yeast cells generate ATP primarily by glycolysis, and the presence of an intact OXPHOS is not essential for growth (Warburg, 1956). As such, to allow growth of *atp2*Δ cells, strains were cultivated on glucose-based media (fermenting conditions) throughout this work. Given that the *CDC28* gene is essential, we used a Cdc28p degron system (*cdc28-td*), based on a C-terminal fusion with a heat-inducible ubiquitin ligase-target peptide (Dohmen *et al.*, 1994), to deplete Cdc28p by shifting cells from 23 ºC to 37 ºC. Cdc28p levels after 3h at the temperatures used in this study are shown in Figure 5.1A. In fermenting conditions, wild type (wt), *atp2*Δ, *cdc28-td* and *atp2*Δ*cdc28-td* cells cultured at the permissive temperature of 23 ºC grew similarly (Figure 5.1B). However, at the semi-permissive temperature of 35 ºC, for which only a mild growth defect is apparent for *cdc28-td* cells, a growth lethality was observed in the *atp2*Δ*cdc28-td* double mutant. Reintroducing wt Cdc28p (from its natural promoter in a low-copy number vector) reverted the *atp2*Δ*cdc28-td* mutant growth defects (Figure 5.8). Growth defects in the *atp2*Δ*cdc28-td* mutant were already evident for temperatures as low as 26 ºC, in which no growth defects are observed for *cdc28-td* cells (Figure 5.1B). At 26 ºC, although *cdc28-td* cells exhibit normal growth, cells exhibited an altered morphology (Figure 5.1B). This indicates that the *cdc28-td* protein activity is suboptimal, and that potential conformational alterations in the mutant due to the presence of the degron tag are not being compensated by the increased protein levels (Figure 5.1A). Absence of Atp2p

aggravated the morphological alterations of *cdc28-td* cells, leading to abnormally large, elongated cells even at 26 ºC (Figure 5.1C). As growth of the *atp2*Δ single mutant is not affected under fermenting conditions, irrespective of the growth temperature, these results suggest a synergistic interaction between *CDC28* and *ATP2*.

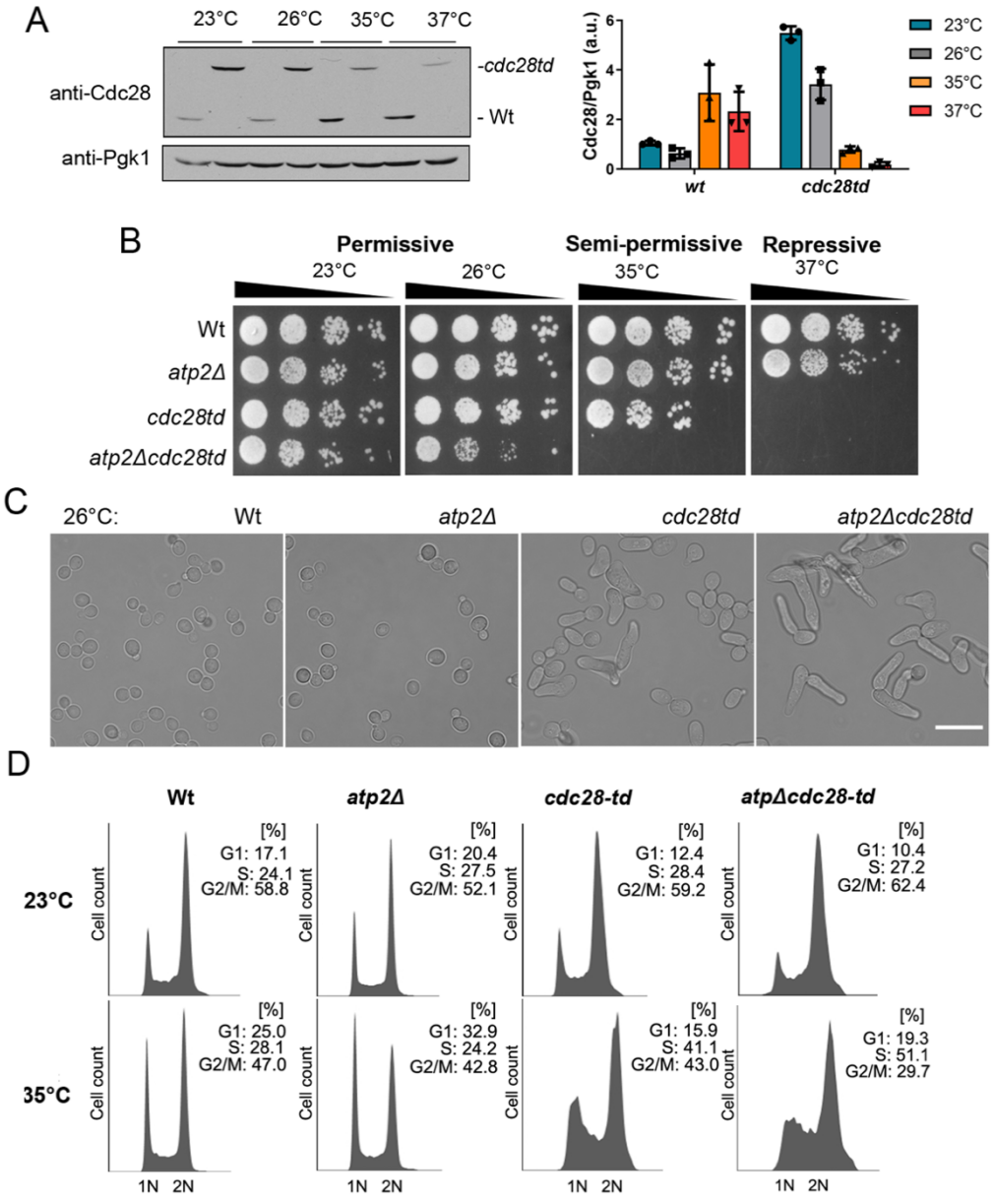

Figure 5.1. *ATP2* displays a negative genetic interaction with *CDC28*. (A) Western blot showing wt Cdc28p and *cdc28-td* levels in wt cells after 4h at the indicated temperatures. Pgk1p is shown as loading control. A quantification is show on the right (mean ± SD, *n* = 4) (B) Fourfold serial dilutions of wt, *atp2*Δ, *cdc28-td* (degron mutant) and *atp2*Δ*cdc28-td* strains are shown after growth at the permissive, semi-permissive and restrictive temperatures, as indicated. The data shown are representative of at least three independent experiments. (C) Micrographs depicting cell morphologies of the indicated haploid strains. Cells were cultured at 26 ºC. Image representative of 4 experiments. Scale bar, 30 μm. (D) Quantitative analysis of DNA content by flow cytometry. Strains were cultured in YPD at 23 ºC to exponential phase and part of the same cultures was shifted at 35 ºC for 3 h.

An analysis of DNA content by flow cytometry showed that at the permissive temperature all strains showed normal distribution in the cell cycle. Although depletion of Cdc28p is expected to arrest the cell cycle at any given cell cycle phase (Papagiannakis *et al.*, 2017), the *cdc28-td* strain showed a mild enrichment in cells at S phase after 4h at the restrictive temperature (37 ºC). Notably, we found this S phase arrest was further aggravated by the loss of Atp2p (Figure 5.1D).

Since distinct temperature sensitive (ts) alleles of Cdc28p are available that cause arrest at specific cell cycle phases, such as G1 (*cdc28-1*) or G2/M (*cdc28-1N*) (Neiman *et al.*, 1990; Surana *et al.*, 1991), we tested whether lethality of *ATP2* disruption might be related to a specific cell cycle phase. We found that *ATP2* deletion also promoted a severe slow growth phenotype in *cdc28-1* and *cdc28-1N* cells (although to a lesser degree), at the respective semi-permissive conditions (Figure 5.2A). Our results are consistent with Atp2p being critical for cell proliferation upon low Cdc28p activity both in G1 (START) and mitosis. In addition, loss of Atp2p did not lead to a growth arrest at a specific cell cycle phase as it aggravated each of the *cdc28* mutant distinctive cell cycle phase arrest profiles at the permissive temperature of 26 ºC (Figure 5.2B).

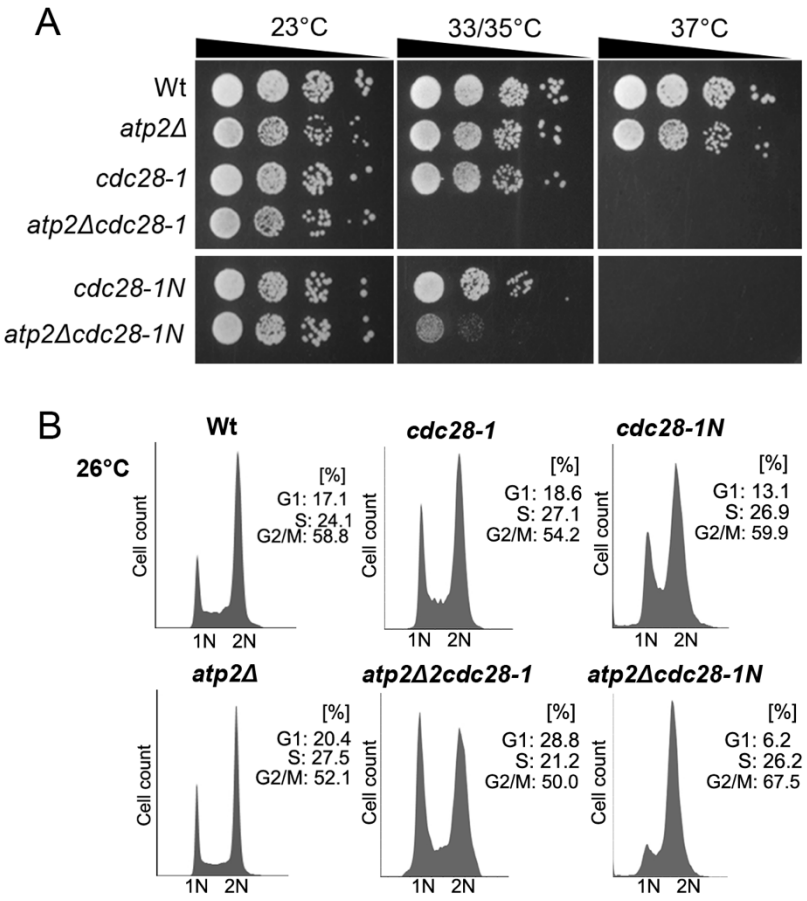

Figure 5.2. *ATP2* deletion aggravate the growth defects of *cdc28-1* and *cdc28-1N ts* mutants. (A) Growth analysis of *atp2*Δ*cdc28-1* and *atp2*Δ*cdc28-1N* strains. Cells were spotted in fourfold serial dilutions and grown at permissive, semi-permissive and restrictive temperatures, as indicated. The semi-permissive temperatures used were 35 ºC for *cdc28-1N* mutants and 33 ºC for *cdc28-1*. A representative image is shown (*n* = 4). (B) Cell cycle analysis by DNA content measurement. Strains were cultured at 26 ºC to exponential phase and analysed for DNA content by flow cytometry. Representative histograms are shown (*n* = 3).

To investigate whether *ATP2* genetically interacts with additional unrelated cell cycle mutants, we introduced in *atp2*Δ cells ts mutations for the yeast Aurora kinase Ipl1p and the anaphase-promoting complex/cyclosome (APC/C) adaptor subunit Cdc20p. Absence of *ATP2* did not affect the growth of either *ipl1-1* or *cdc20-1* cells at respective semi-repressive temperatures (Figure 5.3A). We also found no genetic interaction between *ATP2* and the polo-like kinase encoding gene *CDC5* (Figure 5.9). These data indicates that the growth defect caused by *ATP2* deletion in *cdc28* mutants is not a phenotype shared with other cell cycle mutants. Atp2p, as an essential subunit of an OXPHOS component, plays a vital role in ATP production. Yet, during growth in glucose medium, the glycolytic flux is high and the mitochondrial respiratory chain is repressed and does not contribute significantly to the cellular ATP levels (Warburg, 1956), as evidenced by the normal growth of *atp2*Δ single mutants. In addition, Atp2p may play cellular role(s) unrelated to ATP synthesis (Chen and Clark-Walker, 1999). To support the hypothesis that the negative effect of *ATP2* deletion

when combined with *cdc28-td* allele is related to the role of Atp2p in OXPHOS, genes encoding other ATP synthase subunits, namely *ATP1* (F1 α subunit) and *ATP4* (F_o subunit b) were deleted in *cdc28-td* cells. Deletion of both *ATP1* and *ATP4* strongly inhibited *cdc28-td* proliferation (Figure 5.3B), indicating this is not a β-subunit-specific effect. We next questioned whether this phenotype was restricted to ATP synthase, or common to other OXPHOS complexes. For that, we tested the deletion of *QCR2*, a core subunit of Complex III (cytochrome bc_1), and *COX4*, which encodes for a subunit of complex IV (cytochrome *c* oxidase), in *cdc28-td* cells. Both *qcr2*Δ*cdc28-td* and *cox4*Δ*cdc28-td* strains phenocopied the *atp2*Δ*cdc28-td* double mutant lethality (Figure 5.3B). Ablating mitochondrial DNA in a strain carrying the *cdc28-td* allele (*cdc28-td rho^0)* also resulted in a similar phenotype (Figure 5.10). Overall, these results suggest that mitochondrial respiration in general is essential for growth of cells with reduced Cdc28p levels.

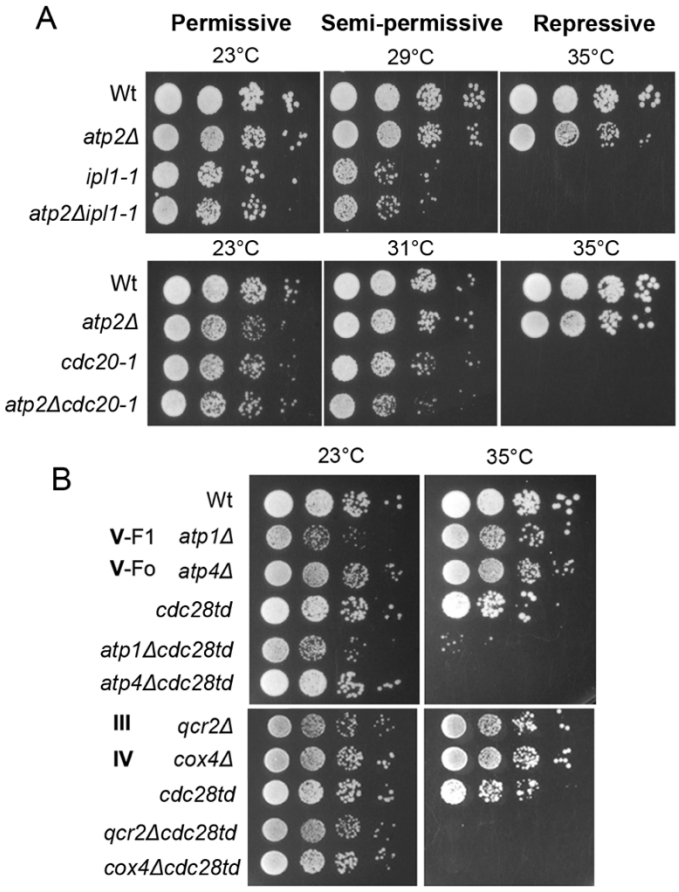

Figure 5.3. *ATP2* does not interact with *IPL1* or *CDC20*, but *CDC28* shows negative genetic interactions with additional genes encoding OXPHOS components. (A) Growth analysis of *atp2*Δ*cdc20-1* and *atp2*Δ*ipl1-1* strains. Cells were spotted in fourfold serial dilutions and grown at permissive, semi-permissive and restrictive temperatures, as indicated. A representative image is shown (*n* = 3). (B) Growth analysis of *atp1*Δ*cdc28-td*, *atp4*Δ*cdc28-td*, *qcr2*Δ*cdc28-td* and *cox4*Δ*cdc28-td* strains. Cells were spotted in fourfold serial dilutions and grown at permissive, semi-permissive and restrictive temperatures, as indicated. A representative image is shown (*n* = 3).

5.2.2. Loss of Cdc28p in the *atp2*Δ mutant aggravates mitochondrial dysfunction, but it does not trigger the retrograde response

The observed aggravating genetic interaction between OXPHOS encoding genes and *CDC28* suggest that they have a functional relationship. Given that previous studies indicated Cdc28p plays a role in mitochondrial function (Devin *et al.*, 1990; Harbauer *et al.*, 2014), we started by addressing whether loss of Cdc28p affected mitochondrial bioenergetics (respiration and mitochondrial membrane potential) and morphology of OXPHOS mutants. For mitochondrial respiration, wt, *atp2*Δ, *cdc28-td* and *atp2*Δ*cdc28-td* strains cells were cultured in glucose medium to mid-log phase and incubated at the semi-permissive temperature (35 ºC) for 3h. The basal oxygen consumption rate (OCR) of intact cells was then measured polarographically. The OCR was strongly reduced in *atp2*Δ and *cox4*Δ cells (2.4 and 0.8 nmol/min, respectively) compared with that found for wt cells (10 nmol/min), as anticipated. The *cdc28-td* mutant, likewise *cdc28-1* or *cdc28-1N* cells (Figure 5.11), exhibited an increase in OCR (16.5 nmol/min) (Figure 5.4A). In addition, OCR was higher in *atp2*Δ*cdc28-td* versus *atp2*Δ cells, indicating some level of mitochondrial uncoupling in the double mutant. As expected, absence of *COX4* drastically reduced the OCR in the *cdc28-td* mutant since it is essential for respiration.

Next, we analysed the mitochondrial morphology of these mutants expressing a mitochondria-targeted green fluorescent protein (mtGFP), and visualized by fluorescence microscopy. In agreement with previous observations, the vast majority (97%) of mitochondria in wt cells displayed a filamentous morphology. Similar results were observed in single mutants (88% for *atp2*Δ and 93% for *cdc28-td* mutant). In contrast, the predominant phenotype of the *atp2*Δ*cdc28-td* double mutant was punctate mitochondrial morphology (69%) indicating fragmentation (Figure 5.4B and Figure 5.12). We also assessed mitochondrial membrane potential (Δψm), as it reflects OXPHOS activity and is essential for mitochondrial function and biogenesis (Martin *et al.*, 1991). The Δψm was evaluated by flow cytometry using the cationic lipophilic dye $DiOC_6(3)$, in cells incubated for 3h in repressive conditions (35 ºC). Addition of the FCCP protonophore, which dissipates the Δψ*m*, led to a substantial reduction in the $DiOC_6(3)$ uptake by all strains (Figure 5.13). We used the FCCP responsive potential, eliminating unspecific binding, in the quantification of the Δψ*m* shown in Fig. 5.4C. The Δψ*m* was also normalized to the mitochondrial mass evaluated using preSU9-GFP, a mitochondrial presequence with low sensitivity to the membrane potential (Vowinckel *et al.*, 2015). We found a significant increase (2.7-fold) of Δψm in *atp2*Δ*cdc28-td* mutants, compared with that in wt cells (Figure 5.4C). For the single mutant strains, no significant differences were observed. The mitochondrial localization of the fluorochrome was checked by epifluorescence microscopy and corroborated the flow cytometry results (see Figure 5.13). These data revealed that Cdc28p impacts on

mitochondrial respiration and loss of Cdc28p in *atp2*Δ cells leads to mitochondrial dysfunction, as indicated by the mitochondrial hyperpolarization, fragmentation and increase of uncoupled respiration.

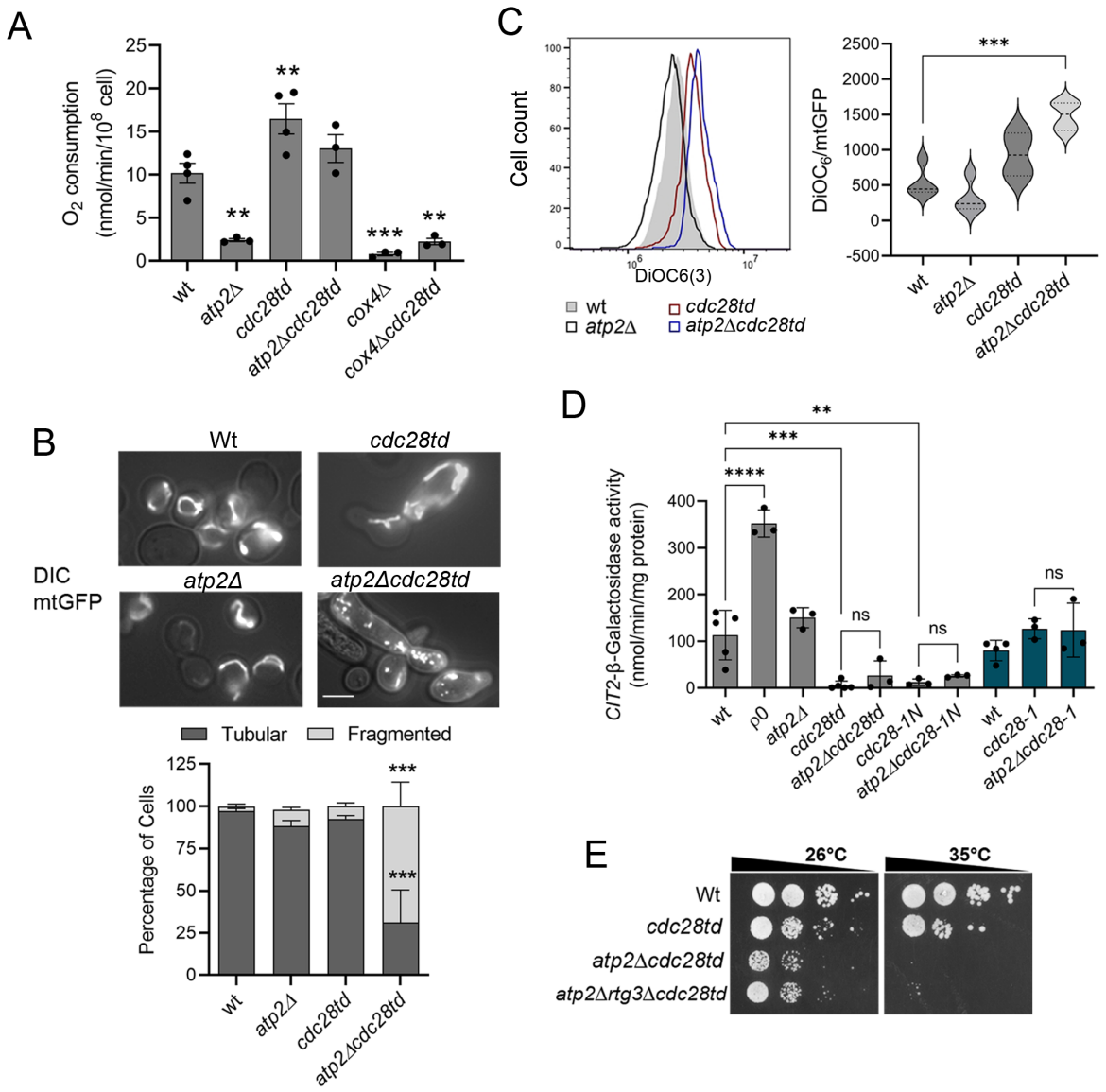

Figure 5.4. Loss of Cdc28p in the *atp2*Δ mutant leads to mitochondrial defects. (A) The basal respiratory rate was determined by measuring oxygen consumption in whole cells grown in glucose medium to mid-log phase at the restrictive temperature. Values are the mean ± SD (n = 4); **, p < 0.01; ***, p < 0.001 compared with wt; one-way ANOVA followed by Turkey's multiple comparison test. (B) Yeast cells expressing mtGFP were analysed by fluorescence microscopy and mitochondrial phenotypes (tubular or fragmented) were ascertained by manually counting. Representative DIC images are merged with maximum intensity projections generated from z-stacks of the mitochondrial green fluorescent signal. Scale bar, 10 μm. Values are the mean ± SD (n = 3); ***, p < 0.001; one-way ANOVA followed by Turkey's multiple comparison test. (C) The indicated strains were stained with the mitochondrial membrane potential probe $DiOC_6(3)$ and analysed by flow cytometry. Images show monoparametric histograms of $DiOC_6(3)$ fluorescence (FL1 area (log)) and violin plots represent FCCP-responsive $DiOC_6(3)$ staining normalized to the mitochondrial mass. Dashed lines show the median and quartile boundaries (n = 4). ***, p < 0.001; one-way ANOVA followed by Šídák's

multiple comparison test. (D) Activation of the retrograde pathway does not underlie the growth defects of the *atp2*Δ*cdc28-td* strain. β-Galactosidase assays were carried out to determine the activity of a *CIT2-lacZ* reporter gene in *cdc28* and *atp2*Δ*cdc28* mutants, as indicated, at semi-permissive conditions (35 ºC for *cdc28-td* and *cdc28-1N* carrying strains, in grey; 33 ºC for *cdc28-1* carrying strains, in blue). Cells lacking mtDNA (*rho*^{0}) are shown as positive control. Values are the mean ± SD (*n* = 6); **, *p* < 0.01; ***, *p* < 0.001; ****, *p* < 0.0001; ns, not significant; one-way ANOVA followed by Turkey's multiple comparison test. (E) Growth analysis of wt, *cdc28-td*, *atp2*Δ*cdc28-td* and *atp2*Δ*rtg3*Δ*cdc28-td.* Cells were spotted in serial dilutions and grown at indicated semi-permissive temperatures. Representative results are shown (*n* = 3).

Mitochondrial dysfunction can trigger an adaptive program named the mitochondrial retrograde response (RTG), a pathway of communication from mitochondria to the nucleus (Butow and Avadhani, 2004). Previous studies have shown that activation of the RTG prevents cell cycle progression by upregulating Swe1p, a Cdc28p inhibitor (Chen *et al.*, 2010), and contributes to cell death during prolonged S/G2 arrest (Zyrina *et al.*, 2015), indicating a link between RTG signalling and cell cycle. This prompted us to examine the possibility that mitochondrial dysfunction in the *atp2*Δ*cdc28-td* mutant could be triggering the RTG, resulting in cell growth arrest.

The classical marker of RTG in yeast is the upregulation of *CIT2*, which encodes a glyoxylate cycle isoform of citrate synthase (Liao *et al.*, 1991). *CIT2* induction was evaluated using a *CIT2-LacZ* reporter that was genomically integrated in the strains under study and in a *rho*^{0} background that served as a positive control. We found that *ATP2* deletion (or *COX4* deletion, not shown) did not induce *CIT2-LacZ* activation, either alone or in combination with the *cdc28-td* allele. Similar results were observed in *cdc28-1* and *cdc28-1N* mutants lacking Atp2p (Figure 5.4D). Intriguingly, LacZ activity was even lower in the *cdc28-td* and *cdc28-1N* single mutants or in combination with Atp2p loss compared to wt, but no changes were observed in *cdc28-1* cells. Alterations in *CIT2* basal expression may be caused by the distinct cell cycle phases at which the mutants arrest, given that *CIT2* expression vary with cell cycle phases (Barberis and Mondeel, 2022; Campbell *et al.*, 2020). Yet, since *CIT2-LacZ* activation was identical for *cdc28* single and *atp2*Δ*cdc28* double mutants, it seems unlikely that the RTG pathway is involved in the growth defects of the *atp2*Δ*cdc28* double mutant. In agreement, downregulation of the RTG pathway by deleting *RTG3* did not rescue the *atp2*Δ*cdc28-td* mutant growth defects (Figure 5.4E). The RTG pathway can be regulated by the levels of glutamate in the medium, whereby low glutamate levels activate and high glutamate levels repress RTG-dependent gene expression (Liu *et al.*, 2001). Corroborating previous results, we found that growth in medium lacking or containing excess of glutamate had no impact on the *atp2*Δ*cdc28-td* mutant growth (Figure 5.14). Overall, these results show that activation of the RTG signalling pathway does not

play a significant role in the lethal phenotype of the *atp2Δcdc28-td* mutant at semi-restrictive temperature.

5.2.3. OXPHOS disruption cause a strong reduction in mutant Cdc28p protein levels

Given that the cell morphology and cell cycle arrest phenotypes of *atp2Δcdc28* mutants resembles an aggravated *cdc28* phenotype, we considered whether Cdc28p steady-state protein levels could be affected in the OXPHOS mutants. We evaluated wt Cdc28p and *cdc28-td* levels in the absence of Atp2p, Qcr2p and Cox4p, in cells grown at the permissive temperature (26 ºC). No alterations in wt Cdc28p levels were observed in the absence of the OXPHOS proteins. However, *cdc28-td* levels were noticeably lower in these cells compared with controls (Figure 5.5A). This phenotype was also observed in the ts mutant *cdc28-1*, which was strongly destabilized by the absence of Atp2p (Figure 5.5B). A 120-min time course analysis of *cdc28-td* levels at restrictive conditions showed that Cdc28p levels decreased overtime both in *cdc28-td* and *atp2Δcdc28-td* strains. However, in the absence of Atp2p, as the Cdc28p protein level was already lower at t0, the detection limit was achieved earlier, after 1h of incubation (Figure 5.5C). Given that Cdc28p is essential for proliferation, our data suggest that the destabilization of *cdc28* upon OXPHOS disruption is the primary cause of the aggravated phenotype in the double mutant.

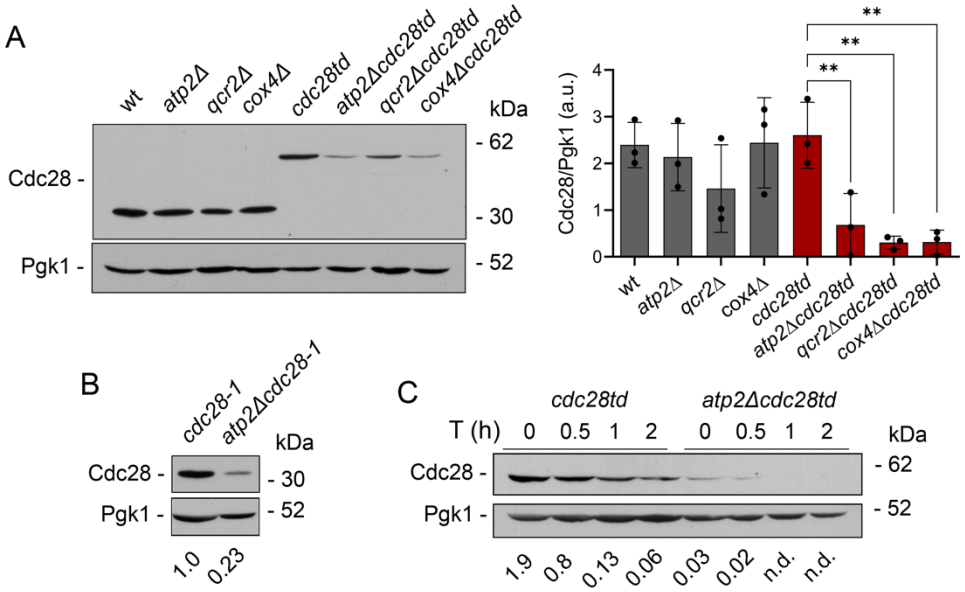

Figure 5.5. Cdc28p protein levels decrease in strains combining OXPHOS defects with impaired Cdc28p activity. (A) Western blot showing wt Cdc28p and *cdc28-td* levels in wt cells and in cells lacking Atp2p, Qcr2p and Cox4p grown at permissive temperature. Fold change was estimated by densitometric scanning of Cdc28p vs Pgk1p (loading control) bands. Values are the mean ± SD (n = 4); **, $p < 0.01$; one-way ANOVA followed by Turkey's multiple comparison test. (B) Immunodetection of *cdc28-1* in wt and *atp2Δ* cells grown at permissive temperature. A representative

blot is shown (*n* = 3). (C) Immunodetection of Cdc28p in *cdc28-td* and *atp2*Δ*cdc28-td* strains during a 120-min time course at the restrictive temperature. A representative blot is shown (*n* = 3). Fold change is indicated.

5.2.4. OXPHOS disruption in *cdc28-td* cells leads to defects in the Hsp90p-Cdc37p chaperone complex

Cdc28p levels are usually constant during cell division. However, Cdc28p folding and/or stabilization requires the co-chaperone Cdc37p (Farrell and Morgan, 2000), a subunit of the chaperone Hsp90p that specifically targets protein kinases (Kimura *et al.*, 1997). Since Cdc37p loss of function mutations can lead to Cdc28p decreased levels (Gerber *et al.*, 1995), we investigated whether defects in this chaperone system could underlie the phenotype of the OXPHOS mutants carrying the *cdc28-td* allele. For that, we tested the sensitivity of the strains to geldanamycin (GA), an Hsp90p inhibitor that prevents the association of Hsp90p-Cdc37p complexes with client protein kinases, inhibiting their maturation (Bandhakavi *et al.*, 2003). As shown in Figure 5.6A, *atp2*Δ*cdc28-td* and *cox4*Δ*cdc28-td* double mutants were hypersensitive to 100 μM GA at the permissive temperature, suggesting that Hsp90p-Cdc37p activity must be affected in OXPHOS/*cdc28* double mutants. Interestingly, OXPHOS and *cdc28-td* single mutants exhibited a sensitivity to GA similar to wt cells.

The Hsp90p-Cdc37p complex controls the folding of a large proportion of protein kinases (Mandal *et al.*, 2007). We investigated the levels of two Hsp90p-Cdc37p client kinases involved in distinct signalling pathways, Slt2p and Yck2p, identified by a reduced accumulation in cells expressing a $Cdc37^{S14A}$ mutant protein (Mandal *et al.*, 2007) that exhibits low Cdc37p activity (Bandhakavi *et al.*, 2003). The steady-state levels of Slt2p and Yck2p were determined in wt, *atp2*Δ, *cdc28-td* and *atp2*Δ*cdc28-td* cells cultured at 30 ºC. Our results show that Slt2p and Yck2p accumulate at reduced levels in *atp2*Δ*cdc28-td* double mutant, but not in single mutants (Figure 5.6B,C). This result indicates that the combination of respiratory and *cdc28* defects impacts on the stability of multiple kinase substrates of the Hsp90p-Cdc37p system. We confirmed the reduced accumulation of these kinases in the $cdc37^{S14A}$ cells (Figure 5.6B).

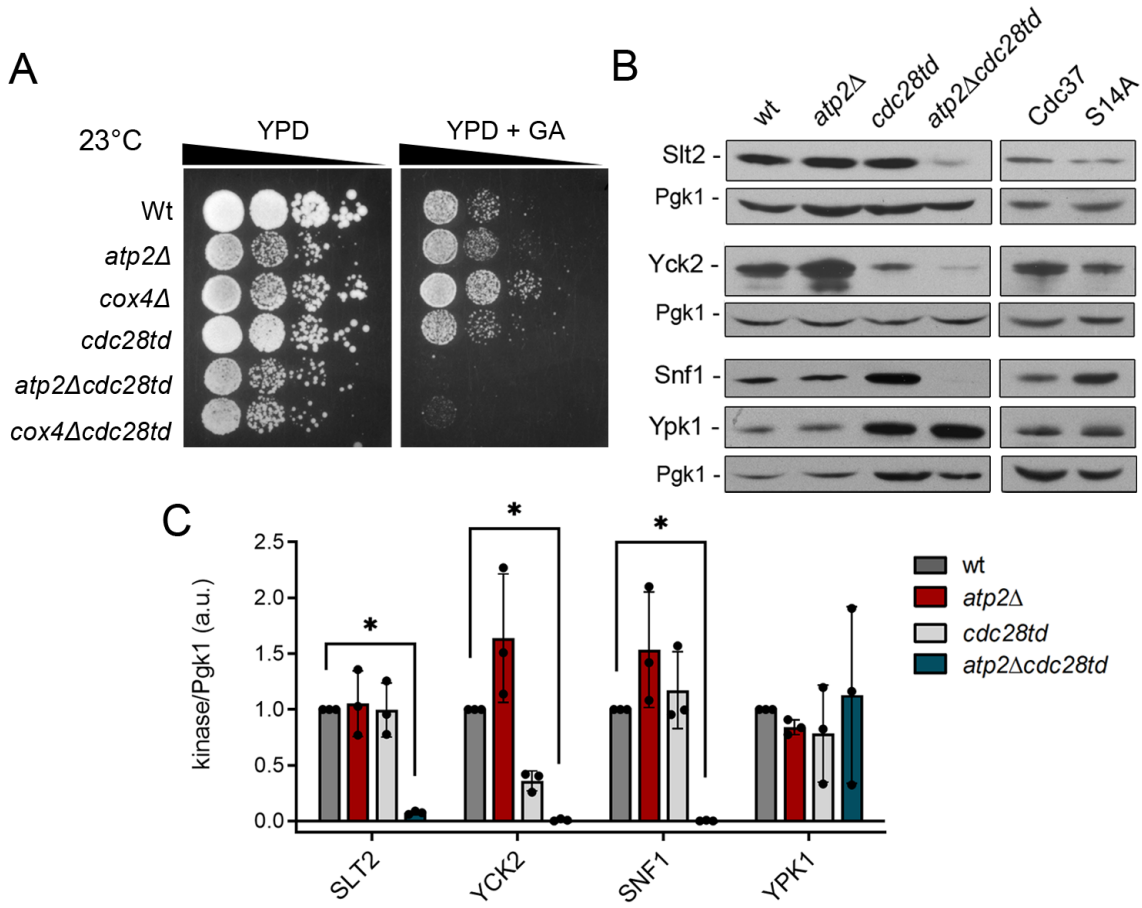

Figure 5.6. Combining OXPHOS and Cdc28p mutations affect the Hsp90p-Cdc37p chaperone complex. (A) Deletion of *ATP2* or *COX4* in *cdc28-td* causes GA sensitivity in yeast. Cultures were grown at 23 ºC to mid-log phase, plated on YPD with solvent (DMSO) or with 100 μM GA, and incubated for 3 days at 23 ºC (permissive temperature). Image representative of 3 experiments. (B) Immunodetection of Hsp90p-Cdc37p client and non-client kinases. wt, *atp2*Δ, *cdc28-td atp2*Δ*cdc28-td* mutants transformed with YEp352-*SLT2–3HA*, pRS316-*SNF1-HA* and p416-*GFP-YCK2* were cultured at 30 ºC (semi-permissive). Slt2p and Snf1p were detected by western blot with anti-HA, Yck2p with anti-GFP and Ypk1p with anti-Ypk1p. Kinase levels in wt and *cdc37*-S14A cells cultured at 30 ºC are shown. (C) Fold change for proteins as in B was estimated by densitometric scanning of each kinase vs Pgk1p bands. Values are the mean ± SD (n = 4); *, $p < 0.05$; one-way ANOVA followed by Turkey's multiple comparison test.

We also investigated the levels of two kinases, Snf1p and Ypk1p, whose levels were reportedly unchanged in cdc37^{S14A} cells (Mandal *et al.*, 2007). As they are not likely Hsp90p-Cdc37p targets, we predicted they would not be affected in the strains in study. Unexpectedly, Snf1p protein levels were also strongly decreased in *atp2*Δ*cdc28-td* cells in comparison with wt and single mutant strains (Figure 5.6B,C). Interestingly, though not statistically significant, both Yck2p and Snf1p exhibit a tendency to accumulate at higher levels in the single *atp2*Δ mutant. Unlike Snf1p, the endogenous Ypk1p levels were unchanged in *atp2*Δ*cdc28-td* cells, as expected (Figure 5.6B,C).

To assess which of the Hsp90p-Cdc37p complex components might be affected in the *atp2*Δ*cdc28-td* cells, we overexpressed Cdc37p and Hsp90p (encoded by *HSC82* and

HSP82 in *S. cerevisiae*) independently. Overexpression of Cdc37p, the component providing kinase specificity, but not Hsc82p or Hsp82p, suppressed the *atp2*Δ*cdc28-td* mutant growth defects at 29 ºC (Figure 5.7A), and had a partial protective effect at higher temperatures (32 ºC). Notably, the growth rescue promoted by Cdc37p overexpression in the *atp2*Δ*cdc28-td* mutant correlated with a partial restoration of Cdc28p and Snf1p levels (Figure 5.7B). These results suggest that Cdc37p activity is affected in the *atp2*Δ*cdc28-td* mutant, underlying its growth defects. Notably, Cdc37p protein levels were not altered in OXPHOS mutants (single or in combination with *cdc28-td*) (Figure 5.7B and Figure 5.15). Thus, it seems post-translational regulation of Cdc37p might be compromised in these mutant cells given that PTMs are vital for its activity (Bandhakavi *et al.*, 2003; Shao *et al.*, 2003). Since phosphorylation on Ser14/Ser17 is essential for Cdc37p function by promoting its protein kinase-binding activity (Bandhakavi *et al.*, 2003; Shao *et al.*, 2003), we evaluated growth of *atp2*Δ*cdc28-td* cells transformed with either empty-vector or the plasmids expressing wild-type Cdc37p, nonphosphorylatable Cdc37-S14A/S17A (Cdc37-AA) or phosphomimetic Cdc37-S14E/S17E (Cdc37-EE). Cdc37p, but not Cdc37-AA or Cdc37-EE, rescued *atp2*Δ*cdc28-td* growth defects in semi-repressive conditions (Figure 5.7C), suggesting that the phosphoregulation of Cdc37p is important for its protective effects.

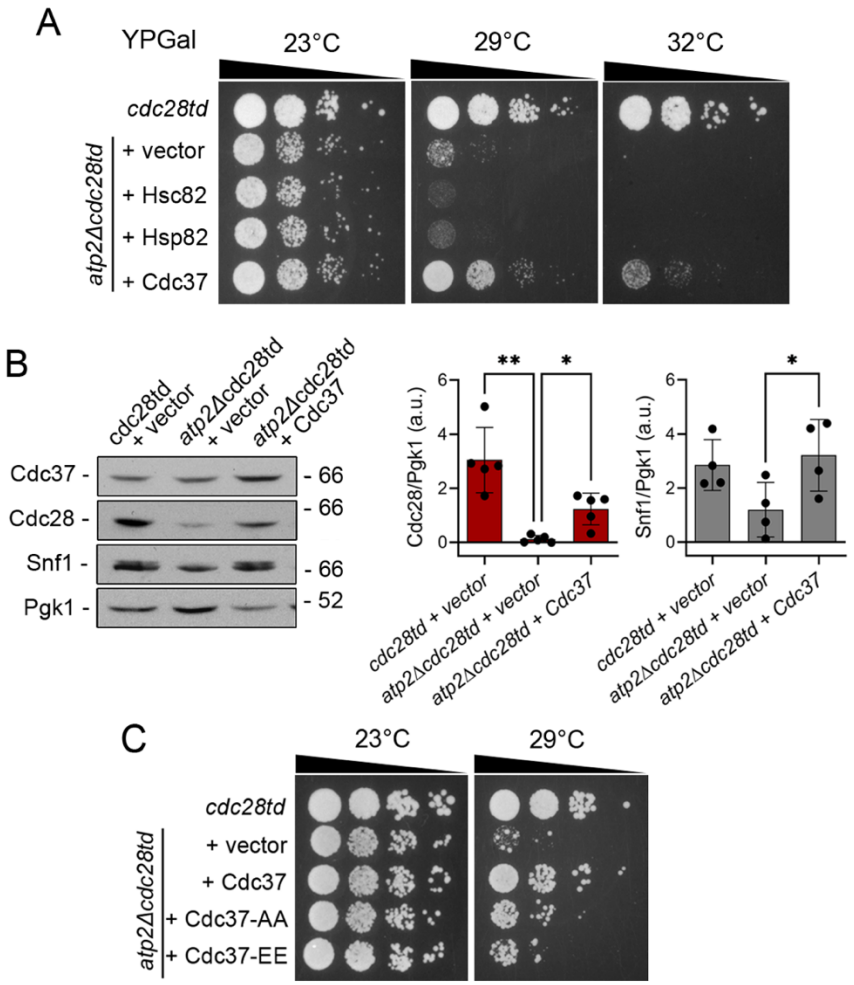

Figure 5.7. Overexpression of *CDC37* partially supresses the *atp2Δcdc28-td* mutant growth defects and restores Cdc28p and Snf1p levels. (A) Growth of *atp2Δcdc28-td* cells overexpressing *HSC82*, *HSP82* and *CDC37* controlled by the *GAL* promoter, on galactose rich medium (YPGal) at permissive (23 ºC) and semi-restrictive temperatures (29 ºC and 32 ºC). (B) Western blot showing Cdc28p, Snf1p and Cdc37p levels in *cdc28-td* and *atp2Δcdc28-td* cells transformed with empty-vector or expressing Cdc37p. Fold change over Pgk1p is shown on the right. Values are the mean ± SD (n = 4); *, $p < 0.05$; one-way ANOVA followed by Turkey's multiple comparison test. (C) Growth of *atp2Δcdc28-td* cells transformed with either empty-vector or the plasmids expressing wt Cdc37p, nonphosphorylatable Cdc37-AA (S14A/S17A) and phosphomimetic Cdc37-EE (S14E/S17E) mutants incubated at permissive and semi-restrictive temperatures. Images in A and C are representative of 4 experiments.

5.3. Discussion

Mitochondria are not only at the centre of aerobic energy production and essential biosynthetic activities but are also tightly interconnected to other cellular processes and signalling cascades important for cell proliferation and survival. The present work point to a role of mitochondria in cell cycle progression by revealing that combined disturbance of mitochondrial respiration and Cdc28p activity inhibits cell proliferation. Importantly, this effect is due to inhibition of Cdc37p, which in turn leads to a further decrease in Cdc28p, underscoring more complex interactions between these proteins than previously

anticipated. Cdc28p plays a major role in cell division and its activity is carefully controlled by checkpoint mechanisms that monitor cues from the environment and their own internal state (Mendenhall and Hodge, 1998). Our results suggest that under less than optimal conditions, when Cdc28p activity is reduced, mitochondrial fitness will be decisive for cell cycle progression decisions.

The aggravated phenotype in the OXPHOS/*cdc28* double mutants (mitochondrial fragmentation and hyperpolarization) suggests that Cdc28p might affect a pathway in common with mitochondrial respiration. Previous reports have already given evidence that Cdc28p/Cdk1 is required for normal mitochondrial function in both yeast and mammals (Genta *et al.*, 1995; Harbauer *et al.*, 2014; Taguchi *et al.*, 2007). In mammalian cells, Cdk1 favours mitochondrial fragmentation during mitosis by phosphorylating the dynamin-related GTPase Drp1 (yeast Dnm1p) (Taguchi *et al.*, 2007). Whether Cdc28p also targets the mitochondrial fusion/fission machinery in yeast is still unknown. Curiously, given that a repressible mutant of Cdc37p also leads to abnormal fragmentation (Altmann and Westermann, 2005), we cannot discard the hypothesis that the observed mitochondrial morphology defects in the OXPHOS/*cdc28* double mutants is a consequence, and not a cause, of Cdc37p inhibition. Apparently, mitochondrial function might affect more and be more affected by the cell cycle machinery than previously anticipated.

A remaining question is how the combined impairment of mitochondrial respiration and Cdc28p activity leads to an inhibition of Cdc37p. In this work we have discarded the hypothesis that the aggravated mitochondrial dysfunction in the OXPHOS/*cdc28* mutants triggers the RTG response. Given that we observed that Cdc37p protein levels are not altered in this strain, Cdc37p inhibition might be associated to changes at the PTMs level. Cdc37p PTMs can occur in several amino acid residues, many of unknown physiological relevance, as listed in the SGD database (Hellerstedt *et al.*, 2017). A prominent PTM is phosphorylation on S14 and/or S17 (residue S13 in the human protein), as this modification is considered essential for Cdc37p function (Bandhakavi *et al.*, 2003; Shao *et al.*, 2003). However, the expression of a phosphomimetic Cdc37-EE version, comparing to the phosphoresistant Cdc37-AA, did not have a protective effect on *atp2*Δ*cdc28-td* mutant, arguing against this hypothesis. Plus, Snf1p stability decreased in the *atp2*Δ*cdc28-td* mutant (our results) but not in cdc37^{S14A} cells (Mandal *et al.*, 2007). In our conditions Snf1p even accumulated at higher levels in cells expressing the Cdc37-S14A mutant. Phosphorylation of S14 is normally crucial for the stabilisation of Cdc37p client kinases, with exceptions. For example, Cak1p accumulates at higher levels upon loss of Cdc37-S14 phosphorylation (Millson *et al.*, 2014). It is conceivable that PTM other than S14 phosphorylation might impact on the Cdc37p activity towards specific kinases.

Expanding our knowledge on the complex interactions between mitochondrial dysfunction and impaired kinase activity will improve our understanding of the multifactorial interactions controlling proliferation and potentially disease. In humans, a prominent number of Cdc37p targets are oncoproteins (Miyata and Nishida, 2004) and aberrant CDK activity also underpins proliferation of tumour cells (Malumbres and Barbacid, 2009), making research on the regulation of these proteins of considerable interest. Plus, mitochondrial metabolism is altered in cancer cells and OXPHOS inhibitors are gaining attention as therapeutic approaches (Ashton *et al.*, 2018). Since inhibition of both Cdc28p and OXPHOS have a strong growth inhibitory effect in our model, we postulate that the synergistic use of CDK and OXPHOS inhibitors might also be advantageous in antitumor therapeutics.

5.4. Material and methods

5.4.1. Yeast strains and growth conditions

The *Saccharomyces cerevisiae* strains used in this study are all BY4741 derivative and are listed in Table 5.1. The *atp1*Δ, *atp4*Δ, *qcr2*Δ and *cox4*Δ strains were constructed by replacing the ORF of each gene by the auxotroph marker *HIS3,* using PCR-mediated homologous recombination. To construct double mutant strains, the cassette containing *cdc28-td:KanMX4*, *cdc28-1:KanMX4*, *cdc20-1:KanMX4* and *ipl1-1:KanMX4* were amplified by PCR and transformed in indicated deletion strains. To construct the *cdc28-1N* expressing strains, *cdc28–1N* sequence was amplified from US102 strain (Loy *et al.*, 1999) and fused to the KanMX6 cassette, using overlap extension PCR. This product was then integrated into wt and *atp2*Δ strains. pBL101-p*CIT2*-LacZ (Liu and Butow, 1999) was linearized by digestion with *Sma*I and integrated into the genomic *CIT2* locus. Correct deletions/insertions were confirmed by PCR. For Hsp90 and Cdc37 overexpression, the auxotroph marker *HIS3* in the *atp2*Δ*cdc28-td* strain was replaced by *URA3* by PCR-mediated recombination and cells were transformed with empty-vector, pAG423*GAL-HSC82*, pAG423*GAL-HSP82* or pAG423*GAL-CDC37* (Lin *et al.*, 2021). For kinase levels assays, wt, *atp2*Δ, *cdc28-td*, *atp2*Δ*cdc28-td* cells were transformed with YEp352-*SLT2-3HA* (Madden *et al.*, 1997), pRS316-*SNF1-HA* (Ye *et al.*, 2008) and p416-ADH-yeGFP-*YCK2*. To generate p416-ADH-yeGFP-*YCK2*, the yeGFP sequence was inserted into the *Xba*I site of p416ADH plasmid followed by insertion of the *YCK2* sequence (*Bam*HI-*Sal*I fragment) amplified. Strains TM141 *cdc37*Δ::*HIS3* [Ycplac111 CDC37-HA] and *cdc37*Δ::*HIS3* [Ycplac111 *CDC37-S14A-HA*] (Hawle *et al.*, 2007) were also transformed with the above plasmids and used as control. For growth assays, Ycplac111-*CDC37*, *CDC37S14/17A* and *CDC37S14/17E* were isolated from TM141 strains (Vaughan *et al.*, 2008) and plasmids used to transform *cdc28-td* and *atp2*Δ*cdc28-td* cells.

Strains were transformed by the standard lithium acetate procedure (Gietz and Schiestl, 2007). To avoid clonal variability, at least 2 different colonies were analyzed in all experiments.

Cells were grown in YPD rich medium (1% (w/v) yeast extract, 2% (w/v) peptone, and 2% (w/v) glucose; Fisher Scientific). YPGal/Raf containing 2% (w/v) galactose (Biosynth) plus 2% (w/v) raffinose (Biosynth) instead of glucose as a carbon source, was used for the induction of gene expression from plasmids with the *GAL1* promoter. Cultures were routinely grown in an orbital shaker at 140 r.p.m.

For clone selection, strains were grown in YPD agar supplemented with 250 μg/mL geneticin (Santa Cruz Biotechonology) or in synthetic complete medium [SC; 0.67% (w/v) Bacto-yeast nitrogen base w/o aminoacids (BD Difco), 2% (w/v) glucose and 0.2% (w/v) Dropout mix; Sigma] lacking histidine or uracil, as appropriate.

For geldanamycin (GA; MedChemExpress) supplemented medium, GA was dissolved in dimethyl sulfoxide and added to a final concentration of 100 μM to warm YPD agar medium before pouring.

Table 5.1. *S. cerevisiae* strains used in this study.

Strain	Genotype	Source
BY4741	Mat *a*; *his3Δ1 leu2Δ0 met15Δ0 ura3Δ0*	Euroscarf
atp2Δ	BY4741; *atp2Δ::HIS3MX6*	Lab collection
cdc28-td	BY4741; *cdc28-td:KanMX4*	Euroscarf (Li *et al.*, 2011)
atp2Δcdc28-td	BY4741; *atp2Δ::HIS3MX6 cdc28-td:KanMX4*	This study
cdc28-1	BY4741; *cdc28-1:KanMX4*	Euroscarf (Li *et al.*, 2011)
atp2Δcdc28-1	BY4741; *atp2Δ::HIS3MX6 cdc28-1:KanMX4*	This study
cdc28-4	BY4741; *cdc28-4:KanMX4*	Euroscarf (Li *et al.*, 2011)
atp2Δcdc28-4	BY4741; *atp2Δ::HIS3MX6 cdc28-4:KanMX4*	This study
cdc28-1N	BY4741; *cdc28-1N:KanMX4*	This study
atp2Δcdc28-1N	BY4741; *atp2Δ::HIS3MX6 cdc28-1N:KanMX4*	This study
cox4Δ	BY4741; *cox4Δ::HIS3MX6*	This study
cox4Δcdc28-td	BY4741; *cox4Δ::HIS3MX6 cdc28-td:KanMX4*	This study
qcr2Δ	BY4741; *qcr2Δ::HIS3MX6*	This study
qcr2Δcdc28-td	BY4741; *qcr2Δ::HIS3MX6 cdc28-td:KanMX4*	This study
atp1Δ	BY4741; *atp1Δ::HIS3MX6*	This study
atp1Δcdc28-td	BY4741; *atp1Δ::HIS3MX6 cdc28-td:KanMX4*	This study
atp4Δ	BY4741; *atp4Δ::HIS3MX6*	This study
atp4Δcdc28-td	BY4741; *atp4Δ::HIS3MX6 cdc28-td:KanMX4*	This study
rtg3Δ	BY4741; *rtg3Δ::URA3MX6*	This study
atp2Δrtg3Δcdc28-td	BY4741; *atp2Δ::HIS3MX rtg3Δ::URA3MX6 cdc28-td:KanMX4*	This study
cdc20-1	BY4741; *cdc20-1:KanMX4*	Euroscarf (Li *et al.*, 2011)
atp2Δcdc20-1	BY4741; *atp2Δ::HIS3MX6 cdc20-1:KanMX4*	This study
ipl1-1	BY4741; *ipl1-1:KanMX4*	Euroscarf (Li *et al.*, 2011)
atp2Δ ipl1-1	BY4741; *atp2Δ::HIS3MX6 ipl1-1:KanMX4*	This study
rho^0 CIT2-LacZ	BY4741; *rho^0 CIT2-LacZ:CIT2*	This study
CIT2-LacZ	BY4741; *CIT2-LacZ:CIT2*	This study
cdc28-td CIT2-LacZ	BY4741; *cdc28-td; CIT2-LacZ*:*CIT2*	This study
atp2Δcdc28-td CIT2-LacZ	BY4741; *atp2Δcdc28-td*; *CIT2-LacZ*:*CIT2*	This study
cdc28-1 CIT2-LacZ	BY4741; *cdc28-1; CIT2-LacZ*:*CIT2*	This study
atp2Δcdc28-1 CIT2-LacZ	BY4741; *atp2Δcdc28-1*; *CIT2-LacZ*:*CIT2*	This study
cdc28-1N CIT2-LacZ	BY4741; *cdc28-1N; CIT2-LacZ*:*CIT2*	This study
atp2Δcdc28-1N CIT2-LacZ	BY4741; *atp2Δcdc28-1N*; *CIT2-LacZ*:*CIT2*	This study
DH211	TM141 *cdc37Δ::HIS3* [Ycplac111 CDC37-HA]	(Hawle *et al.*, 2007)
DH212	TM141 *cdc37Δ::HIS3* [Ycplac111 CDC37-S14A-HA]	(Hawle *et al.*, 2007)

5.4.2. β-galactosidase assay

For the β-galactosidase assay, yeast cells expressing *pCIT2-LacZ* were grown in YPD to exponential phase. Cells were incubated for 3h at the restrictive temperature to inactivate *cdc28-td* (37 ºC)*, cdc28-1N* (37 ºC) and *cdc28-1* (35 ºC). The β-galactosidase activity was measured in a liquid assay using *o*-nitrophenyl-β-D-galactoside (ONPG) as previously described (Almeida *et al.*, 2008), using 60 μg of total protein.

5.4.3. Cell cycle analysis

For cell cycle analysis, strains were cultured overnight in YPD at 24 ºC to mid-log phase. A portion of the cultures was then shifted to 37 ºC for 3 h, while the remaining was maintained at 24 ºC for the same time and used as controls. Cells were fixed overnight and DNA content was analysed by flow cytometry using 10 μM SYTOX Green (Molecular Probes), basically as described in (Haase and Reed, 2002). Cells were analysed using the FL1 detector in a BD Accuri C6. 20000 events were analysed per sample and cell cycle distribution was estimated using FlowJo v10 software version.

5.4.4. Mitochondrial membrane potential

To assess the mitochondrial membrane potential (ΔΨm), cells were incubated for 30 min at 30 ºC with 40 nM of 3,3-dihexyloacarbocynine iodide ($DiOC_6(3)$, Molecular Probes) (Pereira *et al.*, 2014). When used, the uncoupler carbonyl cyanide 4-(trifluoromethoxy)phenylhydrazone (FCCP, Sigma; 10 μM) was added 10 min before loading with $DiOC_6(3)$. At least 20000 cells were analysed per sample using the FL1 detector in a BD Accuri C6 flow cytometer. The collected data was analysed using FlowJo v10 software version to determine the mean green fluorescence intensity.

5.4.5. Oxygen consumption rate

The oxygen consumption rate was measured polarographically in whole cells (1×10^8 in PBS buffer) from cultures grown in YPD medium to late log phase, using a Clark-type oxygen electrode coupled to an Oxygraph plus system (Hansatech). Data were analysed using the OxyTrace$^+$ software. The respiratory rate in the presence and absence of the inhibitor potassium cyanide (700 μM; Merck) was obtained by dividing the oxygen consumed per min by the number of cells used in the experiment.

5.4.6. Microscopy analysis

For the analysis of mitochondrial morphology and volume, samples from strains transformed with a pVT100mtGFP fusion gene (Westermann and Neupert, 2000) were

imaged by fluorescence microscopy. Images were acquired by epifluorescence in a Zeiss Axio Imager Z1 microscope fitted with Nomarski optics with an Axiocam MR3.0 camera and analysed using the Axiovision 4.7 software. Images were collected at 0.4 μm z-intervals and average projected to produce the final image. The mitochondria morphology types were analysed manually in about 100 cells per strain, and the mitochondrial area in the cell was measured using the tools included in the ImageJ software (NIH).

5.4.7. Immunoblotting

Yeast total protein lysates were obtained by boiling in SDS sample buffer (without β-mercapthoethanol) at 95 ºC (5 min). Protein concentration was measured using the Pierce BCA Protein Assay Kit (ThermoFisher Scientific) and β-mercapthoethanol was then added to the lysate. Proteins (40 μg) were separated by SDS-PAGE, electroblotted onto a nitrocellulose membrane (Hybond-C, GE Healthcare) and probed with antibodies using standard protocols. Primary antibodies used were anti-Cdc28p (1:150; sc-515762, Santa Cruz Biotechnology), anti-Cdc37p (1:15000; ab188280, Abcam), anti-Ypk1p (1:500; sc-12051, Santa Cruz Biotechnology), anti-Snf1p (1:100; sc-15622, Santa Cruz Biotechnology), anti-Pgk1p (1:25000; 22C5D8, ThermoFisher), anti-GFP (1:6000; Clontech), and anti-HA (1:5000; sc-7392, Santa Cruz Biotechnology). Secondary antibodies used were anti-mouse IgG-HRP (1:7000, Molecular probes), anti-rabbit IgG-HRP (1:7000, Sigma) and anti-goat IgG-HRP (1:5000, Santa Cruz Biotechnology). Membranes were washed, incubated with WesternBright ECL (Advansta), exposed to LucentBlue X-ray film (Advansta), and scanned on a Molecular Imager GS800. Protein band intensities were quantified using Quantity One 1-D Analysis Software version 4.6 (Bio-Rad).

5.4.8. Statistical analysis

Data were analysed in GraphPad Prism Software v8.4.3 (GraphPad Software). Values were compared by one-way ANOVA, *, $p < 0.05$; **, $p < 0.01$; ***, $p < 0.001$.

5.5. Acknowledgements

The authors acknowledge Uttam Surana (A*STAR, Singapore) for the *cdc28-1N* strain, Zhengchang Liu (University of New Orleans, LA, USA) for the *CIT2-LacZ* plasmid, John Pringle (Stanford University School of Medicine, CA, USA) for the pFA6a- kanMX6-PGAL1-3HA plasmid, and Martin L. Duennwald (University of Western Ontario, Canada) for the *CDC37*, *HSC82* and *HSP82* overexpression plasmids. The Cdc37p (WT), cdc37^{S14A}, cdc37$^{S14/17A}$, and cdc37$^{S14/17E}$ strains were generously provided by Marco Siderius (Vrije Universiteit Amsterdam, Netherlands) and Mehdi Mollapour (Upstate Medical University,

NY, USA). The authors acknowledge the support of the i3S Scientific Platforms Translational Cytometry and Advanced Light Microscopy (member of the national infrastructure PPBI - Portuguese Platform of Bioimaging PPBI-POCI-01-0145-FEDER-022122).

5.6. Supplementary material

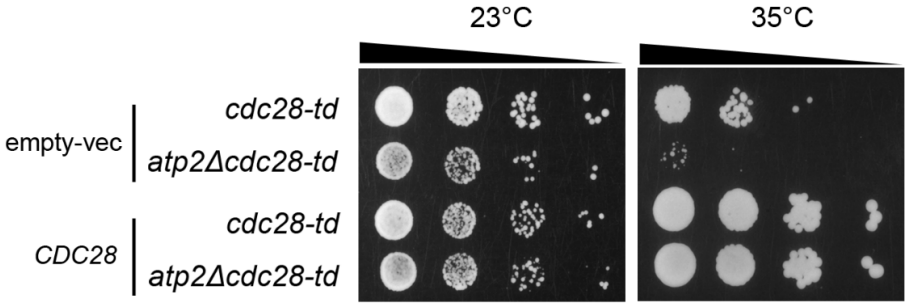

Figure 5.8. Reintroducing wt Cdc28p restored the *atp2*Δ*cdc28-td* mutant growth at semi-permissive temperature. Growth analysis of *cdc28-td* and *atp2*Δ*cdc28-td* transformed with empty-vector (YCP50) or the YCP50-derived pHLP183 vector (expressing *CDC28* from its natural promoter; a gift from Mark C. Hall (Hall *et al.*, 2008)). Cells were spotted in serial dilutions and grown at indicated semi-permissive temperatures. A representative result is shown (*n* = 3).

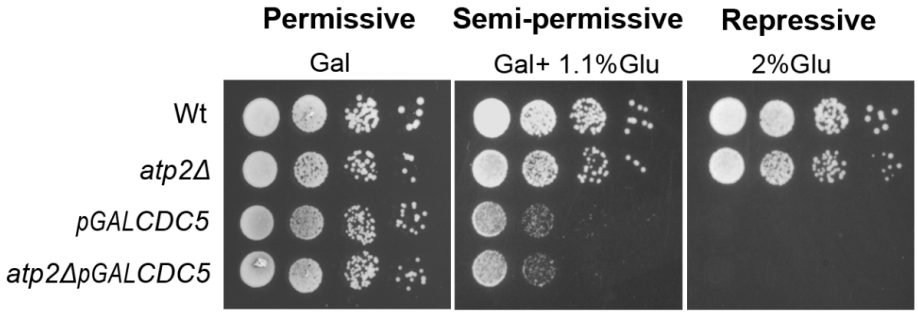

Figure 5.9. *ATP2* does not genetically interact with the polo-like kinase encoding gene *CDC5*. Growth analysis of wt, *atp2*Δ, *pGAL1-CDC5* and *atp2*Δ*pGAL1-CDC5* strains. *CDC5* was placed under the control of *GAL1* promoter and partially or completely downregulated by growing the cells in the presence of the indicated concentrations of glucose. *CDC5* was placed under the control of the *GAL1* promoter by integrating the plasmid pFA6a-KanMX6-PGAL1-3HA into the wt and *atp2*Δ genomes upstream of *CDC5* (Longtine *et al.*, 1998). Cells were spotted in fourfold serial dilutions. A representative image is shown (*n* = 3).

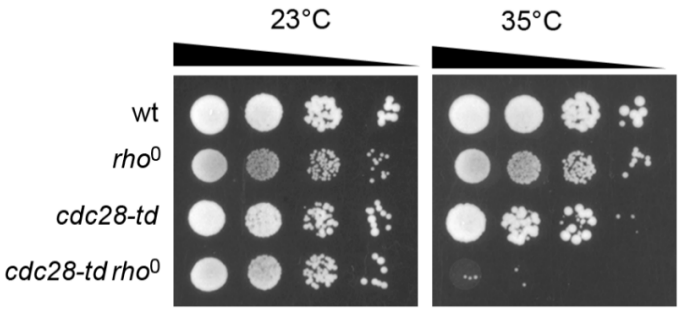

Figure 5.10. Ablating mitochondrial DNA in a strain carrying the *cdc28-td* allele aggravates defective growth at semi-permissive temperature. Growth analysis of wt, *rho*^{0}, *cdc28-td* and *rho*^{0}*cdc28-td* spotted in serial dilutions and grown at permissive and semi-permissive temperatures. A representative result is shown (n = 3). To generate *rho*^{0} strains, cells were grown to saturation twice in liquid YPD medium plus ethidium bromide (25 μg/mL). Individual colonies were selected for growth defects on YPG plates and loss of mtDNA was confirmed by 4′,6-diamidino-2-phenylindole (DAPI) staining.

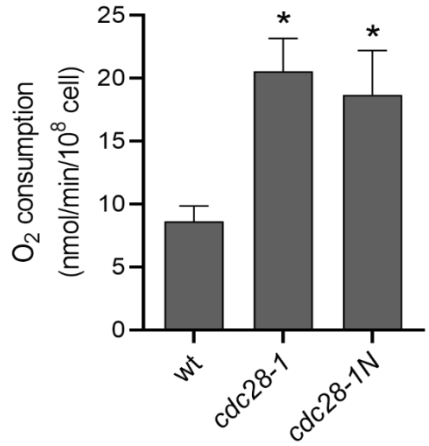

Figure 5.11. Respiratory rate is increased in *cdc28-1* and *cdc28-1N* mutants at restrictive temperature. The basal respiratory rate was determined by measuring oxygen consumption in whole cells from glucose grown mid-log phase cultures at the restrictive temperature. Values are the mean ± SD (n = 4); *, $p < 0.05$; one-way ANOVA followed by Turkey's multiple comparison test.

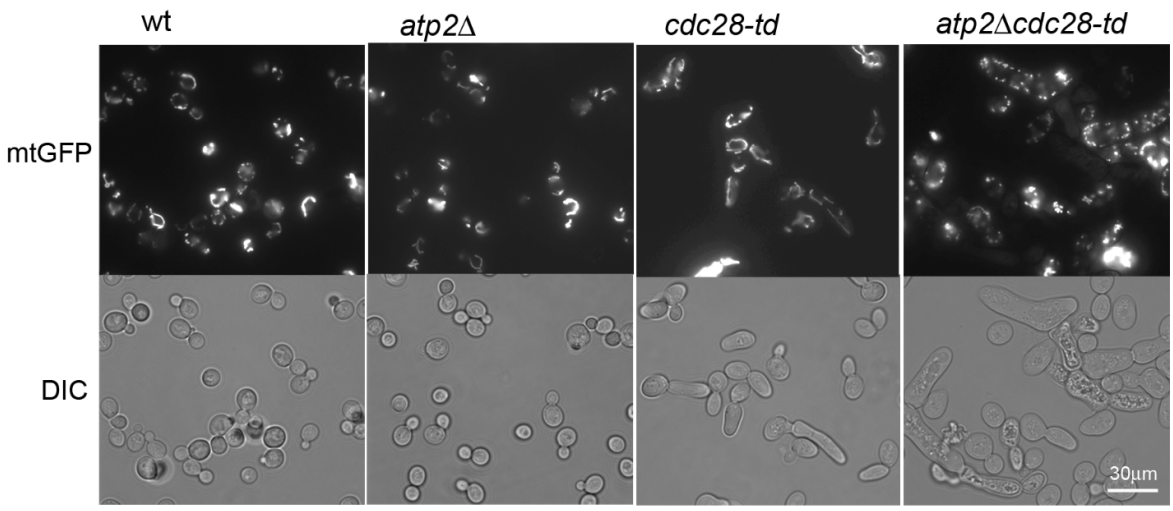

Figure 5.12. Mitochondrial morphology is disrupted in double *atp2Δcdc28-td* strain. Indicated yeast cells expressing mtGFP were analysed by fluorescence microscopy. Representative DIC images are merged with maximum intensity projections generated from z-stacks of the mitochondrial green fluorescent signal. Images were acquired by epifluorescence in a Zeiss Axio Imager Z1 microscope fitted with Nomarski optics with an Axiocam MR3.0 camera and Axiovision 4.7 software.

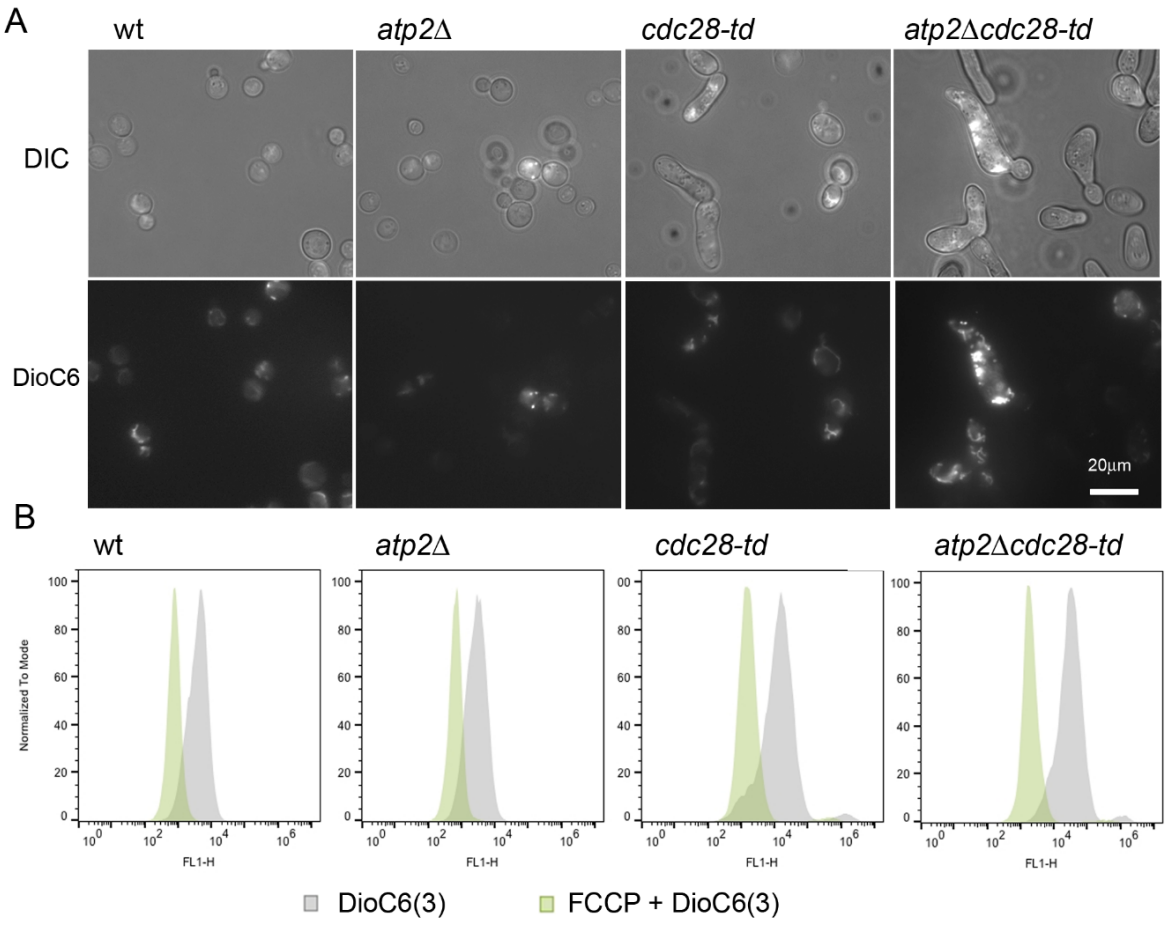

Figure 5.13. Mitochondrial membrane potential is altered in double *atp2Δcdc28-td* mutant. (A) The mitochondrial localization of the fluorochrome $DiOC_6(3)$ was checked by fluorescence

microscopy. Representative DIC images are merged with maximum intensity projections from z-stacks of the $DiOC_6(3)$ staining. (B) Addition of the FCCP protonophore, which dissipates the Δψ*m*, lead to a substantial reduction of the $DiOC_6(3)$ uptake for all strains.

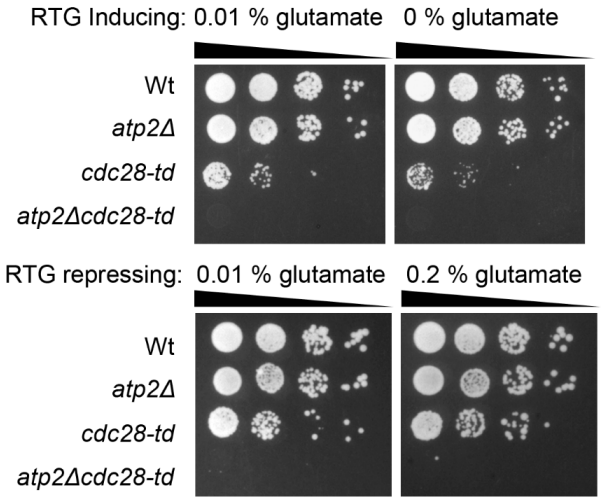

Figure 5.14. Absence or excess of glutamate, a repressor of RTG-dependent gene expression, do not supress the growth defects of the *atp2Δcdc28-td* strain. Serial dilutions of indicated strains after growth at the semi-permissive temperature (35 ºC) in minimal media containing 0.01% glutamate (control), lacking or containing 0.2% glutamate.

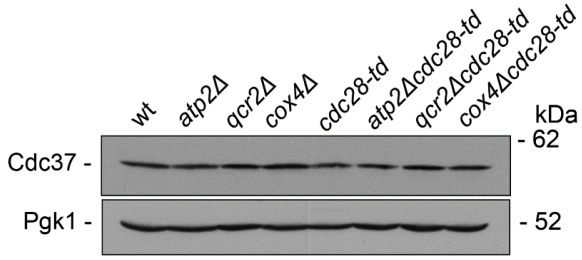

Figure 5.15. Cdc37p levels are unchanged in OXPHOS mutants, single or in combination with *cdc28-td*. Western blot analysis of Cdc37p steady-state protein levels in indicated strain cultures at semi-permissive temperature of 26 ºC. Pgk1p is shown as loading control. A representative blot is shown (*n* = 2).

CHAPTER 6.

General discussion

There is ample evidence of an interplay between mitochondrial physiology and cell cycle progression. Conserved signaling pathways play a key role in the regulation of cell growth and division as well as of mitochondrial inheritance, biogenesis, activity and quality control. The control of mitochondrial activities is important for cell cycle progression, as many mutants affecting mitochondria impact on cell cycle progression, some of them severely, supporting the hypothesis of mitochondrial checkpoints. Despite this, we still do not completely understand the molecular determinants involved in the coordination of mitochondrial inheritance and function with cell cycle progression.

This work aimed to contribute to our understanding of the molecular mechanisms underlying the cross-regulation between mitochondria and cell cycle using *Saccharomyces cerevisiae* as a model. Many of our knowledge on mitochondrial genetics and biochemistry is own to the exceptional fermenting capacity of *Saccharomyces cerevisiae*. Budding yeast tolerate mutations that compromise OXPHOS or even loss of mtDNA, by using ATP derived exclusively from fermentable carbon sources, making it a powerful model for mitochondrial studies. Herein, we have investigated the role of ATP synthase catalytic beta subunit (Atp2p) phosphorylation in cell cycle progression and searched for evidence that cell cycle machinery impacts on mitochondrial function.

The prevailing dogma is that cell division is a cellular process that requires a large amount of energy and that functional mitochondria are required to provide ATP. In line with this, we found that Atp2p levels and phosphorylation oscillate during budding yeast cell cycle, with an increase at G2/M phase. The Atp2-T124/T317 phosphorylation stimulates Δψ, mitochondrial respiration and cellular ATP levels at G2/M, contributing to cell cycle progression presumably by helping meet energetic demands (Figure 6.1). To our knowledge, our study provides the first insight into how a post-translational modification of a protein at the core of the ATP production can influence the cell cycle.

Interestingly, we found two peaks of increased oxygen consumption during cell cycle progression: one at the S phase, independent of Atp2p phosphorylation and likely the result of an increase in mitochondrial mass observed in this phase, and a second peak at G2/M which is dependent on Atp2p phosphorylation. An increase in respiration during S phase may fulfil increased energy requirements for DNA and lipid synthesis. Recent data also points for the maintenance of the cell cycle oscillator controlling mitotic entry and exit as the most energetically costlier processes in cell division (Rodenfels *et al.*, 2019). This is consistent with our observations of an increased yeast mitochondrial activity at G2/M and not during growth phases.

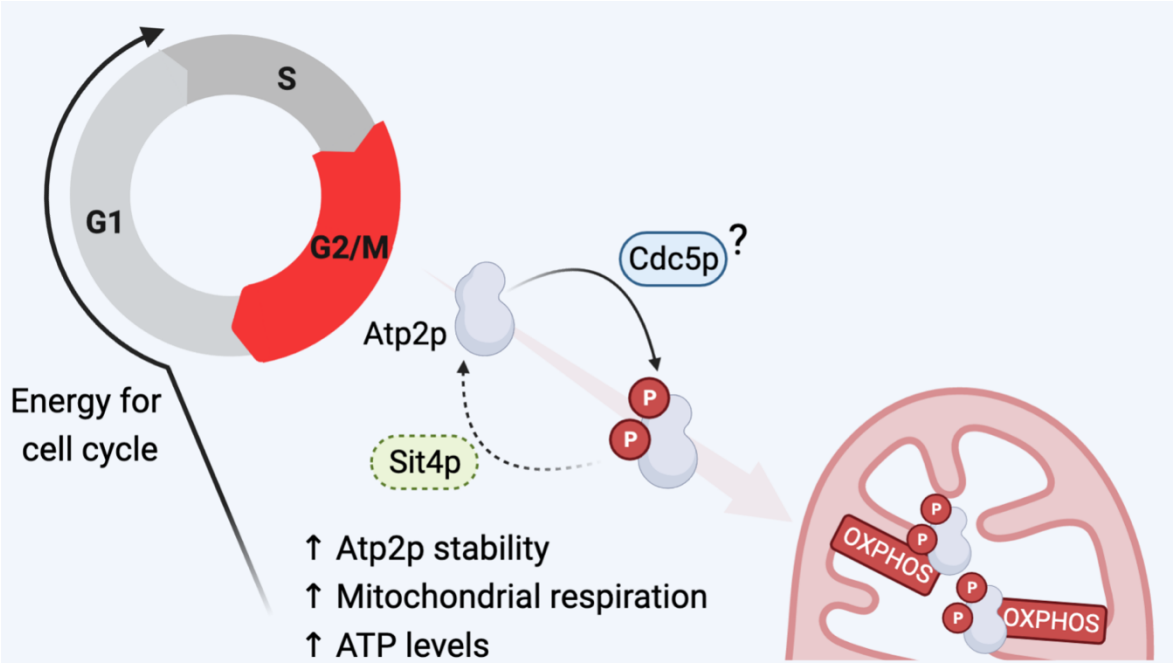

Figure 6.1. Phosphorylation of Atp2p, possibly by the polo-like kinase Cdc5p, stimulates mitochondrial membrane potential, respiration and ATP production at G2/M and promotes cell cycle progression.

The fact that mitochondrial respiration peaks at G2/M together with the evidence that daughter cells inherit the fittest mitochondria poses the question of what is the mitochondrial activity in daughter cells? Is the mitochondrial activity peak occurring asymmetrically in the mother and daughter cells? And does this activity contribute to bud formation? Curiously, a mutation in Atp2p was found to abrogate the asymmetry in the transmission of the fittest mitochondria to the bud (Lai *et al.*, 2002). In addition, our results reveal a higher mtDNA instability in the phosphomimetic Atp2-T124D/T317D mutant, raising the question whether the transient increase in respiration at G2/M may also play a role in mtDNA inheritance.

These changes in mitochondrial activity suggests alteration in ATP levels during cell cycle, but we and others (Takaine *et al.*, 2019) found no significant differences in ATP concentration during cell cycle progression. Yet, in the phosphoresistant Atp2p mutant, ATP levels (estimated by biochemical analysis) decreased specifically at G2/M, suggesting that ATP consumption is counteracted by a higher ATP production. We hypothesized ATP synthesis may be adjusted in accordance with the cellular needs contributing to maintain ATP at a constant level.

It is also still unclear whether mitochondria can support the generation of amino acids and cofactors essential for many processes such as DNA and protein synthesis and activity. It would be interesting to further evaluate whether the role of mitochondria in cell cycle progression goes beyond energy production.

As the results depicted on this thesis establish a novel functional association between Cdh1p and mitochondria (Figure 6.2), future studies are necessary to investigate the exact mechanism by which the APC/C cofactor impacts on mitochondrial function. Although the reason behind the increased Atp2p levels in the absence of the APC/C cofactor Cdh1p remains unclear, one can speculate that such alterations might occur as consequent perturbations in the *ATP2* transcription rate. In fact, our results showed that Cdh1p can affect the activity of transcription factors impacting on mitochondrial proteins abundance. These observations together with the well-known role of APC/C in cell cycle regulation raised the question whether Atp2p is also transcriptionally regulated during cell cycle. In recent years, several transcriptomic studies during the budding yeast cell cycle failed to identify the *ATP2* as a cell cycle regulated gene (Blank *et al.*, 2020; Campbell *et al.*, 2020; Orlando *et al.*, 2008; Spellman *et al.*, 1998). However, we cannot exclude the hypothesis that Cdh1p effect on mitochondrial remodeling is independent on the cell cycle progression. Our results also showed that Atp2p is potentially regulated by polo-like kinase Cdc5p, whose degradation is controlled by APC/C-Cdh1p (Shirayama *et al.*, 1998). Therefore, it is conceivable that the increased Atp2p stability is due to high levels of Cdc5p caused by a failure to degrade Cdc5p protein after *CDH1* deletion.

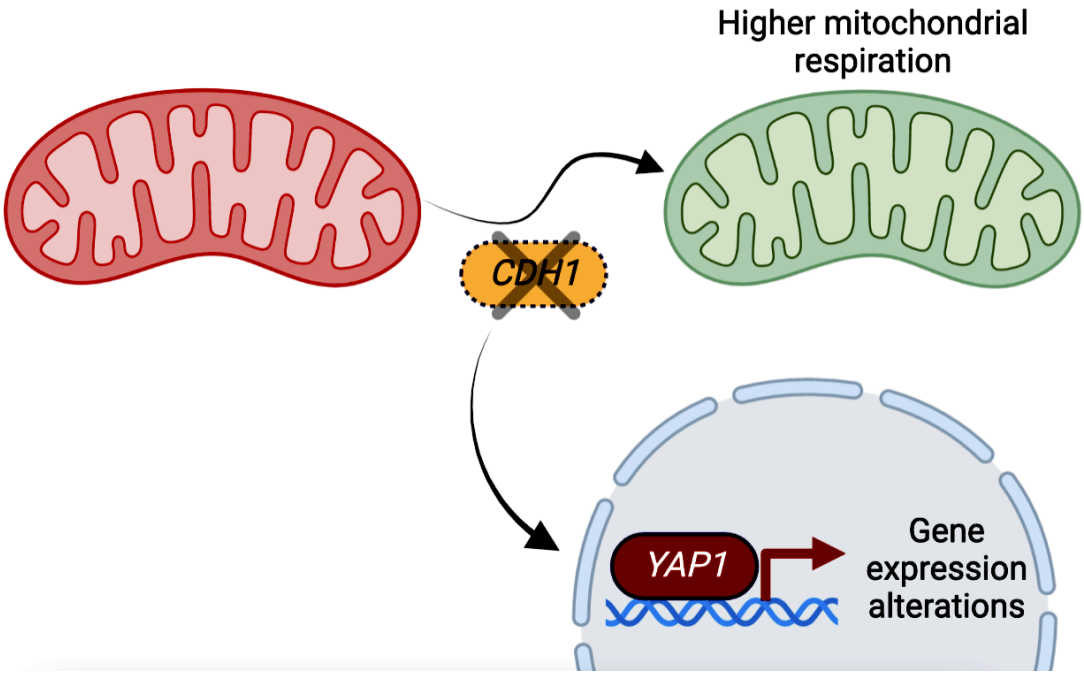

Figure 6.2. APC/C-Cdh1p regulates the mitochondrial metabolic remodelling through Yap1p activity.

Additionally, another interesting question that remains open concerns the effect of Cdh1p on the activity of the transcription factor Yap1p. It is well documented that in mammalian cells, APC/C directly regulates cell cycle transcription factors, namely FOXM1

(Laoukili *et al.*, 2008; Park Hyun *et al.*, 2008) and E2Fs (Peart *et al.*, 2010; Ping *et al.*, 2012) and controls the levels of transcriptional repressors (Boekhout *et al.*, 2016) to ensure the coordination of gene expression essential for cell cycle progression. However, our results suggest that Yap1p stability is not directly controlled by APC/C-Cdh1p complex. We speculate that the increased Yap1p activity may be a downstream event of stabilization of another APC/C-Cdh1p substrate important for Yap1p activation, culminating with the observed mitochondrial proteome remodeling and the consequent increase in mitochondrial respiration. Another possible explanation would be that Yap1p activation is directly triggered by the increase in ROS production determined by the increased mitochondrial respiration inherent of Cdh1p-deficient cells. Additionally, detailed analysis of Yap1p activity during cell cycle progression would provide valuable information to better comprehend the potential existence of an APC/C substrate responsible for modulating the Yap1p activity and whether this activity is important for cell cycle division. Taking in consideration that mitochondrial respiration is synchronized with cell cycle progression and that the high mitochondrial oxygen consumption in the *cdh1*Δ cells decrease upon *YAP1* deletion, we speculate that the APC/C regulation of Yap1p might contribute to the coordination of mitochondrial function with cell cycle progression. Previous studies have shown that deletion or overexpression of Yap1p cause cell cycle arrest at S (Yi *et al.*, 2016) and G2/M (Niu *et al.*, 2008) phases, respectively, probably to the imbalance in ROS production/elimination already pointing for a role of Yap1p in cell cycle progression.

The well-established role of Yap1p in the yeast response to oxidative damage also raised the question whether Yap1p connects the known transient increase in mitochondrial respiration and consequent ROS production with the expression of antioxidants defenses during cell cycle progression. In mammalian cells, it has been shown that mitochondrial ROS increases in a cell cycle-dependent manner, peaking at G2 and mitosis. Importantly, low levels of ROS promote cell cycle progression whereas high levels of ROS induce cell cycle arrest (Havens *et al.*, 2006) showing that cellular redox state is important for cell cycle decisions. Curiously, although the exact mechanism is not yet clear, the APC/C-Cdh1 modulates mitochondrial function and contributes to enhance the production of ROS during mitosis (Lambhate *et al.*, 2021). In contrast, at G1/S transition, APC/C-Cdh1 activity is inhibited by increased endogenous ROS (Havens *et al.*, 2006). It will be interesting to measure the ROS levels during budding yeast cell cycle and assess the expression of Yap1p-dependent genes (e.g., *SOD1*, *TRX2*, *GSH1*) and the activity of antioxidant defenses (e.g., glutathione, superoxide dismutase).

Cdc28p is a master regulator of yeast cell division cycle, and its activity is strictly controlled by checkpoint mechanisms. Our results suggest that, through the modulation of Cdc37p, mitochondrial dysfunction can also trigger cell cycle checkpoint arrest by directly

affecting Cdc28p levels, being decisive for cell cycle progression decisions. Since absence of Cdc28p leads to an enhancement of oxygen consumption rate, Cdc28p might regulate mitochondrial respiration in yeast cells. Further research will be required to determine whether Cdc28p kinase regulates mitochondrial function during cell cycle progression, as proposed for mammalian cells (Wang *et al.*, 2014). Based on our current knowledge we hypothesize that Cdc28p-mediated phosphorylation of mitochondrial respiratory chain subunits during cell cycle stimulates mitochondrial bioenergetics in order to meet the high energy demand to fuel cell cycle progression.

Overall, this thesis provides novel evidence supporting a cross-regulation between mitochondrial function and cell cycle progression in budding yeast. Interestingly, accumulating evidence suggest that mitochondrial reprograming is a central feature of carcinogenesis (Moindjie *et al.*, 2021). Although, mitochondrial respiration increases in some tumors (Zong *et al.*, 2016), the performance of mitochondria is greatly reduced in many forms of cancer (Frezza and Gottlieb, 2009). Therefore, mitochondria have emerging as a promising target in cancer therapy (Moindjie *et al.*, 2021). It would be interesting to assess whether the mechanisms described in yeast model are conserved in mammalian cells and investigate the relationship between dysregulated cell cycle, mitochondria and cancer progression.

List of references

Allen, J.B., Z. Zhou, W. Siede, E.C. Friedberg, and S.J. Elledge. **1994**. The SAD1/RAD53 protein kinase controls multiple checkpoints and DNA damage-induced transcription in yeast. *Genes & Development*. 8:2401-2415.

Almeida, A., J.P. Bolaños, and S. Moncada. **2010**. E3 ubiquitin ligase APC/C-Cdh1 accounts for the Warburg effect by linking glycolysis to cell proliferation. *Proceedings of the National Academy of Sciences*. 107:738-741.

Almeida, T., M. Marques, D. Mojzita, M.A. Amorim, R.D. Silva, B. Almeida, P. Rodrigues, P. Ludovico, S. Hohmann, P. Moradas-Ferreira, M. Côrte-Real, and V. Costa. **2008**. Isc1p plays a key role in hydrogen peroxide resistance and chronological lifespan through modulation of iron levels and apoptosis. *Molecular Biology of the Cell*. 19:865-876.

Altmann, K., and B. Westermann. **2005**. Role of essential genes in mitochondrial morphogenesis in *Saccharomyces cerevisiae*. *Molecular Biology of the Cell*. 16:5410-5417.

Anderson, H.L., J.C. Casler, and L.L. Lackner. **2022**. Hierarchical integration of mitochondrial and nuclear positioning pathways by the Num1 EF hand. *Molecular Biology of the Cell*. 33:ar20.

Aon, M.A., B.A. Stanley, V. Sivakumaran, J.M. Kembro, B. O'Rourke, N. Paolocci, and S. Cortassa. **2012**. Glutathione/thioredoxin systems modulate mitochondrial H_2O_2 emission: An experimental-computational study. *Journal of General Physiology*. 139:479-491.

Arakaki, N., T. Nishihama, H. Owaki, Y. Kuramoto, M. Suenaga, E. Miyoshi, Y. Emoto, H. Shibata, M. Shono, and T. Higuti. **2006**. Dynamics of mitochondria during the cell cycle. *Biological and Pharmaceutical Bulletin*. 29:1962-1965.

Aretz, I., C. Jakubke, and C. Osman. **2020**. Power to the daughters – mitochondrial and mtDNA transmission during cell division. *Biological Chemistry*. 401:533-546.

Ashe, M.P., S.K. De Long, and A.B. Sachs. **2000**. Glucose depletion rapidly inhibits translation initiation in yeast. *Molecular Biology of the Cell*. 11:833-848.

Ashton, T.M., W.G. McKenna, L.A. Kunz-Schughart, and G.S. Higgins. **2018**. Oxidative phosphorylation as an emerging target in cancer therapy. *Clinical Cancer Research*. 24:2482-2490.

Bakker, B.M., K.M. Overkamp, A.J.A. van Maris, P. Kötter, M.A.H. Luttik, J.P. van Dijken, and J.T. Pronk. **2001**. Stoichiometry and compartmentation of NADH metabolism in *Saccharomyces cerevisiae*. *FEMS Microbiology Reviews*. 25:15-37.

Balaban, R.S., S. Nemoto, and T. Finkel. **2005**. Mitochondria, oxidants, and aging. *Cell*. 120:483-495.

Bandhakavi, S., R.O. McCann, D.E. Hanna, and C.V. Glover. **2003**. A positive feedback loop between protein kinase CKII and Cdc37 promotes the activity of multiple protein kinases. *Journal of Biological Chemistry*. 278:2829-2836.

Bao, Y., K. Mukai, T. Hishiki, A. Kubo, M. Ohmura, Y. Sugiura, T. Matsuura, Y. Nagahata, N. Hayakawa, T. Yamamoto, R. Fukuda, H. Saya, M. Suematsu, and Y.A. Minamishima. **2013**. Energy management by enhanced glycolysis in G1-phase in human colon cancer cells *in vitro* and *in vivo*. *Molecular Cancer Research*. 11:973-985.

Barberis, M., and T. Mondeel. **2022**. Unveiling Forkhead-mediated regulation of yeast cell cycle and metabolic networks. *Computational and Structural Biotechnology Journal*. 20:1743-1751.

Barbet, N.C., U. Schneider, S.B. Helliwell, I. Stansfield, M.F. Tuite, and M.N. Hall. **1996**. TOR controls translation initiation and early G1 progression in yeast. *Molecular Biology of the Cell*. 7:25-42.

Barbosa, A.D., C. Pereira, H. Osório, P. Moradas-Ferreira, and V. Costa. **2016**. The ceramide-activated protein phosphatase Sit4p controls lifespan, mitochondrial function and cell cycle progression by regulating hexokinase 2 phosphorylation. *Cell Cycle*. 15:1620-1630.

Bardin, A.J., R. Visintin, and A. Amon. **2000**. A mechanism for coupling exit from mitosis to partitioning of the nucleus. *Cell*. 102:21-31.

Barral, Y., S. Jentsch, and C. Mann. **1995**. G1 cyclin turnover and nutrient uptake are controlled by a common pathway in yeast. *Genes & Development*. 9:399-409.

Barral, Y., M. Parra, S. Bidlingmaier, and M. Snyder. **1999**. Nim1-related kinases coordinate cell cycle progression with the organization of the peripheral cytoskeleton in yeast. *Genes & Development*. 13:176-187.

Bartlett, K., and S. Eaton. **2004**. Mitochondrial β-oxidation. *European Journal of Biochemistry*. 271:462-469.

Bayot, A., M. Gareil, A. Rogowska-Wrzesinska, P. Roepstorff, B. Friguet, and A.-L. Bulteau. **2010**. Identification of novel oxidized protein substrates and physiological partners of the mitochondrial ATP-dependent lon-like protease Pim1. *Journal of Biological Chemistry*. 285:11445-11457.

Blank, H.M., C. Li, J.E. Mueller, L.M. Bogomolnaya, M. Bryk, and M. Polymenis. **2008**. An increase in mitochondrial DNA promotes nuclear DNA replication in yeast. *PLOS Genetics*. 4:e1000047.

Blank, H.M., O. Papoulas, N. Maitra, R. Garge, B.K. Kennedy, B. Schilling, E.M. Marcotte, and M. Polymenis. **2020**. Abundances of transcripts, proteins, and metabolites in the cell cycle of budding yeast reveal coordinate control of lipid metabolism. *Molecular Biology of the Cell*. 31:1069-1084.

Bleazard, W., J.M. McCaffery, E.J. King, S. Bale, A. Mozdy, Q. Tieu, J. Nunnari, and J.M. Shaw. **1999**. The dynamin-related GTPase Dnm1 regulates mitochondrial fission in yeast. *Nature Cell Biology*. 1:298-304.

Böckler, S., X. Chelius, N. Hock, T. Klecker, M. Wolter, M. Weiss, R.J. Braun, and B. Westermann. **2017**. Fusion, fission, and transport control asymmetric inheritance of mitochondria and protein aggregates. *Journal of Cell Biology*. 216:2481-2498.

Bodrug, T., K.A. Welsh, M. Hinkle, M.J. Emanuele, and N.G. Brown. **2021**. Intricate regulatory mechanisms of the anaphase-promoting complex/cyclosome and its role in chromatin regulation. *Frontiers in Cell and Developmental Biology*. 9.

Boekhout, M., R. Yuan, A.P. Wondergem, H.A. Segeren, E.A. van Liere, N. Awol, I. Jansen, R.M.F. Wolthuis, A. de Bruin, and B. Westendorp. **2016**. Feedback regulation between atypical E2Fs and APC/C^{Cdh1} coordinates cell cycle progression. *EMBO reports*. 17:414-427.

Boldogh, I.R., D.W. Nowakowski, H.-C. Yang, H. Chung, S. Karmon, P. Royes, and L.A. Pon. **2003**. A protein complex containing Mdm10p, Mdm12p, and Mmm1p links mitochondrial membranes and DNA to the cytoskeleton-based segregation machinery. *Molecular Biology of the Cell*. 14:4618-4627.

Boldogh, I.R., H.-C. Yang, and L.A. Pon. **2001**. Mitochondrial inheritance in budding yeast. *Traffic*. 2:368-374.

Bonawitz, N.D., M. Chatenay-Lapointe, Y. Pan, and G.S. Shadel. **2007**. Reduced TOR signaling extends chronological life span via increased respiration and upregulation of mitochondrial gene expression. *Cell Metabolism*. 5:265-277.

Booher, R.N., R.J. Deshaies, and M.W. Kirschner. **1993**. Properties of *Saccharomyces cerevisiae* wee1 and its differential regulation of $p34^{CDC28}$ in response to G1 and G2 cyclins. *The EMBO Journal*. 12:3417-3426.

Botchkarev, V.V., and J.E. Haber. **2018**. Functions and regulation of the Polo-like kinase Cdc5 in the absence and presence of DNA damage. *Current Genetics*. 64:87-96.

Boy-Marcotte, E., M. Perrot, F. Bussereau, H. Boucherie, and M. Jacquet. **1998**. Msn2p and Msn4p control a large number of genes induced at the diauxic transition which are repressed by cyclic AMP in *Saccharomyces cerevisiae*. *Journal of Bacteriology*. 180:1044-1052.

Brand, M.D., C. Affourtit, T.C. Esteves, K. Green, A.J. Lambert, S. Miwa, J.L. Pakay, and N. Parker. **2004**. Mitochondrial superoxide: production, biological effects, and activation of uncoupling proteins. *Free Radical Biology and Medicine*. 37:755-767.

Brauer, M.J., A.J. Saldanha, K. Dolinski, and D. Botstein. **2005**. Homeostatic adjustment and metabolic remodeling in glucose-limited yeast cultures. *Molecular Biology of the Cell*. 16:2503-2517.

Burdon, R.H. **1995**. Superoxide and hydrogen peroxide in relation to mammalian cell proliferation. *Free Radical Biology and Medicine*. 18:775-794.

Burton, J.L., and M.J. Solomon. **2000**. Hsl1p, a Swe1p inhibitor, is degraded via the anaphase-promoting complex. *Molecular and Cellular Biology*. 20:4614-4625.

Burton, J.L., and M.J. Solomon. **2001**. D box and KEN box motifs in budding yeast Hsl1p are required for APC-mediated degradation and direct binding to Cdc20p and Cdh1p. *Genes & Development*. 15:2381-2395.

Busnelli, S., F. Tripodi, R. Nicastro, C. Cirulli, G. Tedeschi, R. Pagliarin, L. Alberghina, and P. Coccetti. **2013**. Snf1/AMPK promotes SBF and MBF-dependent transcription in budding yeast. *Biochimica et Biophysica Acta - Molecular Cell Research*. 1833:3254-3264.

Butow, R.A., and N.G. Avadhani. **2004**. Mitochondrial signaling: the retrograde response. *Molecular Cell*. 14:1-15.

Campbell, K., J. Westholm, S. Kasvandik, F. Di Bartolomeo, M. Mormino, and J. Nielsen. **2020**. Building blocks are synthesized on demand during the yeast cell cycle. *Proceedings of the National Academy of Sciences*. 117:7575-7583.

Cardozo, T., and M. Pagano. **2004**. The SCF ubiquitin ligase: insights into a molecular machine. *Nature Reviews Molecular Cell Biology*. 5:739-751.

Carling, D. **2004**. The AMP-activated protein kinase cascade — a unifying system for energy control. *Trends in Biochemical Sciences*. 29:18-24.

Casanovas, A., Richard R. Sprenger, K. Tarasov, David E. Ruckerbauer, Hans K. Hannibal-Bach, J. Zanghellini, Ole N. Jensen, and Christer S. Ejsing. **2015**. Quantitative analysis of proteome and lipidome dynamics reveals functional regulation of global lipid metabolism. *Chemistry & Biology*. 22:412-425.

Castellanos, E., and N.J. Lanning. **2019**. Phosphorylation of OXPHOS machinery subunits: Functional implications in cell biology and disease. *Yale Journal of Biology and Medicine*. 92:523-531.

Charles, J.F., S.L. Jaspersen, R.L. Tinker-Kulberg, L. Hwang, A. Szidon, and D.O. Morgan. **1998**. The Polo-related kinase Cdc5 activates and is destroyed by the mitotic cyclin destruction machinery in *S. cerevisiae*. *Current Biology*. 8:497-507.

Chen, S., D. Liu, R.L. Finley, Jr., and M.L. Greenberg. **2010**. Loss of mitochondrial DNA in the yeast cardiolipin synthase crd1 mutant leads to up-regulation of the protein kinase Swe1p that regulates the G2/M transition. *Journal of Biological Chemistry*. 285:10397-10407.

Chen, X.J., and G.D. Clark-Walker. **1999**. Alpha and beta subunits of F1-ATPase are required for survival of petite mutants in *Saccharomyces cerevisiae*. *Molecular and General Genetics*. 262:898-908.

Chen, Z., E.A. Odstrcil, B.P. Tu, and S.L. McKnight. **2007**. Restriction of DNA replication to the reductive phase of the metabolic cycle protects genome integrity. *Science*. 316:1916-1919.

Cheng, L., L. Hunke, and F.J. Hardy Christopher. **1998**. Cell cycle regulation of the *Saccharomyces cerevisiae* polo-like kinase Cdc5p. *Molecular and Cellular Biology*. 18:7360-7370.

Chernyakov, I., F. Santiago-Tirado, and A. Bretscher. **2013**. Active segregation of yeast mitochondria by Myo2 is essential and mediated by Mmr1 and Ypt11. *Current Biology*. 23:1818-1824.

Chevtzoff, C., J. Vallortigara, N. Avéret, M. Rigoulet, and A. Devin. **2005**. The yeast cAMP protein kinase Tpk3p is involved in the regulation of mitochondrial enzymatic content during growth. *Biochimica et Biophysica Acta - Bioenergetics*. 1706:117-125.

Cho, J.H., Y.K. Lee, and C.B. Chae. **2001**. The modulation of the biological activities of mitochondrial histone Abf2p by yeast PKA and its possible role in the regulation of mitochondrial DNA content during glucose repression. *Biochimica et Biophysica Acta - Gene Structure and Expression*. 1522:175-186.

Cho, R.J., M.J. Campbell, E.A. Winzeler, L. Steinmetz, A. Conway, L. Wodicka, T.G. Wolfsberg, A.E. Gabrielian, D. Landsman, D.J. Lockhart, and R.W. Davis. **1998**. A genome-wide transcriptional analysis of the mitotic cell cycle. *Molecular Cell*. 2:65-73.

Clotet, J., E. Garí, M. Aldea, and J. Ariño. **1999**. The yeast Ser/Thr phosphatases Sit4 and Ppz1 play opposite roles in regulation of the cell cycle. *Molecular and Cellular Biology*. 19:2408-2415.

Clute, P., and J. Pines. **1999**. Temporal and spatial control of cyclin B1 destruction in metaphase. *Nature Cell Biology*. 1:82-87.

Cocklin, R., and M. Goebl. **2011**. Nutrient sensing kinases PKA and Sch9 phosphorylate the catalytic domain of the ubiquitin-conjugating enzyme Cdc34. *PLOS ONE*. 6:e27099.

Cohen-Fix, O., J.M. Peters, M.W. Kirschner, and D. Koshland. **1996**. Anaphase initiation in *Saccharomyces cerevisiae* is controlled by the APC-dependent degradation of the anaphase inhibitor Pds1p. *Genes & Development*. 10:3081-3093.

Coleman Sean, T., A. Epping Eric, M. Steggerda Susanne, and W.S. Moye-Rowley. **1999**. Yap1p activates gene transcription in an oxidant-specific fashion. *Molecular and Cellular Biology*. 19:8302-8313.

Colombo, S.L., M. Palacios-Callender, N. Frakich, S. Carcamo, I. Kovacs, S. Tudzarova, and S. Moncada. **2011**. Molecular basis for the differential use of glucose and glutamine in cell proliferation as revealed by synchronized HeLa cells. *Proceedings of the National Academy of Sciences.* 108:21069-21074.

Colombo, S.L., M. Palacios-Callender, N. Frakich, J. De Leon, C.A. Schmitt, L. Boorn, N. Davis, and S. Moncada. **2010**. Anaphase-promoting complex/cyclosome-Cdh1 coordinates glycolysis and glutaminolysis with transition to S phase in human T lymphocytes. *Proceedings of the National Academy of Sciences*. 107:18868-18873.

Conrad, M., J. Schothorst, H.N. Kankipati, G. Van Zeebroeck, M. Rubio-Texeira, and J.M. Thevelein. **2014**. Nutrient sensing and signaling in the yeast *Saccharomyces cerevisiae*. *FEMS Microbiology Reviews*. 38:254-299.

Conrad, M.N., and C.S. Newlon. **1982**. The regulation of mitochondrial DNA levels in *Saccharomyces cerevisiae*. *Current Genetics*. 6:147-152.

Contamine, V., and M. Picard. **2000**. Maintenance and integrity of the mitochondrial genome: a plethora of nuclear genes in the budding yeast. *Microbiology and Molecular Biology Reviews*. 64:281-315.

Corton, J.M., J.G. Gillespie, and D.G. Hardie. **1994**. Role of the AMP-activated protein kinase in the cellular stress response. *Current Biology*. 4:315-324.

Crider, D.G., L.J. García-Rodríguez, P. Srivastava, L. Peraza-Reyes, K. Upadhyaya, I.R. Boldogh, and L.A. Pon. **2012**. Rad53 is essential for a mitochondrial DNA inheritance checkpoint regulating G1 to S progression. *Journal of Cell Biology*. 198:793-798.

Dejean, L., B. Beauvoit, O. Bunoust, B. Guérin, and M. Rigoulet. **2002**. Activation of Ras cascade increases the mitochondrial enzyme content of respiratory competent yeast. *Biochemical and Biophysical Research Communications*. 293:1383-1388.

Delaunay, A., D. Pflieger, M.-B. Barrault, J. Vinh, and M.B. Toledano. **2002**. A thiol peroxidase is an H_2O_2 receptor and redox-transducer in gene activation. *Cell*. 111:471-481.

Deng, X., F. Gao, and W.S. May, Jr. **2003**. Bcl2 retards G1/S cell cycle transition by regulating intracellular ROS. *Blood*. 102:3179-3185.

Detmer, S.A., and D.C. Chan. **2007**. Functions and dysfunctions of mitochondrial dynamics. *Nature Reviews Molecular Cell Biology*. 8:870-879.

Devin, A.B., T. Prosvirova, V.T. Peshekhonov, O.V. Chepurnaya, M.E. Smirnova, N.A. Koltovaya, E.N. Troitskaya, and I.P. Arman. **1990**. The start gene *CDC28* and the genetic stability of yeast. *Yeast*. 6:231-243.

Di Bartolomeo, F., C. Malina, K. Campbell, M. Mormino, J. Fuchs, E. Vorontsov, C.M. Gustafsson, and J. Nielsen. **2020**. Absolute yeast mitochondrial proteome quantification reveals trade-off between biosynthesis and energy generation during diauxic shift. *Proceedings of the National Academy of Sciences*. 117:7524-7535.

Di Como, C.J., and K.T. Arndt. **1996**. Nutrients, via the Tor proteins, stimulate the association of Tap42 with type 2A phosphatases. *Genes & Development*. 10:1904-1916.

Di Como, C.J., R. Bose, and K.T. Arndt. **1995**. Overexpression of SIS2, which contains an extremely acidic region, increases the expression of *SWI4*, *CLN1* and *CLN2* in *sit4* mutants. *Genetics*. 139:95-107.

Dimmer, K.S., S. Fritz, F. Fuchs, M. Messerschmitt, N. Weinbach, W. Neupert, and B. Westermann. **2002**. Genetic basis of mitochondrial function and morphology in *Saccharomyces cerevisiae*. *Molecular Biology of the Cell*. 13:847-853.

Dohmen, R.J., I. Willers, and A.J. Marques. **2007**. Biting the hand that feeds: Rpn4-dependent feedback regulation of proteasome function. *Biochimica et Biophysica Acta - Molecular Cell Research*. 1773:1599-1604.

Dohmen, R.J., P. Wu, and A. Varshavsky. **1994**. Heat-inducible degron: a method for constructing temperature-sensitive mutants. *Science*. 263:1273-1276.

Drebot, M.A., G.C. Johnston, and R.A. Singer. **1987**. A yeast mutant conditionally defective only for reentry into the mitotic cell cycle from stationary phase. *Proceedings of the National Academy of Sciences*. 84:7948-7952.

Dube, P., F. Herzog, C. Gieffers, B. Sander, D. Riedel, S.A. Müller, A. Engel, J.-M. Peters, and H. Stark. **2005**. Localization of the coactivator Cdh1 and the cullin subunit Apc2 in a cryo-electron microscopy model of vertebrate APC/C. *Molecular Cell*. 20:867-879.

Dutcher, S.K. **1982**. Two cell division cycle mutants of *Saccharomyces cerevisiae* are defective in transmission of mitochondria to zygotes. *Genetics*. 102:9-17.

Elgass, K., J. Pakay, M.T. Ryan, and C.S. Palmer. **2013**. Recent advances into the understanding of mitochondrial fission. *Biochimica et Biophysica Acta - Molecular Cell Research*. 1833:150-161.

Epp, J.A., and J. Chant. **1997**. An IQGAP-related protein controls actin-ring formation and cytokinesis in yeast. *Current Biology*. 7:921-929.

Esposito, M., S. Piatti, L. Hofmann, L. Frontali, A. Delahodde, and T. Rinaldi. **2011**. Analysis of the *rpn11-m1* proteasomal mutant reveals connection between cell cycle and mitochondrial biogenesis. *FEMS Yeast Research*. 11:60-71.

Estela, A., D. Pla-Martín, M. Sánchez-Piris, H. Sesaki, and F. Palau. **2011**. Charcot-Marie-Tooth-related gene *GDAP1* complements cell cycle delay at G2/M phase in *Saccharomyces cerevisiae fis1* gene-defective cells. *Journal of Biological Chemistry*. 286:36777-36786.

Ewald, J.C., A. Kuehne, N. Zamboni, and J.M. Skotheim. **2016**. The yeast cyclin-dependent kinase routes carbon fluxes to fuel cell cycle progression. *Molecular Cell*. 62:532-545.

Farrell, A., and D.O. Morgan. **2000**. Cdc37 promotes the stability of protein kinases Cdc28 and Cak1. *Molecular and Cellular Biology*. 20:749-754.

Fehrmann, S., C. Paoletti, Y. Goulev, A. Ungureanu, H. Aguilaniu, and G. Charvin. **2013**. Aging yeast cells undergo a sharp entry into eenescence unrelated to the loss of mitochondrial membrane potential. *Cell Reports*. 5:1589-1599.

Fernandez-Sarabia, M.J., A. Sutton, T. Zhong, and K.T. Arndt. **1992**. SIT4 protein phosphatase is required for the normal accumulation of *SWI4*, *CLN1*, *CLN2*, and *HCS26* RNAs during late G1. *Genes & Development*. 6:2417-2428.

Flattery-O'Brien, J.A., and I.W. Dawes. **1998**. Hydrogen peroxide causes *RAD9*-dependent cell cycle arrest in G2 in *Saccharomyces cerevisiae* whereas menadione causes G1 arrest independent of *RAD9* function. *Journal of Biological Chemistry*. 273:8564-8571.

Fleming, J.A., E.S. Lightcap, S. Sadis, V. Thoroddsen, C.E. Bulawa, and R.K. Blackman. **2002**. Complementary whole-genome technologies reveal the cellular response to proteasome inhibition by PS-341. *Proceedings of the National Academy of Sciences*. 99:1461-1466.

Flick, J.S., and M. Johnston. **1991**. *GRR1* of *Saccharomyces cerevisiae* is required for glucose repression and encodes a protein with leucine-rich repeats. *Molecular and Cellular Biology*. 11:5101-5112.

Forsburg, S.L., and P. Nurse. **1991**. Cell cycle regulation in the yeasts *Saccharomyces cerevisiae* and *Schizosaccharomyces pombe*. *Annual Review of Cell Biology*. 7:227-256.

Foury, F., T. Roganti, N. Lecrenier, and B. Purnelle. **1998**. The complete sequence of the mitochondrial genome of *Saccharomyces cerevisiae*. *FEBS Letters*. 440:325-331.

Frezza, C., and E. Gottlieb. **2009**. Mitochondria in cancer: Not just innocent bystanders. *Seminars in Cancer Biology*. 19:4-11.

Friedman, J.R., and J. Nunnari. **2014**. Mitochondrial form and function. *Nature*. 505:335-343.

Gancedo, J. M. **1998**. Yeast carbon catabolite repression. *Microbiology and Molecular Biology Reviews*. 62:334-361.

García-Rodríguez, L.J., D.G. Crider, A.C. Gay, I.J. Salanueva, I.R. Boldogh, and L.A. Pon. **2009**. Mitochondrial inheritance is required for MEN-regulated cytokinesis in budding yeast. *Current Biology*. 19:1730-1735.

Genta, H.D., M.E. Mónaco, and M.A. Aon. **1995**. Decreased mitochondrial biogenesis in temperature-sensitive cell division cycle mutants of *Saccharomyces cerevisiae*. *Current Microbiology*. 31:327-331.

Gerber, M.R., A. Farrell, R.J. Deshaies, I. Herskowitz, and D.O. Morgan. **1995**. Cdc37 is required for association of the protein kinase Cdc28 with G1 and mitotic cyclins. *Proceedings of the National Academy of Sciences*. 92:4651-4655.

Ghislain, M., A. Udvardy, and C. Mann. **1993**. *S. cerevisiae* 26S protease mutants arrest cell division in G2/metaphase. *Nature*. 366:358-362.

Gieffers, C., P. Dube, J.R. Harris, H. Stark, and J.-M. Peters. **2001**. Three-dimensional structure of the anaphase-promoting complex. *Molecular Cell*. 7:907-913.

Gietz, R.D., and R.H. Schiestl. **2007**. High-efficiency yeast transformation using the LiAc/SS carrier DNA/PEG method. *Nature Protocols*. 2:31-34.

Glotzer, M., A.W. Murray, and M.W. Kirschner. **1991**. Cyclin is degraded by the ubiquitin pathway. *Nature*. 349:132-138.

Goswami, A.V., M. Samaddar, D. Sinha, J. Purushotham, and P. D'Silva. **2012**. Enhanced J-protein interaction and compromised protein stability of mtHsp70 variants lead to mitochondrial dysfunction in Parkinson's disease. *Human Molecular Genetics*. 21:3317-3332.

Granovskaia, M.V., L.J. Jensen, M.E. Ritchie, J. Toedling, Y. Ning, P. Bork, W. Huber, and L.M. Steinmetz. **2010**. High-resolution transcription atlas of the mitotic cell cycle in budding yeast. *Genome Biology*. 11:R24.

Guerra, P., L.-A.P.E. Vuillemenot, Y.B. van Oppen, M. Been, and A. Milias-Argeitis. **2022**. TORC1 and PKA activity towards ribosome biogenesis oscillates in synchrony with the budding yeast cell cycle. *Journal of Cell Science*. 135:jcs260378.

Gulshan, K., B. Thommandru, and W.S. Moye-Rowley. **2012**. Proteolytic degradation of the Yap1 transcription factor is regulated by subcellular localization and the E3 ubiquitin ligase Not4. *Journal of Biological Chemistry*. 287:26796-26805.

Haase, S.B., and S.I. Reed. **2002**. Improved flow cytometric analysis of the budding yeast cell cycle. *Cell Cycle*. 1:132-136.

Hales, K.G., and M.T. Fuller. **1997**. Developmentally regulated mitochondrial fusion mediated by a conserved, novel, predicted GTPase. *Cell*. 90:121-129.

Hall, M.C., D.E. Jeong, J.T. Henderson, E. Choi, S.C. Bremmer, A.B. Iliuk, and H. Charbonneau. **2008**. Cdc28 and Cdc14 control stability of the anaphase-promoting complex inhibitor Acm1. *Journal of Biological Chemistry*. 283:10396-10407.

Harbauer, A.B., M. Opalińska, C. Gerbeth, S. Herman Josip, S. Rao, B. Schönfisch, B. Guiard, O. Schmidt, N. Pfanner, and C. Meisinger. **2014**. Cell cycle–dependent regulation of mitochondrial preprotein translocase. *Science*. 346:1109-1113.

Hardie, D.G., and D. Carling. **1997**. The AMP-Activated Protein Kinase. *European Journal of Biochemistry*. 246:259-273.

Haurie, V., M. Perrot, T. Mini, P. Jenö, F. Sagliocco, and H. Boucherie. **2001**. The transcriptional activator Cat8p provides a major contribution to the reprogramming of carbon metabolism during the diauxic shift in *Saccharomyces cerevisiae*. *Journal of Biological Chemistry*. 276:76-85.

Havens, C.G., A. Ho, N. Yoshioka, and S.F. Dowdy. **2006**. Regulation of late G1/S phase transition and APC-Cdh1 by Reactive Oxygen Species. *Molecular and Cellular Biology*. 26:4701-4711.

Hawle, P., D. Horst, J.P. Bebelman, X.X. Yang, M. Siderius, and S.M. van der Vies. **2007**. Cdc37p is required for stress-induced high-osmolarity glycerol and protein kinase C mitogen-activated protein kinase pathway functionality by interaction with Hog1p and Slt2p (Mpk1p). *Eukaryotic Cell*. 6:521-532.

Heil-Chapdelaine, R.A., J.R. Oberle, and J.A. Cooper. **2000**. The cortical protein Num1p is essential for dynein-dependent interactions of microtubules with the cortex. *Journal of Cell Biology*. 151:1337-1344.

Hellerstedt, S.T., R.S. Nash, S. Weng, K.M. Paskov, E.D. Wong, K. Karra, S.R. Engel, and J.M. Cherry. **2017**. Curated protein information in the *Saccharomyces* genome database. *Database*. 2017:bax011.

Herzig, R.P., S. Scacco, and R.C. Scarpulla. **2000**. Sequential serum-dependent activation of CREB and NRF-1 leads to enhanced mitochondrial respiration through the induction of cytochrome *c*. *Journal of Biological Chemistry*. 275:13134-13141.

Hess, D.C., C.L. Myers, C. Huttenhower, M.A. Hibbs, A.P. Hayes, J. Paw, J.J. Clore, R.M. Mendoza, B.S. Luis, C. Nislow, G. Giaever, M. Costanzo, O.G. Troyanskaya, and A.A. Caudy. **2009**. Computationally driven, quantitative experiments discover genes required for mitochondrial biogenesis. *PLOS Genetics*. 5:e1000407.

Higuchi, R., Jason D. Vevea, Theresa C. Swayne, R. Chojnowski, V. Hill, Istvan R. Boldogh, and Liza A. Pon. **2013**. Actin dynamics affect mitochondrial quality control and aging in budding yeast. *Current Biology*. 23:2417-2422.

Higuchi-Sanabria, R., J.K. Charalel, M.P. Viana, E.J. Garcia, C.N. Sing, A. Koenigsberg, T.C. Swayne, J.D. Vevea, I.R. Boldogh, S.M. Rafelski, and L.A. Pon. **2016**. Mitochondrial anchorage and fusion contribute to mitochondrial inheritance and quality control in the budding yeast *Saccharomyces cerevisiae*. *Molecular Biology of the Cell*. 27:776-787.

Holt, L.J. **2012**. Regulatory modules: Coupling protein stability to phosphoregulation during cell division. *FEBS Letters*. 586:2773-2777.

Hood, J.K., W.W. Hwang, and P.A. Silver. **2001**. The *Saccharomyces cerevisiae* cyclin Clb2p is targeted to multiple subcellular locations by cis- and trans-acting determinants. *Journal of Cell Science*. 114:589-597.

Hoppins, S. **2014**. The regulation of mitochondrial dynamics. *Current Opinion in Cell Biology*. 29:46-52.

Horn, S.R., M.J. Thomenius, E.S. Johnson, C.D. Freel, J.Q. Wu, J.L. Coloff, C.-S. Yang, W. Tang, J. An, O.R. Ilkayeva, J.C. Rathmell, C.B. Newgard, and S. Kornbluth. **2011**. Regulation of mitochondrial morphology by APC/C^{Cdh1}-mediated control of Drp1 stability. *Molecular Biology of the Cell*. 22:1207-1216.

Hughes, C.S., S. Moggridge, T. Müller, P.H. Sorensen, G.B. Morin, and J. Krijgsveld. **2019**. Single-pot, solid-phase-enhanced sample preparation for proteomics experiments. *Nature Protocols*. 14:68-85.

Igata, M., H. Motoshima, K. Tsuruzoe, K. Kojima, T. Matsumura, T. Kondo, T. Taguchi, K. Nakamaru, M. Yano, D. Kukidome, K. Matsumoto, T. Toyonaga, T. Asano, T. Nishikawa, and E. Araki. **2005**. Adenosine monophosphate-activated protein kinase suppresses vascular smooth muscle cell proliferation through the inhibition of cell cycle progression. *Circulation Research*. 97:837-844.

Imamura, K., T. Ogura, A. Kishimoto, M. Kaminishi, and H. Esumi. **2001**. Cell cycle regulation via p53 phosphorylation by a 5′-AMP activated protein kinase activator, 5-aminoimidazole-4-carboxamide-1-β-d-ribofuranoside, in a human hepatocellular carcinoma cell line. *Biochemical and Biophysical Research Communications*. 287:562-567.

Irniger, S., M. Bäumer, and G.H. Braus. **2000**. Glucose and Ras activity influence the ubiquitin ligases APC/C and SCF in *Saccharomyces cerevisiae*. *Genetics*. 154:1509-1521.

Itoh, T., A. Toh-E, and Y. Matsui. **2004**. Mmr1p is a mitochondrial factor for Myo2p-dependent inheritance of mitochondria in the budding yeast. *The EMBO Journal*. 23:2520-2530.

Jablonka, W., S. Guzmán, J. Ramírez, and M. Montero-Lomelí. **2006**. Deviation of carbohydrate metabolism by the *SIT4* phosphatase in *Saccharomyces cerevisiae*. *Biochimica et Biophysica Acta - General Subjects*. 1760:1281-1291.

Jahnke, V.E., O. Sabido, and D. Freyssenet. **2009**. Control of mitochondrial biogenesis, ROS level, and cytosolic Ca^{2+} concentration during the cell cycle and the onset of differentiation in L6E9 myoblasts. *American Journal of Physiology - Cell Physiology*. 296:C1185-C1194.

Jamieson, D.J. **1992**. *Saccharomyces cerevisiae* has distinct adaptive responses to both hydrogen peroxide and menadione. *Journal of Bacteriology*. 174:6678-6681.

Janke, C., M.M. Magiera, N. Rathfelder, C. Taxis, S. Reber, H. Maekawa, A. Moreno-Borchart, G. Doenges, E. Schwob, E. Schiebel, and M. Knop. **2004**. A versatile toolbox for PCR-based tagging of yeast genes: new fluorescent proteins, more markers and promoter substitution cassettes. *Yeast*. 21:947-962.

Jaquenoud, M., F. van Drogen, and M. Peter. **2002**. Cell cycle-dependent nuclear export of Cdh1p may contribute to the inactivation of APC/C^{Cdh1}. *The EMBO Journal*. 21:6515-6526.

Jiang, Y. **2006**. Regulation of the cell cycle by protein phosphatase 2A in *Saccharomyces cerevisiae*. *Microbiology and Molecular Biology Reviews*. 70:440-449.

Jin, L., A. Williamson, S. Banerjee, I. Philipp, and M. Rape. **2008**. Mechanism of ubiquitin-chain formation by the human anaphase-promoting complex. *Cell*. 133:653-665.

Johnson, J.A., and M. Ogbi. **2011**. Targeting the F1Fo ATP Synthase: Modulation of the bodys powerhouse and its implications for human disease. *Current Medicinal Chemistry*. 18:4684-4714.

Johnston, G.C., J.R. Pringle, and L.H. Hartwell. **1977**. Coordination of growth with cell division in the yeast *Saccharomyces cerevisiae*. *Experimental Cell Research*. 105:79-98.

Jones, R.G., D.R. Plas, S. Kubek, M. Buzzai, J. Mu, Y. Xu, M.J. Birnbaum, and C.B. Thompson. **2005**. AMP-Activated Protein Kinase induces a p53-dependent metabolic checkpoint. *Molecular Cell*. 18:283-293.

Jun, H., T. Kieselbach, and L.J. Jönsson. **2012**. Comparative proteome analysis of *Saccharomyces cerevisiae*: A global overview of *in vivo* targets of the yeast activator protein 1. *BMC Genomics*. 13:230.

Kalucka, J., R. Missiaen, M. Georgiadou, S. Schoors, C. Lange, K. De Bock, M. Dewerchin, and P. Carmeliet. **2015**. Metabolic control of the cell cycle. *Cell Cycle*. 14:3379-3388.

Kanfer, G., and B. Kornmann. **2016**. Dynamics of the mitochondrial network during mitosis. *Biochemical Society Transactions*. 44:510-516.

Kashatus, D.F., K.-H. Lim, D.C. Brady, N.L.K. Pershing, A.D. Cox, and C.M. Counter. **2011**. RALA and RALBP1 regulate mitochondrial fission at mitosis. *Nature Cell Biology*. 13:1108-1115.

Kayikci, Ö., and J. Nielsen. **2015**. Glucose repression in *Saccharomyces cerevisiae*. *FEMS Yeast Research*. 15:fov068.

Kimura, Y., S.L. Rutherford, Y. Miyata, I. Yahara, B.C. Freeman, L. Yue, R.I. Morimoto, and S. Lindquist. **1997**. Cdc37 is a molecular chaperone with specific functions in signal transduction. *Genes & Development*. 11:1775-1785.

King, R.W., J.M. Peters, S. Tugendreich, M. Rolfe, P. Hieter, and M.W. Kirschner. **1995**. A 20S complex containing *CDC27* and *CDC16* catalyzes the mitosis-specific conjugation of ubiquitin to cyclin B. *Cell*. 81:279-288.

Klecker, T., D. Scholz, J. Förtsch, and B. Westermann. **2013**. The yeast cell cortical protein Num1 integrates mitochondrial dynamics into cellular architecture. *Journal of Cell Science*. 126:2924-2930.

Klevecz, R.R., J. Bolen, G. Forrest, and D.B. Murray. **2004**. A genomewide oscillation in transcription gates DNA replication and cell cycle. *Proceedings of the National Academy of Sciences*. 101:1200-1205.

Ko, N., R. Nishihama, G.H. Tully, D. Ostapenko, M.J. Solomon, D.O. Morgan, and J.R. Pringle. **2007**. Identification of yeast *IQGAP* (Iqg1p) as an anaphase-promoting-complex substrate and its role in actomyosin-ring-independent cytokinesis. *Molecular Biology of the Cell*. 18:5139-5153.

Koltovaya, N.A., I.P. Arman, and A.B. Devin. **1998**. Mutations of the *CDC28* gene and the radiation sensitivity of *Saccharomyces cerevisiae*. *Yeast*. 14:133-146.

Kondo-Okamoto, N., K. Ohkuni, K. Kitagawa, J.M. McCaffery, J.M. Shaw, and K. Okamoto. **2006**. The novel F-Box protein Mfb1p regulates mitochondrial connectivity and exhibits asymmetric localization in yeast. *Molecular Biology of the Cell*. 17:3756-3767.

Kraft, C., H.C. Vodermaier, S. Maurer-Stroh, F. Eisenhaber, and J.-M. Peters. **2005**. The WD40 propeller domain of Cdh1 functions as a destruction box receptor for APC/C substrates. *Molecular Cell*. 18:543-553.

Kraft, L.M., and L.L. Lackner. **2017**. Mitochondria-driven assembly of a cortical anchor for mitochondria and dynein. *Journal of Cell Biology*. 216:3061-3071.

Kramer, E.R., N. Scheuringer, A.V. Podtelejnikov, M. Mann, and J.-M. Peters. **2000**. Mitotic regulation of the APC activator proteins *CDC20* and *CDH1*. *Molecular Biology of the Cell*. 11:1555-1569.

Kuge, S., N. Jones, and A. Nomoto. **1997**. Regulation of yAP-1 nuclear localization in response to oxidative stress. *The EMBO Journal*. 16:1710-1720.

Kurat, C.F., H. Wolinski, J. Petschnigg, S. Kaluarachchi, B. Andrews, K. Natter, and S.D. Kohlwein. **2009**. Cdk1/Cdc28-dependent activation of the major triacylglycerol lipase Tgl4 in yeast links lipolysis to cell-cycle progression. *Molecular Cell*. 33:53-63.

Lackner, L.L., H. Ping, M. Graef, A. Murley, and J. Nunnari. **2013**. Endoplasmic reticulum-associated mitochondria–cortex tether functions in the distribution and inheritance of mitochondria. *Proceedings of the National Academy of Sciences*. 110:E458-E467.

Lai, C.-Y., E. Jaruga, C. Borghouts, and S.M. Jazwinski. **2002**. A mutation in the *ATP2* gene abrogates the age asymmetry between mother and daughter cells of the yeast *Saccharomyces cerevisiae*. *Genetics*. 162:73-87.

Lambhate, S., D. Bhattacharjee, and N. Jain. **2021**. APC/C CDH1 ubiquitinates IDH2 contributing to ROS increase in mitosis. *Cellular Signalling*. 86:110087.

Lane, N., and W. Martin. **2010**. The energetics of genome complexity. *Nature*. 467:929-934.

Lange, H., G. Kispal, and R. Lill. **1999**. Mechanism of iron transport to the site of heme synthesis inside yeast mitochondria. *Journal of Biological Chemistry*. 274:18989-18996.

Laoukili, J., M. Alvarez-Fernandez, M. Stahl, and R.H. Medema. **2008**. FoxM1 is degraded at mitotic exit in a Cdh1-dependent manner. *Cell Cycle*. 7:2720-2726.

Lasserre, J.-P., A. Dautant, R.S. Aiyar, R. Kucharczyk, A. Glatigny, D. Tribouillard-Tanvier, J. Rytka, M. Blondel, N. Skoczen, P. Reynier, L. Pitayu, A. Rötig, A. Delahodde, L.M. Steinmetz, G. Dujardin, V. Procaccio, and J.-P. di Rago. **2015**. Yeast as a system for modeling mitochondrial disease mechanisms and discovering therapies. *Disease Models & Mechanisms*. 8:509-526.

Lee, I.H., and T. Finkel. **2013**. Metabolic regulation of the cell cycle. *Current Opinion in Cell Biology*. 25:724-729.

Lee, K.S., J.-E. Park, S. Asano, and C.J. Park. **2005**. Yeast polo-like kinases: functionally conserved multitask mitotic regulators. *Oncogene*. 24:217-229.

Lee, S., S. Kim, X. Sun, J.-H. Lee, and H. Cho. **2007**. Cell cycle-dependent mitochondrial biogenesis and dynamics in mammalian cells. *Biochemical and Biophysical Research Communications*. 357:111-117.

Leite, A.C., T.S. Martins, A. Campos, V. Costa, and C. Pereira. **2022**. Phosphoregulation of the ATP synthase beta subunit stimulates mitochondrial activity for G2/M progression. *Advances in Biological Regulation*. 85:100905.

Lew, D.J. **2003**. The morphogenesis checkpoint: how yeast cells watch their figures. *Current Opinion in Cell Biology*. 15:648-653.

Li, F.N., and M. Johnston. **1997**. Grr1 of *Saccharomyces cerevisiae* is connected to the ubiquitin proteolysis machinery through Skp1: coupling glucose sensing to gene expression and the cell cycle. *The EMBO Journal*. 16:5629-5638.

Li, K.W., M.S. Lu, Y. Iwamoto, D.G. Drubin, and R.T.A. Pedersen. **2021**. A preferred sequence for organelle inheritance during polarized cell growth. *Journal of Cell Science*. 134:jcs258856.

Li, L., S. Bertram, J. Kaplan, X. Jia, and D.M. Ward. **2020**. The mitochondrial iron exporter genes *MMT1* and *MMT2* in yeast are transcriptionally regulated by Aft1 and Yap1. *Journal of Biological Chemistry*. 295:1716-1726.

Li, M., and P. Zhang. **2009**. The function of APC/C^{Cdh1} in cell cycle and beyond. *Cell Division*. 4:2.

Li, W., Y. Li, G. Li, Z. Zhou, X. Chang, Y. Xia, X. Dong, Z. Liu, B. Ren, W. Liu, and Y. Li. **2017**. Ectopic expression of the ATP synthase β subunit on the membrane of PC-3M cells supports its potential role in prostate cancer metastasis. *International Journal of Oncology*. 50:1312-1320.

Li, Z., F.J. Vizeacoumar, S. Bahr, J. Li, J. Warringer, F.S. Vizeacoumar, R. Min, B. Vandersluis, J. Bellay, M. Devit, J.A. Fleming, A. Stephens, J. Haase, Z.Y. Lin, A. Baryshnikova, H. Lu, Z. Yan, K. Jin, S. Barker, A. Datti, G. Giaever, C. Nislow, C. Bulawa, C.L. Myers, M. Costanzo, A.C. Gingras, Z. Zhang, A. Blomberg, K. Bloom, B. Andrews, and C. Boone. **2011**. Systematic exploration of essential yeast gene function with temperature-sensitive mutants. *Nature Biotechnology*. 29:361-367.

Liao, X.S., W.C. Small, P.A. Srere, and R.A. Butow. *1991*. Intramitochondrial functions regulate nonmitochondrial citrate synthase (CIT2) expression in *Saccharomyces cerevisiae*. *Molecular and Cellular Biology*. 11:38-46.

Lill, R., B. Hoffmann, S. Molik, A.J. Pierik, N. Rietzschel, O. Stehling, M.A. Uzarska, H. Webert, C. Wilbrecht, and U. Mühlenhoff. **2012**. The role of mitochondria in cellular iron-sulfur protein biogenesis and iron metabolism. *Biochimica et Biophysica Acta - Molecular Cell Research*. 1823:1491-1508.

Lin, L.T., A. Razzaq, S.E. Di Gregorio, S. Hong, B. Charles, M.H. Lopes, F. Beraldo, V.F. Prado, M.A.M. Prado, and M.L. Duennwald. **2021**. Hsp90 and its co-chaperone Sti1 control TDP-43 misfolding and toxicity. *The FASEB journal*. 35:e21594.

Lisowsky, T. **1994**. ERV1 is involved in the cell-division cycle and the maintenance of mitochondrial genomes in *Saccharomyces cerevisiae*. *Current Genetics*. 26:15-20.

Liu, J., L. Qin, and S. Ferguson-Miller. **2011**. Crystallographic and online spectral evidence for role of conformational change and conserved water in cytochrome oxidase proton pump. *Proceedings of the National Academy of Sciences*. 108:1284-1289.

Liu, M., Y. Xu, Y. Zhou, R. Lang, Z. Shi, J. Zhao, Y. Meng, and L. Bao. **2021**. Integrated analyses reveal the multi-omics and prognostic characteristics of ATP5B in breast cancer. *Frontiers in Genetics*. 12:652474.

Liu, Z., and R.A. Butow. **1999**. A transcriptional switch in the expression of yeast tricarboxylic acid cycle genes in response to a reduction or loss of respiratory function. *Molecular and Cellular Biology*. 19:6720-6728.

Liu, Z., T. Sekito, C.B. Epstein, and R.A. Butow. **2001**. RTG-dependent mitochondria to nucleus signaling is negatively regulated by the seven WD-repeat protein Lst8p. *The EMBO Journal*. 20:7209-7219.

Longtine, M.S., A. McKenzie, 3rd, D.J. Demarini, N.G. Shah, A. Wach, A. Brachat, P. Philippsen, and J.R. Pringle. **1998**. Additional modules for versatile and economical PCR-based gene deletion and modification in *Saccharomyces cerevisiae*. *Yeast*. 14:953-961.

Loy, C.J., D. Lydall, and U. Surana. **1999**. *NDD1*, a high-dosage suppressor of *cdc28-1N*, is essential for expression of a subset of late-S-phase-specific genes in *Saccharomyces cerevisiae*. *Molecular and Cellular Biology*. 19:3312-3327.

Lu, Z.J., Q.F. Song, S.S. Jiang, Q. Song, W. Wang, G.H. Zhang, B. Kan, L.J. Chen, J.L. Yang, F. Luo, Z.Y. Qian, Y.Q. Wei, and L.T. Gou. **2009**. Identification of ATP synthase beta subunit (ATPB) on the cell surface as a non-small cell lung cancer (NSCLC) associated antigen. *BMC Cancer*. 9:16.

Madden, K., Y.J. Sheu, K. Baetz, B. Andrews, and M. Snyder. **1997**. SBF cell cycle regulator as a target of the yeast PKC-MAP kinase pathway. *Science*. 275:1781-1784.

Maechler, P., S. Carobbio, and B. Rubi. **2006**. In beta-cells, mitochondria integrate and generate metabolic signals controlling insulin secretion. *The International Journal of Biochemistry & Cell Biology*. 38:696-709.

Maeta, K., S. Izawa, S. Okazaki, S. Kuge, and Y. Inoue. **2004**. Activity of the Yap1 transcription factor in *Saccharomyces cerevisiae* is modulated by methylglyoxal, a metabolite derived from glycolysis. *Molecular and Cellular Biology*. 24:8753-8764.

Malina, C., C. Larsson, and J. Nielsen. **2018**. Yeast mitochondria: an overview of mitochondrial biology and the potential of mitochondrial systems biology. *FEMS Yeast Research*. 18:foy040.

Malumbres, M., and M. Barbacid. **2009**. Cell cycle, CDKs and cancer: a changing paradigm. *Nature Reviews Cancer*. 9:153-166.

Mandal, A.K., P. Lee, J.A. Chen, N. Nillegoda, A. Heller, S. DiStasio, H. Oen, J. Victor, D.M. Nair, J.L. Brodsky, and A.J. Caplan. **2007**. Cdc37 has distinct roles in protein kinase quality control that protect nascent chains from degradation and promote posttranslational maturation. *Journal of Cell Biology*. 176:319-328.

Mandal, S., P. Guptan, E. Owusu-Ansah, and U. Banerjee. **2005**. Mitochondrial regulation of cell cycle progression during development as revealed by the *tenured* mutation in *Drosophila*. *Developmental Cell*. 9:843-854.

Mannhaupt, G., R. Schnall, V. Karpov, I. Vetter, and H. Feldmann. **1999**. Rpn4p acts as a transcription factor by binding to PACE, a nonamer box found upstream of 26S proteasomal and other genes in yeast. *FEBS Letters*. 450:27-34.

Manzano-López, J., L. Matellán, A. Álvarez-Llamas, J.C. Blanco-Mira, and F. Monje-Casas. **2019**. Asymmetric inheritance of spindle microtubule-organizing centres preserves replicative lifespan. *Nature Cell Biology*. 21:952-965.

Margeot, A., C. Blugeon, J. Sylvestre, S. Vialette, C. Jacq, and M. Corral-Debrinski. **2002**. In *Saccharomyces cerevisiae*, *ATP2* mRNA sorting to the vicinity of mitochondria is essential for respiratory function. *The EMBO Journal*. 21:6893-6904.

Martin, J., K. Mahlke, and N. Pfanner. **1991**. Role of an energized inner membrane in mitochondrial protein import. Delta psi drives the movement of presequences. *The Journal of Biological Chemistry*. 266:18051-18057.

Martínez-Diez, M., G. Santamaría, Á.D. Ortega, and J.M. Cuezva. **2006**. Biogenesis and dynamics of mitochondria during the cell cycle: Significance of 3′UTRs. *PLOS ONE*. 1:e107.

McConnell, S.J., L.C. Stewart, A. Talin, and M.P. Yaffe. **1990**. Temperature-sensitive yeast mutants defective in mitochondrial inheritance. *The Journal of Cell Biology*. 111:967-976.

McCusker, D., C. Denison, S. Anderson, T.A. Egelhofer, J.R. Yates, 3rd, S.P. Gygi, and D.R. Kellogg. **2007**. Cdk1 coordinates cell-surface growth with the cell cycle. *Nature Cell Biology*. 9:506-515.

McFaline-Figueroa, J.R., J. Vevea, T.C. Swayne, C. Zhou, C. Liu, G. Leung, I.R. Boldogh, and L.A. Pon. **2011**. Mitochondrial quality control during inheritance is associated with lifespan and mother–daughter age asymmetry in budding yeast. *Aging Cell*. 10:885-895.

Mehlgarten, C., D. Jablonowski, K.D. Breunig, M.J. Stark, and R. Schaffrath. **2009**. Elongator function depends on antagonistic regulation by casein kinase Hrr25 and protein phosphatase Sit4. *Molecular Microbiology*. 73:869-881.

Mendenhall, M.D., and A.E. Hodge. **1998**. Regulation of Cdc28 cyclin-dependent protein kinase activity during the cell cycle of the yeast *Saccharomyces cerevisiae*. *Microbiology and Molecular Biology Reviews*. 62:1191-1243.

Millson, S., P. van Oosten-Hawle, M.A. Alkuriji, A. Truman, M. Siderius, and P.W. Piper. **2014**. Cdc37 engages in stable, S14A mutation-reinforced association with the most

atypical member of the yeast kinome, Cdk-activating kinase (Cak1). *Cell Stress Chaperones*. 19:695-703.

Mitchell, P. **1961**. Coupling of phosphorylation to electron and hydrogen transfer by a chemi-osmotic type of mechanism. *Nature*. 191:144-148.

Mitra, K., C. Wunder, B. Roysam, G. Lin, and J. Lippincott-Schwartz. **2009**. A hyperfused mitochondrial state achieved at G1–S regulates cyclin E buildup and entry into S phase. *Proceedings of the National Academy of Sciences*. 106:11960-11965.

Miyakawa, I. **2017**. Organization and dynamics of yeast mitochondrial nucleoids. *Proceedings of the Japan Academy, Series B*. 93:339-359.

Miyakawa, I., H. Aoi, N. Sando, and T. Kuroiwa. **1984**. Fluorescence microscopic studies of mitochondrial nucleoids during meiosis and sporulation in the yeast, *Saccharomyces cerevisiae. Journal of Cell Science*. 66:21-38.

Miyata, Y., and E. Nishida. **2004**. Supervision of multiple signaling protein kinases by the CK2-Cdc37 couple, a possible novel cancer therapeutic target. *Annals of the New York Academy of Sciences*. 1030:150-157.

Mizunuma, M., R. Tsubakiyama, T. Ogawa, A. Shitamukai, Y. Kobayashi, T. Inai, K. Kume, and D. Hirata. **2013**. Ras/cAMP-dependent protein kinase (PKA) regulates multiple aspects of cellular events by phosphorylating the Whi3 cell cycle regulator in budding yeast. *Journal of Biological Chemistry*. 288:10558-10566.

Moindjie, H., S. Rodrigues-Ferreira, and C. Nahmias. **2021**. Mitochondrial metabolism in carcinogenesis and cancer therapy. *Cancers*. 13:3311.

Montemurro, C., S. Vadrevu, T. Gurlo, A.E. Butler, K.E. Vongbunyong, A. Petcherski, O.S. Shirihai, L.S. Satin, D. Braas, P.C. Butler, and S. Tudzarova. **2017**. Cell cycle–related metabolism and mitochondrial dynamics in a replication-competent pancreatic beta-cell line. *Cell Cycle*. 16:2086-2099.

Moreno-Torres, M., M. Jaquenoud, and C. De Virgilio. **2015**. TORC1 controls G1–S cell cycle transition in yeast via Mpk1 and the greatwall kinase pathway. *Nature Communications*. 6:8256.

Morgenstern, M., S.B. Stiller, P. Lübbert, C.D. Peikert, S. Dannenmaier, F. Drepper, U. Weill, P. Höß, R. Feuerstein, M. Gebert, M. Bohnert, M. van der Laan, M. Schuldiner, C. Schütze, S. Oeljeklaus, N. Pfanner, N. Wiedemann, and B. Warscheid. **2017**. Definition of a high-confidence mitochondrial proteome at quantitative scale. *Cell Reports*. 19:2836-2852.

Mozdy, A.D., J.M. McCaffery, and J.M. Shaw. **2000**. Dnm1p GTPase-mediated mitochondrial fission is a multi-step process requiring the novel integral membrane component Fis1p. *Journal of Cell Biology*. 151:367-380.

Murray, A.W. **2004**. Recycling the cell cycle: Cyclins revisited. *Cell*. 116:221-234.

Nakamoto, R.K., J.A. Baylis Scanlon, and M.K. Al-Shawi. **2008**. The rotary mechanism of the ATP synthase. *Archives of Biochemistry and Biophysics*. 476:43-50.

Nakashima, A., Y. Maruki, Y. Imamura, C. Kondo, T. Kawamata, I. Kawanishi, H. Takata, A. Matsuura, K.S. Lee, U. Kikkawa, Y. Ohsumi, K. Yonezawa, and Y. Kamada. **2008**. The yeast Tor signaling pathway is involved in G2/M transition via Polo-kinase. *PLOS ONE*. 3:e2223.

Neiman, A.M., F. Chang, K. Komachi, and I. Herskowitz. **1990**. *CDC36* and *CDC39* are negative elements in the signal transduction pathway of yeast. *Cell Regulation*. 1:391-401.

Neupert, W., and J.M. Herrmann. **2007**. Translocation of proteins into mitochondria. *Annual Review of Biochemistry*. 76:723-749.

Newton, C.S., and W.L. Fangman. **1975**. Mitochondrial DNA synthesis in cell cycle mutants of *Saccharomyces cerevisiae*. *Cell*. 5:423-428.

Nicastro, R., F. Tripodi, C. Guzzi, V. Reghellin, S. Khoomrung, C. Capusoni, C. Compagno, C. Airoldi, J. Nielsen, L. Alberghina, and P. Coccetti. **2015**. Enhanced amino acid utilization sustains growth of cells lacking Snf1/AMPK. *Biochimica et Biophysica Acta - Molecular Cell Research*. 1853:1615-1625.

Niedenthal, R.K., L. Riles, M. Johnston, and J.H. Hegemann. **1996**. Green fluorescent protein as a marker for gene expression and subcellular localization in budding yeast. *Yeast*. 12:773-786.

Nilsson, A., and J. Nielsen. **2016**. Metabolic trade-offs in yeast are caused by F1F0-ATP synthase. *Scientific Reports*. 6:22264.

Niu, W., Z. Li, W. Zhan, V.R. Iyer, and E.M. Marcotte. **2008**. Mechanisms of cell cycle control revealed by a systematic and quantitative overexpression screen in *S. cerevisiae*. *PLOS Genetics*. 4:e1000120.

O'Rourke, T.W., N.A. Doudican, H. Zhang, J.S. Eaton, P.W. Doetsch, and G.S. Shadel. **2005**. Differential involvement of the related DNA helicases Pif1p and Rrm3p in mtDNA point mutagenesis and stability. *Gene*. 354:86-92.

Ohlmeier, S., A.J. Kastaniotis, J.K. Hiltunen, and U. Bergmann. **2004**. The yeast mitochondrial proteome, a study of fermentative and respiratory growth. *Journal of Biological Chemistry*. 279:3956-3979.

Oldenburg, K.R., K.T. Vo, S. Michaelis, and C. Paddon. **1997**. Recombination-mediated PCR-directed plasmid construction in vivo in yeast. *Nucleic Acids Research*. 25:451-452.

Orlando, D.A., C.Y. Lin, A. Bernard, J.Y. Wang, J.E. Socolar, E.S. Iversen, A.J. Hartemink, and S.B. Haase. **2008**. Global control of cell-cycle transcription by coupled CDK and network oscillators. *Nature*. 453:944-947.

Osellame, L.D., T.S. Blacker, and M.R. Duchen. **2012**. Cellular and molecular mechanisms of mitochondrial function. *Best Practice & Research Clinical Endocrinology & Metabolism*. 26:711-723.

Osman, C., T.R. Noriega, V. Okreglak, J.C. Fung, and P. Walter. **2015**. Integrity of the yeast mitochondrial genome, but not its distribution and inheritance, relies on mitochondrial fission and fusion. *Proceedings of the National Academy of Sciences*. 112:E947-E956.

Osório, H., C. Silva, M. Ferreira, I. Gullo, V. Máximo, R. Barros, F. Mendonça, C. Oliveira, and F. Carneiro. **2021**. Proteomics analysis of gastric cancer patients with diabetes mellitus. *Journal of Clinical Medicine*. 10: 407.

Ostapenko, D., J.L. Burton, and M.J. Solomon. **2012**. Identification of anaphase promoting complex substrates in *S. cerevisiae*. *PLOS ONE*. 7:e45895.

Otera, H., C. Wang, M.M. Cleland, K. Setoguchi, S. Yokota, R.J. Youle, and K. Mihara. **2010**. Mff is an essential factor for mitochondrial recruitment of Drp1 during mitochondrial fission in mammalian cells. *Journal of Cell Biology*. 191:1141-1158.

Ow, Y.-L.P., D.R. Green, Z. Hao, and T.W. Mak. **2008**. Cytochrome *c*: functions beyond respiration. *Nature Reviews Molecular Cell Biology*. 9:532-542.

Owsianik, G., L. Balzi, and M. Ghislain. **2002**. Control of 26S proteasome expression by transcription factors regulating multidrug resistance in *Saccharomyces cerevisiae*. *Molecular Microbiology*. 43:1295-1308.

Owusu-Ansah, E., A. Yavari, S. Mandal, and U. Banerjee. **2008**. Distinct mitochondrial retrograde signals control the G1-S cell cycle checkpoint. *Nature Genetics*. 40:356-361.

Palmer, C.S., L.D. Osellame, D. Stojanovski, and M.T. Ryan. **2011**. The regulation of mitochondrial morphology: Intricate mechanisms and dynamic machinery. *Cellular Signalling*. 23:1534-1545.

Pan, Y., Elizabeth A. Schroeder, A. Ocampo, A. Barrientos, and Gerald S. Shadel. **2011**. Regulation of yeast chronological life span by TORC1 via adaptive mitochondrial ROS signaling. *Cell Metabolism*. 13:668-678.

Pan, Y., and G.S. Shadel. **2009**. Extension of chronological life span by reduced TOR signaling requires down-regulation of Sch9p and involves increased mitochondrial OXPHOS complex density. *Aging*. 1:131-145.

Papagiannakis, A., J.J. de Jonge, Z. Zhang, and M. Heinemann. **2017**. Quantitative characterization of the auxin-inducible degron: a guide for dynamic protein depletion in single yeast cells. *Scientific Reports*. 7:4704.

Park Hyun, J., H. Costa Robert, F. Lau Lester, L. Tyner Angela, and P. Raychaudhuri. **2008**. Anaphase-promoting complex/cyclosome-Cdh1-mediated proteolysis of the forkhead box M1 transcription factor is critical for regulated entry into S phase. *Molecular and Cellular Biology*. 28:5162-5171.

Park, Y.-Y., and H. Cho. **2012**. Mitofusin 1 is degraded at G2/M phase through ubiquitylation by MARCH5. *Cell Division*. 7:25.

Parker, D.J., A. Iyer, S. Shah, A. Moran, A.B. Hjelmeland, M.K. Basu, R. Liu, and K. Mitra. **2015**. A new mitochondrial pool of cyclin E, regulated by Drp1, is linked to cell-density-dependent cell proliferation. *Journal of Cell Science*. 128:4171-4182.

Passmore, L.A., C.R. Booth, C. Vénien-Bryan, S.J. Ludtke, C. Fioretto, L.N. Johnson, W. Chiu, and D. Barford. **2005**. Structural analysis of the anaphase-promoting complex reveals multiple active sites and insights into polyubiquitylation. *Molecular Cell*. 20:855-866.

Passmore, L.A., E.A. McCormack, S.W.N. Au, A. Paul, K.R. Willison, J.W. Harper, and D. Barford. **2003**. Doc1 mediates the activity of the anaphase-promoting complex by contributing to substrate recognition. *The EMBO Journal*. 22:786-796.

Peart, M.J., M.V. Poyurovsky, E.M. Kass, M. Urist, E. Verschuren, M.K. Summers, P.K. Jackson, and C. Prives. **2010**. APC/C^{Cdc20} targets E2F1 for degradation in prometaphase. *Cell Cycle*. 9:3956-3964.

Peng, Y., and L.S. Weisman. **2008**. The cyclin-dependent kinase Cdk1 directly regulates vacuole inheritance. *Developmental Cell*. 15:478-485.

Pereira, C., L. Miguel Martins, and L. Saraiva. **2014**. LRRK2, but not pathogenic mutants, protects against H_2O_2 stress depending on mitochondrial function and endocytosis in a yeast model. *Biochimica et Biophysica Acta – General*. 1840:2025-2031.

Pereira, C., A.T. Pereira, H. Osório, P. Moradas-Ferreira, and V. Costa. **2018**. Sit4p-mediated dephosphorylation of Atp2p regulates ATP synthase activity and mitochondrial function. *Biochimica et Biophysica Acta - Bioenergetics*. 1859:591-601.

Perez-Riverol, Y., J. Bai, C. Bandla, D. García-Seisdedos, S. Hewapathirana, S. Kamatchinathan, Deepti J. Kundu, A. Prakash, A. Frericks-Zipper, M. Eisenacher, M. Walzer, S. Wang, A. Brazma, and Juan A. Vizcaíno. **2022**. The PRIDE database resources in 2022: a hub for mass spectrometry-based proteomics evidences. *Nucleic Acids Research*. 50:D543-D552.

Pernice, W.M., J.D. Vevea, and L.A. Pon. **2016**. A role for Mfb1p in region-specific anchorage of high-functioning mitochondria and lifespan in *Saccharomyces cerevisiae*. *Nature Communications*. 7:10595.

Perry, S.W., J.P. Norman, J. Barbieri, E.B. Brown, and H.A. Gelbard. **2011**. Mitochondrial membrane potential probes and the proton gradient: a practical usage guide. *BioTechniques*. 50:98-115.

Pessina, S., V. Tsiarentsyeva, S. Busnelli, M. Vanoni, L. Alberghina, and P. Coccetti. **2010**. Snf1/AMPK promotes S-phase entrance by controlling *CLB5* transcription in budding yeast. *Cell Cycle*. 9:2189-2200.

Peters, J.-M. **2006**. The anaphase promoting complex/cyclosome: a machine designed to destroy. *Nature Reviews Molecular Cell Biology*. 7:644-656.

Petroski, M.D., and R.J. Deshaies. **2005**. Function and regulation of cullin–RING ubiquitin ligases. *Nature Reviews Molecular Cell Biology*. 6:9-20.

Pfleger, C.M., and M.W. Kirschner. **2000**. The KEN box: an APC recognition signal distinct from the D box targeted by Cdh1. *Genes & Development*. 14:655-665.

Pfleger, C.M., E. Lee, and M.W. Kirschner. **2001**. Substrate recognition by the Cdc20 and Cdh1 components of the anaphase-promoting complex. *Genes & Development*. 15:2396-2407.

Pines, J. **2006**. Mitosis: a matter of getting rid of the right protein at the right time. *Trends in Cell Biology*. 16:55-63.

Ping, Z., R. Lim, T. Bashir, M. Pagano, and D. Guardavaccaro. **2012**. APC/C^{Cdh1} controls the proteasome-mediated degradation of E2F3 during cell cycle exit. *Cell Cycle*. 11:1999-2005.

Poyton, R.O., B. Goehring, M. Droste, K.A. Sevarino, L.A. Allen, and X.-J. Zhao. **1995**. Cytochrome-*c* oxidase from *Saccharomyces cerevisiae*. In *Methods in Enzymology*. Vol. 260. Academic Press. 97-116.

Qian, W., S. Choi, G.A. Gibson, S.C. Watkins, C.J. Bakkenist, and B. Van Houten. **2012**. Mitochondrial hyperfusion induced by loss of the fission protein Drp1 causes ATM-dependent G2/M arrest and aneuploidy through DNA replication stress. *Journal of Cell Science*. 125:5745-5757.

Rafelski, S.M., M.P. Viana, Y. Zhang, Y.-H.M. Chan, K.S. Thorn, P. Yam, J.C. Fung, H. Li, L.d.F. Costa, and W.F. Marshall. **2012**. Mitochondrial network size scaling in budding yeast. *Science*. 338:822-824.

Rapaport, D., M. Brunner, W. Neupert, and B. Westermann. **1998**. Fzo1p is a mitochondrial outer membrane protein essential for the biogenesis of functional mitochondria in *Saccharomyces cerevisiae*. *Journal of Biological Chemistry*. 273:20150-20155.

Rehman, J., H.J. Zhang, P.T. Toth, Y. Zhang, G. Marsboom, Z. Hong, R. Salgia, A.N. Husain, C. Wietholt, and S.L. Archer. **2012**. Inhibition of mitochondrial fission prevents cell cycle progression in lung cancer. *The FASEB Journal*. 26:2175-2186.

Renvoisé, M., L. Bonhomme, M. Davanture, B. Valot, M. Zivy, and C. Lemaire. **2014**. Quantitative variations of the mitochondrial proteome and phosphoproteome during fermentative and respiratory growth in *Saccharomyces cerevisiae*. *Journal of Proteomics*. 106:140-150.

Rich, P. **2003**. Chemiosmotic coupling: The cost of living. *Nature*. 421:583-583.

Rigbolt, K.T.G., T.A. Prokhorova, V. Akimov, J. Henningsen, P.T. Johansen, I. Kratchmarova, M. Kassem, M. Mann, J.V. Olsen, and B. Blagoev. **2011**. System-wide temporal characterization of the proteome and phosphoproteome of human embryonic stem cell differentiation. *Science Signaling*. 4:rs3.

Rinaldi, T., L. Hofmann, A. Gambadoro, R. Cossard, N. Livnat-Levanon, M.H. Glickman, L. Frontali, and A. Delahodde. **2008**. Dissection of the carboxyl-terminal domain of the proteasomal subunit Rpn11 in maintenance of mitochondrial structure and function. *Molecular Biology of the Cell*. 19:1022-1031.

Rinaldi, T., C. Ricci, D. Porro, M. Bolotin-Fukuhara, and L. Frontali. **1998**. A mutation in a novel yeast proteasomal gene, *RPN11*/*MPR1*, produces a cell cycle arrest, overreplication of nuclear and mitochondrial DNA, and an altered mitochondrial morphology. *Molecular Biology of the Cell*. 9:2917-2931.

Rodenfels, J., K.M. Neugebauer, and J. Howard. **2019**. Heat oscillations driven by the embryonic cell cycle reveal the energetic costs of signaling. *Developmental Cell*. 48:646-658.

Roeder, A.D., G.J. Hermann, B.R. Keegan, S.A. Thatcher, and J.M. Shaw. **1998**. Mitochondrial inheritance is delayed in *Saccharomyces cerevisiae* cells lacking the serine/threonine phosphatase PTC1. *Molecular Biology of the Cell*. 9 4:917-930.

Romero Antonia, M., M. Martínez-Pastor, G. Du, C. Solé, M. Carlos, V. Vergara Sandra, N. Sanvisens, A. Wohlschlegel James, P. Toczyski David, F. Posas, E. de Nadal, T. Martínez-Pastor María, J. Thiele Dennis, and S. Puig. **2018**. Phosphorylation and proteasome recognition of the mRNA-binding protein Cth2 facilitates yeast adaptation to iron deficiency. *mBio*. 9:e01694-18.

Roy, M., P.H. Reddy, M. Iijima, and H. Sesaki. **2015**. Mitochondrial division and fusion in metabolism. *Current Opinion in Cell Biology*. 33:111-118.

Rudner, A.D., and A.W. Murray. **2000**. Phosphorylation by Cdc28 activates the Cdc20-dependent activity of the anaphase-promoting complex. *Journal of Cell Biology*. 149:1377-1390.

Ruiz, A., X. Xu, and M. Carlson. **2011**. Roles of two protein phosphatases, Reg1-Glc7 and Sit4, and glycogen synthesis in regulation of SNF1 protein kinase. *Proceedings of the National Academy of Sciences*. 108:6349-6354.

Salazar-Roa, M., and M. Malumbres. **2017**. Fueling the cell division cycle. *Trends in Cell Biology*. 27:69-81.

Santel, A., and M.T. Fuller. **2001**. Control of mitochondrial morphology by a human mitofusin. *Journal of Cell Science*. 114:867-874.

Sattler, M., T. Winkler, S. Verma, C.H. Byrne, G. Shrikhande, R. Salgia, and J.D. Griffin. **1999**. Hematopoietic growth factors signal through the formation of Reactive Oxygen Species. *Blood*. 93:2928-2935.

Sawyer, E.M., P.R. Joshi, V. Jorgensen, J. Yunus, L.E. Berchowitz, and E. Ünal. **2018**. Developmental regulation of an organelle tether coordinates mitochondrial remodeling in meiosis. *Journal of Cell Biology*. 218:559-579.

Schieke, S.M., J.P. McCoy Jr, and T. Finkel. **2008**. Coordination of mitochondrial bioenergetics with G1 phase cell cycle progression. *Cell Cycle*. 7:1782-1787.

Schmidt, O., A.B. Harbauer, S. Rao, B. Eyrich, R.P. Zahedi, D. Stojanovski, B. Schönfisch, B. Guiard, A. Sickmann, N. Pfanner, and C. Meisinger. **2011**. Regulation of mitochondrial protein import by cytosolic kinases. *Cell*. 144:227-239.

Schwab, M., A.S. Lutum, and W. Seufert. **1997**. Yeast Hct1 is a regulator of Clb2 cyclin proteolysis. *Cell*. 90:683-693.

Schwab, M., M. Neutzner, D. Möcker, and W. Seufert. **2001**. Yeast Hct1 recognizes the mitotic cyclin Clb2 and other substrates of the ubiquitin ligase APC. *The EMBO Journal*. 20:5165-5175.

Sekito, T., J. Thornton, and R.A. Butow. **2000**. Mitochondria-to-nuclear signaling is regulated by the subcellular localization of the transcription factors Rtg1p and Rtg3p. *Molecular Biology of the Cell*. 11:2103-2115.

Sesaki, H., and R.E. Jensen. **1999**. Division versus Fusion: Dnm1p and Fzo1p antagonistically regulate mitochondrial shape. *Journal of Cell Biology*. 147:699-706.

Shao, J., T. Prince, S.D. Hartson, and R.L. Matts. **2003**. Phosphorylation of serine 13 is required for the proper function of the Hsp90 co-chaperone, Cdc37. *Journal of Biological Chemistry*. 278:38117-38120.

Shen, Y., J.W. Sherman, X. Chen, and R. Wang. **2018**. Phosphorylation of CDC25C by AMP-activated protein kinase mediates a metabolic checkpoint during cell-cycle G2/M-phase transition. *Journal of Biological Chemistry*. 293:5185-5199.

Sherr, C.J., and J.M. Roberts. **2004**. Living with or without cyclins and cyclin-dependent kinases. *Genes & Development*. 18:2699-2711.

Shirayama, M., A. Tóth, M. Gálová, and K. Nasmyth. **1999**. APC^{Cdc20} promotes exit from mitosis by destroying the anaphase inhibitor Pds1 and cyclin Clb5. *Nature*. 402:203-207.

Shirayama, M., W. Zachariae, R. Ciosk, and K. Nasmyth. **1998**. The Polo-like kinase Cdc5p and the WD-repeat protein Cdc20p/fizzy are regulators and substrates of the anaphase promoting complex in *Saccharomyces cerevisiae*. *The EMBO Journal*. 17:1336-1349.

Short, M.K., J.P. Hallett, K. Tar, T. Dange, M. Schmidt, R. Moir, I.M. Willis, and P.T. Jubinsky. **2012**. The yeast magmas ortholog Pam16 has an essential function in fermentative growth that involves sphingolipid metabolism. *PLOS ONE*. 7:e39428.

Sies, H. **2017**. Hydrogen peroxide as a central redox signaling molecule in physiological oxidative stress: Oxidative eustress. *Redox Biology*. 11:613-619.

Simon, V.R., S.L. Karmon, and L.A. Pon. **1997**. Mitochondrial inheritance: Cell cycle and actin cable dependence of polarized mitochondrial movements in *Saccharomyces cerevisiae*. *Cell Motility*. 37:199-210.

Simpson-Lavy, K.J., J. Sajman, D. Zenvirth, and M. Brandeis. **2009**. APC/C^{Cdh1} specific degradation of Hsl1 and Clb2 is required for proper stress responses of *S. cerevisiae*. *Cell Cycle*. 8:3006-3012.

Slavov, N., J. Macinskas, A. Caudy, and D. Botstein. **2011**. Metabolic cycling without cell division cycling in respiring yeast. *Proceedings of the National Academy of Sciences*. 108:19090-19095.

Smith, M.E., J.R. Dickinson, and A.E. Wheals. **1990**. Intracellular and extracellular levels of cyclic AMP during the cell cycle of *Saccharomyces cerevisiae*. *Yeast*. 6:53-60.

Spellman, P.T., G. Sherlock, M.Q. Zhang, V.R. Iyer, K. Anders, M.B. Eisen, P.O. Brown, D. Botstein, and B. Futcher. **1998**. Comprehensive identification of cell cycle-regulated genes of the yeast *Saccharomyces cerevisiae* by microarray hybridization. *Molecular Biology of the Cell*. 9:3273-3297.

Stegmeier, F., and A. Amon. **2004**. Closing mitosis: The functions of the Cdc14 phosphatase and its regulation. *Annual Review of Genetics*. 38:203-232.

Stephen, D.W.S., S.L. Rivers, and D.J. Jamieson. 1995. The role of the *YAP1* and *YAP2* genes in the regulation of the adaptive oxidative stress responses of *Saccharomyces cerevisiae*. *Molecular Microbiology*. 16:415-423.

Sudakin, V., D. Ganoth, A. Dahan, H. Heller, J. Hershko, F.C. Luca, J.V. Ruderman, and A. Hershko. **1995**. The cyclosome, a large complex containing cyclin-selective ubiquitin ligase activity, targets cyclins for destruction at the end of mitosis. *Molecular Biology of the Cell*. 6:185-197.

Surana, U., H. Robitsch, C. Price, T. Schuster, I. Fitch, A.B. Futcher, and K. Nasmyth. **1991**. The role of *CDC28* and cyclins during mitosis in the budding yeast *S. cerevisiae*. *Cell*. 65:145-161.

Surana, U., F.M. Yeong, and H.H. Lim. **2002**. MEN, destruction and separation: mechanistic links between mitotic exit and cytokinesis in budding yeast. *BioEssays*. 24:659-666.

Sutton, A., and R. Freiman. **1997**. The Cak1p protein kinase is required at G1/S and G2/M in the budding yeast cell cycle. *Genetics*. 147:57-71.

Sutton, A., D. Immanuel, and K.T. Arndt. **1991**. The SIT4 protein phosphatase functions in late G1 for progression into S phase. *Molecular and Cellular Biology*. 11:2133-2148.

Swayne, Theresa C., C. Zhou, Istvan R. Boldogh, Joseph K. Charalel, José R. McFaline-Figueroa, S. Thoms, C. Yang, G. Leung, J. McInnes, R. Erdmann, and Liza A. Pon. **2011**. Role for cER and Mmr1p in anchorage of mitochondria at sites of polarized surface growth in budding yeast. *Current Biology*. 21:1994-1999.

Sweet, S., and G. Singh. **1999**. Changes in mitochondrial mass, membrane potential, and cellular adenosine triphosphate content during the cell cycle of human leukemic (HL-60) cells. *Journal of Cellular Physiology*. 180:91-96.

Szklarczyk, D., A.L. Gable, D. Lyon, A. Junge, S. Wyder, J. Huerta-Cepas, M. Simonovic, N.T. Doncheva, J.H. Morris, P. Bork, L.J. Jensen, and Christian v. Mering. **2018**. STRING v11: protein–protein association networks with increased coverage, supporting functional discovery in genome-wide experimental datasets. *Nucleic Acids Research*. 47:D607-D613.

Taguchi, N., N. Ishihara, A. Jofuku, T. Oka, and K. Mihara. **2007**. Mitotic phosphorylation of dynamin-related GTPase Drp1 participates in mitochondrial fission. *Journal of Biological Chemistry*. 282:11521-11529.

Takaine, M., M. Ueno, K. Kitamura, H. Imamura, and S. Yoshida. **2019**. Reliable imaging of ATP in living budding and fission yeast. *Journal of Cell Science*. 132:jcs230649.

Taylor, S.D., H. Zhang, J.S. Eaton, M.S. Rodeheffer, M.A. Lebedeva, T.W. O'Rourke, W. Siede, and G.S. Shadel. **2005**. The conserved Mec1/Rad53 nuclear checkpoint pathway regulates mitochondrial DNA copy number in *Saccharomyces cerevisiae*. *Molecular Biology of the Cell*. 16:3010-3018.

Teixeira, L.K., and S.I. Reed. **2013**. Ubiquitin ligases and cell cycle control. *Annual Review of Biochemistry*. 82:387-414.

Teixeira, M.C., R. Viana, M. Palma, J. Oliveira, M. Galocha, M.N. Mota, D. Couceiro, M.G. Pereira, M. Antunes, I.V. Costa, P. Pais, C. Parada, C. Chaouiya, I. Sá-Correia, and P.T. Monteiro. **2022**. YEASTRACT+: a portal for the exploitation of global transcription regulation and metabolic model data in yeast biotechnology and pathogenesis. *Nucleic Acids Research*. 51:785-791.

Thornton, B.R., and D.P. Toczyski. **2003**. Securin and B-cyclin/CDK are the only essential targets of the APC. *Nature Cell Biology*. 5:1090-1094.

Thornton, B.R., and D.P. Toczyski. **2006**. Precise destruction: an emerging picture of the APC. *Genes & Development*. 20:3069-3078.

Tilokani, L., S. Nagashima, V. Paupe, and J. Prudent. **2018**. Mitochondrial dynamics: overview of molecular mechanisms. *Essays in Biochemistry*. 62:341-360.

Torres, J., C.J. Di Como, E. Herrero, and M.A. De La Torre-Ruiz. **2002**. Regulation of the cell integrity pathway by rapamycin-sensitive TOR function in budding yeast. *Journal of Biological Chemistry*. 277:43495-43504.

Toyama, E.Q., S. Herzig, J. Courchet, T.L. Lewis, O.C. Losón, K. Hellberg, N.P. Young, H. Chen, F. Polleux, D.C. Chan, and R.J. Shaw. **2016**. AMP-activated protein kinase mediates mitochondrial fission in response to energy stress. *Science*. 351:275-281.

Tripodi, F., A. Castoldi, R. Nicastro, V. Reghellin, L. Lombardi, C. Airoldi, E. Falletta, E. Maffioli, P. Scarcia, L. Palmieri, L. Alberghina, G. Agrimi, G. Tedeschi, and P. Coccetti. **2018**. Methionine supplementation stimulates mitochondrial respiration. *Biochimica et Biophysica Acta - Molecular Cell Research*. 1865:1901-1913.

Tsai, C.-F., Y.-T. Wang, H.-Y. Yen, C.-C. Tsou, W.-C. Ku, P.-Y. Lin, H.-Y. Chen, A.I. Nesvizhskii, Y. Ishihama, and Y.-J. Chen. **2015**. Large-scale determination of absolute phosphorylation stoichiometries in human cells by motif-targeting quantitative proteomics. *Nature Communications*. 6:6622.

Tu, B.P., A. Kudlicki, M. Rowicka, and S.L. McKnight. **2005**. Logic of the yeast metabolic cycle: Temporal compartmentalization of cellular processes. *Science*. 310:1152-1158.

Turner, J.J., J.C. Ewald, and J.M. Skotheim. **2012**. Cell size control in yeast. *Current Biology*. 22:R350-R359.

Ulery, T.L., S.H. Jang, and J.A. Jaehning. **1994**. Glucose repression of yeast mitochondrial transcription: kinetics of derepression and role of nuclear genes. *Molecular and Cellular Biology*. 14:1160-1170.

Van den Bogert, C., P. Muus, C. Haanen, A. Pennings, T.E. Melis, and A.M. Kroon. **1988**. Mitochondrial biogenesis and mitochondrial activity during the progression of the cell cycle of human leukemic cells. *Experimental Cell Research*. 178:143-153.

Vaughan, C.K., M. Mollapour, J.R. Smith, A. Truman, B. Hu, V.M. Good, B. Panaretou, L. Neckers, P.A. Clarke, P. Workman, P.W. Piper, C. Prodromou, and L.H. Pearl. **2008**. Hsp90-dependent activation of protein kinases is regulated by chaperone-targeted dephosphorylation of Cdc37. *Molecular Cell*. 31:886-895.

Viana, M.P., A.I. Brown, I.A. Mueller, C. Goul, E.F. Koslover, and S.M. Rafelski. **2020**. Mitochondrial fission and fusion dynamics generate efficient, robust, and evenly distributed network topologies in budding yeast cells. *Cell Systems*. 10:287-297.e285.

Vilaça, R., E. Silva, A. Nadais, V. Teixeira, N. Matmati, J. Gaifem, Y.A. Hannun, M.C. Sá Miranda, and V. Costa. **2014**. Sphingolipid signalling mediates mitochondrial dysfunctions

and reduced chronological lifespan in the yeast model of Niemann-Pick type C1. *Molecular Microbiology*. 91:438-451.

Vincent, O., and M. Carlson. **1998**. Sip4, a Snf1 kinase-dependent transcriptional activator, binds to the carbon source-responsive element of gluconeogenic genes. *The EMBO Journal*. 17:7002-7008.

Visintin, R., K. Craig, E.S. Hwang, S. Prinz, M. Tyers, and A. Amon. **1998**. The phosphatase Cdc14 triggers mitotic exit by reversal of Cdk-dependent phosphorylation. *Molecular Cell*. 2:709-718.

Visintin, R., E.S. Hwang, and A. Amon. **1999**. Cfi1 prevents premature exit from mitosis by anchoring Cdc14 phosphatase in the nucleolus. *Nature*. 398:818-823.

Visintin, R., S. Prinz, and A. Amon. **1997**. *CDC20* and *CDH1*: A family of substrate-specific activators of APC-dependent proteolysis. *Science*. 278:460-463.

Vodermaier, H.C., C. Gieffers, S. Maurer-Stroh, F. Eisenhaber, and J.-M. Peters. **2003**. TPR subunits of the anaphase-promoting complex mediate binding to the activator protein CDH1. *Current Biology*. 13:1459-1468.

Vögtle, F.N., J.M. Burkhart, H. Gonczarowska-Jorge, C. Kücükköse, A.A. Taskin, D. Kopczynski, R. Ahrends, D. Mossmann, A. Sickmann, R.P. Zahedi, and C. Meisinger. **2017**. Landscape of submitochondrial protein distribution. *Nature Communications*. 8:290.

Vowinckel, J., J. Hartl, R. Butler, and M. Ralser. **2015**. MitoLoc: A method for the simultaneous quantification of mitochondrial network morphology and membrane potential in single cells. *Mitochondrion*. 24:77-86.

Waizenegger, I.C., S. Hauf, A. Meinke, and J.-M. Peters. **2000**. Two distinct pathways remove mammalian cohesin from chromosome arms in prophase and from centromeres in anaphase. *Cell*. 103:399-410.

Wang, Z., M. Fan, D. Candas, T.-Q. Zhang, L. Qin, A. Eldridge, S. Wachsmann-Hogiu, Kazi M. Ahmed, Brett A. Chromy, D. Nantajit, N. Duru, F. He, M. Chen, T. Finkel, Lee S. Weinstein, and Jian J. Li. **2014**. Cyclin B1/Cdk1 coordinates mitochondrial respiration for cell-cycle G2/M progression. *Developmental Cell*. 29:217-232.

Warburg, O. **1956**. On the origin of cancer cells. *Science*. 123:309-314.

Wemmie, J.A., S.M. Steggerda, and W.S. Moye-Rowley. **1997**. The *Saccharomyces cerevisiae* AP-1 protein discriminates between oxidative stress elicited by the oxidants H2O2 and diamide. *Journal of Biological Chemistry*. 272:7908-7914.

Werner-Washburne, M., E. Braun, G.C. Johnston, and R.A. Singer. **1993**. Stationary phase in the yeast *Saccharomyces cerevisiae*. *Microbiological Reviews*. 57:383-401.

Westermann, B. **2010**. Mitochondrial dynamics in model organisms: What yeasts, worms and flies have taught us about fusion and fission of mitochondria. *Seminars in Cell & Developmental Biology*. 21:542-549.

Westermann, B., and W. Neupert. **2000**. Mitochondria-targeted green fluorescent proteins: convenient tools for the study of organelle biogenesis in *Saccharomyces cerevisiae*. *Yeast*. 16:1421-1427.

Wong, E.D., J.A. Wagner, S.V. Scott, V. Okreglak, T.J. Holewinske, A. Cassidy-Stone, and J. Nunnari. **2003**. The intramitochondrial dynamin-related GTPase, Mgm1p, is a component of a protein complex that mediates mitochondrial fusion. *Journal of Cell Biology*. 160:303-311.

Work, J.J., and O. Brandman. **2020**. Adaptability of the ubiquitin-proteasome system to proteolytic and folding stressors. *Journal of Cell Biology*. 220:e201912041.

Xie, B., S. Wang, N. Jiang, and J.J. Li. **2019**. Cyclin B1/CDK1-regulated mitochondrial bioenergetics in cell cycle progression and tumor resistance. *Cancer Letters*. 443:56-66.

Xie, Y., and A. Varshavsky. **2001**. RPN4 is a ligand, substrate, and transcriptional regulator of the 26S proteasome: A negative feedback circuit. *Proceedings of the National Academy of Sciences*. 98:3056-3061.

Xiong, W., Y. Jiao, W. Huang, M. Ma, M. Yu, Q. Cui, and D. Tan. **2012**. Regulation of the cell cycle via mitochondrial gene expression and energy metabolism in HeLa cells. *Acta Biochimica et Biophysica Sinica*. 44:347-358.

Yalcin, A., B.F. Clem, A. Simmons, A. Lane, K. Nelson, A.L. Clem, E. Brock, D. Siow, B. Wattenberg, S. Telang, and J. Chesney. **2009**. Nuclear targeting of 6-phosphofructo-2-kinase (PFKFB3) increases proliferation via cyclin-dependent kinases. *Journal of Biological Chemistry*. 284:24223-24232.

Yang, H.-C., A. Palazzo, T.C. Swayne, and L.A. Pon. **1999**. A retention mechanism for distribution of mitochondria during cell division in budding yeast. *Current Biology*. 9:1111-S1112.

Yang, H.-C., and L.A. Pon. **2002**. Actin cable dynamics in budding yeast. *b*. 99:751-756.

Ye, T., K. Elbing, and S. Hohmann. **2008**. The pathway by which the yeast protein kinase Snf1p controls acquisition of sodium tolerance is different from that mediating glucose regulation. *Microbiology*. 154:2814-2826.

Yi, D.G., M.J. Kim, J.E. Choi, J. Lee, J. Jung, W.-K. Huh, and W.-H. Chung. **2016**. Yap1 and Skn7 genetically interact with Rad51 in response to oxidative stress and DNA double-strand break in *Saccharomyces cerevisiae*. *Free Radical Biology and Medicine*. 101:424-433.

Yokoyama, H., M. Mizunuma, M. Okamoto, J. Yamamoto, D. Hirata, and T. Miyakawa. **2006**. Involvement of calcineurin-dependent degradation of Yap1p in Ca^{2+}-induced G2 cell-cycle regulation in *Saccharomyces cerevisiae*. *EMBO reports*. 7:519-524.

Young, E.T., C. Zhang, K.M. Shokat, P.K. Parua, and K.A. Braun. **2012**. The AMP-activated protein kinase Snf1 regulates transcription factor binding, RNA Polymerase II activity, and mRNA stability of glucose-repressed genes in *Saccharomyces cerevisiae*. *Journal of Biological Chemistry*. 287:29021-29034.

Youngman, M.J., A.E.A. Hobbs, S.M. Burgess, M. Srinivasan, and R.E. Jensen. **2004**. Mmm2p, a mitochondrial outer membrane protein required for yeast mitochondrial shape and maintenance of mtDNA nucleoids. *Journal of Cell Biology*. 164:677-688.

Zachariae, W., and K. Nasmyth. **1999**. Whose end is destruction: cell division and the anaphase-promoting complex. *Genes & Development*. 13:2039-2058.

Zachariae, W., M. Schwab, K. Nasmyth, and W. Seufert. **1998**. Control of cyclin ubiquitination by CDK-regulated binding of Hct1 to the anaphase promoting complex. *Science*. 282:1721-1724.

Zachariae, W., T.H. Shin, M. Galova, B. Obermaier, and K. Nasmyth. **1996**. Identification of subunits of the anaphase-promoting complex of *Saccharomyces cerevisiae*. *Science*. 274:1201-1204.

Zelenaya-Troitskaya, O., S.M. Newman, K. Okamoto, P.S. Perlman, and R.A. Butow. **1998**. Functions of the high mobility group protein, Abf2p, in mitochondrial DNA segregation, recombination and copy number in *Saccharomyces cerevisiae*. *Genetics*. 148:1763-1776.

Zhou, Q., Y. Zhai, J. Lou, M. Liu, X. Pang, and F. Sun. **2011**. Thiabendazole inhibits ubiquinone reduction activity of mitochondrial respiratory complex II via a water molecule mediated binding feature. *Protein & Cell*. 2:531-542.

Zinzalla, V., M. Graziola, A. Mastriani, M. Vanoni, and L. Alberghina. **2007**. Rapamycin-mediated G1 arrest involves regulation of the Cdk inhibitor Sic1 in *Saccharomyces cerevisiae*. *Molecular Microbiology*. 63:1482-1494.

Zong, W.-X., J.D. Rabinowitz, and E. White. **2016**. Mitochondria and Cancer. *Molecular Cell*. 61:667-676.

Zyrina, A.N., M.I. Sorokin, S.S. Sokolov, D.A. Knorre, and F.F. Severin. **2015**. Mitochondrial retrograde signaling inhibits the survival during prolong S/G2 arrest in *Saccharomyces cerevisiae*. *Oncotarget*. 6:44084-44094.

Zyrina Anna, N., A. Smirnova Ekaterina, V. Markova Olga, F. Severin Fedor, and A. Knorre Dmitry. **2017**. Mitochondrial superoxide dismutase and Yap1p act as a signaling module contributing to ethanol tolerance of the yeast *Saccharomyces cerevisiae*. *Applied and Environmental Microbiology*. 83:e02759-02716.